



Origin and functions of iridescent colours in hummingbirds

Hugo Gruson

► To cite this version:

Hugo Gruson. Origin and functions of iridescent colours in hummingbirds. Populations and Evolution [q-bio.PE]. Université de Montpellier, 2019. English. NNT: . tel-02465397

HAL Id: tel-02465397

<https://theses.hal.science/tel-02465397>

Submitted on 3 Feb 2020

HAL is a multi-disciplinary open access archive for the deposit and dissemination of scientific research documents, whether they are published or not. The documents may come from teaching and research institutions in France or abroad, or from public or private research centers.

L'archive ouverte pluridisciplinaire **HAL**, est destinée au dépôt et à la diffusion de documents scientifiques de niveau recherche, publiés ou non, émanant des établissements d'enseignement et de recherche français ou étrangers, des laboratoires publics ou privés.



Distributed under a Creative Commons Attribution - ShareAlike 4.0 International License

THÈSE POUR OBTENIR LE GRADE DE DOCTEUR DE L'UNIVERSITÉ DE MONTPELLIER

Filière EERGP - Écologie, Évolution, Ressources Génétiques, Paléobiologie
Champ disciplinaire Sciences de l'Évolution et de la Biodiversité

École doctorale GAIA

Unité de recherche CEFE

Origin and functions of iridescent colours in hummingbirds
&
Scientific publication in the technological era

Présentée par Hugo Gruson
Le 18/12/2019

Sous la direction de Claire Doutrelant
et Doris Gomez

Devant le jury composé de

Mathieu Joron, directeur de recherche, CNRS

Président du jury

Daniel C. Osorio, professor, University of Sussex

Rapporteur

Andrew J. Parnell, research fellow, University of Sheffield

Rapporteur

Nicola Nadeau, research fellow, University of Sheffield

Examinateuse

Marianne Elias, directrice de recherche, CNRS

Invitée

Christine Andraud, professeure, MNHN

Invitée

Claire Doutrelant, directrice de recherche, CNRS

Directrice

Doris Gomez, chargée de recherche, CNRS

Directrice



UNIVERSITÉ
DE MONTPELLIER

Contents

Preamble	5
Acknowledgements	7
Origin and functions of iridescent colours in hummingbirds	11
1.1 Introduction: What is colour?	12
Box 1: Measuring spectral reflectance and modelling colour vision	16
1.2 What is iridescence and how to measure it?	18
Box 2: Iridescence by interferences	19
1.3 Iridescence in hummingbirds: proximate and ultimate causes	23
Box 3: Hummingbirds (Trochilidae)	25
Box 4: Comparative analyses	27
1.4 Future directions	36
1.5 Semantics: what is iridescence?	44
1.6 Conclusion	46
References	47
Articles	67
Quantitative characterization of iridescent colours in biological studies: a novel method using optical theory	69
Hummingbird iridescence: an unsuspected structural diversity influences colouration at multiple scales	113
Distribution of iridescent colours in hummingbird communities results from the interplay between selection for camouflage and communication	163
Digest: Disentangling plumage and behavior contributions to iridescent signals	199
Estimation of colour volumes as concave hypervolumes using alphashapes	202
Scientific publication in the technological era	227
2.1 Introduction: The dire state of science	227
2.2 New publishing practices and community initiatives	229
2.3 The danger of proprietary, closed-source software in science	232
2.4 Leveraging technology to reduce human workload	234
2.5 Software and data as valid research outputs	236
2.6 My future projects in this area	238
References	239
Articles	243
rromeo: Access publisher copyright & self-archiving policies via the 'SHERPA/RoMEO' API	245
lightr: Import spectral data and metadata in R	253
When standards go wild - software review for a manuscript	259
pavo 2: New tools for the spectral and spatial analysis of colour in R	265
Résumé grand public en français	277

Preamble

When I initially started this PhD, I expected to work exclusively on iridescence in hummingbirds. But my path led me to spend a lot of time contributing code and advocating for a future where technology was used for the better to improve science practices as well. While discussing with my supervisors, I admitted how much it saddened me to reduce my work to the purely scientific aspect in my thesis, and to neglect all the work I had done in advocacy and meta-research (the research on research practices). My supervisors suggested I simply split my manuscript into two somewhat independent chapters. One that does indeed focus on colour and iridescence, and the other one on meta-research, a kind of editorial describing the world I envision for our community, how I contributed to it until now and more importantly, my plans for the future.

Within each chapter, I wandered away from the usual introduction / articles / discussion format, as the distinction between introduction and discussion appeared somewhat forced and artificial. Furthermore, the articles being pretty much standalone (because they are published or intended to be published in journals on their own), including them between the introduction and the discussion heavily disrupted the flow for the reader. So I simply split everything I wanted to say into thematic sections and put all my articles at the end of each chapter. The main results of each article are *very briefly* reminded in the main text of this thesis but readers should report back to the articles themselves for more information. Instead of copy/pasting in the thesis what I already said in the articles, I used this opportunity to add new details (including many new figures) which could not make it into the articles: the story of how each project came to be, the different strategies I tried, the obstacles I faced, the dead-ends, the surprising observations that are yet to be explained, etc. I hope it will prove useful and pleasant to read.

In accordance to what I present in the second chapter, most of this work is released under a free license:

This work is licensed under a [Creative Commons “Attribution-ShareAlike 4.0 International” license](#).



This means you are free to copy, re-use and adapt the content of this thesis, as long as you provide attribution ([BY clause of the creative commons license](#)) and you release your derived work under the same license (SA clause). Some figures are released under a stricter license (most of the time, forbidding commercial use; [NC clause](#)), to respect the original authors wishes. For such cases, it is always prominently written in the figure caption.

Colour code The electronic version of this thesis contains internal and external hyperlinks. These links are typeset in colour with the following code:

- [internal links to other parts of the thesis \(figures, tables, boxes, sections\)](#)
- [internal links to bibliographic references](#)
- [external links to the web](#)

Acknowledgements

First and foremost, I would like to thank my supervisors for their help and support during this PhD: Doris Gomez, Marianne Elias, Claire Doutrelant and Christine Andraud. You might already know this but every single time someone asked me how I came to work on the evolution of iridescence in hummingbirds, I answered that I didn't choose the topic: I picked the people I wanted to work with. I am extremely happy to have been able to work with you during these 3 years. You have left me many opportunities to explore the topics I was most interested in, even when you didn't share my enthusiasm. You didn't simply reluctantly agree to this, you even encouraged me to pursue my own questions. While I was writing this thesis, I realised how much I've learned during these three years, and I am convinced it would not have been possible without you pushing me forward.

Then, I would like to thank the jury for agreeing to read and evaluate my thesis. I am really glad to be able to welcome people that I admire and appreciate in my jury. Your work and your careers as scientists have greatly inspired me and I look forward to your valuable comments on my thesis.

I would also like to thank Rafael Maia and Tom White for inviting me into the development team for pavo, very early after my first contributions to the package. It has encouraged me to work more in this area, discover a side of research I grew to enjoy more and more every day and as an early career scientist, it gave me my first opportunity to develop collaborations outside my research group. This is exactly the spirit of open, collaborative science as I envision it. Thank you to Matthias Grenié as well who is always up for new crazy side projects instead of working on our respective theses.

It is also important to point out that many people contributed to the work presented in this thesis, at different levels. In chronological order: Juan L. Parra for sharing data, contributing ideas and comments on my first article manuscript, Jérôme Fuchs, Patrick Boussès and Anne Previato from the Muséum National d'Histoire Naturelle, as well as Harold Labrique and Cédric Audibert from the Musée des Confluences for their help with the museum collections, Serge Berthier and Willy Daney de Marcillac for their help with the goniometer and iridescence measurements, and Chakib Djediat for his help with the Transmission Electron Microscope and the sample preparation.

During my thesis, I had the chance to be a teaching assistant at the University of Montpellier. It was a tremendously rewarding and instructive experience and I am sure it would not have gone so well if I had not been surrounded by a great team of caring and kind lecturers.

I am also very grateful to have been able to work with Amélie Fargevieille and Nicola Nadeau for the organisation of a thematic symposium at ESEB2019: "Colour across the evolutionary spectrum: from production to perception." The community aspect of science is very important for me and it was an amazing experience to be able to meet so many '#colsci people' in one place. Putting this together could have been very stressful but it actually went very smoothly working with you both.

Finally, I would like to thank my friends from various places, as well as people from the CEFE and especially the ESP team, for their emotional support during these 3 years. You know who you are. You are probably aware that I'm not one to wear my heart on my sleeve so I won't go into effusive details but rest assured that I love you all very much! If you needed me to tell you this, I have done a pretty poor job at communicating my feelings and I hope to make it up to you very soon.

Peer-reviewed publications

- Gruson, H. (2019). "Digest: Disentangling plumage and behavior contributions to iridescent signals". *Evolution* 73.3, pp. 623–625. <https://doi.org/10.1111/evo.13685>.
- Gruson, H., Andraud, C., Daney de Marcillac, W., Berthier, S., Elias, M., and Gomez, D. (2019). "Quantitative characterization of iridescent colours in biological studies: a novel method using optical theory". *Interface Focus* 9.1, p. 20180049. <https://doi.org/10.1098/rsfs.2018.0049>.
- Gruson, H., White, T. E., and Maia, R. (2019). "lightr: import spectral data and metadata in R". *Journal of Open Source Software* 4.43, p. 1857. <https://doi.org/10.21105/joss.01857>.
- Maia, R., Gruson, H., Endler, J. A., and White, T. E. (2019). "pavo 2: New tools for the spectral and spatial analysis of colour in R". *Methods in Ecology and Evolution* 10.7, pp. 1097–1107. <https://doi.org/10.1111/2041-210X.13174>.

Pre-prints

- Gruson, H. (2019). "Estimation of colour volumes as concave hypervolumes using alphashapes". in revision.
- Gruson, H., Elias, M., Andraud, C., Djediat, C., Berthier, S., Doutrelant, C., and Gomez, D. (2019a). "Hummingbird iridescence: an unsuspected structural diversity influences colouration at multiple scales". *bioRxiv*. in revision, p. 699744. <https://doi.org/10.1101/699744>.
- Gruson, H., Elias, M., Parra, J. L., Andraud, C., Berthier, S., Doutrelant, C., and Gomez, D. (2019b). "Distribution of iridescent colours in hummingbird communities results from the interplay between selection for camouflage and communication". *bioRxiv*. under review at PCI EvolBiol, p. 586362. <https://doi.org/10.1101/586362>.

Invited blog posts

- Butland, S., Golding, N., Grieves, C., Gruson, H., White, T. E., and Hao, Y. (2019). *When Standards Go Wild - Software Review for a Manuscript*. URL: <https://ropensci.org/blog/2019/04/18/wild-standards/>.
- Grenié, M. and Gruson, H. (2019). *Access publisher copyright & self-archiving policies via the 'SHERPA/Romeo' API*. URL: <https://ropensci.org/blog/2019/06/04/rromeo/>.

Conferences and congresses

- Young Natural History scientists Meeting 2017, section Evolutionary Ecology, "Colour competition in Ecuadorian hummingbird communities"
- Young Natural History scientists Meeting 2018, section Methods in Natural Sciences, "New insights in the measurement and characterisation of iridescent colours" (best talk in Methods in Natural Sciences award)
- Living Light 2018, "Diversity and evolution of structures producing iridescence in hummingbirds"
- Evolution 2018, Open Symposium, "Unsuspected structural diversity in multilayers producing iridescent colours in hummingbirds"
- Young Natural History scientists Meeting 2019, section Methods in Natural Sciences, "Digging through the concept of multidimensional niche"
- Evolution 2019, poster in Open Symposium, "Distribution of iridescent colours in hummingbird communities results from the interplay between selection for camouflage and communication"



Origin and functions of iridescent colours in hummingbirds

How vivid is my recollection of the first
hummingbird which met my admiring gaze!
With what delight did I examine its tiny body
and feast my eyes on its glittering plumage!
This early impression, I well remember,
gradually increased into an earnest desire to
attain a more intimate acquaintance with
the lovely group of birds to which it
pertained.

John Gould



1.1 Introduction: What is colour?

In 1859, Darwin published his book '*On the Origin of Species by Means of Natural Selection*' (Darwin, 1859), where he presented a very simple mechanism, which contributes to the extraordinary diversity among living organisms: in a world of limited resources, individuals compete to acquire these resources in order to survive (the *struggle for life*). Because individuals differ in their ability to acquire these resources, some do not manage to survive or find a mate before their death and do not pass their traits onto the next generation, leading to the extinction of their lineage. This process of survival of the fittest is called natural selection.

Colour is one of the most striking aspects of this diversity which arises from natural selection and since the dawn of evolutionary biology, it has been the focus of many studies. For example, Wallace wrote a large corpus of texts and books on colouration in the context of natural selection (Wallace 1877; Wallace 1895; reviewed in Caro 2017). Colour is indeed a good study system to investigate the fine details of evolutionary processes as it is a complex trait which can evolve along several axes of variation (as opposed to body size or weight for example), and which is under the control of multiple forces often acting in opposite directions (Cuthill et al., 2017). Indeed, traits selected by natural selection improve either survival or fecundity. Colour can improve survival by making individuals less conspicuous, more cryptic, to predators (reviewed in Stevens and Merilaita 2011) and it can improve fecundity by making individuals more conspicuous and attractive to potential mates (detailed in Darwin 1872's second most famous book: *The descent of man, and selection in relation to sex*). The interplay between these two forces leads to the evolution of complex signals, which are sometimes spatially organised (as in fig. 1.1). Selection for camouflage and for communication are the commonly studied drivers of the evolution of colour but other drivers likely come into play as well, as I discuss later in this manuscript.



Figure 1.1: Peacock butterfly (*Aglais io*), from the Muséum de Toulouse, by Didier Descouens, CC-BY-SA 4.0. The dorsal side (left panel) has conspicuous colours, with some level of iridescence (blue spots on this picture), which may be involved in both communication and anti-predator strategy while the ventral side (right panel) seems entirely controlled by selection for camouflage.

Before I go any further in the discussion of colour, it is important to point out that colour is not an intrinsic property of an object but on contrary it is dependent on many extrinsic factors. For example, Galileo already highlighted the importance of the viewer in the very existence of the concept of colour (Boghossian and Velleman, 1989):

"Hence I think that these tastes, odors, colors, etc., on the side of the object in which they seem to exist, are nothing else than mere names, but hold their residence solely in the sensitive body; so that if the animal were removed, every such quality would be abolished and annihilated." (Galileo)

In other words, colour is the interaction between the spectral reflectance of said object (intrinsic physical property; box 2 in fig. 1.3) with the viewer's visual and cognitive system (extrinsic property; boxes 3 and 4 in fig. 1.3) (Endler, 1978): this is what philosophers call a secondary quality (Boghossian and Velleman, 1989).¹

The extraordinary diversity of colour I mentioned earlier is paired with a large diversity in the way these colours are perceived by different organisms (visual systems) (Osorio and Vorobyev, 2008). Species differ in their number of photoreceptor classes and the sensitivities of said photoreceptors (Osorio and Vorobyev, 2008). For example, all birds have 4 classes of photoreceptors (called cones) and can perceive so called visible (400 nm to 700 nm) and ultraviolet (UV; 300 nm to 400 nm) radiations but bird visual systems are traditionally divided in two classes, depending on their sensitivity to UV (Vorobyev et al., 1998). In violet-sensitive (VS) birds, the photoreceptor sensitive to UV has an absorbance peak around 355 nm to 380 nm while in ultraviolet-sensitive (UVS) birds, this peak is around 402 nm to 426 nm (Ödeen, Hart, and Håstad, 2009), as illustrated in fig. 1.2. But there is still considerable interspecific variation within these groups (Hart et al., 2000), or even regional variation within a single species (Knott et al., 2017), because of variations in photoreceptor sensitivities or other factors such as ocular medium transmission (Lind et al., 2014). In other taxa, studies have shown a difference in visual system between sexes for a single species (Arikawa et al., 2005; McCulloch, Osorio, and Briscoe, 2016).

Historically, colour was studied through human vision but this is not appropriate for most questions about evolution, as the agents exerting selective pressures do not necessarily see colour in the same way humans do (e.g. a female bird looking at the colours of a potential mate, or a dichromatic mammalian predator hunting its prey). Nowadays, several perceptual models exist to assess how colour is seen by a specific individual, using the characteristics of its visual system and the spectral reflectance of the target object (see box 1 for details on the measurement protocol) (Backhaus, 1991; Vorobyev and Osorio, 1998). Using these models, numerous studies have shown that the use of human vision to study other species colouration is not just a theoretical concern (as detailed in Bennett,

1. In the articles included in this thesis, I have often used 'colour' as a shorthand for 'spectral reflectance' for the sake of brevity and simplicity.

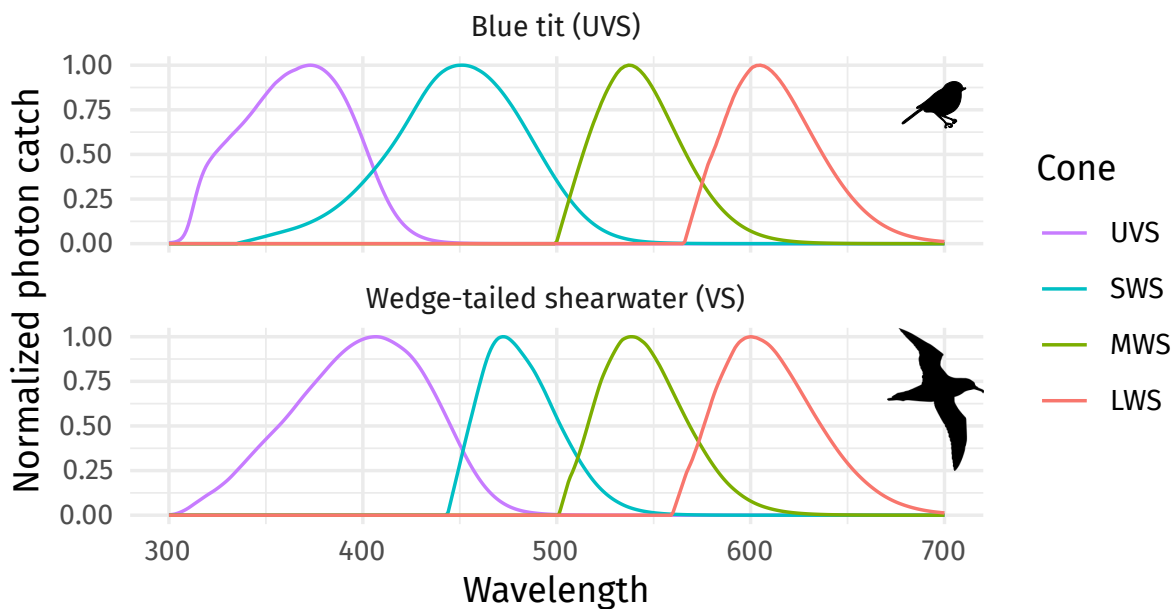


Figure 1.2: Normalised photon catch profiles of photoreceptors (cones) of a UVS bird, the blue tit *Cyanistes caeruleus* (top panel) and a VS bird, the wedge-tailed shearwater *Puffinus pacificus* (bottom panel). Both species have 4 types of photoreceptors but differ in their sensitivity to ultraviolet and small wavelength radiations.

Cuthill, and Norris, 1994) and that it does indeed fail to discern differences visible to other species (Eaton, 2005; Armenta, Dunn, and Whittingham, 2008). Colour is also processed by the brain in a complex way we do not yet fully understand for all species (box 4 in fig. 1.3). For example, a recent study showed that zebra finches (*Taeniopygia guttata*) make colour categories, even though their visual system could allow them to discern colours from a given category (Caves et al., 2018). This capacity was only attributed to humans until now and I do not know any perceptual model that takes this new research into account yet.

Finally, colour is also influenced by ambient light (box 1 in fig. 1.3). Let us imagine any object that is illuminated by blue light (similarly to what happens in the depth of the oceans for example), it cannot reflect anything else than this blue light, no matter its characteristics. Illuminants are varied in nature depending on the weather and the surrounding vegetation (Endler, 1993) and multiple studies have shown that this plays an important role in the evolution of colours (Endler and Thery, 1996; Heindl and Winkler, 2003a; Heindl and Winkler, 2003b; Gomez and Théry, 2004; Douglas et al., 2007).

The spectral reflectance that ultimately gives rise to colour can be produced by two non-exclusive mechanisms (Gadow, 1882), which divide colours in two classes:

- Pigmentary colours, in which wavelengths of the incoming light are selectively absorbed by a specific molecular entity, called pigment. The reflected light is therefore depleted in some wavelengths compared to the incoming light.

- Structural colours (reviewed in Kinoshita, Yoshioka, and Miyazaki, 2008), where the physical interaction between light with micro- and nano-structures produces the spectral reflectance because of dispersion, diffraction, interferences (the process by which interferences generate the spectral reflectance is detailed in **box 2**).

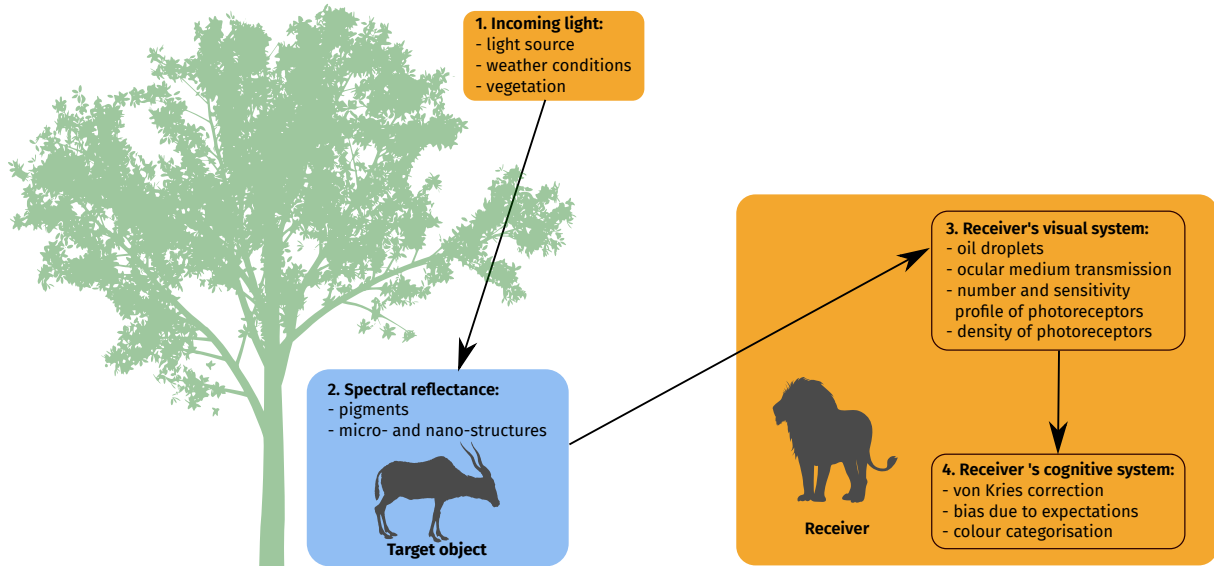


Figure 1.3: Drawing showing the different intrinsic (in blue) and extrinsic (in orange) components that creates the colour of an object in the brain of the receiver.

Box 1: Measuring spectral reflectance and modelling colour vision

Colour results from the interaction between spectral reflectance of the object (intrinsic physical property), incoming light and the receiver's visual and cognitive system (extrinsic properties). The first step to measuring colour in a reliable way, according to a given visual system, is thus to measure the spectral reflectance in an objective and reproducible way. For this, we use a spectrophotometer, which is a device that:

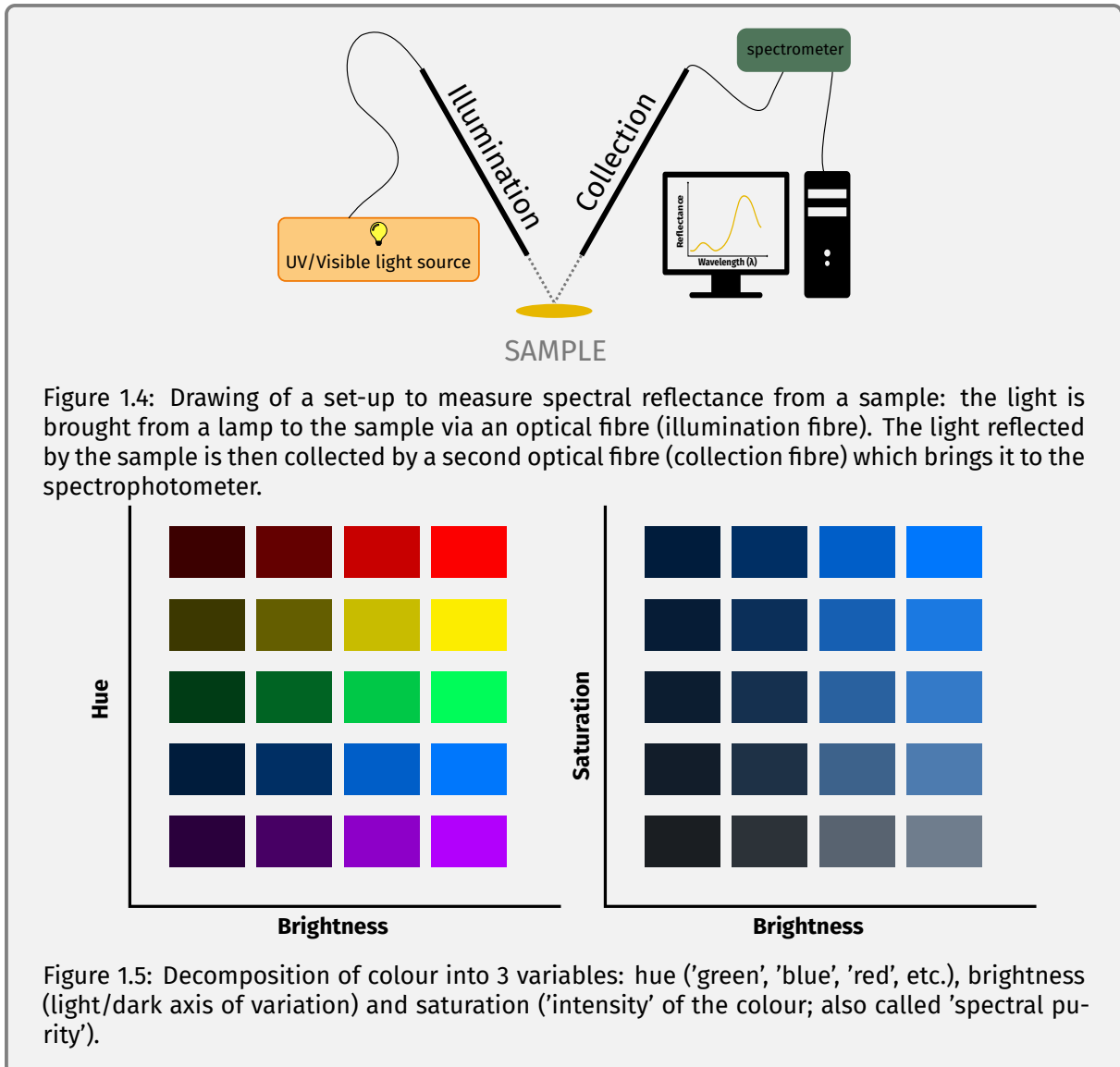
1. Separates the light radiation into discrete wavelength bins (diffraction step)
2. Counts the number of photons (roughly speaking the 'amount' of light) for each of these bins

Each spectrometer has its specific sensitivity to the different wavelengths and the reflected light depends on the incoming light, as mentioned before. As a consequence, to be able to use the resulting data in vision models with a chosen incoming light and visual system, we need to produce a measurement that is independent from the incoming light and spectrometer (receiver in this case). This is achieved by normalising all measurements relative to a 'white' reference (usually an achromatic Lambertian surface) and a 'dark' reference (representing the baseline signal in the absence of a sample, caused by stray light in the room and electrical noise).

This spectrometer collects light reflected by the sample via an optical fibre (called the collection fibre). We can only collect the full range of the spectral reflectance if the incoming light hitting the sample itself contains the full wavelength range perceived by potential receivers. For birds, we must then use a lamp that emits light in the UV and visible range (i.e. emitting over the 300 nm to 700 nm range). The light is brought from the lamp to the sample via a second optical fibre called the illumination fibre. This set-up is illustrated in [fig. 1.4](#).

The resulting reflectance spectrum then consists of several hundred data points for each measurement (one point for each of the aforementioned bin). They are usually summarised in 3 variables which convey different type of information: hue, brightness and saturation (illustrated in [fig. 1.5](#)). These variables are either extracted directly from the spectrum or after processing via a vision model, ad done in Vorobyev and Osorio ([1998](#)).

The protocol is slightly more involved for iridescent colours. Because the reflectance depends on the angle of illumination or collection, the precise position of the two fibres must be precisely controlled. See Gruson et al. ([2019a](#)) for a detailed presentation of the new method I developed during my PhD to measure and analyse iridescent colours in a precise and efficient way.



1.2 What is iridescence and how to measure it?

Iridescence is a specific type of structural colour, where the spectral reflectance changes with the illumination or observation angle (but see section 1.5 for discussion on this definition). It is quite a common phenomenon, found even in everyday objects, such as compact disks, soap bubbles or oil spills on the road. Iridescence can be produced by two mechanisms: diffraction or interferences (see box 2 for more details). For example, iridescent colours in bird feathers are produced by interferences caused by the reflection of light on multilayer structures (Dürrer, 1977). These multilayers are composed of organelles which contain melanin (refractive index $n \approx 1.8$; Stavenga et al. 2015), called melanosomes (reviewed by D'Alba and Shawkey, 2018), embedded in a keratin matrix (refractive index $n \approx 1.5$; Leertouwer, Wilts, and Stavenga 2011), as detailed later. Iridescence in many flowers on the other hand is due to diffraction (Whitney et al., 2009; Glover and Whitney, 2010), but not exclusively, as reviewed in Vignolini et al. (2013), while both interferences and diffraction contribute to the blue iridescent colours of *Morpho* butterflies (Vukusic et al., 1999). In many cases, iridescent colours are also highly directional, meaning that they are only visible over a narrow range of angles (directional colours) (Osorio and Ham, 2002; Pantelić et al., 2011). On the contrary, other species present specific adaptations that increase this angle range (diffuse colours) (Vukusic et al., 1999; Osorio and Ham, 2002).

Why study iridescence as evolutionary biologists?

I briefly explained the importance of the study of colours as a tool to better understand evolution but in this section, I would like to expand on why iridescence in particular is an especially valuable study system. Iridescent colours are widespread in many species across all groups in the tree of life (as illustrated in fig. 1.7) including bacteria (Kientz et al., 2016; Johansen et al., 2018), bony fishes (Lythgoe and Shand, 1989; Gur et al., 2014; Gur et al., 2015), arthropods and especially insects (Parker, McKenzie, and Large, 1998; Fabricant et al., 2013; Stavenga, 2014; Parnell et al., 2018; Pasteels et al., 2016) and spiders (Lim and Li, 2013), some bird groups (Dürrer, 1977), gastropods (Brink, van der Berg, and Botha, 2002) and even one mammal (Snyder et al., 2012) (see table 1 in Gruson et al. 2019a for a more complete list of taxa in which iridescence reflectance was measured and the method used or the more detailed version in Gruson et al. 2018). In spite of this large prevalence of iridescence, and in spite of the interest it sparked in early naturalists already (Gould, 1849; Wallace, 1895), much remains unknown about iridescence in natural objects. More specifically, most of its putative functions in natural objects (reviewed in Doucet and Meadows, 2009) have only been tested in a very limited number of species, and until very recently, we knew nearly nothing about its developmental process and genetic determinants (detailed in section 1.4).

Box 2: Iridescence by interferences

Iridescent colours are a specific type of structural colour, defined by a dependency to the angle of observation or illumination. It can be produced by interference of light on a thin-film^a or a multilayer structure. The simplest model to understand interferences comes from considering light as a wave^b. In this model, like for a mechanical wave, adjacent rays can be in phase or out of phase. Out of phase rays cancel one another (destructive interference). This phase difference arises when light goes through a multilayer structure, whose layers have different refractive indices ([table 1.1](#)). All light rays do not necessarily take the same path and if the length of the path difference is not a multiple of the wavelength, they get partially out of phase. Because this depends on the wavelength, the reflected light is depleted in some wavelengths (because of destructive interference) more than others relative to the incoming light, as shown in [fig. 1.6](#). This optical path difference also depends on the incidence angle, which explains the angle dependency of hue in iridescent colours.

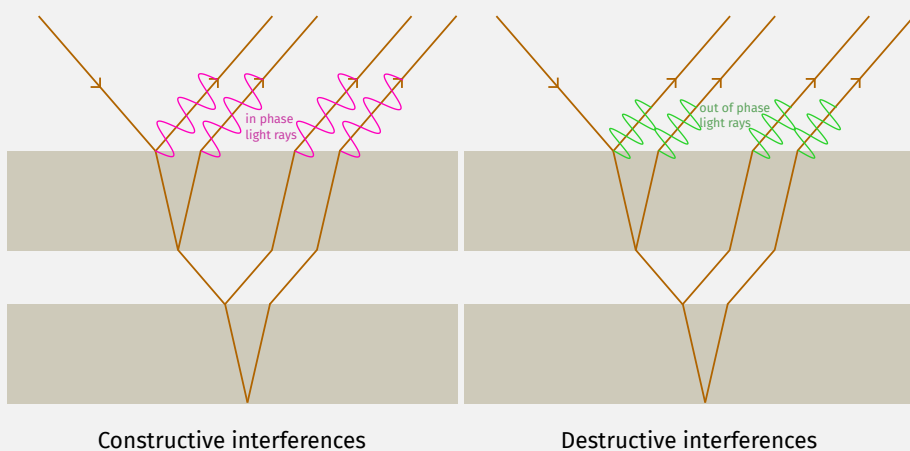


[Figure 1.6](#): Illustration of constructive and destructive interference. In this example, the wavelengths corresponding to a green hue will not be visible as they destructively interfere. The sample will appear pink, because the wavelengths corresponding to pink constructively interfere.

Material	Refractive index (n)	Reference
Keratin	1.56	Leertouwer, Wilts, and Stavenga (2011)
Chitin	1.55	
Melanin	1.8	Stavenga et al. (2015)
Air	1	

[Table 1.1](#): Example of usual materials found in animal multilayer structures and their refractive indices. Here, I present average values but the refractive index actually is a function of the wavelength (Leertouwer, Wilts, and Stavenga, [2011](#); Stavenga et al., [2015](#)).

a. an empirical distinction is made when the layer thickness exceeds $1\mu\text{m}$ and some authors use term 'thick-film' but the physical process is the same.

b. this model does not accurately describe the actual physical process but it works well enough for simple examples like this one.



Figure 1.7: A sample of the diversity of organisms displaying iridescence: Rainbow scarab beetle *Phanaeus vindex*, by Sebastian Eder, CC-BY-SA, green-tailed sunbird *Aethopyga nipalensis* by Dibyendu Ash, CC-BY-SA, peacock spider *Maratus volans* by Jürgen Otto, CC-BY-SA, *Morpho* sp. by Vera Kratochvil, CCO, Indian peafowl *Pavo cristatus* by Peter Kraayvanger, CCO, *Xenopeltis* sp. by wikipedia user bochr, CC-BY-SA, mantis shrimp *Odontodactylus scyllarus* by flickr user prilfish, CC-BY, cuckoo wasp *Hedychrum rutilans*, by Frank Vassen, CC-BY, sharknose goby *Elacatinus evelynae* by Ilyes Laszlo, CC-BY

How to measure iridescence? The first obstacle in its study

Iridescence has been largely neglected by evolutionary biologists until now likely in part because of the high difficulty to even reliably measure and quantify it. Indeed, it is a complex trait whose study requires a good grasp of the underlying optical principles. Until recently, there was no protocol publicly available to measure iridescence and only research groups with physicists were able to perform measurements, often using a custom method, which could not always be compared across studies. Most studies also generally focused on a single, iconic, species within a group (e.g. Zi et al., 2003; Plattner, 2004; Stavenga et al., 2011a; Fabricant et al., 2013; Parnell et al., 2015; Wilts, Giraldo, and Stavenga, 2016; Giraldo, Parra, and Stavenga, 2018). Yet, for evolutionary biologists, it is of paramount importance to be able to assess the variability within a clade (as done in Parnell et al. 2018) or even within a single species (as in Meadows, Roudybush, and McGraw 2012; Fabricant et al. 2013; Piszter et al. 2016; Ornelas et al. 2016), making it absolutely crucial to develop a standard protocol. For my first study during my PhD ([Distribution of iridescent colours in hummingbird communities results from the interplay between selection for camouflage and communication](#); under review by Peer Community In EvolBiol), I used a method derived from Meadows et al. (2011) to measure iridescence. As reported by the original authors, it did produce repeatable measurements. From this method, I defined a variable specific to iridescent colours: hue shift, as the difference in hue between two angular positions (as in Dakin

and Montgomerie 2013). But I noticed that the values of hue and hue shift were highly correlated, as already reported in Dakin and Montgomerie (2013), and I later proved this correlation theoretically (section B.3.2 of Gruson et al., 2019a). This strong correlation drastically reduced statistical power and made difficult any investigation on hue shift. In Gruson et al. (2019a), I used optical theory to show that iridescent colours due to interferences (box 2) vary in a predictable way in the angle space (fig. 1.8). This means that a limited number (16 angle configurations) of well-chosen measurements is sufficient to mathematically derive the variations in the entire angle space, which represents a huge time gain compared to the systematic exploration (120 angles configurations). Based on this proof, I proposed a standard protocol and described 6 indices (hue H_{\max} , angle dependency of hue γ_H , brightness B_{\max} , angle dependency of brightness γ_B , structure orientation t , saturation S_{\max}) to entirely summarise iridescent in the angle space and allow comparisons across studies. Following the advice of one reviewer, I also numerically verified the validity of the simplifying assumptions made in this paper by using simulations of the spectral reflectance produced by a multilayer structure (Supplementary Information presented in Gruson et al., 2018). I then tested this method on two phylogenetically distant clades: hummingbirds and *Morpho* butterflies, and showed that it produced reliable and repeatable values (reported in table 1.2).

taxon	variable	param.	mean	SD	RSD (%)	ICC	p (likel.)	p (perm.)
hummingbirds	brightness	B_{\max}	36.60	47.54	14.79	0.947	<0.0001	0.001
		t	14.61	18.21	7.428	0.968	<0.0001	0.001
		γ_B	13.67	7.85	11.19	0.875	0.0009	0.002
	hue	H_{\max}	556.80	65.66	0.3004	0.997	<0.0001	0.001
		γ_H	0.64	0.18	2.281	0.689	0.028	0.098
		B_{\max}	148.80	99.78	6.91	0.936	<0.0001	0.001
butterflies	brightness	t	2.94	4.83	32.96	0.268	0.18	0.098
		γ_B	5.35	5.12	4.76	0.769	<0.0001	0.004
		H_{\max}	492.69	27.87	0.2484	0.993	<0.0001	0.001
	hue	γ_H	0.73	0.14	2.993	0.853	<0.0001	0.001

Table 1.2: Repeatability of the method developed in Gruson et al. (2019a) for hummingbirds and butterflies. I tested repeatability by computing the intra-class coefficient (ICC column), which compares variability between measurements at the intraspecific level and at the interspecific level (i.e. is the method precise enough to capture differences between species?) and its statistical significance via two methods (last two columns). I also computed the relative standard deviation (RSD column), also called coefficient of variation which is the standard deviation divided by the mean, and which gives a index of the similarity of successive measurements of the same sample. Table 1 from Gruson et al. (2019a).

This method is based on spectral descriptors and not on variables derived from vision models, which means in its current state, it is not appropriate for all questions in evolutionary biology. But it can still be used in studies that focus on spectral reflectance (and not necessarily how it translates into colour), like [Hummingbird iridescence: an unsuspected structural diversity influences colouration at multiple scales](#). I plan on trying to expand this method to work with vision models in the future.

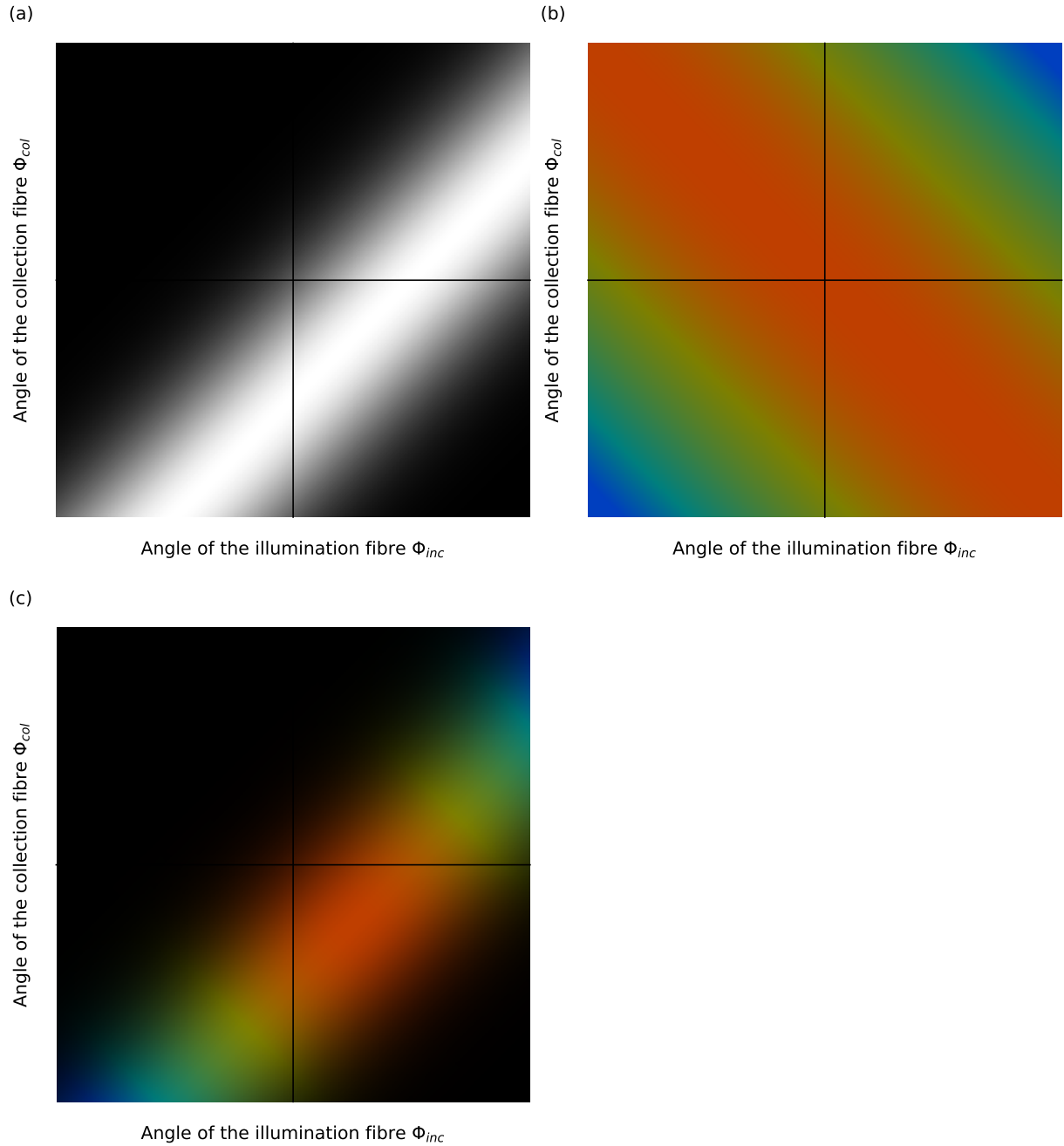


Figure 1.8: Colour variables ((a): brightness; (b): hue; (c): hue + brightness) of an iridescent multilayer change in a predictable fashion in the angle space. This means a limited number of measurement, to estimate the parameters of the underlying mathematical functions, is sufficient to reconstruct the variations in the angle space. Figure 3 from Gruson et al. (2019a).

1.3 Iridescence in hummingbirds: proximate and ultimate causes

In the rest of my PhD, I mainly focused on hummingbirds (see [box 3](#) for a brief general presentation of this family). Hummingbirds are a good system to study visual communication and iridescence, or even evolution in general (as exemplified by the fact that Wallace 1895 wrote a chapter titled 'Hummingbirds of Juan Fernandez as illustrating Variation and Natural Selection'), for several conceptual and technical reasons:

- Indeed, in few clades are iridescent colours as striking as in the hummingbirds. This extreme angle dependency and brightness are illustrated in [fig. 1.9](#) and by the following quote (see also Osorio and Ham 2002 for a precise quantification in the magnificent hummingbird *Eugenes fulgens*):

"We were examining a Hummingbird, the gorget of which was an intense emerald-green, but on changing the light (that is altering its angle of incidence) the emerald was changed into velvet black." Gould, 1849



Figure 1.9: Two views of the same Anna's hummingbird (*Calypte anna*) individual a couple of seconds apart, demonstrating the dramatic effect of angle on the colour of the face. This collage was created from a video of Mick Thompson, CC-BY-NC, <https://flic.kr/p/JDwh9K>.

All of the 365 hummingbird species have iridescent colours (sometimes alongside pigmentary colours), and hues can be wildly different between species, even when they diverged fairly recently (Clark, Feo, and Escalante, 2011), providing a good statistical power.

"The hue of every precious stone and the lustre of every metal is here represented; and such terms as topaz, amethyst, beryl, emerald, garnet, ruby, sapphire; golden, golden-green, coppery, fiery, glowing, iridescent, resplendent, celestial, glittering, shining, are constantly used to name or describe the different species." Wallace, 1895

- Almost all species are present in large numbers in museum collections. Indeed, the small size and shiny colours of hummingbirds made them prime targets for collectors during the 19th and 20th century. Gould (1849) reports that “[f]rom Santa Fe de Bogota alone many thousands of skins [were] annually sent to London and Paris”. For example, the Musée des Confluences in Lyon, France, has one of the largest hummingbird collections in the world, with about 16 000 skins. There are issues associated with such large numbers, especially related to data curation and accessibility that I discuss in the second part of this manuscript but museum collections represent a valuable tool for many experiments in natural sciences (Linck et al., 2017). During my PhD, I worked on museum specimens because it would have been too time consuming to travel all across the Americas to collect specimens. Additionally, the protocol to measure iridescence cannot be easily used in the field, as it requires a dark room (more details in Gruson et al. 2019a). We also know that museum specimens are appropriate to measure structural colours. Doucet and Hill (2009) have shown that reflectance characteristics are similar between live wild birds and museum skins in the structural blue patch of the long-tailed manakin *Chiroxiphia linearis*: brightness and saturation remain constant no matter the specimen age but hue tends to increase slightly with age. Similarly, Martin, Gaskett, and Friesen (2018) showed that seabird feather colours, as seen by seabirds, do not significantly change with specimen age. As a side note, it seems that pigmentary colours are more sensitive to colour alteration with time (McNnett and Marchetti, 2005). Hummingbirds do have pigmentary colours as well but my work has mainly focused on their iridescent colours.
- The phylogeny of hummingbirds is well resolved. Indeed, McGuire et al. provided sequences that led to the elaboration of two phylogenies by different teams. One by the team that generated the sequences (McGuire et al., 2007; McGuire et al., 2014) and the other by a team that built a general phylogeny for all birds (Jetz et al., 2012). The two phylogenies are quite similar, which is not surprising since they use the same genetic data as their basis. The main difference lies in the position of one clade: the topazes (as shown in fig. 1.10). Because of this similarity and because the number of topazes in my studies was low (1 species for Distribution of iridescent colours in hummingbird communities results from the interplay between selection for camouflage and communication and and 2 for Hummingbird iridescence: an unsuspected structural diversity influences colouration at multiple scales), I do not expect this to have an important impact on my results. In all the studies during my PhD, I used Jetz et al. (2012)'s phylogeny for the reasons developed in the second part of the manuscript.

But analyses at large taxonomic scale remain scarce in the field of iridescence, with most studies focusing on a single species (but see Maia, Rubenstein, and Shawkey 2013) and measuring iridescence at a single angle configuration, thus making impossible any investigation on hue or brightness angle

Box 3: Hummingbirds (Trochilidae)

Hummingbirds are a speciose family of small birds, which split from their sister group 42 million years ago (McGuire et al., 2014). They are famous for their hovering flight and shiny colours. Although they are often considered as exclusively nectarivorous in popular culture, several studies have shown they also eat small arthropods, especially during nesting season (Gould, 1849; Wallace, 1895; Montgomerie and Redsell, 1980). Despite their apparent similarity, the 365 species from this very speciose clade occupy a large diversity of habitats, regions, and climate (Schuchmann and Bonan, 2019). They live exclusively in the Americas but some species can be found in very cold regions such as Alaska or the high Andean plateau, as well as extremely arid regions such as the Sonoran desert (fig. 1.11).

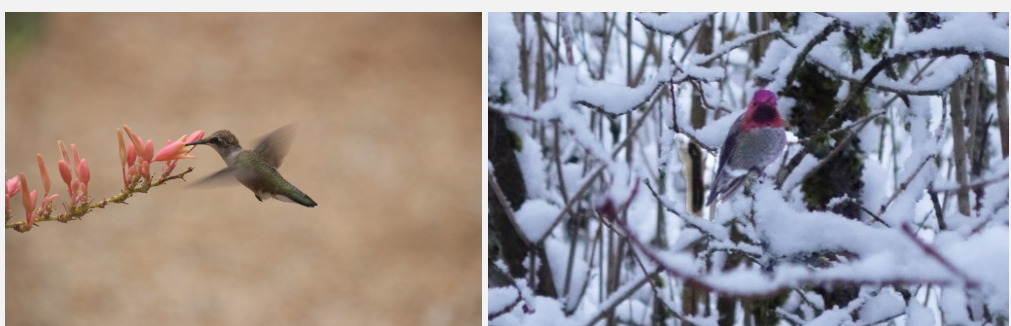


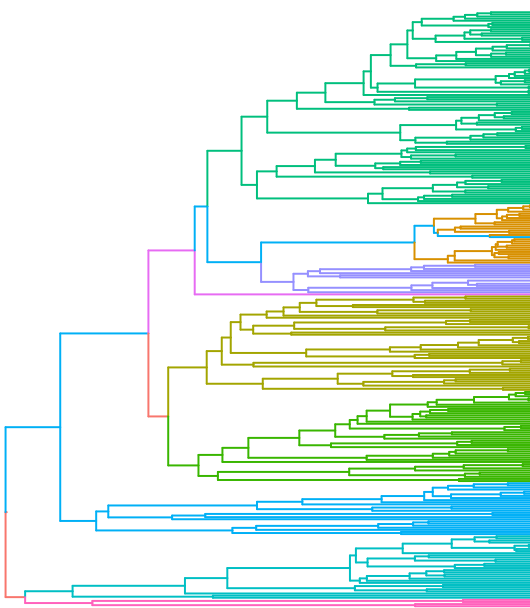
Figure 1.11: Black-chinned hummingbird (*Archilochus alexandri*) in the desert near Phoenix, Arizona (picture by Corey Seeman, <https://flic.kr/p/KyxgwR>, CC-BY-NC-SA) and Anna's hummingbird (*Calypte anna*) in the snow (picture by Bea Minus, CC0).

Their small size and costly hovering flight are linked to an extreme metabolism (Suarez, 1992). They are constantly refuelling and present specific adaptations which reduce catabolism during sleep, when they are unable to feed. They enter a state close to hibernation called torpor, where their internal temperature and heart rate drop (Hainsworth, Collins, and Wolf, 1977). During the day, this constant need for food creates a very high competition for access to the best foraging patches. Hummingbirds are indeed often described as territorial and pugnacious, attacking even species much larger than themselves (Pitelka, 1942; Stiles and Wolf, 1970; Stiles, 1982):

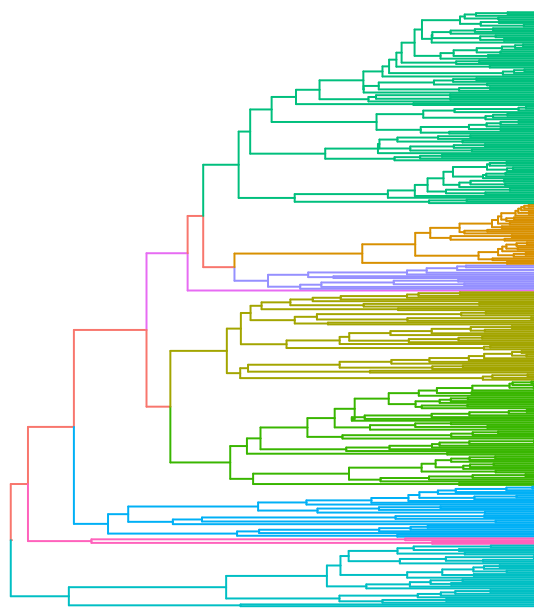
"Every observer who has written upon them has not failed to descant upon their boldness and pugnacity: not only do they attack birds of much larger size than themselves, but it is even asserted that they will tilt at the Eagle if he approaches within the precincts of the nest; nor is man exempt from their assaults." Gould, 1849

They are usually divided in 9 clades: Bees, Brilliants, Colettes, Emeralds, Hermits, Mangoes, Mountain Gems, Patagona, Topazes (fig. 1.10), which differ in their overall appearance and behaviour. It is common for species, even from different genera, to interbreed, which leads to the production of hybrids (Banks and Johnson, 1961; Lynch and Ames, 1970; Graves and Zusi, 1990; Stiles and Cortés-Herrera, 2015).

McGuire



Jetz



Clade — Bees — Coquettes — Hermits — MtGems — Topazes
— Briliants — Emeralds — Mangoes — Patagona

Figure 1.10: Differences between McGuire et al. (2014) and Jetz et al. (2012) phylogenies for hummingbirds. The clades are marked in different colours. The tips are not necessarily in the same order.

dependency. Additionally, studies on hummingbirds date back from a time where we did not have the technical tools to measure them precisely or investigate the structure involved in iridescence (Dorst, 1951; Dürrer, 1977). These studies also often focused on a limited number of species and remained quite descriptive. In particular, they did not investigate possible trait correlations among species. Yet, this is an interesting question for evolutionary biologists as it can reveal possible functions or constraints.

During my PhD, I looked at two facets of iridescence in hummingbirds: the evolutionary drivers at the community level in [Distribution of iridescent colours in hummingbird communities](#) results from the interplay between selection for camouflage and communication (ultimate cause) and the structural basis in [Hummingbird iridescence: an unsuspected structural diversity influences colouration at multiple scales](#) (proximate cause).

Ultimate causes (Gruson et al., 2019c)

My very first study ([Distribution of iridescent colours in hummingbird communities](#) results from the interplay between selection for camouflage and communication) took an unusual approach. I focused on evolutionary questions but used a geographical scale and methods which are more often used in community ecology. I looked at clustering or overdispersion patterns for colour on different patches

Box 4: Comparative analyses

All species emerged from a common ancestor and their shared evolutionary history means they are not independent replicates. For this reason, classical statistical approaches, which rely on the independence of residuals, cannot be used when working at the interspecific level. In all my analyses during this PhD, I took into account the phylogeny to correct for this non-independence (Felsenstein, 1985). Specific methods to achieve this correction are detailed in each article.

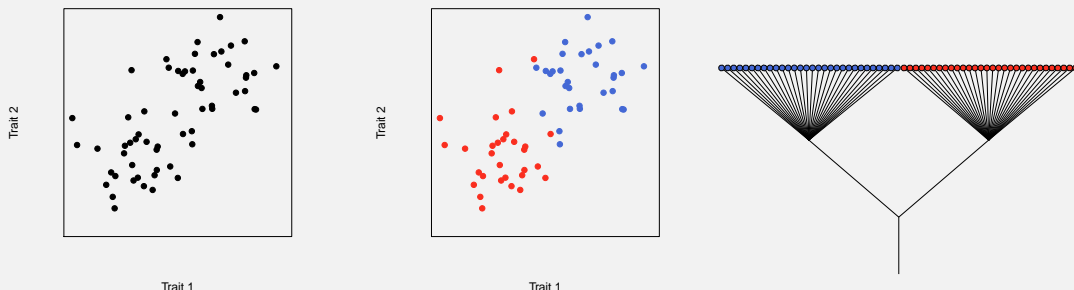


Figure 1.12: The shared evolutionary history of species (represented on a phylogenetic tree) introduces non-independence in the data points, which can create spurious correlations. If we do not pay attention to the phylogeny, as in the first panel, there seems to be a correlation between Trait 1 and Trait 2 but this correlation is entirely due to the evolutionary history of species. This becomes obvious when ones colours the data point (as in the second panel) based on the species position in the phylogeny (third panel). We see that the correlation is entirely driven by the difference between the blue and the red group, which is a single evolutionary event. Figure redrawn from Felsenstein (1985). The plots were done in R by drawing data points from a bivariate normal distribution with different means for the blue and red points.

in 189 communities from Ecuador, tallying 112 hummingbird species. I formulated predictions based on the reproductive character displacement (RCD) theory (Butlin, 1987): co-occurring species are subject to reproductive interference, i.e. individuals from a given species might interbreed with another species, leading to the production of low-fitness hybrids (Gröning and Hochkirch, 2008). This low fitness of hybrids should lead to the selection of adaptations preventing interbreeding, such as divergence in signals involved in species recognition. In particular, I expect divergence on colour in co-occurring species for patches often exposed to conspecifics: facial and ventral patches (Delhey, 2019), leading to a phenotypic overdispersion pattern at the community level (fig. 1.13). On the other hand, dorsal patches are often not displayed to conspecifics and are usually suspected to be more under selection for camouflage (Gomez and Théry, 2007; Delhey, 2019). Because co-occurring hummingbird species share the same predators and vegetation background, it is likely that selection for camouflage will drive them to harbour the same colours, leading to a phenotypic clustering pattern at the community level (fig. 1.13). To evaluate the phenotypic structure, I used the τ_{ST} defined in Baraloto et al. (2012), whose sign indicates phenotypic clustering ($\tau_{ST} > 0$) or overdispersion ($\tau_{ST} < 0$). This character displacement question is especially interesting for iridescent colours because I expect a higher evolvability (Kirschner and Gerhart, 1998) for iridescent colours than non-iridescent ones. Indeed, the same template can produce a large array of different colours with minute changes in the underlying structure.

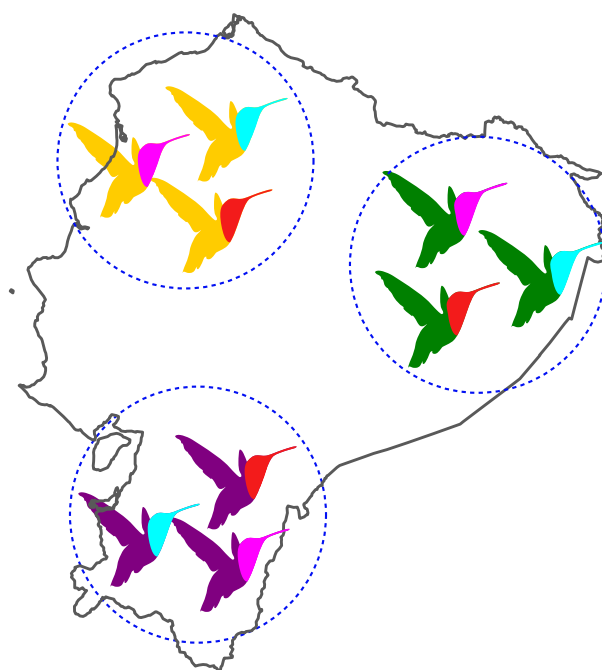


Figure 1.13: Representation of my predictions for the phenotypic structure of colour on the different body patches of hummingbirds at the community level in Ecuador (with unrealistic colours here for explanatory purposes): I predict phenotypic clustering on dorsal patches and phenotypic overdispersion on facial patches. The method used in this article compares intra-communities trait variation to the total (intra and inter-communities) variation, which means both traits with low and high variability can appear as either clustered or overdispersed.

In this study, taking into account the effect of the shared evolutionary of species (which is necessary for the reasons explained in [box 4](#)) was a real challenge. The phylogenetic structure of the community was assessed using Π_{ST} , which works exactly in the same manner as τ_{ST} , with positive values indicating phylogenetic clustering and negative values indicating phylogenetic overdispersion (Hardy and Senterre, [2007](#)). Preliminary results showed a very strong phylogenetic clustering (species living together are more related than expected by chance). This is an issue because it makes it difficult to determine whether the phenotypic clustering we might observe on colour is caused by evolutionary pressures on colour itself or if it is only a by-product of the phylogenetic clustering, which might be caused by evolutionary pressures on other traits linked to the habitat such as temperature tolerance.

The solution came with the publication of an article from de Bello et al. ([2017](#)): they proposed a function to decouple the effect of the phylogeny and evolution from an observed pattern. I thus defined a new value of τ_{ST} based on the decoupled trait values, that I denoted $d\tau_{ST}$. The comparison of τ_{ST} and $d\tau_{ST}$ allowed us to infer whether the observed pattern was mainly due to the phylogeny or to evolution (Table 1 in Gruson et al., [2019c](#)).

I did indeed find phenotypic clustering on the back, coherent with a possible role in camouflage, but an absence of phenotypic structure on most other body patches (as opposed to the phenotypic overdispersion I predicted), excepted for the hue on the belly which was indeed overdispersed. I proposed several hypotheses to explain this partial mismatch with our predictions: why are facial patches and most ventral patches not overdispersed?

- The overdispersion on a single patch (the belly) is enough to enable species recognition. For example, Bitton and Doucet ([2016](#)) used fake trogon models where the colour of a single patch was manipulated compared to the usual phenotype and showed that this was enough to prevent aggression by conspecifics in some cases, even though they were broadcasting species-specific songs at the same time.
- Co-occurring species are still different enough to enable species recognition, even on patches that do not display phenotypic overdispersion. Because the method I used in the article compares variability within communities to variability across communities, and does not look at absolute variability, my study cannot test this hypothesis.
- Species recognition happens on traits other than colour, such as modified tail feathers (Møller and Cuervo, [1998](#)) which are present in many hummingbird species (see for example the white-booted racket-tail *Ocreatus underwoodii* in [fig. 1.15](#)), song (Matyjasik, [2005](#); Luther, [2009](#)), non-vocal noises made by some hummingbird species (Clark and Feo, [2008](#); Clark, Elias, and Prum, [2011](#); Clark, [2011](#)), or behaviour (Simpson and McGraw [2019a](#) showed that, in spite of the similar static appearance, closely related North American bee hummingbird species use different iridescence features during display)

As a conclusion, the original approach taken in this study offers a new argument to support the idea that dorsal patches are indeed involved in camouflage. While other studies often support this by comparing contrasts (Gomez and Théry, 2007; Delhey, 2019) for ventral and dorsal patches, my study looked at the community pattern expected under this hypothesis of selection for camouflage. The major upside of this method is that it does not require heavy hypotheses on the vegetation background used in contrasts computation. On the other hand, it requires a detailed dataset of the local assemblages, which thankfully already existed and was kindly provided by Juan L. Parra, and we miss a possible micro-evolutionary signal (e.g. the same species might look different in two localities depending on the other co-occurring species). This first work also showed me the extraordinary diversity of colours among hummingbird species, and even across body patches from the same individuals, which sparks my curiosity about the underlying structures: are they as diverse?

Proximate causes (Gruson et al., 2019b)

I then tried to answer this question and investigated the proximate causes of iridescence in hummingbirds. Until my work [Hummingbird iridescence: an unsuspected structural diversity influences colouration at multiple scales](#), it was thought that all hummingbird species had the same type of structure producing iridescence (hollow melanin platelets). Yet, Dürrer (1977) describes 4 different types of structures that produce iridescence in birds (illustrated in [fig. 1.14](#)) and Maia, Rubenstein, and Shawkey (2013)'s work on African starlings showed that these 4 types could be present within a single family or even a single genus. Additionally, the structures of only 14 species among the 365 extremely different looking hummingbirds had been investigated (Greenewalt, Brandt, and Friel, 1960; Schmidt and Ruska, 1962; Dürrer, 1977; Shawkey, Morehouse, and Vukusic, 2009; Giraldo, Parra, and Stavenga, 2018; Nordén et al., 2019) and preliminary observations by Doris Gomez few years earlier on 8 species suggested that at least one species (a mango: the purple-throated carib *Eulampis jugularis*) had a different type of melanosomes (solid melanin platelets instead of hollow melanin platelets). I set out to explore more the diversity of multilayer structures within hummingbirds. Because my first study ([Distribution of iridescent colours in hummingbird communities results from the interplay between selection for camouflage and communication](#)) suggested that facial and dorsal patches were under very different selective regimes, I also decided to sample the throat and the back for 36 species, which display very different hues, occupy various habitats and are evenly spread across the phylogeny.

My first Transmission Electronic Microscope (TEM) observations of melanosomes in hummingbird feathers revealed that the structures were way more diverse than previously suspected: in particular, many species did not have hollow melanin platelets but had solid melanin platelets instead. This was not so big a surprise for us as the preliminary observations of Doris Gomez already hinted at this. But my observations also brought more unexpected results:

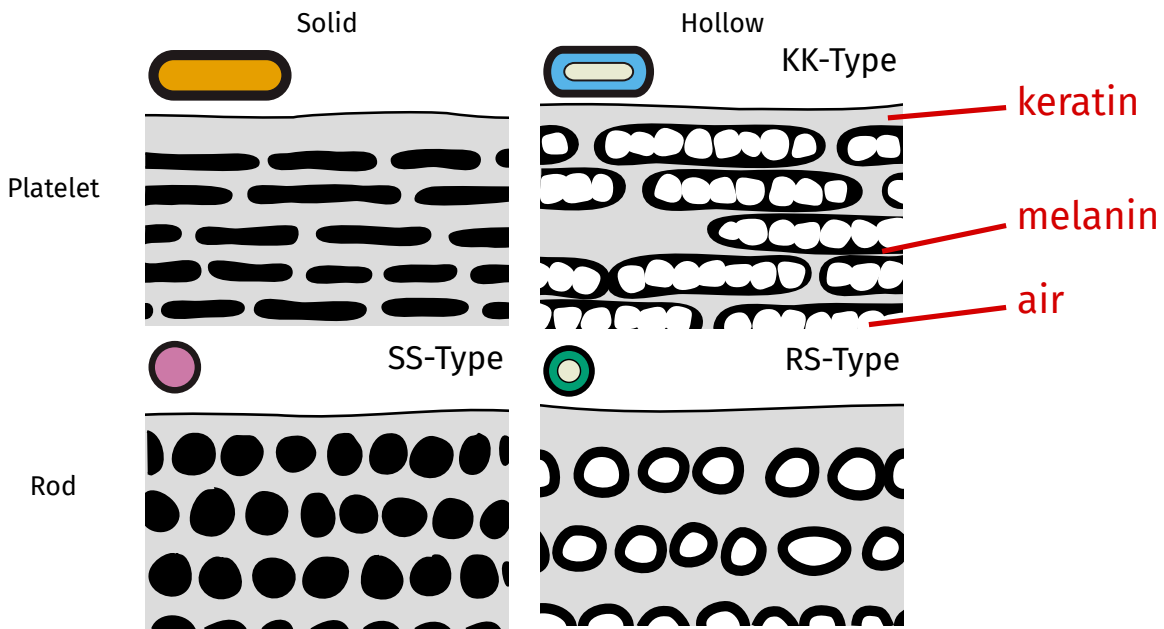


Figure 1.14: Illustration of the 4 types of melanosomes described by Dürrer (1977). Melanosomes are organelles filled with melanin (with sometimes a central air cavity), embedded in a keratin matrix. The 14 hummingbird species investigated until my study ([Hummingbird iridescence: an unsuspected structural diversity influences colouration at multiple scales](#)) had hollow melanin platelets but my study revealed that many species also had solid melanin platelets.

- In some samples, the outermost layer of melanosomes was thinner than the following ones, sometimes even being entirely solid when the rest of the multilayer had hollow melanosomes. This has been observed but not commented in details at the same time by Giraldo, Parra, and Stavenga (2018) in their study on Anna's hummingbird *Calypte anna* and it was already visible in some of Dürrer (1977)'s historic photographs (but he did not comment it either). I named this new multilayer type the "mixed" type.
- The two body patches from a single species sometimes had different melanosome types (see the example of the white-booted racket-tail *Ocreatus underwoodii* in [fig. 1.15](#)). This has not been documented in any other species to our knowledge but until now, most studies only observed the structure of one patch per species as assumed that this was representative of the whole species (Dürrer, 1977).

At some point, I suspected that the different melanosome types (hollow vs solid) corresponded to different stages of development of a single type, in accordance with what Shawkey et al. (2015) found in the wild turkey *Meleagris gallopavo*: melanosomes start as solid rods and their core is degraded through development, leading to the formation of a central air cavity. However, this seems to happen at early stages of feather development and the authors warn that this process might be specific to this species or clade. Additionally, if this were the case for hummingbirds, some of my observations would likely have been inconsistent with the existing literature (Greenewalt, Brandt, and Friel, 1960; Schmidt and Ruska, 1962; Dürrer, 1977; Shawkey, Morehouse, and Vukusic, 2009; Giraldo, Parra, and

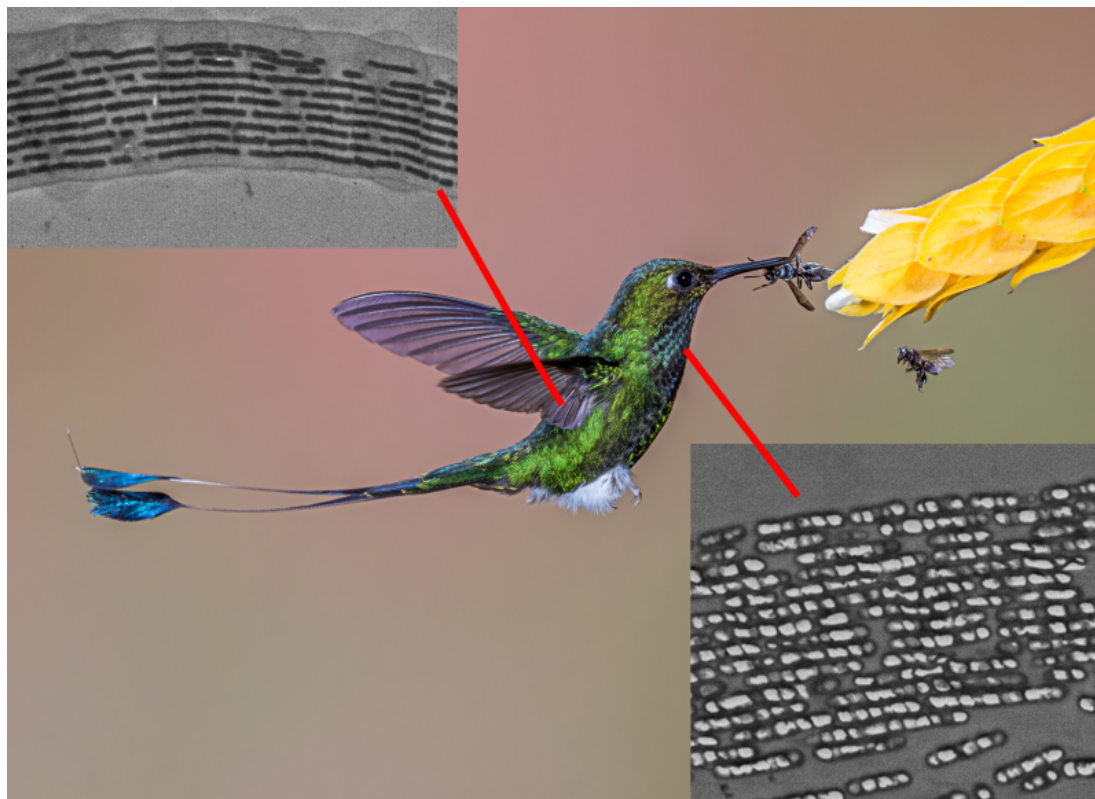


Figure 1.15: The white-booted racket-tail *Ocreatus underwoodii* has two different types of melanosomes depending on the patch location on the body. On the back, the multilayer structures are made of solid melanin platelets while on the throat, they are made of hollow melanin platelets. Overlayed images are Transmission Electron Microscope observations of cross-sections of barbules. Hummingbird picture by Andy Morffew, CC0, <https://pxhere.com/en/photo/383361>.

Stavenga, 2018; Nordén et al., 2019) or the independent preliminary observations from Doris Gomez (on other individuals from the same species). This was not the case, which suggests that solid and hollow melanosomes are indeed two different types.

The next step in this study was to investigate the effect of various structure features on the resulting spectral reflectance. For this, I measured the colour of the different patches that I previously observed in TEM and I computed correlations between colour and structure while taking into account the effect of the phylogeny (as explained in [box 4](#)). But, even though it was a large increase compared to previous studies, my sample size remained low. Additionally, observed correlations, or increase in colour gamut, may be due to evolutionary reasons, or developmental constraints (Eliason and Shawkey, 2012) and not to the physics underlying iridescence (as illustrated in [fig. 1.16](#)). For example, Eliason and Shawkey (2012) showed that the actual colour space occupied by duck feathers is much smaller than the theoretically possible space. To prevent this and increase the sample size, I also tested all correlations in a system where evolution and developmental constraints are absent: computer simulations.

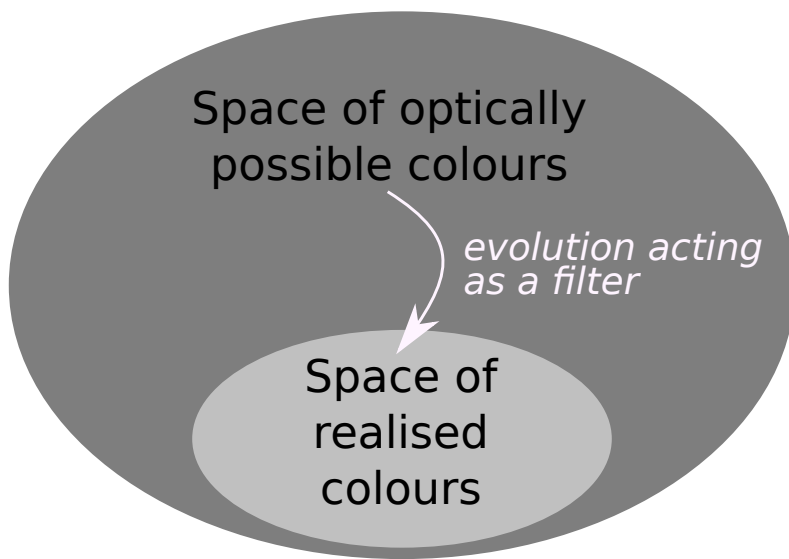


Figure 1.16: Illustration of the role of evolution as a filter limiting the space of realised possibilities from the space of possibilities. This explains why it is not appropriate to study physical processes only through the lens of what happens in living organisms. Many options may be physically possible but weeded out by evolution. Similarly, an observed increase in the space of realised colours (as in Maia, Rubenstein, and Shawkey 2013) does not necessarily reflect an increase in the space of optically possible colours.

I initially suspected that the outermost layer in the new "mixed" type did not have any influence on the resulting reflectance (because it was only one layer out of up to 25), and that the increased melanin content in this layer only had a protective function against damaging UV radiations (melanin pigments absorb more in shorter wavelengths). But simulations showed that, on the contrary, relative absorbance in the UV (S1UV in Montgomerie 2006) did not differ between the mixed and hollow multilayer types while brightness, saturation, hue, and angle dependency of hue did.

In one species, there was a highly unusual structure that I could not explain: the gorget of the chestnut-breasted coronet *Boissonneaua matthewsii* has hollow melanin platelets but also granules of melanin (whose appearance differs a lot from solid melanin platelets), as illustrated in [fig. 1.17](#)



Figure 1.17: TEM observation (left) of the cross-section of iridescent barbules from the gorget of the chestnut-breasted coronet *Boissonneaua matthewsii* (right; picture by Andy Morffew, CC-BY). It is the only species where I have observed hollow melanin platelets intermixed with melanin granules. This may be cause the highly unusual appearance of the gorget in this species. As visible in the photograph, there is intra-feather patterning, with the feather edge looking almost non-iridescent from this angle.

Another striking peculiarity of hummingbird feathers which deserves more detailed investigations is the shape of their barbules: in some species, on some body patches, the barbules have a sickle-like shape (with two part named *speculum* and *velum*), as already described by Dürrer (1977) and as illustrated in [fig. 1.18](#). My initial idea was that the two different multilayers played a role in the resulting spectral reflectance but it seems unlikely as one cannot devise a scenario where light rays can reach the second multilayer (on the *velum*; see [fig. 1.18](#)) and then be reflected in a direction where it could be caught by an observer. It is much more likely that this shape is linked to a better interlocking of adjacent barbules, as reported in other species by Schmidt and Ruska (1962) and Dürrer and Villiger (1970), which could in turn influence the spectral reflectance, feather hydrophobicity or aerodynamics (these hypotheses are not mutually exclusive). I did indeed find curved barbules were linked with more reflective and more directional colours than flat barbules, suggesting a role of selection for colour. However, if the second multilayer does not have any function, it remains unclear why its production has not been counter-selected. There are several (non mutually exclusive) possible explanations that future studies should test: (i) the production of these multilayer has low or no cost for the hummingbirds (discussed in details later). (ii) developmental constraints make it impossible to produce a multilayer structure only on the *speculum* and not the *velum*. Sickle-shaped barbules are indeed a derived form of ancestral, flat, barbules, that have melanosomes along their entire length. It

is possible that there is no way to selectively turn off the production and migration of melanosomes to a specific region of the barbule. But there seems to be some flexibility nevertheless because the two multilayers do not have the same number of layers (the *speculum* always have more layers than the *velum*).

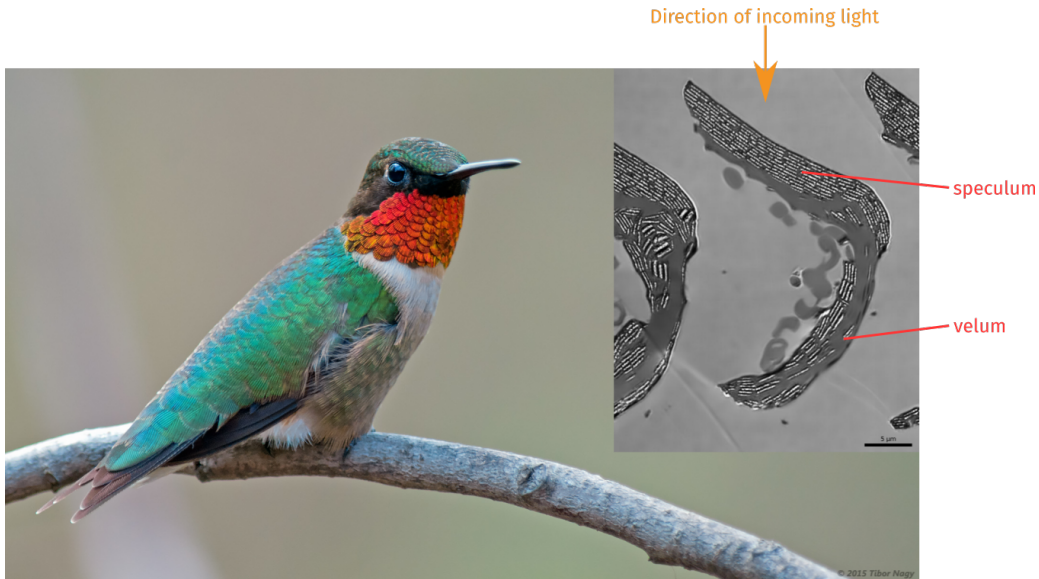


Figure 1.18: Illustration of the shape of the barbules from the orange iridescent gorget of the ruby-throated hummingbird *Archilochus colubris*. It remains unclear if the evolution of this peculiar shape is linked to selection on colour and if so, how it does influence colour. Background image by Tibor Nagy, CC-BY-NC, <https://flic.kr/p/svg5mV>.

Finally, it would be very interesting for future studies on this topic to sample more species and use ancestral state reconstruction to infer the full evolutionary history of multilayer structures in hummingbirds and compute the transition rates from one type to the other, as Maia, Rubenstein, and Shawkey (2013) did for the starlings. Indeed, my limited sampling suggests at least 2 transitions on the back, and 3 on the throat from hollow to solid melanosomes, while Maia, Rubenstein, and Shawkey (2013) found that this transition was highly unlikely in starlings. This difference may be due to the different ecological conditions these two families (starlings and hummingbirds) face or differences in the way multilayer structures are produced, which would make it easier for hummingbirds to go from one type to the other.

1.4 Future directions

Hummingbird predators and visual system

One major issue I encountered at every corner of my PhD is the very poor knowledge of the hummingbirds' ecology. For example, we only have few anecdotal accounts and no systematic study of predation on hummingbirds. This is an issue because camouflage from predators is often a strong evolutionary determinant of the spectral reflectance of species and I needed to specifically test this in [Distribution of iridescent colours in hummingbird communities results from the interplay between selection for camouflage and communication](#). Yet, I could not determine the intensity of this selective pressure nor the visual system of the predators. Some limited information exists in old articles from ornithology journals (the Auk: Miller and Gass [1985](#), the Condor: Stiles [1982](#), the Wilson Journal of Ornithology: Lima [1993](#); Robinson [2003](#), etc.) or in non-English journals (Ornitología Neotropical: Restrepo-Cardona et al. [2018](#); Ayazo, Flórez-Díaz, and González-Charrasquel [2019](#)) but these articles are difficult to come across. It is also likely that many predation observations do not get published because it now falls outside the scope of most journals, as being 'too descriptive'. This issue could be solved by carefully combing through specialized literature, including journals in Spanish and Portuguese and by looking at personal blogs, picture hosting websites (e.g. Flickr), etc. This highlights the importance of modern tools and search engines for scientific literature and the importance of public, collaborative databases, as discussed in the second part of this manuscript.

Similarly, although it has long been known that hummingbirds can see UV (Huth and Burkhardt, [1972](#); Goldsmith, [1980](#)), the exact sensitivity profile of their photoreceptors remains debated. Studies by different groups using different methods find conflicting data. Chen and Goldsmith ([1986](#)) and Herrera et al. ([2008](#)) performed electroretinography (ERG) on eyes from the ruby-throated hummingbird (*Archilocus colubris*) and the green-backed firecrown (*Sephanoides sephaniodes*) respectively, and found results consistent with the vision of an UVS species. On the other hand, Ödeen and Håstad ([2010](#)) used genetic data for the SWS1 opsin gene, which controls the sensitivity of the (U)VS photoreceptor (Ödeen, Hart, and Håstad, [2009](#)) and found sequences suggesting VS vision for 3 hummingbird species from different clades (Hermits: *Phaethornis pretrei*, Briliants: *Heliodoxa rubinoides*, Emeralds: *Hylocharis chrysura*). This suggests either a variability and complex evolutionary history within the group or inadequate methods (Herrera et al. [2008](#) warns that their data could support both VS or UVS vision). In my work, I performed visual modelling as if all hummingbirds species were VS, which is coherent with the most recent and most conclusive literature (Ödeen and Håstad, [2010](#)). Other studies have also shown that this choice likely had quite little influence on the final results (Gomez and Théry, [2007](#); Cain et al., [2019](#)).

Integration of behaviour in iridescence study thanks to hyperspectral photography

My work during this PhD focused on the static aspect of colours. But, as mentioned earlier, iridescent colours depend on the angle of illumination or observation, which means that behaviour can play a huge role in the resulting signal, adding yet another component to colour (fig. 1.19)

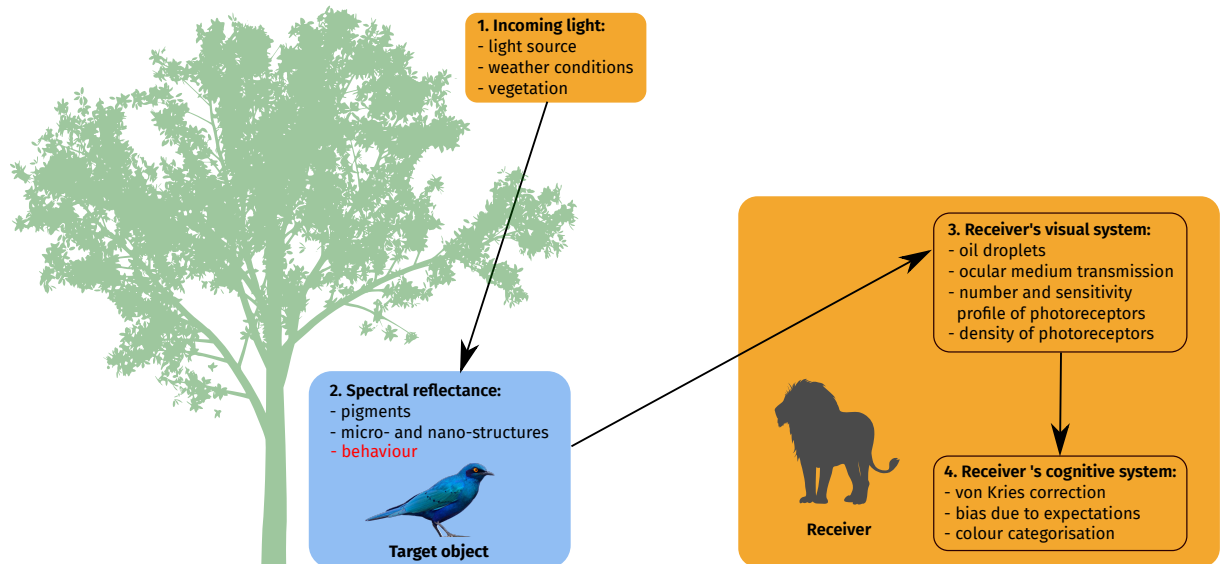


Figure 1.19: Alteration of fig. 1.3 to add the possible role of behaviour in the resulting colour for iridescent colours.

"See it darting through the air almost as quick as thought! - now it is within a yard of your face! - in an instant it is gone! - now it flutters from flower to flower to sip the silver dew - it is now a ruby - now a topaz - now an emerald - now all burnished." Gould, 1849

Some studies have looked at the effect of behaviour in other organisms displaying iridescent colours, such as Schultz and Fincke (2009) on the damselfly *Megaloprepus caerulatus*, Legagneux et al. (2010) on the peacock *Pavo cristatus*, Stavenga et al. (2011a) on Lawes' parotia *Parotia lawesi* or White, Zeil, and Kemp (2015) on the butterfly *Hypolimnas bolina*. But similar studies on hummingbirds have remained scarce until very recently (Hamilton, 1965; Clark, Feo, and Escalante, 2011) and are only now really taking off, with for example the work of Simpson and McGraw on 6 species of North America bee hummingbirds (Simpson and McGraw, 2018b; Simpson and McGraw, 2018a; Simpson and McGraw, 2019a; Simpson and McGraw, 2019b), on which I have published a digest in Evolution (Gruson, 2019), and the ongoing work of Hogan and Stoddard (2018).

This is made possible by the emergence of multi- or hyperspectral photography, with UV-transparent lenses, and free open-source tools to analyse them (Troscianko and Stevens, 2015; van den Berg et al., 2019). While standard cameras mimic human vision and use three types of sensors to catch different component of light (red, green and blue sensors), hyperspectral cameras have many more sensors and can capture the intensity of light in a given scene for many wavelengths, sometimes almost allowing

the complete reconstruction of the reflectance spectrum. This is a much more convenient and efficient measurement method than spectrophotometry and it allows scientists to measure colours directly on the field, while the birds are displaying (Stevens et al., 2007).

Colour pattern analysis

Similarly, many natural objects are not monochromatic but display different colours on different parts. Studying each colour patch separately does not provide a complete picture of the use of colour by an organism. A possible way is to look at the volume occupied by the different patches in the colour space. In [Estimation of colour volumes as concave hypervolumes using alphashapes](#), I explain why the current method to compute colour volume can lead to biased estimates and I propose a more robust method to prevent these biases (illustrated in [fig. 1.20](#)). Briefly, we often need to measure the volume of multidimensional data in ecology and evolution and the choice has historically been to use the convex hull because of its conceptual, computational and mathematical simplicity. But this choice makes a very strong underlying assumption (that the solid in question is convex) and this causes issues in all areas where it is used: functional ecology, palaeontology, biogeography, colour science (detailed in [table 1.3](#)). I propose to use instead a more flexible tool which does not have the same limitations: α -shapes (Edelsbrunner, Kirkpatrick, and Seidel, 1983).

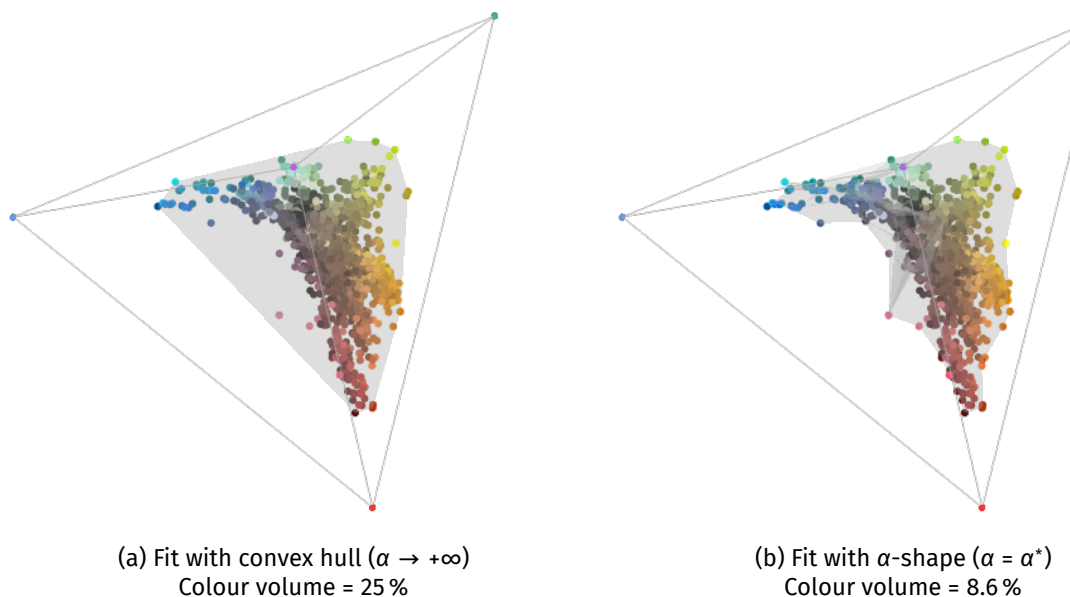


Figure 1.20: Comparison of the fits with (a) a convex hull and (b) an α -shape. Each point is the colour of one patch from birds living in the Nouragues rainforest, in French Guiana, represented in the colour space of an average VS bird species, under ideal illumination. The colour of the points corresponds to the colour of the data points as seen in human colour vision. The colour measurements were performed by Doris Gomez. Figure from [Estimation of colour volumes as concave hypervolumes using alphashapes](#).

Field (use)	Used in	Criticized in
Functional ecology (Functional Richness FRic)	Cornwell, Schwilk, and Ackerly (2006) and Villéger, Mañón, and Mouillot (2008)	Blonder et al. (2014) and Blonder (2018)
Palaeontology (Body mass from skeleton)	Sellers et al. (2012)	
Morphometrics (Morphospace volume)	Kotrc and Knoll (2015)	Kotrc and Knoll (2015) and Nordén et al. (2019)
Biogeography (Home range estimation)	Céspedes et al. (2019)	Galton and Duckham (2006) and Duckham et al. (2008)
Colour Science (Colour volume)		Stoddard and Prum (2011), Langmore et al. (2011), Stoddard (2012), Prum et al. (2012), Spottiswoode and Stevens (2012), Ödeen et al. (2012), Galván et al. (2013), Hanley et al. (2013), Pérez i de Lanuza, Font, and Montde (2013), Renoult, Courtiol, and Schaefer (2013), Stournaras et al. (2013), Burd et al. (2014), Muchhalia, Johnson, and S. D. Smith (2014), Delhey (2015), Doutrelant et al. (2016), Ornelas et al. (2016), Bukovac et al. (2017), Enbody, Lantz, and Karubian (2017), White et al. (2017), Dalrymple et al. (2018), and Merwin, B. T. Smith, and Seeholzer (2018)

Table 1.3: List of fields where convex hulls are used and what for. In all these fields, the use of convex hull has been criticized because it leads to biased estimation. α -shapes could be a solution to these criticisms. The list of publications using convex hulls is only (almost) exhaustive for the colour science row and only contains some examples of publications for the other fields.

But colours can be arranged in complex patterns and simply computing the colour volume does not take this into account. Numerous recent studies propose methods to include the organisation of colours on the body into analyses (Endler, 2012; Le Poul et al., 2014; van Belleghem et al., 2018; Endler, Cole, and Kranz, 2018; van den Berg et al., 2019; Stoddard and Osorio, 2019). This is again made easier by the development of multispectral photography, which makes it possible to image and record spectral reflectance on different body areas at the same time. However, some of these methods remain (almost) unused as they were not bundled with a convenient, user-friendly, and free tool to run them (but see van den Berg et al. 2019 for a good counter-example). Programming such methods can be very difficult and time-consuming and can represent an insurmountable barrier for some research teams. During my thesis, I have contributed to the R package *pavo* (Maia et al., 2019) which offers a user-friendly tool to use Endler (2012)'s method (although I want to highlight that most of the work on this aspect of *pavo* has been spearheaded by Thomas White). I talk more about this in the second part of this manuscript and I detail how we could encourage more the development of such tools.

Other possible evolutionary drivers of iridescent colours

Even at the end of my PhD, it remains unclear to me whether the angle dependency of hue has a function or if it is simply a by-product of selection on hue itself. Pigments in birds can only produce a limited range of colours (reviewed in Hill and McGraw, 2006), and most notably not blue or violet hues, while multilayer structures on the other hand can produce any hue, with very bright and saturated colours, opening up the space of possible colours (Maia, Rubenstein, and Shawkey, 2013). It is then very well possible that angle dependency is a simple consequence of having multilayer structures and that only hue and brightness are selected but not angle dependency (Doucet and Meadows, 2009). My first study [Distribution of iridescent colours in hummingbird communities results from the interplay between selection for camouflage and communication](#) attempted to tackle this question but the strong correlation between hue shift and hue due to the method I used led to a large decrease in statistical power and I was unable to answer this question with certainty. However, the hue angle dependency for colours produced by photonic crystals can be disrupted by introducing disorder in the nanostructures, as described in Welch et al. (2007) and Colomer et al. (2012). This possibility suggests that hue angle dependency is not counter-selected in hummingbirds (but it might be neutral).

Additionally, in this thesis, I mainly discussed the communication function of colours but spectral reflectance (and as a consequence colour) is also involved in various non-communicative functions. These non-communicative functions no doubt also exist for iridescent colours (Doucet and Meadows, 2009) but it remains difficult to precisely assess to which extent they influence iridescence evolution in hummingbirds. For example, it is well-known that iridescence can be simply a by-product of mechanical strengthening in some organisms. The brilliant nacre of many marine molluscs probably does not

have any communication function as it remains hidden from predators and oysters themselves lack visual structures. The sheen of the pearls is a direct consequence of the successive layering around a nucleus (Land, 1972). This effect could potentially be important in hummingbirds whose intricate aerodynamics impose strong mechanical constraints on the wings and feathers (Altshuler, Dudley, and McGuire, 2004).

Hummingbirds are also among the world smallest homeotherms (Lasiewski, 1963; Chai, Chang, and Dudley, 1998), and we know that colour can play an important role in thermoregulation (Roulin, 2014; K. R. Smith et al., 2016). This leads to large-scale macroecological patterns of colours caused by regional variations in temperature and precipitations (Delhey et al., 2019). However, while many studies have looked at physiological adaptations to cope with low temperatures such as torpor (Lasiewski, 1963) or heat production during their hovering flight (Chai, Chang, and Dudley, 1998), I could not find any study that looked at the link between thermal physiology and colour in hummingbirds. If we were to work in this direction, recent studies have highlighted the possibly important role of near-infrared (700 nm to 2500 nm) in thermoregulation (Stuart-Fox, Newton, and Clusella-Trullas, 2017) for both endotherms (birds Medina et al. 2018) and ectotherms (butterflies Munro et al. 2019, lizards K. R. Smith et al. 2016). This however requires an additional set of measurements with a specific spectrometer which is sensitive to longer wavelengths. However, I do not know of any study which looked at near-infrared reflectance in hummingbirds (see Shawkey et al. 2017 for an investigation of near-infrared in sunbirds).

Finally, it remains unclear how costly the production of iridescent colours is. Various teams reported a link between iridescence and body condition either by correlational (Fitzstephens and Getty, 2000; Doucet, 2002; Legagneux et al., 2010; Lim and Li, 2013; Youngblood, 2014; Van Wijk et al., 2016) or experimental studies (McGraw et al., 2002; Hill, Doucet, and Buchholz, 2005; Kemp, Vukusic, and Rutowski, 2006; Meadows, Roudybush, and McGraw, 2012; Pegram et al., 2013; Leclaire et al., 2014). Similarly, the fact that it is used in mate choice (Doucet and Montgomerie, 2003; Dakin and Montgomerie, 2013; Kemp and Rutowski, 2007; Kemp, 2008) suggests a possible role in quality advertising. However all these studies used methods which only captured partial or inaccurate information about iridescence (using for example human vision, or measurements at a fixed angle configuration), which clouds any result about the possible cost of iridescence. Additionally, Maia, Macedo, and Shawkey (2012) suggest that the formation of multilayer structures in the blue-black grassquit *Volatinia jacarina* happens via a passive mechanism, which disputes the idea that the regularity of multilayers is inherently costly.

In the same vein, the link between iridescence and water repellency (hydrophobicity) remains unclear. Early studies presumed that structures responsible for iridescence enhanced hydrophobicity (reviewed in Doucet and Meadows, 2009). However, two years later, a study from Eliason and Shawkey

(2011) on the mallard *Anas platyrhynchos* suggested that iridescent feathers were less hydrophobic (contact angle $\theta_c = 115^\circ$) than non-iridescent ones ($\theta_c = 143.83^\circ$), thereby representing a possible cost of iridescence. But a more recent study showed on the contrary that iridescent feathers were super hydrophobic ($\theta_c = 156^\circ$) in the Nicobar pigeon *Caloenas nicobarica* (Rashid et al., 2018). More studies in other taxa are needed to test this possible link between iridescence and hydrophobicity. This question could be crucial for hummingbirds, whose small size makes very sensitive to extra weight due to soaked feathers (Ortega-Jimenez and Dudley, 2012b) and which have evolved specific behavioural strategies to cope (Ortega-Jimenez and Dudley, 2012a).

But selective pressures are not the only important factors to understand the evolution of iridescent colours, in hummingbirds and in other groups. Species are restricted in their evolution by genetic and developmental constraints. For this reason, it would be extremely valuable to know the genetic bases of iridescence, as well as its developmental pathways, which can have a large impact of the evolution of colour (Maia, Rubenstein, and Shawkey, 2016). Unfortunately, for animals, this remains an active topic of research where much still needs to be uncovered (but see Thayer, Allen, and Patel 2019). One notable discovery in the area is the involvement of the *optix* gene in the blue iridescence of some butterflies (Zhang, Mazo-Vargas, and Reed, 2017). A more recent studies suggests the involvement of a region on the Z sex chromosome in the blue iridescent *Heliconius erato* (Brien et al., 2019). Unfortunately, no similar study has been done in birds yet to my knowledge (I know however that some groups are currently working on this topic in the domestic chicken *Gallus gallus*).

Intraspecific variation

Because of a lack of time, I did not have the opportunity to work much on the intraspecific variation of the spectral reflectance and the underlying structures. Yet, this is an interesting question for evolutionary biologists as variability is the basis on which selection can act. Moreover, intraspecific variation across the species range can hint at the role of local adaptation.

Additionally, I performed preliminary colour measurements on a set of feathers from 20 male purple-throated caribs *Eulampis jugularis*, sampled by Claire Doutrelant on two different islands in the Antilles. Using the method from Gruson et al. (2019a), I was able to produce repeatable measurement, i.e. the accuracy of the measurements was high enough to capture the interindividual variability, even at the intraspecific level. From this, I was planning on exploring different questions:

- is there a correlation between some characteristics of iridescence and morphology or condition?

This would add up to the literature looking at the cost of iridescence, as mentioned in the previous section. A similar study by Legagneux et al. (2012) on 1052 Eurasian teal *Anas crecca* for example found a positive link between wing colour contrast and body size.

- is there a regional variability of iridescence characteristics linked to the local habitat? As explained in this introduction of this thesis, cursory observation via human vision might not be able to detect cryptic polymorphism, as reported for example in the case of a sailfin silverside fish *Telmatherina anthoniae* (Pfaender et al., 2014).
- is there a correspondence between variability at the structure level and at the reflectance level? It is possible that the resulting reflectance is robust to the variation of some structural features.

As I mentioned, a lack of time prevented me to explore this question any further but everything is ready for this project (proof of concept for the methods, biological material and measurement tools). It is likely to happen in the near future, either done by myself, or by someone else (likely a Masters student).

Hummingbirds and sunbirds as a study system to investigate evolutionary convergence

Although it has been suspected that hummingbirds (Trochilidae; Caprimulgiformes) were closely related to swifts even long before the dawn of molecular methods (Wallace, 1895), they share a striking resemblance with a phylogenetically distant family, including 147 species: sunbirds (Nectariniidae; Passeriformes) (Cheke, Mann, and Bonan, 2019). Indeed, birds from both families can use stationary flight, feed on flower nectar and display striking iridescent colours, as illustrated in fig. 1.21. Additionally, in both families, some species display elongated and modified ornamental tail feathers (Evans and Thomas, 1992; Clark, 2010).



Figure 1.21: Lesser double-collared sunbird (*Cinnyris chalybeus*) from Francesco Veronesi, CC-BY-SA and Violet-crowned woodnymph (*Thalurania colombica*) by Sam May, CC-BY.

The two families however present interesting differences which fuel the interest of a comparison: for example while hummingbirds seem to have a VS vision, sunbirds are reported to have a UVS vision (Ödeen and Håstad, 2010). This would be a perfect model to study convergence between two distant taxa:

- How to explain the multiple similarities between the two families? Is the emergence of one trait mechanistically correlated (e.g. stationary flight) to the emergence of the other (e.g. iridescence)? If so, in which order do they emerge?
- Our current knowledge is that sunbird melanosomes are solid melanin platelets (Dürer and Villiger, 1968) but this is again based on a limited number of species. Future studies should investigate whether they actually display an unsuspected structural diversity similar to what I have found out in hummingbirds.
- Do the two families use the same type of structures to produce similar hues or is there an evolutionary convergence pattern where different structures can produce similar spectral reflectances?
- Is the genetic basis of iridescence the same in the two families?

But sunbirds also have interesting differences with hummingbirds. In particular, they use carotenoid pigmentary colours alongside melanin pigmentary and iridescent structural colours (Shawkey et al., 2017). Yet, iridescent colours are often presented as a key evolutionary innovation in the sense that they largely increase the range of possible colours (Maia, Rubenstein, and Shawkey, 2013). Additionally, some carotenoid colours have been shown to be costly to produce for birds (Hill and McGraw, 2006). It would be worthwhile to investigate if carotenoid colours allow sunbirds to produce unique colours, which cannot be produced by iridescent colours. Alternatively, other characteristics of iridescence (hue and brightness angle dependency) may be selected against.

1.5 Semantics: what is iridescence?

While explaining my work to new acquaintances during these 3 years of work, I came to the realisation that some concepts I used extensively are loosely defined and/or of little interest.

First, the distinction structural versus pigmentary colour seems artificial. In both cases, the modification of the reflected light compared to the incoming light comes from the interaction with the electronic structure of the matter. Additionally, it is often very hard to disentangle the pigmentary from the structural component of a given spectral reflectance. Indeed, most structures involved in structural colours are made of pigments (e.g. melanin in the case of hummingbirds, as detailed in [Hummingbird iridescence: an unsuspected structural diversity influences colouration at multiple scales](#)). As a result, reflectance is influenced by both effects in many cases (Vukusic, Sambles, and Lawrence, 2000; Shawkey and Hill, 2005; Shawkey, Morehouse, and Vukusic, 2009; Stavenga, Giraldo, and Leertouwer, 2010; Trzeciak et al., 2012; D'Alba, Kieffer, and Shawkey, 2012; Shawkey and D'Alba, 2017; Taysom, Stuart-Fox, and Cardoso, 2011; McCoy et al., 2019).

Iridescence itself seems poorly defined as a concept. The usual definition and the one that I used in the introduction of the manuscript is: colour which depends on the angle of illumination or observation. Yet, this angle dependency exists even in colours that are usually considered as non-iridescent (Barreira et al., 2016; McCoy et al., 2019). One could be tempted to define iridescence based on the physical mechanism which gives rise to it (interferences or diffraction) but a sufficient level of disorder in these structures can break the angle dependency (Welch et al., 2007; Colomer et al., 2012). Similarly, a definition based on the structures (e.g. presence of a multilayer structure) would be too restrictive as Stavenga et al. (2011b) showed that the spongy structure in the barbs of the common kingfisher (*Alcedo atthis*) were responsible for the blue iridescent colour. An anonymous reviewer of Gruson et al. (2019a) said: “nearly all substances have reflectance that is angular dependent. The only counter examples are perfect Lambertian reflectors. There are also pigment colors with strong angular dependence, certain fuchsins for example. So I would say that iridescence is characterized by a strong angular dependence in a structural color”. This however remains unsatisfactory as it relies on a subjective appreciation (“strong angular dependence”) but I do not have any better definition to propose.

This vagueness does not however prevent us to work on colours in a given group and to develop specific methods to measure and analyse these colours, no matter the exact terminology we use. For example, in Gruson et al. (2019a), I added a specific paragraph to adapt the method I proposed to iridescent colours which also have a strong pigmentary component (Appendix C in Gruson et al., 2019a).

1.6 Conclusion

In spite of its abundance in nature and the many questions it raises in terms of evolution, some facets of iridescence have largely remained understudied until now. In this thesis, I explored iridescence focusing on hummingbirds' iridescent colours and using original methods. I used a strongly interdisciplinary approach, combining evolution and physics to make both methodological and scientific contributions. The originality of my work compared to many other studies on iridescence is its large taxonomic scale, which allowed me to use methods from community ecology to try and understand the macro-ecological patterns of iridescence in hummingbirds. Because of this large taxonomic scale, I was also able to describe an unsuspected diversity in the structures producing iridescence in hummingbirds. I highlighted possible evolutionary drivers to this diversity but some structures are so unusual they will probably require more focused studies (at the species-specific level this time). However, the impact of my contributions is not limited to hummingbirds or even to colour science. The new standard method I proposed to measure iridescence can be applied to a huge range of organisms, and will hopefully prove useful to many teams with limited equipment and physical knowledge. Similarly, my work on the colour analysis R package *pavo* (discussed hereafter) provides an easy way to work on colour, without the need for an advanced theoretical knowledge of colour science or programming skills. Additionally, even though I focused the discussion on my area of expertise (the study of colour), my work on convex hulls and α -shapes can provide a solution to issues encountered in other fields and I have already started discussing with community and functional ecologists to see if they could use it in their own research. In spite of this, much remains to be done. If my work benefits from the large taxonomic sampling, it also suffers from the drawbacks common to all studies of the sort: the data collection step took an enormous amount of time and I had to use (sometimes crude) automated tools and do many simplifying hypotheses to analyse the resulting data. This prevented me from exploring some questions (such as the role of behaviour, or the developmental pathways) but I know other research groups are already tackling these questions and I look forward to more discoveries about iridescence in nature.

References

- Altshuler, D. L., Dudley, R., and McGuire, J. A. (2004). "Resolution of a paradox: Hummingbird flight at high elevation does not come without a cost". *Proceedings of the National Academy of Sciences* 101.51, pp. 17731–17736. <https://doi.org/10.1073/pnas.0405260101>. pmid: 15598748 (cit. on p. 41).
- Arikawa, K., Wakakuwa, M., Qiu, X., Kurasawa, M., and Stavenga, D. G. (2005). "Sexual dimorphism of short-wavelength photoreceptors in the small white butterfly, *Pieris rapae crucivora*". *Journal of Neuroscience* 25.25, pp. 5935–5942. <https://doi.org/10.1523/JNEUROSCI.1364-05.2005>. pmid: 15976082 (cit. on p. 13).
- Armenta, J. K., Dunn, P. O., and Whittingham, L. A. (2008). "Quantifying avian sexual dichromatism: a comparison of methods". *Journal of Experimental Biology* 211.15, pp. 2423–2430. <https://doi.org/10.1242/jeb.013094>. pmid: 18626076 (cit. on p. 14).
- Ayazo, R. D., Flórez-Díaz, V. L., and González-Charrasquel, C. (2019). "A rufous-tailed hummingbird (*Amazilia tzacatl*) caught in a spider web of *Eriophora fuliginea* (Araneae: Araneidae)". *Ornitología Neotropical* 30.0, pp. 1–3 (cit. on p. 36).
- Backhaus, W. (1991). "Color opponent coding in the visual system of the honeybee". *Vision Research* 31.7, pp. 1381–1397. [https://doi.org/10.1016/0042-6989\(91\)90059-E](https://doi.org/10.1016/0042-6989(91)90059-E) (cit. on p. 13).
- Banks, R. C. and Johnson, N. K. (1961). "A review of North American hybrid hummingbirds". *The Condor* 63.1, pp. 3–28. <https://doi.org/10.2307/1365419> (cit. on p. 25).
- Baraloto, C., Hardy, O. J., Paine, C. E. T., Dexter, K. G., Cruaud, C., Dunning, L. T., Gonzalez, M.-A., Molino, J.-F., Sabatier, D., Savolainen, V., and Chave, J. (2012). "Using functional traits and phylogenetic trees to examine the assembly of tropical tree communities". *Journal of Ecology* 100.3, pp. 690–701. <https://doi.org/10.1111/j.1365-2745.2012.01966.x> (cit. on p. 28).
- Barreira, A. S., García, N. C., Lougheed, S. C., and Tubaro, P. L. (2016). "Viewing geometry affects sexual dichromatism and conspicuousness of noniridescent plumage of Swallow Tanagers (*Tersina viridis*)". *The Auk* 133.3, pp. 530–543. <https://doi.org/10.1642/AUK-15-170.1> (cit. on p. 45).
- Bennett, A. T. D., Cuthill, I. C., and Norris, K. J. (1994). "Sexual selection and the mismeasure of color". *The American Naturalist* 144.5, pp. 848–860. <https://doi.org/10.1086/285711> (cit. on p. 13).
- Bitton, P.-P. and Doucet, S. M. (2016). "Sympatric black-headed and elegant trogons focus on different plumage characteristics for species recognition". *Animal Behaviour* 116, pp. 213–221. <https://doi.org/10.1016/j.anbehav.2016.03.035> (cit. on p. 29).
- Blonder, B. (2018). "Hypervolume concepts in niche- and trait-based ecology". *Ecography* 41.9, pp. 1441–1455. <https://doi.org/10.1111/ecog.03187> (cit. on p. 39).

- Blonder, B., Lamanna, C., Violle, C., and Enquist, B. J. (2014). "The n-dimensional hypervolume". *Global Ecology and Biogeography* 23.5, pp. 595–609. <https://doi.org/10.1111/geb.12146> (cit. on p. 39).
- Boghossian, P. A. and Velleman, J. D. (1989). "Colour as a secondary quality". *Mind* 98.389, pp. 81–103. <https://doi.org/10.1093/mind/XCVIII.389.81> (cit. on p. 13).
- Brien, M. N., Enciso-Romero, J., Parnell, A. J., Salazar, P. A., Morochz, C., Chalá, D., Bainbridge, H. E., Zinn, T., Curran, E. V., and Nadeau, N. J. (2019). "Phenotypic variation in *Heliconius erato* crosses shows that iridescent structural colour is sex-linked and controlled by multiple genes". *Interface Focus* 9.1, p. 20180047. <https://doi.org/10.1098/rsfs.2018.0047> (cit. on p. 42).
- Brink, D. J., van der Berg, N. G., and Botha, A. J. (2002). "Iridescent colors on seashells: an optical and structural investigation of *Helcion pruinosus*". *Applied Optics* 41.4, pp. 717–722. <https://doi.org/10.1364/AO.41.000717> (cit. on p. 18).
- Bukovac, Z., Shrestha, M., Garcia, J. E., Burd, M., Dorin, A., and Dyer, A. G. (2017). "Why background colour matters to bees and flowers". *Journal of Comparative Physiology A* 203.5, pp. 369–380. <https://doi.org/10.1007/s00359-017-1175-7> (cit. on p. 39).
- Burd, M., Stayton, C. T., Shrestha, M., and Dyer, A. G. (2014). "Distinctive convergence in Australian floral colours seen through the eyes of Australian birds". *Proc. R. Soc. B* 281.1781, p. 20132862. <https://doi.org/10.1098/rspb.2013.2862>. pmid: 24573847 (cit. on p. 39).
- Butlin, R. (1987). "Speciation by reinforcement". *Trends in Ecology & Evolution* 2.1, pp. 8–13. [https://doi.org/10.1016/0169-5347\(87\)90193-5](https://doi.org/10.1016/0169-5347(87)90193-5) (cit. on p. 28).
- Cain, K. E., Hall, M. L., Medina, I., Leitao, A. V., Delhey, K., Brouwer, L., Peters, A., Pruett-Jones, S., Webster, M. S., Langmore, N. E., and Mulder, R. A. (2019). "Conspicuous plumage does not increase predation risk: a continent-wide test using model songbirds". *The American Naturalist* 193.3, pp. 359–372. <https://doi.org/10.1086/701632> (cit. on p. 36).
- Caro, T. (2017). "Wallace on coloration: contemporary perspective and unresolved insights". *Trends in Ecology & Evolution* 32.1, pp. 23–30. <https://doi.org/10.1016/j.tree.2016.10.003> (cit. on p. 12).
- Caves, E. M., Green, P. A., Zipple, M. N., Peters, S., Johnsen, S., and Nowicki, S. (2018). "Categorical perception of colour signals in a songbird". *Nature* 560.7718, pp. 365–367. <https://doi.org/10.1038/s41586-018-0377-7> (cit. on p. 14).
- Céspedes, L. N., Pavan, L. I., Hazlehurst, J. A., and Jankowski, J. E. (2019). "The behavior and diet of the Shining Sunbeam (*Aglaeactis cupripennis*): A territorial high-elevation hummingbird". *The Wilson Journal of Ornithology* 131.1, pp. 24–34. <https://doi.org/10.1676/18-79> (cit. on p. 39).
- Chai, P., Chang, A. C., and Dudley, R. (1998). "Flight thermogenesis and energy conservation in hovering hummingbirds". *Journal of Experimental Biology* 201.7, pp. 963–968. pmid: 9487101 (cit. on p. 41).

- Cheke, R., Mann, C., and Bonan, A. (2019). "Sunbirds (Nectariniidae)". In: *Handbook of the Birds of the World Alive*. Ed. by del Hoyo, J., Elliott, A., Sargatal, J., Christie, D. A., and de Juana, E. Lynx Edicions. Barcelona (cit. on p. 43).
- Chen, D.-M. and Goldsmith, T. H. (1986). "Four spectral classes of cone in the retinas of birds". *Journal of Comparative Physiology A* 159.4, pp. 473–479. <https://doi.org/10.1007/BF00604167> (cit. on p. 36).
- Clark, C. J. (2010). "The evolution of tail shape in hummingbirds". *The Auk* 127.1, pp. 44–56. <https://doi.org/10.1525/auk.2009.09073> (cit. on p. 43).
- (2011). "Wing, tail, and vocal contributions to the complex acoustic signals of courting Calliope hummingbirds". *Current Zoology* 57.2, pp. 187–196. <https://doi.org/10.1093/czoolo/57.2.187> (cit. on p. 29).
- Clark, C. J., Elias, D. O., and Prum, R. O. (2011). "Aeroelastic flutter produces hummingbird feather songs". *Science* 333.6048, pp. 1430–1433. <https://doi.org/10.1126/science.1205222>. pmid: 21903810 (cit. on p. 29).
- Clark, C. J. and Feo, T. J. (2008). "The Anna's hummingbird chirps with its tail: a new mechanism of sonation in birds". *Proceedings of the Royal Society of London B: Biological Sciences* 275.1637, pp. 955–962. <https://doi.org/10.1098/rspb.2007.1619>. pmid: 18230592 (cit. on p. 29).
- Clark, C. J., Feo, T. J., and Escalante, I. (2011). "Courtship displays and natural history of scintillant (*Selasphorus scintilla*) and volcano (*S. flammula*) hummingbirds". *The Wilson Journal of Ornithology* 123.2, pp. 218–228. <https://doi.org/10.1676/10-076.1> (cit. on pp. 23, 37).
- Colomer, J.-F., Simonis, P., Bay, A., Cloetens, P., Suhonen, H., Rassart, M., Vandenbem, C., and Vigneron, J. P. (2012). "Photonic polycrystal in the greenish-white scales of the African longhorn beetle *Prosopocera lactator* (Cerambycidae)". *Physical Review E* 85.1, p. 011907. <https://doi.org/10.1103/PhysRevE.85.011907> (cit. on pp. 40, 45).
- Cornwell, W. K., Schwilk, D. W., and Ackerly, D. D. (2006). "A trait-based test for habitat filtering: convex hull volume". *Ecology* 87.6, pp. 1465–1471. [https://doi.org/10.1890/0012-9658\(2006\)87\[1465:ATTFHF\]2.0.CO;2](https://doi.org/10.1890/0012-9658(2006)87[1465:ATTFHF]2.0.CO;2) (cit. on p. 39).
- Cuthill, I. C., Allen, W. L., Arbuckle, K., Caspers, B., Chaplin, G., Hauber, M. E., Hill, G. E., Jablonski, N. G., Jiggins, C. D., Kelber, A., Mappes, J., Marshall, J., Merrill, R., Osorio, D. C., Prum, R., Roberts, N. W., Roulin, A., Rowland, H. M., Sherratt, T. N., Skelhorn, J., Speed, M. P., Stevens, M., Stoddard, M. C., Stuart-Fox, D., Talas, L., Tibbetts, E., and Caro, T. (2017). "The biology of color". *Science* 357.6350, eaan0221. <https://doi.org/10.1126/science.aan0221>. pmid: 28774901 (cit. on p. 12).
- D'Alba, L., Kieffer, L., and Shawkey, M. D. (2012). "Relative contributions of pigments and biophotonic nanostructures to natural color production: a case study in budgerigar (*Melopsittacus undulatus*)

- feathers". *Journal of Experimental Biology* 215.8, pp. 1272–1277. <https://doi.org/10.1242/jeb.064907>. pmid: 22442364 (cit. on p. 44).
- D'Alba, L. and Shawkey, M. D. (2018). "Melanosomes: Biogenesis, Properties, and Evolution of an Ancient Organelle". *Physiological Reviews* 99.1, pp. 1–19. <https://doi.org/10.1152/physrev.00059.2017> (cit. on p. 18).
- Dakin, R. and Montgomerie, R. (2013). "Eye for an eyespot: how iridescent plumage ocelli influence peacock mating success". *Behavioral Ecology* 24.5, pp. 1048–1057. <https://doi.org/10.1093/beheco/art045> (cit. on pp. 20, 21, 41).
- Dalrymple, R. L., Flores, Moreno, H., Kemp, D. J., White, T. E., Laffan, S. W., Hemmings, F. A., Hitchcock, T. D., and Moles, A. T. (2018). "Abiotic and biotic predictors of macroecological patterns in bird and butterfly coloration". *Ecological Monographs* 88.2, pp. 204–224. <https://doi.org/10.1002/ecm.1287> (cit. on p. 39).
- Darwin, C. (1859). *On the origin of species by means of natural selection, or the preservation of favoured races in the struggle for life*. London: John Murray (cit. on p. 12).
- (1872). *The descent of man, and selection in relation to sex*. Vol. 2. London: John Murray (cit. on p. 12).
- De Bello, F., Šmilauer, P., Diniz-Filho, J. A. F., Carmona, C. P., Lososová, Z., Herben, T., and Götzenberger, L. (2017). "Decoupling phylogenetic and functional diversity to reveal hidden signals in community assembly". *Methods in Ecology and Evolution* 8.10, pp. 1200–1211. <https://doi.org/10.1111/2041-210X.12735> (cit. on p. 29).
- Delhey, K. (2015). "The colour of an avifauna: A quantitative analysis of the colour of Australian birds". *Scientific Reports* 5, p. 18514. <https://doi.org/10.1038/srep18514> (cit. on p. 39).
- (2019). "Revealing the colourful side of birds: Spatial distribution of conspicuous plumage colours on the body of Australian birds". *Journal of Avian Biology*. <https://doi.org/10.1111/jav.02222> (cit. on pp. 28, 30).
- Delhey, K., Dale, J., Valcu, M., and Kempenaers, B. (2019). "Reconciling ecogeographical rules: rainfall and temperature predict global colour variation in the largest bird radiation". *Ecology Letters* 22.4, pp. 726–736. <https://doi.org/10.1111/ele.13233> (cit. on p. 41).
- Dorst, J. (1951). "Recherches sur la structure des plumes des trochilidés". OCLC: 14220401. Paris: Université de Paris. 260 pp. (cit. on p. 26).
- Doucet, S. M. (2002). "Structural plumage coloration, male body size, and condition in the blue-black grassquit". *The Condor* 104.1, pp. 30–38. [https://doi.org/10.1650/0010-5422\(2002\)104\[0030:SPCMBS\]2.0.CO;2](https://doi.org/10.1650/0010-5422(2002)104[0030:SPCMBS]2.0.CO;2) (cit. on p. 41).
- Doucet, S. M. and Hill, G. E. (2009). "Do museum specimens accurately represent wild birds? A case study of carotenoid, melanin, and structural colours in long-tailed manakins *Chiroxiphia linearis*".

- Journal of Avian Biology* 40.2, pp. 146–156. <https://doi.org/10.1111/j.1600-048X.2009.03763.x> (cit. on p. 24).
- Doucet, S. M. and Meadows, M. G. (2009). “Iridescence: a functional perspective”. *Journal of The Royal Society Interface* 6 (Suppl 2), S115–S132. <https://doi.org/10.1098/rsif.2008.0395.focus>. pmid: 19336344 (cit. on pp. 18, 40, 41).
- Doucet, S. M. and Montgomerie, R. (2003). “Multiple sexual ornaments in satin bowerbirds: ultraviolet plumage and bowsers signal different aspects of male quality”. *Behavioral Ecology* 14.4, pp. 503–509. <https://doi.org/10.1093/beheco/arg035> (cit. on p. 41).
- Douglas, J. M., Cronin, T. W., Chiou, T.-H., and Dominy, N. J. (2007). “Light habitats and the role of polarized iridescence in the sensory ecology of neotropical nymphalid butterflies (Lepidoptera: Nymphalidae)”. *Journal of Experimental Biology* 210.5, pp. 788–799. <https://doi.org/10.1242/jeb.02713>. pmid: 17297139 (cit. on p. 14).
- Doutrelant, C., Paquet, M., Renoult, J. P., Grégoire, A., Crochet, P.-A., and Covas, R. (2016). “Worldwide patterns of bird colouration on islands”. *Ecology Letters* 19.5, pp. 537–545. <https://doi.org/10.1111/ele.12588> (cit. on p. 39).
- Duckham, M., Kulik, L., Worboys, M., and Galton, A. (2008). “Efficient generation of simple polygons for characterizing the shape of a set of points in the plane”. *Pattern Recognition* 41.10, pp. 3224–3236. <https://doi.org/10.1016/j.patcog.2008.03.023> (cit. on p. 39).
- Dürrer, H. (1977). “Schillerfarben der Vogelfeder als Evolutionsproblem”. Medizinischen Fakultät der Universität Basel (cit. on pp. 18, 26, 30, 31, 34).
- Dürrer, H. and Villiger, W. (1970). “Schillerradien des Goldkuckucks (*Chrysococcyx cupreus* (Shaw)) im Elektronenmikroskop”. *Zeitschrift für Zellforschung und Mikroskopische Anatomie* 109.3, pp. 407–413. <https://doi.org/10.1007/BF02226912> (cit. on p. 34).
- Dürrer, H. and Villiger, W. (1968). “Schillerfarben der Nektarvögel (Nectariniidae)”. *Rev Suisse Zool* 69.38, pp. 801–814 (cit. on p. 44).
- Eaton, M. D. (2005). “Human vision fails to distinguish widespread sexual dichromatism among sexually “monochromatic” birds”. *Proceedings of the National Academy of Sciences* 102.31, pp. 10942–10946. <https://doi.org/10.1073/pnas.0501891102>. pmid: 16033870 (cit. on p. 14).
- Edelsbrunner, H., Kirkpatrick, D. G., and Seidel, R. (1983). “On the shape of a set of points in the plane”. *IEEE Transactions on Information Theory* 29.4, pp. 551–559. <https://doi.org/10.1109/TIT.1983.1056714> (cit. on p. 38).
- Eliason, C. M. and Shawkey, M. D. (2011). “Decreased hydrophobicity of iridescent feathers: a potential cost of shiny plumage”. *The Journal of Experimental Biology* 214 (Pt 13), pp. 2157–2163. <https://doi.org/10.1242/jeb.055822>. pmid: 21653809 (cit. on p. 41).

- Eliason, C. M. and Shawkey, M. D. (2012). "A photonic heterostructure produces diverse iridescent colours in duck wing patches". *Journal of The Royal Society Interface* 9.74, pp. 2279–2289. <https://doi.org/10.1098/rsif.2012.0118>. pmid: 22491981 (cit. on p. 33).
- Eliason, C. M., Shawkey, M. D., and Clarke, J. A. (2016). "Evolutionary shifts in the melanin-based color system of birds". *Evolution* 70.2, pp. 445–454. <https://doi.org/10.1111/evo.12855>. pmid: 26044706 (cit. on p. 39).
- Enbody, E. D., Lantz, S. M., and Karubian, J. (2017). "Production of plumage ornaments among males and females of two closely related tropical passerine bird species". *Ecology and Evolution* 7.11, pp. 4024–4034. <https://doi.org/10.1002/ece3.3000> (cit. on p. 39).
- Endler, J. A. (1978). "A predator's view of animal color patterns". In: *Evolutionary Biology*. Ed. by Hecht, M. K., Steere, W. C., and Wallace, B. *Evolutionary Biology*. Boston, MA: Springer US, pp. 319–364. ISBN: 978-1-4615-6956-5. https://doi.org/10.1007/978-1-4615-6956-5_5 (cit. on p. 13).
- (1993). "The color of light in forests and its implications". *Ecological Monographs* 63.1, pp. 1–27. <https://doi.org/10.2307/2937121> (cit. on p. 14).
 - (2012). "A framework for analysing colour pattern geometry: adjacent colours". *Biological Journal of the Linnean Society* 107.2, pp. 233–253. <https://doi.org/10.1111/j.1095-8312.2012.01937.x> (cit. on p. 40).
- Endler, J. A., Cole, G. L., and Kranz, A. M. (2018). "Boundary strength analysis: Combining colour pattern geometry and coloured patch visual properties for use in predicting behaviour and fitness". *Methods in Ecology and Evolution* 9.12. Ed. by Blomberg, S., pp. 2334–2348. <https://doi.org/10.1111/2041-210X.13073> (cit. on p. 40).
- Endler, J. A. and Thery, M. (1996). "Interacting effects of lek placement, display behavior, ambient light, and color patterns in three neotropical forest-dwelling birds". *The American Naturalist* 148.3, pp. 421–452. <https://doi.org/10.1086/285934>. pmid: 454 (cit. on p. 14).
- Evans, M. R. and Thomas, A. L. R. (1992). "The aerodynamic and mechanical effects of elongated tails in the scarlet-tufted malachite sunbird: measuring the cost of a handicap". *Animal Behaviour* 43.2, pp. 337–347. [https://doi.org/10.1016/S0003-3472\(05\)80229-5](https://doi.org/10.1016/S0003-3472(05)80229-5) (cit. on p. 43).
- Fabricant, S. A., Kemp, D. J., Krajiček, J., Bosáková, Z., and Herberstein, M. E. (2013). "Mechanisms of color production in a highly variable shield-back stinkbug, *Tectocoris diophthalmus* (Heteroptera: Scutelleridae), and why it matters". *PLOS ONE* 8.5, e64082. <https://doi.org/10.1371/journal.pone.0064082>. pmid: 23675520 (cit. on pp. 18, 20).
- Felsenstein, J. (1985). "Phylogenies and the comparative method". *The American Naturalist* 125.1, pp. 1–15. <https://doi.org/10.1086/284325> (cit. on p. 27).

- Fitzstephens, D. M. and Getty, T. (2000). "Colour, fat and social status in male damselflies, *Calopteryx maculata*". *Animal Behaviour* 60.6, pp. 851–855. <https://doi.org/10.1006/anbe.2000.1548> (cit. on p. 41).
- Gadow, D. H. (1882). "On the colour of feathers as affected by their structure." *Proceedings of the Zoological Society of London* 50.3, pp. 409–422. <https://doi.org/10.1111/j.1096-3642.1882.tb02748.x> (cit. on p. 14).
- Galton, A. and Duckham, M. (2006). "What Is the region occupied by a set of points?" In: *Geographic Information Science*. Ed. by Raubal, M., Miller, H. J., Frank, A. U., and Goodchild, M. F. Lecture Notes in Computer Science. Springer Berlin Heidelberg, pp. 81–98. ISBN: 978-3-540-44528-9 (cit. on p. 39).
- Galván, I., Negro, J. J., Rodríguez, A., and Carrascal, L. M. (2013). "On showy dwarfs and sober giants: Body Size as a Constraint for the Evolution of Bird Plumage Colouration". *Acta Ornithologica* 48.1, pp. 65–80. <https://doi.org/10.3161/000164513X670007> (cit. on p. 39).
- Giraldo, M. A., Parra, J. L., and Stavenga, D. G. (2018). "Iridescent colouration of male Anna's hummingbird (*Calypte anna*) caused by multilayered barbules". *Journal of Comparative Physiology A* 204.12, pp. 965–975. <https://doi.org/10.1007/s00359-018-1295-8> (cit. on pp. 20, 30, 31).
- Glover, B. J. and Whitney, H. M. (2010). "Structural colour and iridescence in plants: the poorly studied relations of pigment colour". *Annals of Botany* 105.4, pp. 505–511. <https://doi.org/10.1093/aob/mcq007> (cit. on p. 18).
- Goldsmith, T. H. (1980). "Hummingbirds see near ultraviolet light". *Science* 207.4432, pp. 786–788. <https://doi.org/10.1126/science.7352290>. pmid: 7352290 (cit. on p. 36).
- Gomez, D. and Théry, M. (2004). "Influence of ambient light on the evolution of colour signals: comparative analysis of a Neotropical rainforest bird community". *Ecology Letters* 7.4, pp. 279–284. <https://doi.org/10.1111/j.1461-0248.2004.00584.x> (cit. on p. 14).
- (2007). "Simultaneous crypsis and conspicuousness in color patterns: comparative analysis of a neotropical rainforest bird community". *The American Naturalist* 169.s1, S42–S61. <https://doi.org/10.1086/510138> (cit. on pp. 28, 30, 36).
- Gould, J. (1849). *A monograph of the Trochilidae, or family of humming-birds*. 5 vols. London: Printed by Taylor and Francis. 314 pp. <https://doi.org/10.5962/bhl.title.51056> (cit. on pp. 18, 23–25, 37).
- Graves, G. R. and Zusi, R. L. (1990). "An intergeneric hybrid hummingbird (*Heliodoxa leadbeateri* × *Heliangelus amethysticollis*) from Northern Colombia". *The Condor* 92.3, pp. 754–760. <https://doi.org/10.2307/1368695> (cit. on p. 25).
- Greenewalt, C. H., Brandt, W., and Friel, D. D. (1960). "Iridescent colors of hummingbird feathers". *Journal of the Optical Society of America* 50.10, pp. 1005–1013. <https://doi.org/10.1364/JOSA.50.001005> (cit. on pp. 30, 31).

- Gröning, J. and Hochkirch, A. (2008). "Reproductive interference between animal species". *The Quarterly Review of Biology* 83.3, pp. 257–282. <https://doi.org/10.1086/590510> (cit. on p. 28).
- Gruson, H. (2019). "Digest: Disentangling plumage and behavior contributions to iridescent signals". *Evolution* 73.3, pp. 623–625. <https://doi.org/10.1111/evo.13685> (cit. on p. 37).
- Gruson, H., Andraud, C., Daney de Marcillac, W., Berthier, S., Elias, M., and Gomez, D. (2018). "Supplementary material from "Quantitative characterization of iridescent colours in biological studies: a novel method using optical theory"". <https://doi.org/10.6084/m9.figshare.c.4275911.v2> (cit. on pp. 18, 21).
- (2019a). "Quantitative characterization of iridescent colours in biological studies: a novel method using optical theory". *Interface Focus* 9.1, p. 20180049. <https://doi.org/10.1098/rsfs.2018.0049> (cit. on pp. 16, 18, 21, 22, 24, 42, 45).
- Gruson, H., Elias, M., Andraud, C., Djediat, C., Berthier, S., Doutrelant, C., and Gomez, D. (2019b). "Hummingbird iridescence: an unsuspected structural diversity influences colouration at multiple scales". *bioRxiv*. in revision, p. 699744. <https://doi.org/10.1101/699744> (cit. on p. 30).
- Gruson, H., Elias, M., Parra, J. L., Andraud, C., Berthier, S., Doutrelant, C., and Gomez, D. (2019c). "Distribution of iridescent colours in hummingbird communities results from the interplay between selection for camouflage and communication". *bioRxiv*. under review at PCI EvolBiol, p. 586362. <https://doi.org/10.1101/586362> (cit. on pp. 26, 29).
- Gur, D., Leshem, B., Oron, D., Weiner, S., and Addadi, L. (2014). "The structural basis for enhanced silver reflectance in koi fish scale and skin". *Journal of the American Chemical Society* 136.49, pp. 17236–17242. <https://doi.org/10.1021/ja509340c> (cit. on p. 18).
- Gur, D., Palmer, B. A., Leshem, B., Oron, D., Fratzl, P., Weiner, S., and Addadi, L. (2015). "The mechanism of color change in the neon tetra fish: a light-induced tunable photonic crystal array". *Angewandte Chemie International Edition* 54.42, pp. 12426–12430. <https://doi.org/10.1002/anie.201502268> (cit. on p. 18).
- Hainsworth, F. R., Collins, B. G., and Wolf, L. L. (1977). "The function of torpor in hummingbirds". *Physiological Zoology* 50.3, pp. 215–222. <https://doi.org/10.1086/physzool.50.3.30155724> (cit. on p. 25).
- Hamilton, W. J. (1965). "Sun-oriented display of the Anna's hummingbird". *The Wilson Bulletin* 77.1, pp. 38–44. JSTOR: 4159342 (cit. on p. 37).
- Hanley, D., Stoddard, M. C., Cassey, P., and Brennan, P. L. (2013). "Eggshell conspicuousness in ground nesting birds: do conspicuous eggshells signal nest location to conspecifics?" *Avian Biology Research* 6.2, pp. 147–156. <https://doi.org/10.3184/175815513X13617279883973> (cit. on p. 39).

- Hardy, O. J. and Senterre, B. (2007). "Characterizing the phylogenetic structure of communities by an additive partitioning of phylogenetic diversity". *Journal of Ecology* 95.3, pp. 493–506. <https://doi.org/10.1111/j.1365-2745.2007.01222.x> (cit. on p. 29).
- Hart, N. S., Partridge, J. C., Cuthill, I. C., and Bennett, A. T. D. (2000). "Visual pigments, oil droplets, ocular media and cone photoreceptor distribution in two species of passerine bird: the blue tit (*Parus caeruleus* L.) and the blackbird (*Turdus merula* L.)" *Journal of Comparative Physiology A* 186.4, pp. 375–387. <https://doi.org/10.1007/s003590050437> (cit. on p. 13).
- Heindl, M. and Winkler, H. (2003a). "Interacting effects of ambient light and plumage color patterns in displaying Wire-tailed Manakins (Aves, Pipridae)". *Behavioral Ecology and Sociobiology* 53.3, pp. 153–162. <https://doi.org/10.1007/s00265-002-0562-3> (cit. on p. 14).
- (2003b). "Vertical lek placement of forest-dwelling manakin species (Aves, Pipridae) is associated with vertical gradients of ambient light". *Biological Journal of the Linnean Society* 80.4, pp. 647–658. <https://doi.org/10.1111/j.1095-8312.2003.00264.x>. pmid: 410 (cit. on p. 14).
- Herrera, G., Zagal, J. C., Diaz, M., Fernández, M. J., Vielma, A., Cure, M., Martínez, J., Bozinovic, F., and Palacios, A. G. (2008). "Spectral sensitivities of photoreceptors and their role in colour discrimination in the green-backed firecrown hummingbird (*Sephanoides sephaniodes*)". *Journal of Comparative Physiology A* 194.9, p. 785. <https://doi.org/10.1007/s00359-008-0349-8>. pmid: 18584181 (cit. on p. 36).
- Hill, G. E., Doucet, S. M., and Buchholz, R. (2005). "The effect of coccidial infection on iridescent plumage coloration in wild turkeys". *Animal Behaviour* 69.2, pp. 387–394. <https://doi.org/10.1016/j.anbehav.2004.03.013> (cit. on p. 41).
- Hill, G. E. and McGraw, K. J., eds. (2006). *Bird coloration, volume 1: Mechanisms and measurements*. Vol. 1. 2 vols. Harvard University Press. 640 pp. ISBN: 978-0-674-01893-8 (cit. on pp. 40, 44).
- Hogan, B. G. and Stoddard, M. C. (2018). "Synchronization of speed, sound and iridescent color in a hummingbird aerial courtship dive". *Nature Communications* 9.1, p. 5260. <https://doi.org/10.1038/s41467-018-07562-7> (cit. on p. 37).
- Huth, H.-H. and Burkhardt, D. (1972). "Der spektrale Sehbereich eines Violettohr-Kolibris". *Naturwissenschaften* 59.12, pp. 650–650. <https://doi.org/10.1007/BF00609559> (cit. on p. 36).
- Jetz, W., Thomas, G. H., Joy, J. B., Hartmann, K., and Mooers, A. O. (2012). "The global diversity of birds in space and time". *Nature* 491.7424, pp. 444–448. <https://doi.org/10.1038/nature11631>. pmid: 23123857 (cit. on pp. 24, 26).
- Johansen, V. E., Catón, L., Hamidjaja, R., Oosterink, E., Wilts, B. D., Rasmussen, T. S., Sherlock, M. M., Ingham, C. J., and Vignolini, S. (2018). "Genetic manipulation of structural color in bacterial colonies". *Proceedings of the National Academy of Sciences* 115.11, pp. 2652–2657. <https://doi.org/10.1073/pnas.1716214115>. pmid: 29472451 (cit. on p. 18).

- Kemp, D. J., Vukusic, P., and Rutowski, R. L. (2006). "Stress-mediated covariance between nano-structural architecture and ultraviolet butterfly coloration". *Functional Ecology* 20.2, pp. 282–289. <https://doi.org/10.1111/j.1365-2435.2006.01100.x> (cit. on p. 41).
- Kemp, D. J. (2008). "Female mating biases for bright ultraviolet iridescence in the butterfly *Eurema hecabe* (Pieridae)". *Behavioral Ecology* 19.1, pp. 1–8. <https://doi.org/10.1093/beheco/arm094> (cit. on p. 41).
- Kemp, D. J. and Rutowski, R. L. (2007). "Condition dependence, quantitative genetics, and the potential signal content of iridescent ultraviolet butterfly coloration". *Evolution* 61.1, pp. 168–183. <https://doi.org/10.1111/j.1558-5646.2007.00014.x> (cit. on p. 41).
- Kientz, B., Luke, S., Vukusic, P., Péteri, R., Beaudry, C., Renault, T., Simon, D., Mignot, T., and Rosenfeld, E. (2016). "A unique self-organization of bacterial sub-communities creates iridescence in *Cellulophaga lytica* colony biofilms". *Scientific Reports* 6, p. 19906. <https://doi.org/10.1038/srep19906> (cit. on p. 18).
- Kinoshita, S., Yoshioka, S., and Miyazaki, J. (2008). "Physics of structural colors". *Reports on Progress in Physics* 71.7, p. 076401. <https://doi.org/10.1088/0034-4885/71/7/076401> (cit. on p. 15).
- Kirschner, M. and Gerhart, J. (1998). "Evolvability". *Proceedings of the National Academy of Sciences* 95.15, pp. 8420–8427. <https://doi.org/10.1073/pnas.95.15.8420>. pmid: 9671692 (cit. on p. 28).
- Knott, B., Berg, M. L., Ribot, R. F. H., Endler, J. A., and Bennett, A. T. D. (2017). "Intraspecific geographic variation in rod and cone visual pigment sensitivity of a parrot, *Platycercus elegans*". *Scientific Reports* 7.1, pp. 1–8. <https://doi.org/10.1038/srep41445> (cit. on p. 13).
- Kotrc, B. and Knoll, A. H. (2015). "A morphospace of planktonic marine diatoms. I. Two views of disparity through time". *Paleobiology* 41.1, pp. 45–67. <https://doi.org/10.1017/pab.2014.4> (cit. on p. 39).
- Land, M. F. (1972). "The physics and biology of animal reflectors". *Progress in Biophysics and Molecular Biology* 24, pp. 75–106. [https://doi.org/10.1016/0079-6107\(72\)90004-1](https://doi.org/10.1016/0079-6107(72)90004-1). pmid: 4581858 (cit. on p. 41).
- Langmore, N. E., Stevens, M., Maurer, G., Heinsohn, R., Hall, M. L., Peters, A., and Kilner, R. M. (2011). "Visual mimicry of host nestlings by cuckoos". *Proceedings of the Royal Society B: Biological Sciences* 278.1717, pp. 2455–2463. <https://doi.org/10.1098/rspb.2010.2391> (cit. on p. 39).
- Lasiewski, R. C. (1963). "Oxygen consumption of torpid, resting, active, and flying hummingbirds". *Physiological Zoology* 36.2, pp. 122–140. <https://doi.org/10.1086/physzool.36.2.30155436> (cit. on p. 41).
- Le Poul, Y., Whibley, A., Chouteau, M., Prunier, F., Llaurens, V., and Joron, M. (2014). "Evolution of dominance mechanisms at a butterfly mimicry supergene". *Nature Communications* 5.1, pp. 1–8. <https://doi.org/10.1038/ncomms6644> (cit. on p. 40).

- Leclaire, S., Pierret, P., Chatelain, M., and Gasparini, J. (2014). "Feather bacterial load affects plumage condition, iridescent color, and investment in preening in pigeons". *Behavioral Ecology* 25.5, pp. 1192–1198. <https://doi.org/10.1093/beheco/aru109> (cit. on p. 41).
- Leertouwer, H. L., Wilts, B. D., and Stavenga, D. G. (2011). "Refractive index and dispersion of butterfly chitin and bird keratin measured by polarizing interference microscopy". *Optics Express* 19.24, pp. 24061–24066. <https://doi.org/10.1364/OE.19.024061> (cit. on pp. 18, 19).
- Legagneux, P., Clark, R. G., Guillemain, M., Eraud, C., Théry, M., and Bretagnolle, V. (2012). "Large-scale geographic variation in iridescent structural ornaments of a long-distance migratory bird". *Journal of Avian Biology* 43.4, pp. 355–361. <https://doi.org/10.1111/j.1600-048X.2012.05666.x> (cit. on p. 42).
- Legagneux, P., Théry, M., Guillemain, M., Gomez, D., and Bretagnolle, V. (2010). "Condition dependence of iridescent wing flash-marks in two species of dabbling ducks". *Behavioural Processes* 83.3, pp. 324–330. <https://doi.org/10.1016/j.beproc.2010.01.017> (cit. on pp. 37, 41).
- Lim, M. L. M. and Li, D. (2013). "UV-green iridescence predicts male quality during jumping spider contests". *PLOS ONE* 8.4, e59774. <https://doi.org/10.1371/journal.pone.0059774> (cit. on pp. 18, 41).
- Lima, S. L. (1993). "Ecological and evolutionary perspectives on escape from predatory attack: A Survey of North American birds". *The Wilson Bulletin* 105.1, pp. 1–47 (cit. on p. 36).
- Linck, E. B., Hanna, Z., Sellas, A., and Dumbacher, J. P. (2017). "Evaluating hybridization capture with RAD probes as a tool for museum genomics with historical bird specimens". *bioRxiv*, p. 100867. <https://doi.org/10.1101/100867> (cit. on p. 24).
- Lind, O., Mitkus, M., Olsson, P., and Kelber, A. (2014). "Ultraviolet vision in birds: the importance of transparent eye media". *Proceedings of the Royal Society B: Biological Sciences* 281.1774, p. 20132209. <https://doi.org/10.1098/rspb.2013.2209> (cit. on p. 13).
- Luther, D. (2009). "The influence of the acoustic community on songs of birds in a neotropical rain forest". *Behavioral Ecology* 20.4, pp. 864–871. <https://doi.org/10.1093/beheco/arp074> (cit. on p. 29).
- Lynch, J. F. and Ames, P. L. (1970). "A new hybrid hummingbird, *Archilochus alexandri* × *Selasphorus sasin*". *The Condor* 72.2, pp. 209–212. <https://doi.org/10.2307/1366633> (cit. on p. 25).
- Lythgoe, J. N. and Shand, J. (1989). "The structural basis for iridescent colour changes in dermal and corneal iridophores in fish". *Journal of Experimental Biology* 141.1, pp. 313–325 (cit. on p. 18).
- Maia, R., Gruson, H., Endler, J. A., and White, T. E. (2019). "pavo 2: New tools for the spectral and spatial analysis of colour in R". *Methods in Ecology and Evolution* 10.7, pp. 1097–1107. <https://doi.org/10.1111/2041-210X.13174> (cit. on p. 40).

- Maia, R., Macedo, R. H. F., and Shawkey, M. D. (2012). "Nanostructural self-assembly of iridescent feather barbules through depletion attraction of melanosomes during keratinization". *Journal of The Royal Society Interface* 9.69, pp. 734–743. <https://doi.org/10.1098/rsif.2011.0456> (cit. on p. 41).
- Maia, R., Rubenstein, D. R., and Shawkey, M. D. (2013). "Key ornamental innovations facilitate diversification in an avian radiation". *Proceedings of the National Academy of Sciences* 110.26, pp. 10687–10692. <https://doi.org/10.1073/pnas.1220784110>. pmid: 23754395 (cit. on pp. 24, 30, 33, 35, 40, 44).
- (2016). "Selection, constraint, and the evolution of coloration in African starlings". *Evolution* 70.5, pp. 1064–1079. <https://doi.org/10.1111/evo.12912> (cit. on p. 42).
- Maia, R. and White, T. E. (2018). "Comparing colors using visual models". *Behavioral Ecology* 29.3, pp. 649–659. <https://doi.org/10.1093/beheco/ary017> (cit. on p. 39).
- Martin, A. L. B., Gaskell, A. C., and Friesen, M. R. (2018). "Feather colours of live birds and museum specimens look similar when viewed by seabirds". *Ibis* 160.1, pp. 185–189. <https://doi.org/10.1111/ibi.12501> (cit. on p. 24).
- Matyjasik, P. (2005). "Birds associate species-specific acoustic and visual cues: recognition of heterospecific rivals by male blackcaps". *Behavioral Ecology* 16.2, pp. 467–471. <https://doi.org/10.1093/beheco/ari012> (cit. on p. 29).
- McCoy, D. E., Shultz, A. J., Vidoudez, C., Heide, E. van der, Trauger, S. A., and Haig, D. (2019). "Microstructures amplify seemingly honest signals in carotenoid-colored tanagers". *bioRxiv*, p. 799783. <https://doi.org/10.1101/799783> (cit. on pp. 44, 45).
- McCulloch, K. J., Osorio, D. C., and Briscoe, A. D. (2016). "Sexual dimorphism in the compound eye of *Heliconius erato*: a nymphalid butterfly with at least five spectral classes of photoreceptor". *Journal of Experimental Biology* 219.15, pp. 2377–2387. <https://doi.org/10.1242/jeb.136523>. pmid: 27247318 (cit. on p. 13).
- McGraw, K. J., Mackillop, E. A., Dale, J., and Hauber, M. E. (2002). "Different colors reveal different information: how nutritional stress affects the expression of melanin- and structurally based ornamental plumage". *Journal of Experimental Biology* 205.23, pp. 3747–3755. pmid: 12409501 (cit. on p. 41).
- McGuire, J. A., Witt, C. C., Altshuler, D. L., and Remsen, J. V. J. (2007). "Phylogenetic systematics and biogeography of hummingbirds: Bayesian and maximum likelihood analyses of partitioned data and selection of an appropriate partitioning strategy". *Systematic Biology* 56.5, pp. 837–856. <https://doi.org/10.1080/10635150701656360>. pmid: 17934998 (cit. on p. 24).
- McGuire, J. A., Witt, C. C., Remsen, J. V. J., Corl, A., Rabosky, D. L., Altshuler, D. L., and Dudley, R. (2014). "Molecular phylogenetics and the diversification of hummingbirds". *Current Biology* 24.8, pp. 910–916. <https://doi.org/10.1016/j.cub.2014.03.016>. pmid: 24704078 (cit. on pp. 24–26).

- McNett, G. D. and Marchetti, K. (2005). "Ultraviolet degradation in carotenoid patches: Live versus museum specimens of wood warblers (Parulidae)". *The Auk* 122.3, pp. 793–802. <https://doi.org/10.1093/auk/122.3.793> (cit. on p. 24).
- Meadows, M. G., Morehouse, N. I., Rutowski, R. L., Douglas, J. M., and McGraw, K. J. (2011). "Quantifying iridescent coloration in animals: a method for improving repeatability". *Behavioral Ecology and Sociobiology* 65.6, pp. 1317–1327. <https://doi.org/10.1007/s00265-010-1135-5>. pmid: 876 (cit. on p. 20).
- Meadows, M. G., Roudybush, T. E., and McGraw, K. J. (2012). "Dietary protein level affects iridescent coloration in Anna's hummingbirds, *Calypte anna*". *Journal of Experimental Biology* 215.16, pp. 2742–2750. <https://doi.org/10.1242/jeb.069351>. pmid: 22837446 (cit. on pp. 20, 41).
- Medina, I., Newton, E., Kearney, M. R., Mulder, R. A., Porter, W. P., and Stuart-Fox, D. (2018). "Reflection of near-infrared light confers thermal protection in birds". *Nature Communications* 9.1, pp. 1–7. <https://doi.org/10.1038/s41467-018-05898-8> (cit. on p. 41).
- Merwin, J. T., Smith, B. T., and Seeholzer, G. F. (2018). "Macroevolutionary bursts and constraints generate a rainbow in a clade of tropical birds". *bioRxiv*, p. 489419. <https://doi.org/10.1101/489419> (cit. on p. 39).
- Miller, R. S. and Gass, C. L. (1985). "Survivorship in hummingbirds: Is predation important?" *The Auk* 102.1, pp. 175–178. <https://doi.org/10.2307/4086840>. JSTOR: 4086840 (cit. on p. 36).
- Møller, A. P. and Cuervo, J. J. (1998). "Speciation and feather ornamentation in birds". *Evolution* 52.3, pp. 859–869. <https://doi.org/10.1111/j.1558-5646.1998.tb03710.x> (cit. on p. 29).
- Montgomerie, R. (2006). "Analyzing colors". In: *Bird Coloration, Volume 1: Mechanisms and Measurements*. Ed. by Hill, G. E. and McGraw, K. J. Vol. 1. 2 vols. Bird Coloration. Harvard University Press, p. 640. ISBN: 978-0-674-01893-8 (cit. on p. 33).
- Montgomerie, R. and Redsell, C. A. (1980). "A Nesting Hummingbird Feeding Solely on Arthropods". *The Condor* 82.4, p. 463. <https://doi.org/10.2307/1367577> (cit. on p. 25).
- Muchhalal, N., Johnsen, S., and Smith, S. D. (2014). "Competition for hummingbird pollination shapes flower color variation in Andean Solanaceae". *Evolution* 68.8, pp. 2275–2286. <https://doi.org/10.1111/evo.12441>. pmid: 24766107 (cit. on p. 39).
- Munro, J. T., Medina, I., Walker, K., Moussalli, A., Kearney, M. R., Dyer, A. G., Garcia, J., Rankin, K. J., and Stuart-Fox, D. (2019). "Climate is a strong predictor of near-infrared reflectance but a poor predictor of colour in butterflies". *Proceedings of the Royal Society B: Biological Sciences* 286.1898, p. 20190234. <https://doi.org/10.1098/rspb.2019.0234> (cit. on p. 41).
- Nordén, K. K., Faber, J. W., Babarović, F., Stubbs, T. L., Selly, T., Schiffbauer, J. D., Štefanić, P. P., Mayr, G., Smithwick, F. M., and Vinther, J. (2019). "Melanosome diversity and convergence in the evolution

- of iridescent avian feathers—Implications for paleocolor reconstruction". *Evolution* 73.1, pp. 15–27. <https://doi.org/10.1111/evo.13641> (cit. on pp. 30, 33, 39).
- Ödeen, A., Hart, N. S., and Håstad, O. (2009). "Assessing the use of genomic DNA as a predictor of the maximum absorbance wavelength of avian SWS1 opsin visual pigments". *Journal of Comparative Physiology A* 195.2, pp. 167–173. <https://doi.org/10.1007/s00359-008-0395-2> (cit. on pp. 13, 36).
- Ödeen, A. and Håstad, O. (2010). "Pollinating birds differ in spectral sensitivity". *Journal of Comparative Physiology A* 196.2, pp. 91–96. <https://doi.org/10.1007/s00359-009-0474-z> (cit. on pp. 36, 43).
- Ödeen, A., Pruett-Jones, S., Driskell, A. C., Armenta, J. K., and Håstad, O. (2012). "Multiple shifts between violet and ultraviolet vision in a family of passerine birds with associated changes in plumage coloration". *Proceedings of the Royal Society B: Biological Sciences* 279.1732, pp. 1269–1276. <https://doi.org/10.1098/rspb.2011.1777>. pmid: 21976683 (cit. on p. 39).
- Ornelas, J. F., González, C., Hernández-Baños, B. E., and García-Moreno, J. (2016). "Molecular and iridescent feather reflectance data reveal recent genetic diversification and phenotypic differentiation in a cloud forest hummingbird". *Ecology and Evolution* 6.4, pp. 1104–1127. <https://doi.org/10.1002/ece3.1950> (cit. on pp. 20, 39).
- Ortega-Jimenez, V. M. and Dudley, R. (2012a). "Aerial shaking performance of wet Anna's hummingbirds". *Journal of The Royal Society Interface* 9.70, pp. 1093–1099. <https://doi.org/10.1098/rsif.2011.0608>. pmid: 22072447 (cit. on p. 42).
- (2012b). "Flying in the rain: hovering performance of Anna's hummingbirds under varied precipitation". *Proceedings of the Royal Society B: Biological Sciences* 279.1744, pp. 3996–4002. <https://doi.org/10.1098/rspb.2012.1285> (cit. on p. 42).
- Osorio, D. C. and Ham, A. D. (2002). "Spectral reflectance and directional properties of structural coloration in bird plumage". *Journal of Experimental Biology* 205.14, pp. 2017–2027. pmid: 12089207 (cit. on pp. 18, 23).
- Osorio, D. C. and Vorobyev, M. (2008). "A review of the evolution of animal colour vision and visual communication signals". *Vision Research. Vision Research Reviews* 48.20, pp. 2042–2051. <https://doi.org/10.1016/j.visres.2008.06.018>. pmid: 18627773 (cit. on p. 13).
- Pantelić, D., Ćurčić, S., Savić-Šević, S., Korać, A., Kovačević, A., Ćurčić, B., and Bokić, B. (2011). "High angular and spectral selectivity of purple emperor (Lepidoptera: *Apatura iris* and *A. ilia*) butterfly wings". *Optics Express* 19.7, pp. 5817–5826. <https://doi.org/10.1364/OE.19.005817> (cit. on p. 18).
- Parker, A. R., McKenzie, D. R., and Large, M. C. J. (1998). "Multilayer reflectors in animals using green and gold beetles as contrasting examples". *Journal of Experimental Biology* 201.9, pp. 1307–1313. pmid: 9547312 (cit. on p. 18).
- Parker, A. R. (2000). "515 million years of structural colour". *Journal of Optics A: Pure and Applied Optics* 2.6, R15–R28. <https://doi.org/10.1088/1464-4258/2/6/201>.

- Parnell, A. J., Bradford, J. E., Curran, E. V., Washington, A. L., Adams, G., Brien, M. N., Burg, S. L., Morochz, C., Fairclough, J. P. A., Vukusic, P., Martin, S. J., Doak, S., and Nadeau, N. J. (2018). "Wing scale ultrastructure underlying convergent and divergent iridescent colours in mimetic *Heliconius* butterflies". *Journal of The Royal Society Interface* 15.141, p. 20170948. <https://doi.org/10.1098/rsif.2017.0948>. pmid: 29669892 (cit. on pp. 18, 20).
- Parnell, A. J., Washington, A. L., Mykhaylyk, O. O., Hill, C. J., Bianco, A., Burg, S. L., Dennison, A. J. C., Snape, M., Cadby, A. J., Smith, A., Prevost, S., Whittaker, D. M., Jones, R. A. L., Fairclough, J. P. A., and Parker, A. R. (2015). "Spatially modulated structural colour in bird feathers". *Scientific Reports* 5, p. 18317. <https://doi.org/10.1038/srep18317> (cit. on p. 20).
- Pasteels, J. M., Deparis, O., Mouchet, S. R., Windsor, D. M., and Billen, J. (2016). "Structural and physical evidence for an endocuticular gold reflector in the tortoise beetle, *Charidotella ambita*". *Arthropod Structure & Development* 45.6, pp. 509–518. <https://doi.org/10.1016/j.asd.2016.10.008> (cit. on p. 18).
- Pegram, K. V., Nahm, A. C., Rutowski, R. L., and Todd, S. (2013). "Warning color changes in response to food deprivation in the pipevine swallowtail butterfly, *Battus philenor*". *Journal of Insect Science* 13.1. <https://doi.org/10.1673/031.013.11001> (cit. on p. 41).
- Pérez i de Lanuza, G., Font, E., and Monterde, J. L. (2013). "Using visual modelling to study the evolution of lizard coloration: sexual selection drives the evolution of sexual dichromatism in lacertids". *Journal of Evolutionary Biology* 26.8, pp. 1826–1835. <https://doi.org/10.1111/jeb.12185> (cit. on p. 39).
- Pfaender, J., Gray, S. M., Rick, I. P., Chapuis, S., Hadiaty, R. K., and Herder, F. (2014). "Spectral data reveal unexpected cryptic colour polymorphism in female sailfin silverside fish from ancient Lake Matano". *Hydrobiologia* 739.1, pp. 155–161. <https://doi.org/10.1007/s10750-013-1557-y> (cit. on p. 43).
- Piszter, G., Kertész, K., Bálint, Z., and Biró, L. P. (2016). "Variability of the structural coloration in two butterfly species with different prezygotic mating strategies". *PLOS ONE* 11.11, e0165857. <https://doi.org/10.1371/journal.pone.0165857> (cit. on p. 20).
- Pitelka, F. A. (1942). "Territoriality and related problems in North American hummingbirds". *The Condor* 44.5, pp. 189–204. <https://doi.org/10.2307/1364129>. JSTOR: 1364129 (cit. on p. 25).
- Plattner, L. (2004). "Optical properties of the scales of *Morpho rhetenor* butterflies: theoretical and experimental investigation of the back-scattering of light in the visible spectrum". *Journal of The Royal Society Interface* 1.1, pp. 49–59. <https://doi.org/10.1098/rsif.2004.0006>. pmid: 16849152 (cit. on p. 20).
- Prum, R. O., LaFountain, A. M., Berro, J., Stoddard, M. C., and Frank, H. A. (2012). "Molecular diversity, metabolic transformation, and evolution of carotenoid feather pigments in cotingas (Aves: Cotingi-

- dae)". *Journal of Comparative Physiology B* 182.8, pp. 1095–1116. <https://doi.org/10.1007/s00360-012-0677-4> (cit. on p. 39).
- Rashid, I., Hassan, M. U., Khandwalla, A., Ameen, R. M., Yetisen, A. K., Dai, Q., and Butt, H. (2018). "Structural coloration in *Caloenas nicobarica* pigeons and refractive index modulated sensing". *Advanced Optical Materials* 6.9, p. 1701218. <https://doi.org/10.1002/adom.201701218> (cit. on p. 42).
- Renoult, J. P., Courtiol, A., and Schaefer, H. M. (2013). "A novel framework to study colour signalling to multiple species". *Functional Ecology* 27.3, pp. 718–729. <https://doi.org/10.1111/1365-2435.12086> (cit. on p. 39).
- Renoult, J. P., Kelber, A., and Schaefer, H. M. (2017). "Colour spaces in ecology and evolutionary biology". *Biological Reviews* 92.1, pp. 292–315. <https://doi.org/10.1111/brv.12230> (cit. on p. 39).
- Restrepo-Cardona, J. S., Marín-C, D., Sánchez-Bellaizá, D. M., Rodríguez-Villamil, D. R., Berrío, S., Vargas, L., and Mikkola, H. (2018). "Diet of barn owl (*Tyto alba*), spectacled owl (*Pulsatrix perspicillata*) and rufous-banded owl (*Strix albitarsis*) in the Western Andes of Colombia". *Ornitología Neotropical* 29.1, pp. 193–198 (cit. on p. 36).
- Robinson, W. D. (2003). "White-necked puffbird captures rufous-tailed hummingbird". *The Wilson Journal of Ornithology* 115.4, pp. 486–487. <https://doi.org/10.1676/02-105> (cit. on p. 36).
- Roulin, A. (2014). "Melanin-based colour polymorphism responding to climate change". *Global Change Biology* 20.11, pp. 3344–3350. <https://doi.org/10.1111/gcb.12594>. pmid: 24700793 (cit. on p. 41).
- Schmidt, W. J. and Ruska, H. (1962). "Über das schillernde Federmelanin bei *Heliangelus* und *Lophophorus*". *Zeitschrift für Zellforschung und Mikroskopische Anatomie* 57.1. <https://doi.org/10.1007/BF00338926> (cit. on pp. 30, 31, 34).
- Schuchmann, K. and Bonan, A. (2019). "Hummingbirds (Trochilidae)". In: *Handbook of the Birds of the World Alive*. Ed. by del Hoyo, J., Elliott, A., Sargatal, J., Christie, D. A., and de Juana, E. Lynx Edicions. Barcelona (cit. on p. 25).
- Schultz, T. D. and Fincke, O. M. (2009). "Structural colours create a flashing cue for sexual recognition and male quality in a Neotropical giant damselfly". *Functional Ecology* 23.4, pp. 724–732. <https://doi.org/10.1111/j.1365-2435.2009.01584.x> (cit. on p. 37).
- Sellers, W. I., Hepworth-Bell, J., Falkingham, P. L., Bates, K. T., Brassey, C. A., Egerton, V. M., and Manning, P. L. (2012). "Minimum convex hull mass estimations of complete mounted skeletons". *Biology Letters*, rsbl20120263. <https://doi.org/10.1098/rsbl.2012.0263>. pmid: 22675141 (cit. on p. 39).
- Shawkey, M. D. and D'Alba, L. (2017). "Interactions between colour-producing mechanisms and their effects on the integumentary colour palette". *Philosophical Transactions of the Royal Society B: Biological Sciences* 372.1724, p. 20160536. <https://doi.org/10.1098/rstb.2016.0536> (cit. on p. 44).

- Shawkey, M. D., D'Alba, L., Xiao, M., Schutte, M., and Buchholz, R. (2015). "Ontogeny of an iridescent nanostructure composed of hollow melanosomes". *Journal of Morphology* 276.4, pp. 378–384. <https://doi.org/10.1002/jmor.20347>. pmid: 25427951 (cit. on p. 31).
- Shawkey, M. D., Igic, B., Rogalla, S., Goldenberg, J., Clusella-Trullas, S., and D'Alba, L. (2017). "Beyond colour: consistent variation in near infrared and solar reflectivity in sunbirds (Nectariniidae)". *The Science of Nature* 104.9, p. 78. <https://doi.org/10.1007/s00114-017-1499-8> (cit. on pp. 41, 44).
- Shawkey, M. D., Morehouse, N. I., and Vukusic, P. (2009). "A protean palette: colour materials and mixing in birds and butterflies". *Journal of The Royal Society Interface* 6 (Suppl 2), S221–S231. <https://doi.org/10.1098/rsif.2008.0459.focus>. pmid: 19141430 (cit. on pp. 30, 31, 44).
- Shawkey, M. D. and Hill, G. E. (2005). "Carotenoids need structural colours to shine". *Biology Letters* 1.2, pp. 121–124. <https://doi.org/10.1098/rsbl.2004.0289> (cit. on p. 44).
- Simpson, R. K. and McGraw, K. J. (2018a). "It's not just what you have, but how you use it: solar-positional and behavioural effects on hummingbird colour appearance during courtship". *Ecology Letters* 21.9, pp. 1413–1422. <https://doi.org/10.1111/ele.13125> (cit. on p. 37).
- (2018b). "Two ways to display: male hummingbirds show different color-display tactics based on sun orientation". *Behavioral Ecology* 29.3, pp. 637–648. <https://doi.org/10.1093/beheco/ary016> (cit. on p. 37).
 - (2019a). "Experimental trait mis-matches uncover specificity of evolutionary links between multiple signaling traits and their interactions in hummingbirds". *Evolution* 73.3, pp. 436–451. <https://doi.org/10.1111/evo.13662> (cit. on pp. 29, 37).
 - (2019b). "Interspecific covariation in courtship displays, iridescent plumage, solar orientation, and their Interactions in hummingbirds". *The American Naturalist* 194.4, pp. 441–454. <https://doi.org/10.1086/704774> (cit. on p. 37).
- Smith, K. R., Cadena, V., Endler, J. A., Kearney, M. R., Porter, W. P., and Stuart-Fox, D. (2016). "Color change for thermoregulation versus camouflage in free-ranging lizards". *The American Naturalist* 188.6, pp. 668–678. <https://doi.org/10.1086/688765> (cit. on p. 41).
- Snyder, H. K., Maia, R., D'Alba, L., Shultz, A. J., Rowe, K. M. C., Rowe, K. C., and Shawkey, M. D. (2012). "Iridescent colour production in hairs of blind golden moles (Chrysochloridae)". *Biology Letters* 8.3, pp. 393–396. <https://doi.org/10.1098/rsbl.2011.1168>. pmid: 22279154 (cit. on p. 18).
- Spottiswoode, C. N. and Stevens, M. (2012). "Host-parasite arms races and rapid changes in bird egg appearance". *The American Naturalist* 179.5, pp. 633–648. <https://doi.org/10.1086/665031> (cit. on p. 39).
- Stavenga, D. G. (2014). "Thin film and multilayer optics cause structural colors of many Insects and birds". *Materials Today: Proceedings*. Living Light: Uniting biology and photonics – A memorial meet-

- ing in honour of Prof Jean-Pol Vigneron 1, pp. 109–121. <https://doi.org/10.1016/j.matpr.2014.09.007> (cit. on p. 18).
- Stavenga, D. G., Giraldo, M. A., and Leertouwer, H. L. (2010). "Butterfly wing colors: glass scales of *Graphium sarpedon* cause polarized iridescence and enhance blue/green pigment coloration of the wing membrane". *Journal of Experimental Biology* 213.10, pp. 1731–1739. <https://doi.org/10.1242/jeb.041434>. pmid: 20435824 (cit. on p. 44).
- Stavenga, D. G., Leertouwer, H. L., Marshall, N. J., and Osorio, D. C. (2011a). "Dramatic colour changes in a bird of paradise caused by uniquely structured breast feather barbules". *Proceedings of the Royal Society of London B: Biological Sciences* 278.1715, pp. 2098–2104. <https://doi.org/10.1098/rspb.2010.2293>. pmid: 21159676 (cit. on pp. 20, 37).
- Stavenga, D. G., Leertouwer, H. L., Osorio, D. C., and Wilts, B. D. (2015). "High refractive index of melanin in shiny occipital feathers of a bird of paradise". *Light: Science & Applications* 4.1, e243. <https://doi.org/10.1038/lsa.2015.16> (cit. on pp. 18, 19).
- Stavenga, D. G., Tinbergen, J., Leertouwer, H. L., and Wilts, B. D. (2011b). "Kingfisher feathers - colouration by pigments, spongy nanostructures and thin films". *Journal of Experimental Biology* 214.23, pp. 3960–3967. <https://doi.org/10.1242/jeb.062620>. pmid: 22071186 (cit. on p. 45).
- Stevens, M. and Merilaita, S. (2011). *Animal camouflage: mechanisms and function*. 1st ed. Cambridge University Press. ISBN: 978-0-521-19911-7 (cit. on p. 12).
- Stevens, M., Párraga, C. A., Cuthill, I. C., Partridge, J. C., and Troscianko, T. S. (2007). "Using digital photography to study animal coloration". *Biological Journal of the Linnean Society* 90.2, pp. 211–237. <https://doi.org/10.1111/j.1095-8312.2007.00725.x> (cit. on p. 38).
- Stiles, F. G. (1982). "Aggressive and courtship displays of the male Anna's hummingbird". *The Condor* 84.2, pp. 208–225. <https://doi.org/10.2307/1367674>. JSTOR: 1367674 (cit. on pp. 25, 36).
- Stiles, F. G. and Cortés-Herrera, J. O. (2015). "Diagnosis and observations of a hybrid hummingbird (*Metallura tyrianthina* x *Aglaeocercus kingi*) in the Eastern Andes of Colombia". *Revista de la Academia Colombiana de Ciencias Exactas, Físicas y Naturales* 39.153, pp. 481–490. <https://doi.org/10.18257/raccefyn.260> (cit. on p. 25).
- Stiles, F. G. and Wolf, L. L. (1970). "Hummingbird territoriality at a tropical flowering tree". *The Auk* 87.3, pp. 467–491. <https://doi.org/10.2307/4083791>. JSTOR: 4083791 (cit. on p. 25).
- Stoddard, M. C. (2012). "Mimicry and masquerade from the avian visual perspective". *Current Zoology* 58.4, pp. 630–648. <https://doi.org/10.1093/czoolo/58.4.630> (cit. on p. 39).
- Stoddard, M. C. and Osorio, D. C. (2019). "Animal coloration patterns: Linking spatial vision to quantitative analysis". *The American Naturalist* 193.2, pp. 164–186. <https://doi.org/10.1086/701300> (cit. on p. 40).

- Stoddard, M. C. and Prum, R. O. (2011). "How colorful are birds? Evolution of the avian plumage color gamut". *Behavioral Ecology* 22.5, pp. 1042–1052. <https://doi.org/10.1093/beheco/arr088> (cit. on p. 39).
- Stournaras, K. E., Lo, E., Böhning-Gaese, K., Cazetta, E., Matthias Dehling, D., Schleuning, M., Stoddard, M. C., Donoghue, M. J., Prum, R. O., and Martin Schaefer, H. (2013). "How colorful are fruits? Limited color diversity in fleshy fruits on local and global scales". *New Phytologist* 198.2, pp. 617–629. <https://doi.org/10.1111/nph.12157> (cit. on p. 39).
- Stuart-Fox, D., Newton, E., and Clusella-Trullas, S. (2017). "Thermal consequences of colour and near-infrared reflectance". *Philosophical Transactions of the Royal Society B: Biological Sciences* 372.1724, p. 20160345. <https://doi.org/10.1098/rstb.2016.0345> (cit. on p. 41).
- Suarez, R. K. (1992). "Hummingbird flight: sustaining the highest mass-specific metabolic rates among vertebrates". *Experientia* 48.6, pp. 565–570. <https://doi.org/10.1007/BF01920240> (cit. on p. 25).
- Taysom, A. J., Stuart-Fox, D., and Cardoso, G. C. (2011). "The contribution of structural-, psittacofulvin- and melanin-based colouration to sexual dichromatism in Australasian parrots". *Journal of Evolutionary Biology* 24.2, pp. 303–313. <https://doi.org/10.1111/j.1420-9101.2010.02166.x> (cit. on p. 44).
- Thayer, R. C., Allen, F. I., and Patel, N. H. (2019). "Structural color in *Junonia* butterflies evolves by tuning scale lamina thickness". *bioRxiv*, p. 584532. <https://doi.org/10.1101/584532> (cit. on p. 42).
- Troscianko, J. and Stevens, M. (2015). "Image calibration and analysis toolbox – a free software suite for objectively measuring reflectance, colour and pattern". *Methods in Ecology and Evolution* 6.11, pp. 1320–1331. <https://doi.org/10.1111/2041-210X.12439> (cit. on p. 37).
- Trzeciak, T. M., Wilts, B. D., Stavenga, D. G., and Vukusic, P. (2012). "Variable multilayer reflection together with long-pass filtering pigment determines the wing coloration of papilionid butterflies of the nireus group". *Optics Express* 20.8, pp. 8877–8890. <https://doi.org/10.1364/OE.20.008877> (cit. on p. 44).
- Van den Berg, C. P., Troscianko, J., Endler, J. A., Marshall, N. J., and Cheney, K. L. (2019). "Quantitative colour pattern analysis (QCPA): A comprehensive framework for the analysis of colour patterns in nature". *bioRxiv*, p. 592261. <https://doi.org/10.1101/592261> (cit. on pp. 37, 40).
- Van Wijk, S., Bourret, A., Béliele, M., Garant, D., and Pelletier, F. (2016). "The influence of iridescent coloration directionality on male tree swallows' reproductive success at different breeding densities". *Behavioral Ecology and Sociobiology* 70.9, pp. 1557–1569. <https://doi.org/10.1007/s00265-016-2164-5> (cit. on p. 41).
- Van Belleghem, S. M., Papa, R., Ortiz-Zuazaga, H., Hendrickx, F., Jiggins, C. D., McMillan, W. O., and Counterman, B. A. (2018). "patternize: An R package for quantifying colour pattern variation". *Methods*

- in Ecology and Evolution* 9.2, pp. 390–398. <https://doi.org/10.1111/2041-210X.12853> (cit. on p. 40).
- Vignolini, S., Moyroud, E., Glover, B. J., and Steiner, U. (2013). “Analysing photonic structures in plants”. *Journal of The Royal Society Interface* 10.87, p. 20130394. <https://doi.org/10.1098/rsif.2013.0394>. pmid: 23883949 (cit. on p. 18).
- Villéger, S., Mason, N. W. H., and Mouillot, D. (2008). “New multidimensional functional diversity indices for a multifaceted framework in functional ecology”. *Ecology* 89.8, pp. 2290–2301. <https://doi.org/10.1890/07-1206.1> (cit. on p. 39).
- Vorobyev, M. and Osorio, D. C. (1998). “Receptor noise as a determinant of colour thresholds”. *Proceedings of the Royal Society of London B: Biological Sciences* 265.1394, pp. 351–358. <https://doi.org/10.1098/rspb.1998.0302>. pmid: 9523436 (cit. on pp. 13, 16).
- Vorobyev, M., Osorio, D. C., Bennett, A. T. D., Marshall, N. J., and Cuthill, I. C. (1998). “Tetrachromacy, oil droplets and bird plumage colours”. *Journal of Comparative Physiology A* 183.5, pp. 621–633. <https://doi.org/10.1007/s003590050286>. pmid: 9839454 (cit. on p. 13).
- Vukusic, P., Sambles, J. R., and Lawrence, C. R. (2000). “Colour mixing in wing scales of a butterfly”. *Nature* 404.6777, pp. 457–457. <https://doi.org/10.1038/35006561> (cit. on p. 44).
- Vukusic, P., Sambles, J. R., Lawrence, C. R., and Wootton, R. J. (1999). “Quantified interference and diffraction in single Morpho butterfly scales”. *Proceedings of the Royal Society of London B: Biological Sciences* 266.1427, pp. 1403–1411. <https://doi.org/10.1098/rspb.1999.0794> (cit. on p. 18).
- Wallace, A. R. (1877). “The colors of animals and plants”. *The American Naturalist* 11.11, pp. 641–662. <https://doi.org/10.1086/271979> (cit. on p. 12).
- (1895). *Natural selection and tropical nature; essays on descriptive and theoretical biology*. In collab. with Cornell University Library. London and New York, Macmillan and Co. 512 pp. (cit. on pp. 12, 18, 23, 25, 43).
- Welch, V., Lousse, V., Deparis, O., Parker, A., and Vigneron, J. P. (2007). “Orange reflection from a three-dimensional photonic crystal in the scales of the weevil *Pachyrrhynchus congestus pavonius* (Curculionidae)”. *Physical Review E* 75.4, p. 041919. <https://doi.org/10.1103/PhysRevE.75.041919> (cit. on pp. 40, 45).
- White, T. E., Dalrymple, R. L., Herberstein, M. E., and Kemp, D. J. (2017). “The perceptual similarity of orb-spider prey lures and flower colours”. *Evolutionary Ecology* 31.1, pp. 1–20. <https://doi.org/10.1007/s10682-016-9876-x> (cit. on p. 39).
- White, T. E., Zeil, J., and Kemp, D. J. (2015). “Signal design and courtship presentation coincide for highly biased delivery of an iridescent butterfly mating signal”. *Evolution* 69.1, pp. 14–25. <https://doi.org/10.1111/evo.12551> (cit. on p. 37).

- Whitney, H. M., Kolle, M., Andrew, P., Chittka, L., Steiner, U., and Glover, B. J. (2009). "Floral iridescence, produced by diffractive optics, acts as a cue for animal pollinators". *Science* 323.5910, pp. 130–133. <https://doi.org/10.1126/science.1166256>. pmid: 19119235 (cit. on p. 18).
- Wilts, B. D., Giraldo, M. A., and Stavenga, D. G. (2016). "Unique wing scale photonics of male Rajah Brooke's birdwing butterflies". *Frontiers in Zoology* 13, p. 36. <https://doi.org/10.1186/s12983-016-0168-7> (cit. on p. 20).
- Youngblood, W. (2014). "Parasitism and feather reflectance in mourning doves (*Zenaida macroura*)". Undergraduate thesis. University of Mississippi. 63 pp. (cit. on p. 41).
- Zhang, L., Mazo-Vargas, A., and Reed, R. D. (2017). "Single master regulatory gene coordinates the evolution and development of butterfly color and iridescence". *Proceedings of the National Academy of Sciences* 114.40, pp. 10707–10712. <https://doi.org/10.1073/pnas.1709058114> (cit. on p. 42).
- Zi, J., Yu, X., Li, Y., Hu, X., Xu, C., Wang, X., Liu, X., and Fu, R. (2003). "Coloration strategies in peacock feathers". *Proceedings of the National Academy of Sciences* 100.22, pp. 12576–12578. <https://doi.org/10.1073/pnas.2133313100>. pmid: 14557541 (cit. on p. 20).



Research

Cite this article: Gruson H, Andraud C, Daney de Marcillac W, Berthier S, Elias M, Gomez D. 2018 Quantitative characterization of iridescent colours in biological studies: a novel method using optical theory. *Interface Focus* 9: 20180049.

<http://dx.doi.org/10.1098/rsfs.2018.0049>

Accepted: 11 October 2018

One contribution of 11 to a theme issue 'Living light: optics, ecology and design principles of natural photonic structures'.

Subject Areas:

biomaterials, biophysics, environmental science

Keywords:

iridescence, structural colours, thin-film interferences, hummingbirds, Lepidoptera, visual signals

Author for correspondence:

Hugo Gruson

e-mail: hugo.gruson@normalesup.org

Electronic supplementary material is available online at <https://dx.doi.org/10.6084/m9.figshare.c.4275911>.

Quantitative characterization of iridescent colours in biological studies: a novel method using optical theory

Hugo Gruson¹, Christine Andraud², Willy Daney de Marcillac³, Serge Berthier³, Marianne Elias⁴ and Doris Gomez^{1,3}

¹CEFE, Univ Montpellier, CNRS, Univ Paul Valéry Montpellier 3, EPHE, IRD, Montpellier, France

²CRC, MNHN, Ministère de la Culture et de la Communication, CNRS, Paris, France

³INSP, Sorbonne Université, CNRS, Paris, France

⁴ISYEB, CNRS, MNHN, EPHE, Sorbonne Université, Paris, France

HG, 0000-0002-4094-1476; ME, 0000-0002-1250-2353; DG, 0000-0002-9144-3426

Iridescent colours are colours that change with viewing or illumination geometry. While they are widespread in many living organisms, most evolutionary studies on iridescence do not take into account their full complexity. Few studies try to precisely characterize what makes iridescent colours special: their angular dependency. Yet, it is likely that this angular dependency has biological functions and is therefore submitted to evolutionary pressures. For this reason, evolutionary biologists need a repeatable method to measure iridescent colours as well as variables to precisely quantify the angular dependency. In this study, we use a theoretical approach to propose five variables that allow one to fully describe iridescent colours at every angle combination. Based on the results, we propose a new measurement protocol and statistical method to reliably characterize iridescence while minimizing the required number of time-consuming measurements. We use hummingbird iridescent feathers and butterfly iridescent wings as test cases to demonstrate the strengths of this new method. We show that our method is precise enough to be potentially used at intraspecific level while being also time-efficient enough to encompass large taxonomic scales.

1. Introduction

Most interactions between organisms, whether between different species (interspecific) or different individuals of the same species (intraspecific), involve communication. Communication can have different purposes (e.g. warning, camouflage, display) and use different channels (e.g. olfactory, acoustic, visual) [1]. In particular, colour is a specific kind of communication channel that can be produced through two non-mutually exclusive mechanisms: pigmentary colours are generated by the selective absorption of some wavelengths by special molecules called pigments while structural colours are generated by the physical interaction of light with matter, causing dispersion, diffraction or interferences [2].

Among structural colours, iridescent colours change depending on the illumination or observation angle. They can be produced by interferences of light after reflection by a thin-film or multilayer structure, or diffraction on a grating. Iridescent colours are present in many taxa, and particularly widespread among bony fishes (Actinopterygii), insects, as well as some birds (see detailed review in table 1 for studies on each one of these taxa). Iridescent colours seem to be involved in many important biological processes [123] and their angular dependency is likely under selection to produce complex visual signals [74,87,115,124]. In some cases, however, angular dependency may be selected against [125]. In all those cases, the study of the evolution of iridescent colours requires a precise quantification of the angular dependency. However, the inherent physical complexity of iridescent colours has hampered the development of quantitative methods to fully describe them in the angle space.

Table 1. Review of the methods used in the literature to study iridescent colours from multilayer or thin-film structures. The criteria we used for studies to be included in the table were the following: (i) at least one quantitative reflectance measurement using a spectrometer, (ii) functioning with white light (no monochromatic illumination), and (iii) the patch measured had to be described as iridescent in the article. A more detailed version of this table, with all angle configurations and colour variables used for each study is available in the electronic supplementary material. The terms ‘constant illumination’, ‘constant collection’, ‘constant angle bisector’ and ‘constant span’ are defined in figure 3d.

no. measurements	fibre configuration (no. studies)	birds	arthropods	others
single measurement	single fixed angle (53)	[3–33]	[34–48]	bony fishes [49]; mammals [50]; plants [51–54]
	single measurement relative to the structure orientation (6)	—	[55–60]	—
multiple measurements along a single line	constant illumination (5) constant collection (2) constant angle bisector (16) constant span (16)	[61] [66] [68–78] [84–87]	[62–64] [67] [79–83] [88–96]	bacteria [65] — — bony fishes [97]; lizards [98,99]
multiple measurement lines	multiple constant illuminations (4) multiple constant collections (1) multiple constant spans (1) constant illumination and bisector (3) multiple illumination and bisector (1) constant illumination and span (3) constant span and bisector (6) constant illumination, span and bisector (4)	[100] [104] [105] — — [110,111] [113–115] [120,121]	[101,102] — — [106,107] [109] [112] [116–118] [102,122]	bacteria [103] — — bacteria [108] — — gastropods [119] —

We reviewed all studies that performed reflectance measurements of biological samples with iridescent colours produced by a multilayer or a thin-film structure in table 1. We notice two main trends: (i) many studies measure iridescence at a single fixed angle (first row in table 1). In these studies, authors generally remain cautious and warn they are not attempting to measure angle dependency. However, the multilayer or thin film producing iridescent colours may not be parallel to the sample surface [67,80,96,102,109], and the angle between them and the sample surface may vary between species or even between individuals of the same species [105]. Hence, even though the angle of the measuring optical fibres relative to the macroscopic is constant, the angle relative to the structures is not. This jeopardizes any biological interpretation of differences between samples because the effects of many different parameters are intertwined.

(ii) Other studies take measurements at multiple angles but few attempt to precisely quantify angle dependency ('Literature review' folder in electronic supplementary material). Even when angle dependency is quantified, variables never stem from a theoretical approach, which leads to a large diversity of custom variables for each author. This heterogeneity in the methods, variable naming and sign conventions has likely hindered the spread of new concepts and results among researchers working on iridescence in living organisms.

Osorio & Ham [110] and Meadows *et al.* [114] started to address this heterogeneity in measurement methods and advocated for the use of a goniometer to reliably measure colour in a controlled angle configuration. However, they did not propose a detailed protocol or statistical tools to study angular dependency. Here, we use the optical laws that govern iridescence to propose a set of parameters to characterize

angle dependency of brightness, hue and saturation of iridescent colours. Next, we confirm the validity of these equations for complex biological structures using two highly different groups of organisms well known for their iridescent colours: Trochilidae (hummingbirds) and Lepidoptera (i.e. butterflies and moths), including the iconic *Morpho* butterflies that harbour large wings with bright iridescent blue colours. The standard framework we propose here makes iridescent colours comparable across taxa and across studies, opening up new perspectives in the study of their biological functions.

2. Model

2.1. Choice of colour variables

Since we want to produce a general method that would not depend on any specific vision system, we use variables directly derived from spectra, without computing vision models. We define brightness B as the average reflectance over a range between the minimal (λ_{\min}) and maximal (λ_{\max}) wavelengths (B_2 in Montgomerie [126]), saturation S as the full width at half maximum reflectance and hue H as the wavelength at which reflectance is maximal (H_1 in Montgomerie [126]). These three variables are represented in figure 1 and are the most common measures of brightness, hue and saturation in studies about iridescence (see the literature review in the electronic supplementary material).

2.2. Assumptions and equations

Our method relies on three assumptions that greatly simplify the equations for brightness, hue and saturation in the angle

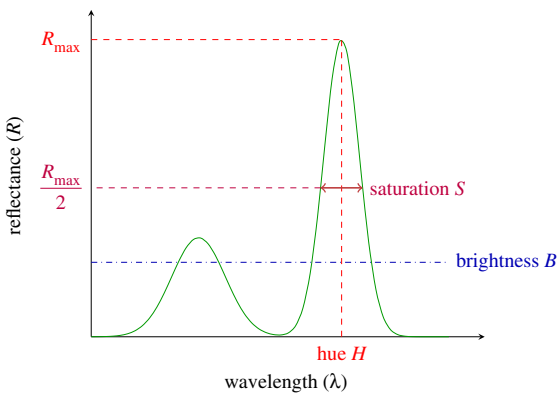


Figure 1. Graphical representation of the variables we used for hue H (wavelength at peak reflectance R_{\max} ; called H_1 in Montgomerie [126]), brightness B (average of reflectance over the wavelength range of interest; B_2 in Montgomerie [126]) and saturation S (full width at half maximum; no equivalent in Montgomerie [126]). (Online version in colour.)

space. See appendix A for mathematical proofs of the equations and the role of each one of these assumptions:

- (1) Small angles (less than or equal to 30°). Outside of this range, the signal due to iridescence is often very low and all that remains is the effect of the underlying pigments, which can be measured through traditional methods. For all thin films, and in some multilayers (depending on chemical composition), it is possible to consider angles up to 45° , as illustrated in the electronic supplementary material. This may help in producing more repeatable parameter estimates. For instance, a 45° angle can correspond to a viewer standing next to the viewed iridescent patch illuminated from above. Many previous studies have in this way mimicked the position of the bird relative to the sun in their measurements [66,87,98,105,114,118].
- (2) The orientation of the layers within the multilayer structure is affected by Gaussian noise. Many developmental processes are controlled by a large array of independent factors of small effect each, causing subsequent errors to often be Gaussian (due to the central limit theorem). This assumption is also empirically supported by the results of Gur *et al.* [127], who looked at the orientation of guanine crystals in neon tetra fishes (*Paracheirodon innesi*) using wide-angle X-ray scattering. Fitting a Cauchy distribution (fatter tail distribution) instead of a Gaussian distribution yields similar values of parameter estimates. For simplicity, we here only present the results with Gaussian noise.
- (3) Multilayers are ideal, i.e. the optical thickness (layer thickness times optical index) of each layer is constant: $n_1e_1 = n_2e_2$. This is a common assumption [36,54,67,97, 107,119,128–130] which is thought to be valid for most animal reflectors [131] because it produces the brightest and most saturated signals with a minimal number of layers (but see Schultz & Rankin [35] and Parker *et al.* [132] for beetles, Kinoshita *et al.* [133] for neon tetra).

This set of assumptions allows us to formally derive simple analytic expressions of brightness B , hue H and saturation S (figure 1) in the angle space (Φ_{inc} , Φ_{col}). All variables used in this study with their notations and their possible values are listed in table 2 and illustrated whenever possible in figure 2.

$$B(\Phi_{\text{inc}}, \Phi_{\text{col}}) = B_{\max} \exp - \frac{((\Phi_{\text{inc}} - \Phi_{\text{col}})/2 - t)^2}{2\gamma_B^2}, \quad (\text{A } 4 \text{ bis})$$

$$H(\Phi_{\text{inc}}, \Phi_{\text{col}}) = H_{\max} \cos \left(\gamma_H \frac{\Phi_{\text{inc}} + \Phi_{\text{col}}}{2} \right) \quad (\text{A } 14 \text{ bis})$$

and

$$S(\Phi_{\text{inc}}, \Phi_{\text{col}}) = S_{\max}. \quad (2.1)$$

Hereafter, we focus on brightness B and hue H because saturation S is constant no matter the angle configuration. The brightness $B(\Phi_{\text{inc}}, \Phi_{\text{col}})$ in the angle space is entirely defined by three parameters: B_{\max} , t and γ_B . The tilt t is the angle between the multilayer structure and the sample surface (as illustrated in figure 2). B_{\max} is the maximum reflectance produced by the multilayer or thin-film structure, reached when the fibres are placed in a symmetrical configuration relative to the normal of the multilayer. γ_B is the parameter quantifying the disorder in the alignment of the multilayer structure. This disorder in the structure results in a reflected signal that is not purely specular but instead contains a diffuse component, meaning it can be seen at multiple angle configurations. For this reason, from a macroscopic point of view, γ_B is correlated with the angular dependency of brightness. Earlier studies used a binary classification of iridescent colours depending on the angle range at which the colour was visible ('diffuse/directional' in Osorio & Ham [110], 'wide-angle/flashing' in Huxley [55], 'limited view' of Vukusic *et al.* [134]). This classification is positively correlated with $1/\gamma_B$.

The hue $H(\Phi_{\text{inc}}, \Phi_{\text{col}})$ in the angle space is defined by two parameters: H_{\max} which is the hue at coincident geometry (when using a bifurcated probe for example) and γ_H is the angular dependency of hue.

The variations of brightness and hue in the angle space, according to equations (A 4) and (A 14), respectively, are represented in figure 3.

2.3. Angle and notation conventions

In the rest of this study, we measure the incoming light ray angles (θ_i and Φ_{inc}) counter-clockwise and the outgoing light ray angles (θ_r and Φ_{col}) clockwise. For both incoming and outgoing angles, the origin is the normal to the structures (θ_i and θ_r) or the normal to the sample (Φ_{inc} and Φ_{col}). These conventions are represented in figure 2 where the direction of the arrows on angles represents the positive direction. The tilt t corresponds to the angle between the multilayer and the surface of the sample and is defined as $t = \Phi_{\text{inc}} - \theta_i = \theta_r - \Phi_{\text{col}}$ (see appendix A for more details about t). In other words, t is positive when the multilayer is tilted towards the illumination and negative otherwise (i.e. t is measured clockwise).

3. Methods

3.1. Study system: hummingbirds and butterflies

We used hummingbirds and butterflies (more precisely some *Morpho* and *Papilio* species) as study systems. Hummingbirds make an ideal example to test our framework for numerous reasons. First, they belong to a speciose family where all species are iridescent [135], which allows us to work on a large number of species that diverged fairly recently [136]. Upon visual examination, they display highly different types of iridescent colours, with either 'diffuse' (usually on dorsal patches) or 'directional' (usually on facial or

Table 2. List of parameters used in this study, with their domains of definition and their meanings.

symbol	range	meaning
θ_i	$[-\frac{\pi}{2}; \frac{\pi}{2}]$	incident light angle relative to the multilayer
θ_r	$[-\frac{\pi}{2}; \frac{\pi}{2}]$	reflected light angle relative to the multilayer
θ_1	$[0; \frac{\pi}{2}]$	angle between the incident ray and the interface between layers 1 and 2
θ_2	$[0; \frac{\pi}{2}]$	angle between the transmitted ray and the interface between layers 1 and 2
m	\mathbb{N}	angle between the incident ray and the interface between layers 2 and 1
B	\mathbb{R}^+	interference order/rank
H	$[\lambda_{\min}; \lambda_{\max}]$	brightness at a given configuration
S	\mathbb{R}^+	hue at a given angle configuration
B_{\max}	\mathbb{R}^+	saturation at a given angle configuration
t	$[-\frac{\pi}{2}; \frac{\pi}{2}]$	maximal brightness value (achieved for specular position)
γ_B	\mathbb{R}^+	angle between the multilayer surface and the sample surface (=tilt)
H_{\max}	$[\lambda_{\min}; \lambda_{\max}]$	disorder of the layer alignment in the multilayer/angular dependency of brightness
γ_H	\mathbb{R}^+	maximal hue value (achieved at normal incidence geometry)
n	\mathbb{C}	angular dependency of hue
e	\mathbb{R}^+	optical index of the material
Φ_{inc}	$[-\frac{\pi}{2}; \frac{\pi}{2}]$	thickness of the layer(s)
Φ_{col}	$[-\frac{\pi}{2}; \frac{\pi}{2}]$	angle between incidence fibre and sample surface (measured counterclockwise)
const.	\mathbb{R}	angle between collection fibre and sample surface (measured clockwise)
		used to denote a constant whose value is not important for the calculations

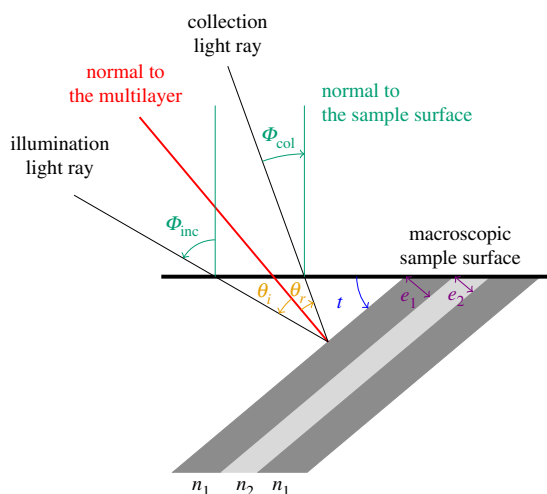


Figure 2. Schematic of a tilted multilayer (angle between the multilayer and the sample surface or tilt $t = 40^\circ$) and incoming and reflected light rays relative to the multilayer structure (with angles θ_i and θ_r , respectively) and relative to the sample surface (with angles Φ_{inc} and Φ_{col} , respectively). There is a relationship involving the tilt t between angles relative to the multilayer structure (θ_i and θ_r) and angles relative to the sample surface (Φ_{inc} and Φ_{col}): $\theta_i = \Phi_{\text{inc}} - t$ and $\theta_r = \Phi_{\text{col}} + t$. The positive direction for each angle is figured by an arrowhead. The multilayer is composed of an alternance of two layers characterized by the optical indices n_1 and n_2 and their thicknesses e_1 and e_2 . A schematic at a different scale, focusing on the goniometer, is available in the electronic supplementary material. (Online version in colour.)

ventral patches) iridescence (*sensu* Osorio & Ham [110]). In addition, many species have highly tilted multilayers, providing a good test case to estimate the tilt t [110,114]. Finally, most species

are available in large numbers in museum collections. We obtained the authorization from the Muséum National d'Histoire Naturelle to carefully cut feathers using surgical scissors. We selected one male from 36 species, evenly distributed across the phylogeny, from which we took feathers on two patches, one diffuse and one directional (*sensu* Osorio & Ham [110]).

Because the exclusive use of hummingbirds as a test taxon for a new method has been criticized in previous studies [86], we also test our method on a very different group: butterflies. Butterflies are phylogenetically distant from birds and have different structures producing iridescence. For these reasons, the fact our method works in both taxa is a compelling argument for its universality. We used 17 butterfly species known to have multilayer structures [101,137]. The full list of species we used for our measurements is available in the electronic supplementary material, for both hummingbirds and butterflies.

The method presented is also valid for whole specimens (whole birds instead of plucked feathers, for example). We nonetheless opted for the use of single feathers to maximize repeatability. Indeed, the precision of the goniometer measurements relies on the fact that the sample is precisely located at the centre of rotation of both fibres, which is more difficult to ensure for whole specimens.

3.2. Reflectance measurements

We measured reflectance at various angles using a purpose-built goniometer, following the recommendations of Meadows *et al.* [114]. The light emitted by a xenon lamp (300 W) over the 300–700 nm range of wavelengths to which birds are sensitive [138] was brought to the sample through an illuminating UV-visible optical fibre collimated to get a 1 mm light spot at normal illumination. Light reflected by the sample was then collected by a second identical collimated optical fibre and conducted toward an Oceanoptics USB4000 spectrophotometer. This set-up allows for a precise independent rotation of the illumination and the collection fibres, necessary for the measurements of iridescent colours.

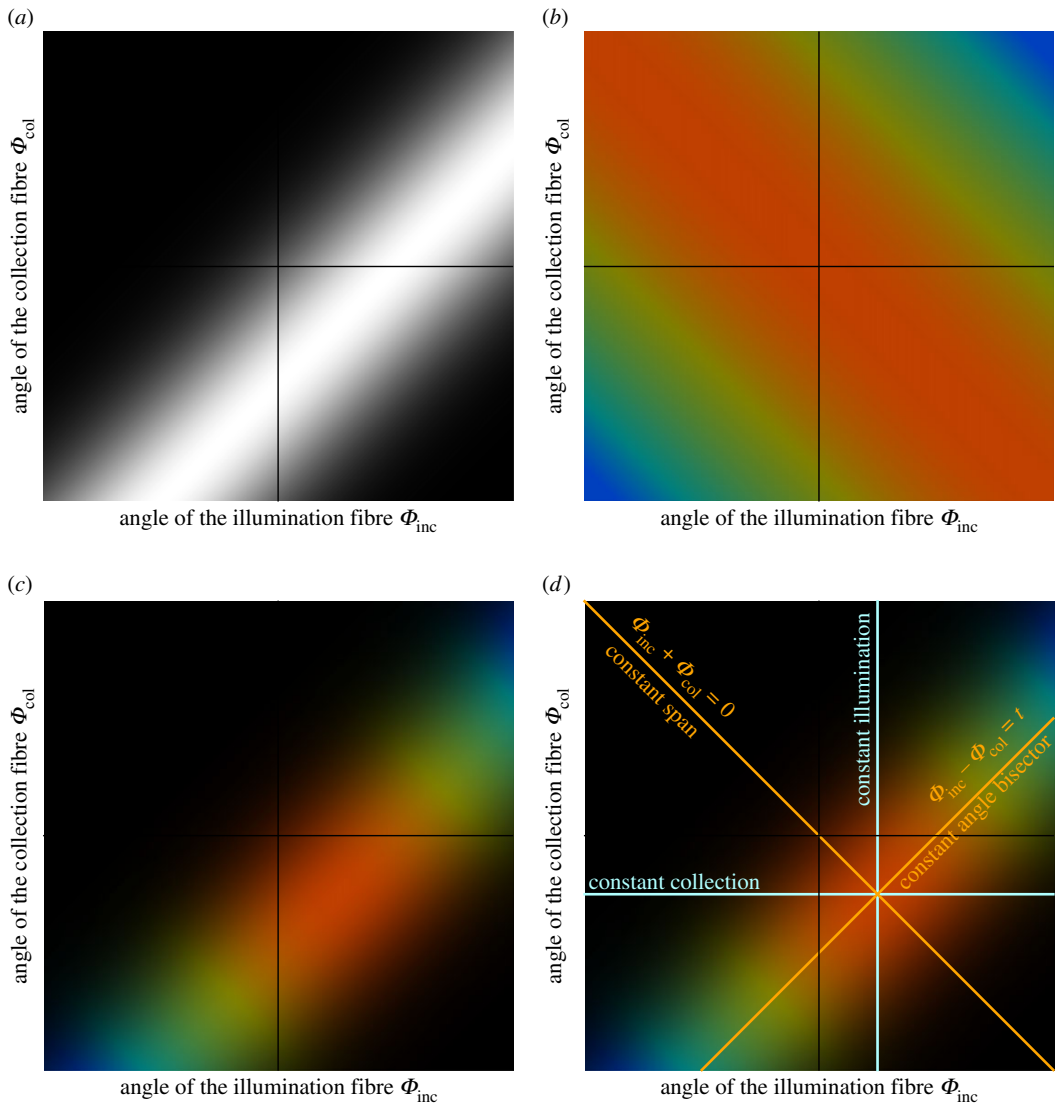


Figure 3. Colour variables (a) brightness, (b) hue, (c) and (d) hue and brightness of an iridescent multilayer (with tilt $t \neq 0$) in the angle space relative to the sample surface (Φ_{inc} , Φ_{col}). The colour lines in (d) indicate alternative bases: the angle space relative to the multilayer structure (θ_i , θ_r) in blue and ($\Phi_{\text{inc}} = 0$, $\Phi_{\text{inc}} - \Phi_{\text{col}} = t$) in orange and illustrates the terms ‘constant illumination’, ‘constant collection’, ‘constant angle bisector’ and ‘constant span’ used in table 1 and throughout this article.

Our previous mathematical exploration (detailed in appendix A.2) revealed that hue is constant along the $\Phi_{\text{inc}} + \Phi_{\text{col}} = \text{const}$. line (constant span) and brightness along the $\Phi_{\text{inc}} - \Phi_{\text{col}} = \text{const}$. line (constant angle bisector), as illustrated in figure 3. We thus only need to take measurements in two orthogonal directions: in the direction $\Phi_{\text{inc}} - \Phi_{\text{col}} = \text{const}$. to quantify hue variation and in the direction $\Phi_{\text{inc}} + \Phi_{\text{col}} = \text{const}$. to quantify brightness variations. This will allow us to infer all parameters controlling hue and brightness, and therefore to potentially compute all values of hue and brightness in the entire angle space (Φ_{inc} , Φ_{col}).

The shape and size of the light spot on the sample depend on the position of the illuminating fibre relative to the sample. As the angle of illumination θ_i increases, the light spot becomes more and more elongated, according to a θ_i cosine function. This means the amount of light received by the spectrometer decreases when θ_i increases, independently of sample characteristics. This can also be empirically observed by taking measurements of the white reference (which is a Lambertian surface, i.e. reflectance does not depend on the angle) at different angles. To control for this, we took white reference measurements at several angle configurations (detailed in the protocol below). The white standard for this study was an Avantes reference tile WS-2. Because this is a diffuse (Lambertian) white reference and because some iridescent colours are very directional

(i.e. all reflected light is focused in a single direction), it is expected to sometimes get values of brightness that can be over 100%.

The detailed protocol we used for our measurements is similar to Waldron *et al.* [118] and inspired from Osorio & Ham [110] and Meadows *et al.* [114]. A detailed walk-through of the measurement protocol is presented in box 1, and a worked example is available in the electronic supplementary material.

We repeated each measurement twice, on different days, by two different experimenters for hummingbirds and butterflies. We performed statistical analyses after the completion of the measurement session to prevent experimenter bias.

3.3. Statistical analyses

As explained in the previous section, the angle configuration changes the shape of the light spot and thus the total possible amount of light collected by the collection fibre. To address this issue, we first pre-processed spectra to normalize count data using the appropriate reference white spectrum (script available in the electronic supplementary material). Resulting csv files were then imported in pavo R package [139]. Hue values were discarded (i.e. converted to NA) when brightness was lower than 8.5% because hue is not defined for black colours.

Box 1. Measurement protocol.

- (1) Move one of the two fibres of the goniometer to find the position where you get a signal of maximal intensity. This position depends on the tilt t of the multilayer and is therefore different for every sample. Once this is done, this means the angle bisector of the two fibres is close to the normal to the multilayer structure (red line in figure 2).
- (2) While keeping the same angle bisector, take measurements at different angular spans (orange line $\Phi_{\text{inc}} - \Phi_{\text{col}} = t$ in figure 3d). These measurements will be used to estimate hue parameters. To have a sample size large enough for reliable estimation and to stay at small angles, we recommend measurements at $(\Phi_{\text{inc}}, \Phi_{\text{col}}) \in \{(t + 5^\circ, t + 5^\circ), (t + 10^\circ, t + 10^\circ), (t + 15^\circ, t + 15^\circ), (t + 20^\circ, t + 20^\circ), (t + 25^\circ, t + 25^\circ)\}$.
- (3) Take measurements while keeping the angular span between the two fibres constant (e.g. $\Phi_{\text{col}} - \Phi_{\text{inc}} = 20^\circ$) and moving the angle bisector (if you cannot do this, because for example, one of your fibres is not mobile, see appendix B.2). This will be used to estimate parameters related to brightness. We recommend three measurements on each side of the supposed normal to the multilayer structure (seven measurements in total) and a span of 20° : $(\Phi_{\text{inc}}, \Phi_{\text{col}}) \in \{(t - 5^\circ, t + 25^\circ), (t^\circ, t + 20^\circ), (t + 5^\circ, t + 15^\circ), (t + 10^\circ, t + 10^\circ), (t + 15^\circ, t + 5^\circ), (t + 20^\circ, t + 0^\circ), (t + 25^\circ, t - 5^\circ)\}$. Depending on how directional your sample is, it may be needed to increase the resolution of the measurement grid and only move the angle bisector of 2.5° or 5° at each step.
- (4) Take white reference measurements with the same angular spans as before but using the normal to the goniometer as angle bisector (same measurements as in 2 but with $t = 0^\circ$). If you have followed our advice for measurements, you should now take white measurements at $(\Phi_{\text{inc}}, \Phi_{\text{col}}) \in \{(5^\circ, 5^\circ), (10^\circ, 10^\circ), (15^\circ, 15^\circ), (20^\circ, 20^\circ), (25^\circ, 25^\circ), (30^\circ, 30^\circ)\}$.
- (5) Take white reference measurements with a constant span but various angle bisectors (same measurements as in 3 but with $t = 0^\circ$). If you have followed our advice of three measurements on each side to the supposed normal to the multilayer structure and a span of 20° , you should now take white measurement at $(\Phi_{\text{inc}}, \Phi_{\text{col}}) \in \{(-5^\circ, 25^\circ), (0^\circ, 20^\circ), (5^\circ, 15^\circ), (10^\circ, 10^\circ), (15^\circ, 5^\circ), (20^\circ, 0^\circ), (25^\circ, -5^\circ)\}$.

Iridescence parameters can be estimated using various methods, including least-squares optimization and Bayesian non-linear regression. We used a least-squares optimization as it is more common in biological sciences. We tested the Bayesian approach as well but it returned similar results and it is therefore not presented here.

We used two indices to estimate the variability of the parameters resulting from our method: (i) relative standard deviation (RSD, also called coefficient of variation or CV) as the standard deviation divided by the absolute value of the mean. (Absolute) standard deviation (SD) is a common measure of the noise in a dataset. RSD is a way to quantify the signal-to-noise ratio. Because it is normalized by the mean value of the parameter, it is dimensionless and can be compared between parameters. It represents the precision of the experimental and statistical framework and does not depend on the sample population. (ii) Repeatability as the intra-class coefficient (ICC) computed with the rptR package [140]. ICC assesses whether the method allows one to discriminate individual samples among the population by comparing intra- and inter-sample standard deviation. ICC is therefore highly dependent on the sample population and on the biological question.

RSD and ICC complement each other. A very precise method can still lead to non-repeatable measurements if there is no variability in the population. Conversely, a coarse method can work well enough to discriminate between samples and be repeatable if the variability between samples is high.

4. Results and discussion

Spectra from measurement along the ‘constant span’ ($\Phi_{\text{inc}} + \Phi_{\text{col}} = 20^\circ$) and ‘constant angle bisector’ ($\Phi_{\text{inc}} - \Phi_{\text{col}} = \text{const.}$) lines after correction by the appropriate white reference are displayed in figure 4 for the iridescent blue of the breast of the hummingbird *Heliodoxa jacquelinii*. We also show values of hue H and brightness B along these two measurement lines as well as the result from parameter estimation.

4.1. Relative error and repeatability

Variability and repeatability results are summarized in table 3. We find low values of RSD for hue-related variables for both hummingbirds and butterflies, indicating that our framework provides precise estimations of parameters. For brightness-related parameters, RSD is higher, as is usually the case, even for non-iridescent colours [141–143]. Despite relatively high RSD, all values for brightness remain repeatable, expected tilt t for butterflies because of a low inter-species variability, as demonstrated by the low value of SD.

4.2. Correlation between parameters

4.2.1. Correlation between B_{max} and γ_B

Madsen *et al.* [105] noticed a negative relationship between brightness angular dependency and maximum brightness. From an evolutionary point of view, this means there is a trade-off between the signal brightness at a given angle and the range of angle at which it is not black (i.e. directionality *sensu* Osorio & Ham [110]).

This correlation can also be proved theoretically. Indeed, the total energy of light that is reflected by the sample cannot exceed the received light energy. In other words, if absorption is similar across samples, the total brightness reflected in all directions is constant across samples:

$$\int \int B(\Phi_{\text{inc}}, \Phi_{\text{col}}) d\Phi_{\text{inc}} d\Phi_{\text{col}} = \text{const.} \quad (4.1)$$

The value of this double integral is known ($B(\Phi_{\text{inc}}, \Phi_{\text{col}})$ is a bivariate Gaussian function) and when we compute it, we find

$$B_{\text{max}} \sqrt{2\pi\gamma_B^2} = \text{const.} \quad (4.2)$$

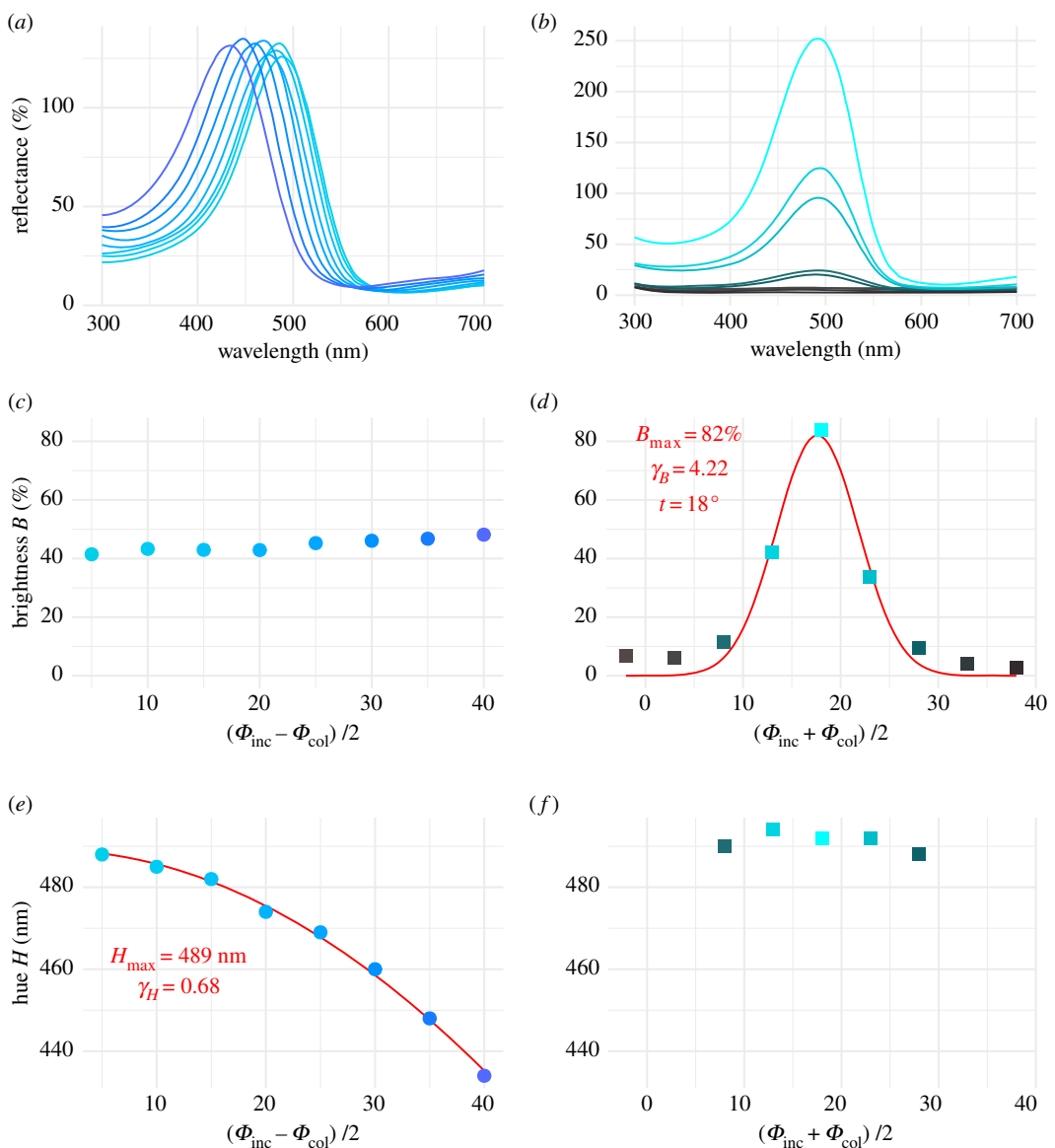


Figure 4. Spectra (*a*,*b*) and corresponding values of brightness (*c*,*d*) and hue (*e*,*f*) at different angle configurations for the breast patch of the hummingbird *Heliomaster furcifer* along the $\Phi_{\text{inc}} - \Phi_{\text{col}} = \text{const}$. (*a*,*c*,*e*; data points with round shape) and $\Phi_{\text{inc}} + \Phi_{\text{col}} = \text{const}$. (*b*,*d*,*f*; data points with square shape) lines. Colours correspond to the conversion of the spectra in human vision using the CIE10 visual system. As expected, brightness is constant when $\Phi_{\text{inc}} - \Phi_{\text{col}} = \text{const}$. and has a Gaussian shape when $\Phi_{\text{inc}} + \Phi_{\text{col}} = \text{const}$. Conversely, hue has a cosine shape when $\Phi_{\text{inc}} - \Phi_{\text{col}} = \text{const}$. and is constant when $\Phi_{\text{inc}} + \Phi_{\text{col}} = \text{const}$. The red lines correspond to the fit of the functions after parameter estimation, with the values of the parameters. The R script to produce this figure is available in electronic supplementary material.

Table 3. Repeatability (ICC with likelihood ratio and permutation *p*-values) and standard deviations (SD and RSD) of iridescence parameters for hummingbirds and butterflies.

taxon	variable	param.	mean	SD	RSD (%)	ICC	<i>p</i> (likel.)	<i>p</i> (perm.)
hummingbirds	brightness	B_{max}	36.60	47.54	14.79	0.947	<0.0001	0.001
		t	14.61	18.21	7.428	0.968	<0.0001	0.001
		γ_B	13.67	7.85	11.19	0.875	0.0009	0.002
	hue	H_{max}	556.80	65.66	0.3004	0.997	<0.0001	0.001
butterflies	brightness	B_{max}	148.80	99.78	6.91	0.936	<0.0001	0.001
		t	2.94	4.83	32.96	0.268	0.18	0.098
		γ_B	5.35	5.12	4.76	0.769	<0.0001	0.004
	hue	H_{max}	492.69	27.87	0.2484	0.993	<0.0001	0.001
	γ_H	0.73	0.14	2.993	0.853	<0.0001	0.001	

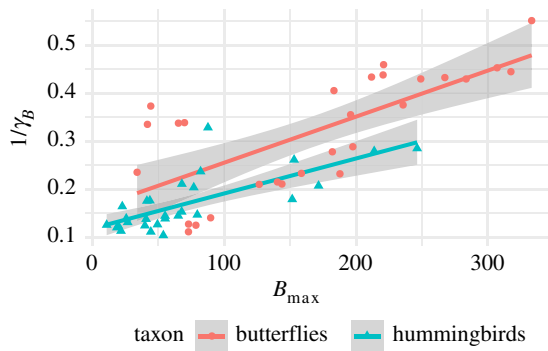


Figure 5. Correlation between B_{\max} and directionality $1/\gamma_B$. The dots are the data points. The lines show the result of the generalized linear model. (Online version in colour.)

and

$$B_{\max} \propto \frac{1}{\gamma_B}. \quad (4.3)$$

We indeed find a positive correlation between B_{\max} and $1/\gamma_B$ in the empirical data ($F = 147.0742$, d.f. = 1, $p < 0.0001$), illustrated in figure 5. We also notice an effect of the taxon (butterflies or hummingbirds) on the slope of the correlation ($F_1 = 8.3198$, $p = 0.0057$). Because the link between B_{\max} and $1/\gamma_B$ was proven when ignoring absorption (equation (4.3)), this may suggest that absorption is higher in hummingbirds than in butterflies.

4.2.2. Correlation between angular dependency for hue γ_H and other parameters.

Osorio & Ham [110] found that γ_H and γ_B are negatively correlated among 15 bird species from different families. We do not find support for such correlation for either the hummingbirds or the butterflies ($F_1 = 3.1994$, $p = 0.074$; figure in electronic supplementary material). Additionally, as discussed later in appendix B.3.2, many studies use variables that are correlated to H_{\max} to quantify hue angular dependence. On the contrary, we find that the parameters used in our method, H_{\max} and γ_H , are not correlated ($F_1 = 0.5167$, $p = 0.47$; figure in electronic supplementary material).

5. Conclusion

Using both a theoretical and an experimental approach we find that hue and brightness can be easily characterized for all angle configurations using a set of five parameters (H_{\max} and γ_H for hue; B_{\max} , t and γ_B for brightness). Additionally, we show that a relatively small number of measurements is sufficient to reliably estimate these parameter values. This is made possible by the fact that hue is constant when the angular span between the two fibres remains constant ($\Phi_{\text{inc}} - \Phi_{\text{col}} = \text{const.}$), and that brightness is constant for small angles as long as the angle bisector remains in the same position ($\Phi_{\text{inc}} + \Phi_{\text{col}} = \text{const.}$) (as illustrated in figures 3 and 4). These properties have been previously noticed empirically for hue H_1 by Osorio & Ham [110] on 15 bird species sampled from different families and Meadows *et al.* [114] on *Calyptra anna*. Without being formalized, it had been illustrated for brightness in Eliason & Shawkey [104] and Stavenga *et al.* [77] for B_3 as well as Stavenga *et al.* [78] for B_1 .

Our contribution unlocks new perspectives for studies on iridescent colours, such as the evolution of complex visual signals leveraging angular dependency properties of iridescent colours.

The proofs for the equation in this article are based on the multilayer theory. However, it is possible that parts of it may work for iridescence from diffraction gratings. Future studies should aim at integrating iridescence from diffraction into our framework. This would allow for a standard set of variables to describe iridescence, no matter its physical origin. Further investigation is also required to assess whether it is possible to relax some of the assumptions made in the paper under certain conditions.

Data accessibility. Data used in this study as well as scripts to apply the described method are available in the electronic supplementary material.

Authors' contributions. H.G. conducted the study (model construction, data analysis) and wrote the first version of this manuscript. H.G. performed measurements on hummingbirds and D.G. on butterflies. W.D.d.M. designed and built the goniometer. C.A., D.G., M.E. and S.B. contributed to the design of the goniometer. C.A., D.G. and W.D.d.M. helped with measurement protocol. D.G. and M.E. participated in the discussion for biological significance and pitfalls. All authors contributed to the final version of this article.

Competing interests. The authors declare no competing interests.

Funding. No funding has been received for this article.

Acknowledgements. We are grateful to C. Doutrelant and two anonymous reviewers for their valuable comments on the manuscript. We would also like to thank the Muséum National d'Histoire Naturelle and in particular J. Fuchs, P. Boussès and A. Prevato for letting us sample feathers from museum hummingbird specimens, as well as V. Debat for lending us *Morpho* specimens to explore *Morpho* iridescence. Finally, we thank the Living Light conference organizers for putting together this special issue on structural colours in living organisms.

Appendix A. Mathematical proof of the equations

A.1. Brightness B in the angle space (Φ_{inc} , Φ_{col})

For a perfectly regular multilayer, all the reflected signal is focused in the specular direction, at an angle θ_r equal to the incident angle θ_i . The brightness B is proportional to the reflected signal intensity, meaning

$$B(\theta_i, \theta_r) = \begin{cases} B(\theta_i) & \text{if } \theta_i = \theta_r \\ 0 & \text{if } \theta_i \neq \theta_r, \end{cases} \quad (\text{A } 1)$$

where $B(\theta_i)$ is defined by the Fresnel factor in the case of a thin-film structure (equation and R code to compute the Fresnel factor available in the electronic supplementary material). However, because we are dealing with small angles (assumption 1), we can approximate $B(\theta_i)$ to a constant B_{\max} (as illustrated in the electronic supplementary material):

$$B(\theta_i, \theta_r) \approx \begin{cases} B_{\max} & \text{if } \theta_i = \theta_r \\ 0 & \text{if } \theta_i \neq \theta_r. \end{cases} \quad (\text{A } 2)$$

But because biological structures are not entirely flat, and because the different layers of the multilayer structure are not perfectly aligned, there is also some amount of light reflected outside of the specular reflection (often referred as diffuse reflection). We thus assume a Gaussian decay of the brightness B around the specular position $\theta_i = \theta_r$ (assumption 2), controlled

by a parameter γ_B related to the disorder of the multilayer:

$$B(\theta_i, \theta_r) \approx B_{\max} \exp - \frac{((\theta_i - \theta_r)/2)^2}{2\gamma_B^2}. \quad (\text{A } 3)$$

In the case of a perfectly regular multilayer with no disorder, we have $\gamma_B = 0$ and we find equation (A 2). Conversely, if $\gamma_B = +\infty$, the brightness value is the same for all angle configurations, which means we are dealing with a Lambertian surface.

Additionally, the multilayer structure is not always parallel to the sample surface. It is the case, for example, for hummingbirds included in this study, as well as for *Morpho* butterflies in Berthier *et al.* [67], for the rainbow stag beetle, *Phalacognathus muelleri*, structures described by Edo *et al.* [109], six pierid butterflies in Pirih *et al.* [102], 10 species of butterflies in Wickham *et al.* [80], and for six species of *Heliconius* butterflies in Parnell *et al.* [96]. So the illuminating angle Φ_{inc} and the collection Φ_{col} at the macroscopic scale do not necessarily match θ_i and θ_r (as illustrated in figure 2). If we denote t the angle between the multilayer surface and the macroscopic sample surface (called *tilt* hereafter, as in Madsen *et al.* [105] and Osorio & Ham [110]), we get

$$B(\Phi_{\text{inc}}, \Phi_{\text{col}}) \approx B_{\max} \exp - \frac{((\Phi_{\text{inc}} - \Phi_{\text{col}})/2 - t)^2}{2\gamma_B^2}. \quad (\text{A } 4)$$

Using equation (A 4), we only have three parameters (B_{\max} , t and γ_B) to estimate to be able to reconstruct all values of brightness B in the angle space defined by $(\Phi_{\text{inc}}, \Phi_{\text{col}})$. The resulting brightness in this space is plotted in figure 3.

A.2. Hue H in the angle space $(\Phi_{\text{inc}}, \Phi_{\text{col}})$

We defined the hue H as the wavelength for which reflectance is maximal. In the context of interferences, it is therefore the wavelength for which reflected light interferes constructively. For a regular multilayer, this happens when

$$mH(\theta_1, \theta_2) = 2(n_1e_1 \cos \theta_1 + n_2e_2 \cos \theta_2), \quad (\text{A } 5)$$

where m is an integer (interference order), θ_1 is the angle between the incident light ray and the multilayer structure at the interface between layer 1 and 2, θ_2 is the angle between the transmitted ray after going through the first interface between layers 1 and 2 and the multilayer structure, n_1 and n_2 are the optical indices of the layers, and e_1 and e_2 the thicknesses of the layers. The products n_1e_1 and n_2e_2 are often called optical thicknesses of the layers 1 and 2 (respectively).

The relationship between θ_1 and θ_2 is given by Snell's Law:

$$n_1 \sin \theta_1 = n_2 \sin \theta_2. \quad (\text{A } 6)$$

Because $\theta_1 \in [0; \pi/2]$, hue H increases when angle θ_1 decreases according to equation (A 5). This means a maximum value for hue H_{\max} is achieved when $\theta_1 = 0$ (in this case $\theta_2 = 0$ as well because of Snell's Law; equation (A 6)):

$$mH_{\max} = 2(n_1e_1 + n_2e_2). \quad (\text{A } 7)$$

We can replace n_1e_1 and n_2e_2 in equation (A 5) using equation (A 7):

$$\begin{aligned} mH(\theta_1, \theta_2) &= mH_{\max}(\cos \theta_1 + \cos \theta_2) \\ &\quad - 2(n_1e_1 \cos \theta_2 + n_2e_2 \cos \theta_1). \end{aligned} \quad (\text{A } 8)$$

By adding equation (A 8) and equation (A 5), we obtain

$$\begin{aligned} 2mH(\theta_1, \theta_2) &= mH_{\max}(\cos \theta_1 + \cos \theta_2) \\ &\quad + 2(\cos \theta_1 - \cos \theta_2)(n_1e_1 - n_2e_2). \end{aligned} \quad (\text{A } 9)$$

We consider here the case of an ideal multilayer, meaning that $n_1e_1 = n_2e_2$ (assumption 3). This allows us to simplify equation (A 9) into

$$H(\theta_1, \theta_2) = H_{\max} \frac{\cos \theta_1 + \cos \theta_2}{2}. \quad (\text{A } 10)$$

Because we are working with small angles (assumption 1), Snell's Law (equation (A 6)) can be approximated by

$$\theta_2 \approx \frac{n_1}{n_2} \theta_1 \quad (\text{A } 11)$$

and

$$H(\theta_1, \theta_2) \approx H_{\max} \frac{\cos \theta_1 + \cos(n_1/n_2)\theta_1}{2}. \quad (\text{A } 12)$$

For small angles (assumption 1), this sum of cosine functions can be approximated by a single cosine function with twice the amplitude (numerical proof in the electronic supplementary material):

$$H(\theta_1, \theta_2) \approx H_{\max} \cos \gamma_H \theta_1, \quad (\text{A } 13)$$

where $\gamma_H \approx \sqrt{(1 + (n_1/n_2)^2)/2}$ (after identification of the coefficients of the second-order Taylor series expansions in equations (A 12) and (A 13)).

This reasoning is valid for ideal thin-film structures and multilayers and tells what happens at the specular position. But as explained in the previous section, biological structures are noisy and there is signal outside the specular position. As previously, if there is signal, this means that there is a multilayer for which the position of the fibres is specular. And in this case, we can apply equation (A 13) as well:

$$H(\Phi_{\text{inc}}, \Phi_{\text{col}}) = H_{\max} \cos \left(\gamma_H \frac{\Phi_{\text{inc}} + \Phi_{\text{col}}}{2} \right). \quad (\text{A } 14)$$

We only need two parameters (H_{\max} and γ_H) to plot all hue values in the angle space $(\Phi_{\text{inc}}, \Phi_{\text{col}})$ as in figure 3. In the case of non-iridescent colours, we have $\gamma_H = 0$.

A.3. Saturation S in the angle space $(\Phi_{\text{inc}}, \Phi_{\text{col}})$

A.3.1. Along the 'constant span' direction $(\Phi_{\text{inc}} + \Phi_{\text{col}} = \text{const.})$

We know that along the $\Phi_{\text{inc}} + \Phi_{\text{col}} = \text{const.}$ direction (constant span), hue is constant (as shown in equation (A 14) and figure 3b). Using a similar reasoning as in appendix A.1, we find that the reflectance R for a wavelength λ at a given angle configuration $(\Phi_{\text{inc}}, \Phi_{\text{col}})$ is given by

$$R(\Phi_{\text{inc}}, \Phi_{\text{col}}, \lambda) = R_{\text{bisector}}(\lambda) \exp - \frac{((\Phi_{\text{inc}} - \Phi_{\text{col}})/2 - t)^2}{2\gamma_B^2}. \quad (\text{A } 15)$$

This means that reflectance spectra at all angle configurations along the 'constant span' axis ($\Phi_{\text{inc}} + \Phi_{\text{col}} = \text{const.}$) can be derived by scaling of the spectrum at another angle configuration.

The saturation $S(\Phi_{\text{inc}}, \Phi_{\text{col}})$ is defined as the full width at half maximum of the reflectance spectrum $R(\Phi_{\text{inc}}, \Phi_{\text{col}}, \lambda)$. Let us call R the reflectance spectrum at a given angle configuration

$(\Phi_{\text{inc}}^{\text{pos}1}, \Phi_{\text{col}}^{\text{pos}1})$. Then the saturation S at this configuration is

$$\left. \begin{aligned} S &= \lambda_1 - \lambda_2, \\ R(\lambda_1) = R(\lambda_2) &= \frac{R_{\max}}{2} \\ \lambda_1 &> \lambda_2. \end{aligned} \right\} \quad (\text{A } 16)$$

and

If the reflectance spectrum R' at $(\Phi_{\text{inc}}^{\text{pos}2}, \Phi_{\text{col}}^{\text{pos}2})$ is equal to R scaled by a factor s , then the saturation S' is

$$\left. \begin{aligned} S' &= \lambda'_1 - \lambda'_2, \\ R'(\lambda'_1) = R'(\lambda'_2) &= \frac{R'_{\max}}{2} \\ \lambda'_1 &> \lambda'_2, \end{aligned} \right\} \quad (\text{A } 17)$$

and

where

$$\left. \begin{aligned} R'(\lambda'_1) &= \frac{R(\lambda'_1)}{s}, \\ R'(\lambda'_2) &= \frac{R(\lambda'_2)}{s} \\ R'_{\max} &= \frac{R_{\max}}{s}. \end{aligned} \right\} \quad (\text{A } 18)$$

From this, we find that

$$\frac{R(\lambda'_2)}{s} = \frac{R(\lambda'_1)}{s} = \frac{R_{\max}}{2s} \quad (\text{A } 19)$$

and

$$R(\lambda'_2) = R(\lambda'_1) = \frac{R_{\max}}{2}. \quad (\text{A } 20)$$

This means that $\lambda'_1 = \lambda_1$ and $\lambda'_2 = \lambda_2$. In other words, the full width at half maximum is stable by scaling, which results in the saturation S remaining constant along the $\Phi_{\text{inc}} + \Phi_{\text{col}} = \text{const.}$ axis (constant span).

A.3.2. Along the 'constant angle bisector' direction ($\Phi_{\text{inc}} - \Phi_{\text{col}} = \text{const.}$)

Additionally, along the $\Phi_{\text{inc}} - \Phi_{\text{col}} = \text{const.}$ axis (constant angle bisector), brightness is constant and only hue changes. This means spectra are translations of one another. The full width at half maximum is also stable by translation so the saturation S remains constant along $\Phi_{\text{inc}} - \Phi_{\text{col}} = \text{const.}$ axis (constant angle bisector).

A.3.3. In the general case

All points in the $(\Phi_{\text{inc}}, \Phi_{\text{col}})$ space can be reached by a combination of moves along the orthogonal 'constant span' ($\Phi_{\text{inc}} + \Phi_{\text{col}} = \text{const.}$) and 'constant angle bisector' ($\Phi_{\text{inc}} - \Phi_{\text{col}} = \text{const.}$) axes. We just showed the saturation S is constant along these two axes so it is actually constant in the whole $(\Phi_{\text{inc}}, \Phi_{\text{col}})$ space.

Appendix B. Comparison with other methods

B.1. Measurements at fixed angle configuration

The angle t between the multilayer structure and the normal to the surface of the feather (tilt) is highly variable between species of the same family (SD = 19.36° in hummingbirds, as reported in table 3). This is in agreement with Osorio & Ham [110] who found tilt values t ranging from -20° to 40°. Even if the angle configuration $(\Phi_{\text{inc}}, \Phi_{\text{col}})$ is constant

at the macroscopic scale, the configuration relative to the multilayer structure (θ_i, θ_r) may not be constant because of the variation in the tilt t between samples. This means measurements at fixed geometry cannot be compared between samples. For this reason, we warn against measurements of iridescent colours at a fixed angle, even when angular dependency is not studied.

B.2. Parameter estimation using constant illumination

Some goniometers only allow for the rotation of the collection fibre while the illumination fibre stays at a fixed position. Measurements realized with a such protocol can still be used with our method but this leads to a loss of statistical power.

If illumination is provided at a fixed angle $\Phi_{\text{inc}} = \alpha$:

$$\begin{aligned} B(\Phi_{\text{col}}) &= B_{\max} \exp - \frac{((\alpha - \Phi_{\text{col}})/2 - t)^2}{2\gamma_B^2} \\ &= B_{\max} \exp - \frac{(\Phi_{\text{col}} + 2t - \alpha)^2}{8\gamma_B^2}. \end{aligned} \quad (\text{B } 1)$$

So, $B(\Phi_{\text{col}})$ is still a normal function of Φ_{col} with the same maximum value B_{\max} but with parameters $t^* = 2t - \alpha$ and $\gamma_B^* = 2\gamma_B$ for mean and standard deviation, respectively.

Because the estimation of the parameters of a normal function through a regression is more reliable when the standard deviation is low, using anything else than a fixed normal as measurement line, such as a fixed illumination, to study brightness parameters will result in less accurate values.

Additionally, depending on the exact value of α , it may not be possible to have a fibre configuration where $(\alpha + \Phi_{\text{col}})/2 = t$ but the span between the fibres is still less than 90° (small angles assumption). In this case, data points never reach the maximum B_{\max} , which makes parameter estimation very unreliable.

Finally, the new value of the mean t^* does not have a direct biological and physical interpretation, as opposed to t which is the tilt of the multilayer of thin-film structure.

For hue, if illumination is at fixed angle α

$$H(\Phi_{\text{col}}) = H_{\max} \cos \left(\gamma_H \frac{\alpha}{2} + \frac{\gamma_H}{2} \Phi_{\text{col}} \right). \quad (\text{B } 2)$$

The equation for hue at fixed illumination has a shape different from its general form depending on the span between the fibres, $(\Phi_{\text{inc}} + \Phi_{\text{col}})/2$. There is a constant term in the cosine function and the new term for hue angular dependency is $\gamma_H^* = \gamma_H/2$. As we explain in the next section, the estimation of the parameters is more reliable for high values of γ_H . For this reason, the parameter estimation at fixed illumination may not be as precise as along the $\Phi_{\text{inc}} + \Phi_{\text{col}} = \text{const.}$ line.

B.3. Link with other variables of angular dependency for hue

B.3.1. Linear regression

Linear regression instead of cosine regression to estimate H_{\max} and γ_H is common [63,75,110,121]. Because the curvature of the cosine function in equation (A 14), defining hue depending on the angular span, is often small, we obtain congruent results using either cosine or linear regression. However, this creates a systematic bias where H_{\max} is more overestimated for samples with larger angle dependency γ_H . Indeed, a linear regression

overestimates more the intercept value as the curvature of the function increases.

B.3.2. Difference between two angle configurations with the same angle bisector

The difference in hue between two angle configurations is sometimes used as a proxy for iridescence [71]. However, it is problematic because it leads to a very high correlation between hue and iridescence, as reported in Dakin & Montgomerie [66] ($R^2 > 0.95$).

We can prove mathematically this linear correlation. Let us focus on the difference between hue $H_{\text{pos}1}$ at a given angle configuration $(\Phi_{\text{inc}}^1, \Phi_{\text{col}}^1)$ and hue H_{max} at coincident geometry (i.e. $\Phi_{\text{inc}} + \Phi_{\text{col}} = \theta_i + \theta_r = 0$). It follows from equation (A 14) that defines the hue at any angle configuration that:

$$H_{\text{pos}1} - H_{\text{max}} = H_{\text{max}} \left[\cos \left(\gamma_H \frac{\Phi_{\text{inc}}^1 + \Phi_{\text{col}}^1}{2} \right) - 1 \right]. \quad (\text{B } 3)$$

From this equation, we see that if γ_H is constant or displays low variability between samples, $H_{\text{pos}1} - H_{\text{max}}$ is proportional to H_{max} :

$$H_{\text{pos}1} - H_{\text{max}} \propto H_{\text{max}}. \quad (\text{B } 4)$$

We can apply the same reasoning and prove the difference $H_{\text{pos}2} - H_{\text{max}}$ between hue $H_{\text{pos}2}$ at $(\Phi_{\text{inc}}^2, \Phi_{\text{col}}^2)$ and H_{max} is proportional to H_{max} :

$$H_{\text{pos}2} - H_{\text{max}} \propto H_{\text{max}}. \quad (\text{B } 5)$$

Thus (doing equations (B 4) and (B 5)), the difference in hue between any two angle configurations $(\Phi_{\text{inc}}^1, \Phi_{\text{col}}^1)$ and $(\Phi_{\text{inc}}^2, \Phi_{\text{col}}^2)$ is proportional to H_{max} :

$$H_{\text{pos}1} - H_{\text{pos}2} \propto H_{\text{max}}. \quad (\text{B } 6)$$

This correlation between the two variables characterizing hue in the angle space can lead to errors in subsequent statistical inferences. On the opposite and as reported in §4.2.2, the parameters proposed in this study (H_{max} and γ_H) do not have the same issue.

B.4. Link with other variables of angular dependency for brightness

We are providing the following comparison with variables that have been previously used in the literature to describe brightness angular dependency. This means that values from previous studies using these variables can still be used in a meta-analysis or a discussion using our new variables B_{max} , t and γ_B . We however explain why they are less precise, less versatile and/or more time consuming than those measured under our unified framework.

B.4.1. Full width at half maximum and angular breadth

We have shown brightness is a Gaussian function of standard deviation γ_B along the line of ‘constant span’ ($\Phi_{\text{inc}} + \Phi_{\text{col}} = \text{const. direction}$). Many studies previously characterized angular dependency in this direction using the full width at half maximum (hereafter FWHM) [80,102,107,110,113]. For a Gaussian function, there is an easy link between standard deviation and

FWHM:

$$\begin{aligned} \text{FWHM} &= 2\gamma_B^* \sqrt{2 \ln 2} \\ &= 4\gamma_B \sqrt{2 \ln 2} \\ &\approx 4.71\gamma_B. \end{aligned} \quad (\text{B } 7)$$

Similarly, some studies use what they call *angular breadth* [85,86,88–92,112], which they define as the range of angle where brightness is higher than 3% of its maximum (threshold at 10% for [112]):

$$\begin{aligned} \text{ang. breadth} &= 2\gamma_B^* \sqrt{4 \ln 10 - 2 \ln 3} \\ &= 4\gamma_B \sqrt{4 \ln 10 - 2 \ln 3} \\ &\approx 10.59\gamma_B. \end{aligned} \quad (\text{B } 8)$$

We see that these variables are proportional to γ_B in theory. However because they are computed from raw data, without any pre-processing or curve fitting, they are more sensitive to noise.

B.4.2. Hunter’s specular gloss and integrating sphere

Multiple studies [75,144,145] use Hunter’s gloss [146], defined by the ratio of specular to diffuse reflectance. This method is convenient because it can easily be achieved using an integrating sphere to capture the needed spectra in two measurements only (one at specular position without the sphere and one with the sphere to capture diffuse and specular reflectance).

This is equivalent to keeping the illumination at a fixed angle and measuring reflectance at all collection angles. We already know the brightness at the specular position is B_{max} . The diffuse reflection is the integral on all angle configurations of the brightness. Hence Hunter’s specular gloss G using the notation defined in this study is

$$G = \frac{B_{\text{max}}}{\iint B(\Phi_{\text{inc}}, \Phi_{\text{col}}) d\Phi_{\text{inc}} d\Phi_{\text{col}}}. \quad (\text{B } 9)$$

The integral of brightness for every angle configurations is $B_{\text{max}} \gamma_B^* \sqrt{2\pi}$ (integral of the normal with maximum B_{max} and standard deviation γ_B^*), which gives

$$G = \frac{1}{\gamma_B^* \sqrt{2\pi}} = \frac{1}{2\gamma_B \sqrt{2\pi}}. \quad (\text{B } 10)$$

However, this is assuming the measurement of B_{max} was actually done at the normal to the multilayer ($\Phi_{\text{inc}} + \Phi_{\text{col}}/2 = t$). But there is no way to know whether it is the case without doing several goniometer measurements with different normal positions. Once this is done, γ_B can be estimated without doing additional integrating sphere measurements.

B.4.3. Difference/quotient between maximum and another position with the same span

Some studies [84,86,111] use the difference or the quotient between the brightness at the fibre position where it is maximum and another position. With this approach, they find t and B_{max} .

The difference or the quotient between these two positions can easily be linked to γ_B because we know that $B(\Phi_{\text{inc}}, \Phi_{\text{col}})$ is a normal function of parameters t and γ_B .

However, this is very sensitive to noise and measurement error because B_{max} and t are estimated with only one data point and γ_B (or its equivalent variable) with only two data points.

Appendix C. Structural colours with pigmentary component

The framework we presented here focuses on purely structural iridescent colours. However many colours integrate both pigmentary and structural components [147,148]. If there is a pigmentary component, it adds constant term B_{pigment} to brightness B :

$$B(\Phi_{\text{inc}}, \Phi_{\text{col}}) = B_{\text{irid}} + B_{\text{pigment}} \quad (\text{C } 1)$$

and

$$\begin{aligned} B(\Phi_{\text{inc}}, \Phi_{\text{col}}) &= B_{\max} \exp - \frac{((\Phi_{\text{inc}} - \Phi_{\text{col}})/2 - t)^2}{2\gamma_B^2} \\ &\quad + B_{\text{pigment}}. \end{aligned} \quad (\text{C } 2)$$

This can easily be investigated using our protocol and statistical framework. The only difference is that four parameters (B_{\max} , t , γ_B and B_{pigment}) instead of three need to be estimated by running a nonlinear regression on equation (C 2) instead of equation (A 4).

There are cases where the structural and pigmentary components of colour act on very different regions of the light spectrum. This happens, for example, in *Colias eurytheme* [62], where iridescence is restricted to the UV region while the visible region colour is caused by pigments. In this case, our method can be applied directly by restricting the studied wavelength range to the region of interest (this option is available in the code provided in the electronic supplementary material).

References

- Maynard Smith J, Harper DA 2009 *Animal signals*. Oxford Series in Ecology and Evolution. Oxford, UK: Oxford University Press.
- Parker AR. 2000 515 million years of structural colour. *J. Opt. A: Pure Appl. Opt.* **2**, R15–R28. (doi:10.1088/1464-4258/2/6/201)
- Bennett ATD, Cuthill IC, Partridge JC, Lunau K. 1997 Ultraviolet plumage colors predict mate preferences in starlings. *Proc. Natl Acad. Sci. USA* **94**, 8618–8621. (doi:10.1073/pnas.94.16.8618)
- Perrier C, de Lope F, Möller AP, Ninni P. 2002 Structural coloration and sexual selection in the barn swallow *Hirundo rustica*. *Behav. Ecol.* **13**, 728–736. (doi:10.1093/beheco/13.6.728)
- Doucet SM, Montgomerie R. 2003 Multiple sexual ornaments in satin bowerbirds: ultraviolet plumage and bows signal different aspects of male quality. *Behav. Ecol.* **14**, 503–509. (doi:10.1093/beheco/arg035)
- Doucet SM, Montgomerie R. 2003 Structural plumage colour and parasites in satin bowerbirds *Ptilonorhynchus violaceus*: implications for sexual selection. *J. Avian Biol.* **34**, 237–242. (doi:10.1034/j.1600-048X.2003.03113.x)
- Zi J, Yu X, Li Y, Hu X, Xu C, Wang X, Liu X, Fu R. 2003 Coloration strategies in peacock feathers. *Proc. Natl Acad. Sci. USA* **100**, 12 576–12 578. (doi:10.1073/pnas.2133313100)
- McGraw KJ. 2004 Multiple UV reflectance peaks in the iridescent neck feathers of pigeons. *Naturwissenschaften* **91**, 125–129. (doi:10.1007/s00114-003-0498-0)
- Costa FJV, Macedo RH. 2005 Coccidian oocyst parasitism in the blue-black grassquit: influence on secondary sex ornaments and body condition. *Anim. Behav.* **70**, 1401–1409. (doi:10.1016/j.anbehav.2005.03.024)
- Hill GE, Doucet SM, Buchholz R. 2005 The effect of coccidial infection on iridescent plumage coloration in wild turkeys. *Anim. Behav.* **69**, 387–394. (doi:10.1016/j.anbehav.2004.03.013)
- Komdeur J, Oorebeek M, van Overveld T, Cuthill IC. 2005 Mutual ornamentation, age, and reproductive performance in the European starling. *Behav. Ecol.* **16**, 805–817. (doi:10.1093/beheco/ari059)
- Shawkey MD, Hauber ME, Estep LK, Hill GE. 2006 Evolutionary transitions and mechanisms of matte and iridescent plumage coloration in grackles and allies (Icteridae). *J. R. Soc. Interface* **3**, 777–786. (doi:10.1098/rsif.2006.0131)
- Bitton P-P, O'Brien EL, Dawson RD. 2007 Plumage brightness and age predict extrapair fertilization success of male tree swallows, *Tachycineta bicolor*. *Anim. Behav.* **74**, 1777–1784. (doi:10.1016/j.anbehav.2007.03.018)
- Bitton P-P, Dawson RD. 2008 Age-related differences in plumage characteristics of male tree swallows *Tachycineta bicolor*: hue and brightness signal different aspects of individual quality. *J. Avian Biol.* **39**, 446–452. (doi:10.1111/j.0908-8857.2008.04283.x)
- Bitton P-P, Dawson RD, Ochs CL. 2008 Plumage characteristics, reproductive investment and assortative mating in tree swallows *Tachycineta bicolor*. *Behav. Ecol. Sociobiol.* **62**, 1543–1550. (doi:10.1007/s00265-008-0583-7)
- Galván I, Möller AP. 2009 Different roles of natural and sexual selection on senescence of plumage colour in the barn swallow. *Funct. Ecol.* **23**, 302–309. (doi:10.1111/j.1365-2435.2008.01504.x)
- Eliason CM, Shawkey MD. 2010 Rapid, reversible response of iridescent feather color to ambient humidity. *Opt. Express* **18**, 21 284–21 292. (doi:10.1364/OE.18.021284)
- Legagneux P, Théry M, Guillemain M, Gomez D, Bretagnolle V. 2010 Condition dependence of iridescent wing flash-marks in two species of dabbling ducks. *Behav. Processes* **83**, 324–330. (doi:10.1016/j.beproc.2010.01.017)
- Maia R, Macedo RH. 2011 Achieving luster: prenuptial molt pattern predicts iridescent structural coloration in blue-black grassquits. *J. Ornithol.* **152**, 243–252. (doi:10.1007/s10336-010-0576-y)
- Savard J-F, Keagy J, Borgia G. 2011 Blue, not UV, plumage color is important in satin bowerbird *Ptilonorhynchus violaceus* display. *J. Avian Biol.* **42**, 80–84. (doi:10.1111/j.1600-048X.2010.05128.x)
- Eliason CM, Shawkey MD. 2011 Decreased hydrophobicity of iridescent feathers: a potential cost of shiny plumage. *J. Exp. Biol.* **214**, 2157–2163. (doi:10.1242/jeb.055822)
- Lee E, Miyazaki J, Yoshioka S, Lee H, Sugita S. 2012 The weak iridescent feather color in the jungle crow *Corvus macrorhynchos*. *Ornithol. Sci.* **11**, 59–64. (doi:10.2326/osj.11.59)
- Legagneux P, Clark RG, Guillemain M, Eraud C, Théry M, Bretagnolle V. 2012 Large-scale geographic variation in iridescent structural ornaments of a long-distance migratory bird. *J. Avian Biol.* **43**, 355–361. (doi:10.1111/j.1600-048X.2012.05666.x)
- Maia R, Rubenstein DR, Shawkey MD. 2013 Key ornamental innovations facilitate diversification in an avian radiation. *Proc. Natl Acad. Sci. USA* **110**, 10 687–10 692. (doi:10.1073/pnas.1220784110)
- Leclaire S, Pierret P, Chatelain M, Gasparini J. 2014 Feather bacterial load affects plumage condition, iridescent color, and investment in preening in pigeons. *Behav. Ecol.* **25**, 1192–1198. (doi:10.1093/beheco/aru109)
- Eliason CM, Maia R, Shawkey MD. 2015 Modular color evolution facilitated by a complex nanostructure in birds. *Evolution* **69**, 357–367. (doi:10.1111/evo.12575)
- Lee C-C, Liao S-F, Vukusic P. 2015 Measuring and modelling the reflectance spectra of male Swinhoe's pheasant feather barbules. *J. R. Soc. Interface* **12**, 20141354. (doi:10.1098/rsif.2014.1354)
- Maapatra BB, Marathe SA, Meyer-Rochow VB, Mishra M. 2016 A closer look at the feather coloration in the male purple sunbird, *Nectarinia asiatica*. *Micron* **85**, 44–50. (doi:10.1016/j.micron.2016.04.001)
- Maia R, Rubenstein DR, Shawkey MD. 2016 Selection, constraint, and the evolution of coloration in African starlings. *Evolution* **70**, 1064–1079. (doi:10.1111/evo.12912)

30. Nam H-Y, Lee S-I, Lee J, Choi C-Y, Choe JC. 2016 Multiple structural colors of the plumage reflect age, sex, and territory ownership in the Eurasian magpie *Pica pica*. *Acta Ornithol.* **51**, 83–92. (doi:10.3161/00016454AO2016.51.1.007)
31. Ornelas JF, González C, Hernández-Baños BE, García-Moreno J. 2016 Molecular and iridescent feather reflectance data reveal recent genetic diversification and phenotypic differentiation in a cloud forest hummingbird. *Ecol. Evol.* **6**, 1104–1127. (doi:10.1002/ece3.1950)
32. Vaquero-Alba I, McGowan A, Pincheira-Donoso D, Evans MR, Dall SRX. 2016 A quantitative analysis of objective feather color assessment: measurements in the laboratory do not reflect true plumage color. *Auk* **133**, 325–337. (doi:10.1642/AUK-16-19.1)
33. Quinard A, Cézilly F, Motreuil S, Rossi J-M, Biard C. 2017 Reduced sexual dichromatism, mutual ornamentation, and individual quality in the monogamous Zenaida dove *Zenaida aurita*. *J. Avian Biol.* **48**, 489–501. (doi:10.1111/jav.00902)
34. Mossakowski D. 1979 Reflection measurements used in the analysis of structural colours of beetles. *J. Microsc.* **116**, 351–364. (doi:10.1111/j.1365-2818.1979.tb00220.x)
35. Schultz TD, Rankin MA. 1985 The ultrastructure of the epicuticular interference reflectors of tiger beetles (*Cicindela*). *J. Exp. Biol.* **117**, 87–110.
36. Chae J, Nishida S. 1999 Spectral patterns of the iridescence in the males of *Sapphirina* (Copepoda: Poecilostomatoida). *J. Mar. Biol. Assoc. UK* **79**, 437–443. (doi:10.1017/S0025315498000563)
37. Tada H, Mann SE, Miaoulis IN, Wong PY. 1999 Effects of a butterfly scale microstructure on the iridescent color observed at different angles. *Opt. Express* **5**, 87–92. (doi:10.1364/OE.5.000087)
38. Vukusic P, Sambles R, Lawrence C, Wakely G. 2001 Sculpted-multilayer optical effects in two species of *Papilio* butterfly. *Appl. Opt.* **40**, 1116–1125. (doi:10.1364/AO.40.001116)
39. Hariyama T, Takaku Y, Hironaka M, Horiguchi H, Komiya Y, Kurachi M. 2002 The origin of the iridescent colors in coleopteran elytron. *Forma* **17**, 123–132.
40. Kurachi M, Takaku Y, Komiya Y, Hariyama T. 2002 The origin of extensive colour polymorphism in *Plateumaris sericea* (Chrysomelidae, Coleoptera). *Naturwissenschaften* **89**, 295–298. (doi:10.1007/s00114-002-0332-0)
41. Liu F, Dong BQ, Liu XH, Zheng YM, Zi J. 2009 Structural color change in longhorn beetles *Tmesisternus isabellae*. *Opt. Express* **17**, 16183–16191. (doi:10.1364/OE.17.016183)
42. Schultz TD, Fincke OM. 2009 Structural colours create a flashing cue for sexual recognition and male quality in a Neotropical giant damselfly. *Funct. Ecol.* **23**, 724–732. (doi:10.1111/j.1365-2435.2009.01584.x)
43. Ingram AL, Deparis O, Boulenguez J, Kennaway G, Berthier S, Parker AR. 2011 Structural origin of the green iridescence on the chelicerae of the red-backed jumping spider, *Phidippus johnsoni* (Salticidae: Araneae). *Arthrop. Struct. Dev.* **40**, 21–25. (doi:10.1016/j.asd.2010.07.006)
44. Kuitunen K, Gorb SN. 2011 Effects of cuticle structure and crystalline wax coverage on the coloration in young and old males of *Calopteryx splendens* and *Calopteryx virgo*. *Zoology* **114**, 129–139. (doi:10.1016/j.zool.2011.01.003)
45. Gur D, Leshem B, Farstey V, Oron D, Addadi L, Weiner S. 2016 Light-induced color change in the sapphirinid copepods: tunable photonic crystals. *Adv. Funct. Mater.* **26**, 1393–1399. (doi:10.1002/adfm.201504339)
46. Wilts BD, Giraldo MA, Stavenga DG. 2016 Unique wing scale photonics of male Rajah Brooke's birdwing butterflies. *Front. Zool.* **13**, 36. (doi:10.1186/s12983-016-0168-7)
47. Onelli OD, van de Kamp T, Skepper JN, Powell J, Rolo TDS, Baumbach T, Vignolini S. 2017 Development of structural colour in leaf beetles. *Sci. Rep.* **7**, 1373. (doi:10.1038/s41598-017-01496-8)
48. Trzeciak TM, Wilts BD, Stavenga DG, Vukusic P. 2012 Variable multilayer reflection together with long-pass filtering pigment determines the wing coloration of papilionid butterflies of the nireus group. *Opt. Express* **20**, 8877–8890. (doi:10.1364/OE.20.008877)
49. Gur D, Leshem B, Oron D, Weiner S, Addadi L. 2014 The structural basis for enhanced silver reflectance in koi fish scale and skin. *J. Am. Chem. Soc.* **136**, 17 236–17 242. (doi:10.1021/ja509340c)
50. Snyder HK, Maia R, D'Alba L, Shultz AJ, Rowe KMC, Rowe KC, Shawkey MD. 2012 Iridescent colour production in hairs of blind golden moles (Chrysochloridae). *Biol. Lett.* **8**, 393–396. (doi:10.1098/rsbl.2011.1168)
51. Lee DW. 1991 Ultrastructural basis and function of iridescent blue colour of fruits in *Elaeocarpus*. *Nature* **349**, 260–262. (doi:10.1038/349260a0)
52. Lee DW, Taylor GT, Irvine AK. 2000 Structural fruit coloration in *Delarbrea mitchieana* (Araliaceae). *Int. J. Plant Sci.* **161**, 297–300. (doi:10.1086/314249)
53. Vignolini S, Rudall PJ, Rowland AV, Reed A, Moyroud E, Faden RB, Baumberg JJ, Glover BJ, Steiner U. 2012 Pointillist structural color in Pollia fruit. *Proc. Natl Acad. Sci. USA* **109**, 15 712–15 715. (doi:10.1073/pnas.1210105109)
54. Chandler CJ, Wilts BD, Vignolini S, Brodie J, Steiner U, Rudall PJ, Glover BJ, Gregory T, Walker RH. 2015 Structural colour in *Chondrus crispus*. *Sci. Rep.* **5**, 11645. (doi:10.1038/srep11645)
55. Huxley J. 1975 The basis of structural colour variation in two species of *Papilio*. *J. Entomol. Ser. A Gen. Entomol.* **50**, 9–22. (doi:10.1111/j.1365-3032.1975.tb00087.x)
56. Kemp DJ. 2006 Heightened phenotypic variation and age-based fading of ultraviolet butterfly wing coloration. *Evol. Ecol. Res.* **8**, 515–527.
57. Papke RS, Kemp DJ, Rutowski RL. 2007 Multimodal signalling: structural ultraviolet reflectance predicts male mating success better than pheromones in the butterfly *Colias eurytheme* L. (Pieridae). *Anim. Behav.* **73**, 47–54. (doi:10.1016/j.anbehav.2006.07.004)
58. Pegram KV, Nahm AC, Rutowski RL, Todd S. 2013 Warning color changes in response to food deprivation in the pipevine swallowtail butterfly, *Battus philenor*. *J. Insect Sci.* **13**, 1–16. (doi:10.1673/031.013.11001)
59. Kemp DJ, Jones D, Macedonia JM, Krockenberger AK. 2014 Female mating preferences and male signal variation in iridescent *Hypolimnas* butterflies. *Anim. Behav.* **87**, 221–229. (doi:10.1016/j.anbehav.2013.11.001)
60. Thurman TJ, Seymour BM. 2016 A bird's eye view of two mimetic tropical butterflies: coloration matches predator's sensitivity. *J. Zool.* **298**, 159–168. (doi:10.1111/jzo.12305)
61. Parra JL. 2010 Color evolution in the hummingbird genus *Coeligena*. *Evolution* **64**, 324–335. (doi:10.1111/j.1558-5646.2009.00827.x)
62. Rutowski RL, Macedonia JM, Morehouse NI, Taylor-Taft L. 2005 Pterin pigments amplify iridescent ultraviolet signal in males of the orange sulphur butterfly, *Colias eurytheme*. *Proc. R. Soc. B* **272**, 2329–2335. (doi:10.1098/rspb.2005.3216)
63. Rutowski RL, Macedonia JM, Kemp DJ, Taylor-Taft L. 2007 Diversity in structural ultraviolet coloration among female sulphur butterflies (Coliadinae, Pieridae). *Arthrop. Struct. Dev.* **36**, 280–290. (doi:10.1016/j.asd.2006.11.005)
64. Imafuku M, Ogihara N. 2016 Wing scale orientation alters reflection directions in the green hairstreak *Chrysophyphus smaragdinus* (Lycaenidae; Lepidoptera). *Zool. Sci.* **33**, 616–622. (doi:10.2108/zs160041)
65. Kientz B, Ducret A, Luke S, Vukusic P, Mignot T, Rosenfeld E. 2012 Glitter-like iridescence within the Bactrodidetes especially *Cellulophaga* spp.: optical properties and correlation with gliding motility. *PLoS ONE* **7**, e52900. (doi:10.1371/journal.pone.0052900)
66. Dakin R, Montgomerie R. 2013 Eye for an eyespot: how iridescent plumage ocelli influence peacock mating success. *Behav. Ecol.* **24**, 1048–1057. (doi:10.1093/beheco/art045)
67. Berthier S, Charron E, Boulenguez J. 2006 Morphological structure and optical properties of the wings of Morphidae. *Insect Sci.* **13**, 145–158. (doi:10.1111/j.1744-7917.2006.00077.x)
68. Doucet SM, Shawkey MD, Hill GE, Montgomerie R. 2006 Iridescent plumage in satin bowerbirds: structure, mechanisms and nanostructural predictors of individual variation in colour. *J. Exp. Biol.* **299**, 380–390. (doi:10.1242/jeb.01988)
69. Yin H et al. 2006 Iridescence in the neck feathers of domestic pigeons. *Phys. Rev. E* **74**, 051916. (doi:10.1103/PhysRevE.74.051916)
70. Yoshioka S, Nakamura E, Kinoshita S. 2007 Origin of two-color iridescence in rock dove's feather. *J. Phys. Soc. Jpn.* **76**, 013801. (doi:10.1143/JPSJ.76.013801)
71. Maia R, Caetano JAV, Bão SN, Macedo RH. 2009 Iridescent structural colour production in male blue-black grassquit feather barbules: the role of keratin and melanin. *J. R. Soc. Interface* **6**, S203–S211. (doi:10.1098/rsif.2008.0460.focus)
72. Shawkey MD, D'Alba L, Wozny J, Eliason C, Koop JAH, Jia L. 2011 Structural color change following

- hydration and dehydration of iridescent mourning dove (*Zenaida macroura*) feathers. *Zoology* **114**, 59–68. (doi:10.1016/j.zool.2010.11.001)
73. Yoshioka S, Kinoshita S. 2011 Direct determination of the refractive index of natural multilayer systems. *Phys. Rev. E* **83**, 051917. (doi:10.1103/PhysRevE.83.051917)
74. Wilts BD, Michelsen K, Raedt HD, Stavenga DG. 2014 Sparkling feather reflections of a bird-of-paradise explained by finite-difference time-domain modeling. *Proc. Natl. Acad. Sci. USA* **111**, 4363–4368. (doi:10.1073/pnas.1323611111)
75. Igic B *et al.* 2015 A nanostructural basis for gloss of avian eggshells. *J. R. Soc. Interface* **12**, 20141210. (doi:10.1098/rsif.2014.1210)
76. Stavenga DG, Leertouwer HL, Osorio DC, Wilts BD. 2015 High refractive index of melanin in shiny occipital feathers of a bird of paradise. *Light: Sci. Appl.* **4**, e243. (doi:10.1038/lsa.2015.16)
77. Stavenga DG, Leertouwer HL, Wilts BD. 2018 Magnificent magpie colours by feathers with layers of hollow melanosomes. *J. Exp. Biol.* **221**, jeb174656. (doi:10.1242/jeb.174656)
78. Stavenga DG, van der Kooij CJ, Wilts BD. 2017 Structural coloured feathers of mallards act by simple multilayer photonics. *J. R. Soc. Interface* **14**, 20170407. (doi:10.1098/rsif.2017.0407)
79. Vukusic P, Wootton RJ, Sambles JR. 2004 Remarkable iridescence in the hindwings of the damselfly *Neurobasis chinensis chinensis* (Linnaeus) (Zygoptera: Calopterygidae). *Proc. R. Soc. Lond. B* **271**, 595–601. (doi:10.1098/rspb.2003.2595)
80. Wickham S, Large MCJ, Poladian L, Jermiin LS. 2006 Exaggeration and suppression of iridescence: the evolution of two-dimensional butterfly structural colours. *J. R. Soc. Interface* **3**, 99–109. (doi:10.1098/rsif.2005.0071)
81. Stavenga DG, Giraldo MA, Leertouwer HL. 2010 Butterfly wing colors: glass scales of *Graphium sarpedon* cause polarized iridescence and enhance blue/green pigment coloration of the wing membrane. *J. Exp. Biol.* **213**, 1731–1739. (doi:10.1242/jeb.041434)
82. Yoshioka S, Kinoshita S, Iida H, Hariyama T. 2012 Phase-adjusting layers in the multilayer reflector of a jewel beetle. *J. Phys. Soc. Jpn.* **81**, 054801. (doi:10.1143/JPSJ.81.054801)
83. Mouchet SR, Lobet M, Kolaric B, Kaczmarek AM, Van Deun R, Vukusic P, Deparis O, Van Hooijdonk E. 2017 Photonic scales of *Hoplia coerulea* beetle: any colour you like. *Mater. Tod. Proc.* **4**, 4979–4986. (doi:10.1016/j.matpr.2017.04.104)
84. Meadows MG, Roudybush TE, McGraw KJ. 2012 Dietary protein level affects iridescent coloration in Anna's hummingbirds, *Calypte anna*. *J. Exp. Biol.* **215**, 2742–2750. (doi:10.1242/jeb.069351)
85. Van Wijk S, Bourret A, Bélisle M, Garant D, Pelletier F. 2016 The influence of iridescent coloration directionality on male tree swallows' reproductive success at different breeding densities. *Behav. Ecol. Sociobiol.* **70**, 1557–1569. (doi:10.1007/s00265-016-2164-5)
86. Van Wijk S, Bélisle M, Garant D, Pelletier F. 2016 A reliable technique to quantify the individual variability of iridescent coloration in birds. *J. Avian Biol.* **47**, 227–234. (doi:10.1111/jav.00750)
87. Simpson RK, McGraw KJ. 2018 It's not just what you have, but how you use it: solar-positional and behavioural effects on hummingbird colour appearance during courtship. *Ecol. Lett.* **21**, 1413–1422. (doi:10.1111/ele.13125)
88. Kemp DJ, Vukusic P, Rutowski RL. 2006 Stress-mediated covariance between nano-structural architecture and ultraviolet butterfly coloration. *Funct. Ecol.* **20**, 282–289. (doi:10.1111/j.1365-2435.2006.01100.x)
89. Kemp DJ, Rutowski RL. 2007 Condition dependence, quantitative genetics, and the potential signal content of iridescent ultraviolet butterfly coloration. *Evolution* **61**, 168–183. (doi:10.1111/j.1558-5646.2007.00014.x)
90. Rutowski RL, Macedonia JM, Merry JW, Morehouse NI, Yturralde K, Taylor-Taft L, Gaalema D, Kemp DJ, Papke RS. 2007 Iridescent ultraviolet signal in the orange sulphur butterfly (*Colias eurytheme*): spatial, temporal and spectral properties. *Biol. J. Linnean Soc.* **90**, 349–364. (doi:10.1111/j.1095-8312.2007.00749.x)
91. Kemp DJ, Macedonia JM, Ball TS, Rutowski RL. 2008 Potential direct fitness consequences of ornament-based mate choice in a butterfly. *Behav. Ecol. Sociobiol.* **62**, 1017–1026. (doi:10.1007/s00265-007-0529-5)
92. Kemp DJ. 2008 Female mating biases for bright ultraviolet iridescence in the butterfly *Eurema hecabe* (Pieridae). *Behav. Ecol.* **19**, 1–8. (doi:10.1093/beheco/arm094)
93. Ghate E, Bhoraskar SV, Kulkarni GR. 2013 Study of nano-architecture of the wings of *Paris Peacock* butterfly. *Proc. SPIE* **8598**, 859805. (doi:10.1117/12.2003061)
94. Gur D, Leshem B, Pierantoni M, Farstey V, Oron D, Weiner S, Addadi L. 2015 Structural basis for the brilliant colors of the sapphirinid copepods. *J. Am. Chem. Soc.* **137**, 8408–8411. (doi:10.1021/jacs.5b05289)
95. Piszter G, Kertész K, Bálint Z, Bíró LP. 2016 Variability of the structural coloration in two butterfly species with different prezygotic mating strategies. *PLoS ONE* **11**, e0165857. (doi:10.1371/journal.pone.0165857)
96. Parnell AJ *et al.* 2018 Wing scale ultrastructure underlying convergent and divergent iridescent colours in mimetic *Heliconius* butterflies. *J. R. Soc. Interface* **15**, 20170948. (doi:10.1098/rsif.2017.0948)
97. Mäthger LM, Land MF, Siebeck UE, Marshall NJ. 2003 Rapid colour changes in multilayer reflecting stripes in the paradise whiptail, *Pentapodus paradiseus*. *J. Exp. Biol.* **206**, 3607–3613. (doi:10.1242/jeb.00599)
98. i de Lanuza GP, Font E. 2014 Now you see me, now you don't: iridescence increases the efficacy of lizard chromatic signals. *Naturwissenschaften* **101**, 831–837. (doi:10.1007/s00114-014-1224-9)
99. i de Lanuza GP, Font E. 2016 Iridescent (angle-dependent reflectance) properties of dorsal coloration in *Podarcis muralis* (Laurenti, 1768). *Amphibia-Reptilia* **37**, 441–445.
100. Santos SI, Lumeij JT, Westers P, van Wandelen BB. 2007 Sexual dichromatism in the European magpie *Pica pica*. Not as black and white as expected. *Ardea* **95**, 299–310. (doi:10.5253/078.095.0212)
101. Plattner L. 2004 Optical properties of the scales of *Morpho rhetenor* butterflies: theoretical and experimental investigation of the back-scattering of light in the visible spectrum. *J. R. Soc. Interface* **1**, 49–59. (doi:10.1098/rsif.2004.0006)
102. Pirih P, Wilts BD, Stavenga DG. 2011 Spatial reflection patterns of iridescent wings of male pierid butterflies: curved scales reflect at a wider angle than flat scales. *J. Comp. Physiol. A* **197**, 987–997. (doi:10.1007/s00359-011-0661-6)
103. Kientz B, Luke S, Vukusic P, Péteri R, Beaudry C, Renault T, Simon D, Mignot T, Rosenfeld E. 2016 A unique self-organization of bacterial sub-communities creates iridescence in *Cellulophaga lytica* colony biofilms. *Sci. Rep.* **6**, 19906. (doi:10.1038/srep19906)
104. Eliason CM, Shawkey MD. 2012 A photonic heterostructure produces diverse iridescent colours in duck wing patches. *J. R. Soc. Interface* **9**, 2279–2289. (doi:10.1098/rsif.2012.0118)
105. Madsen V, Dabelsteen T, Osorio D, Osorno JL. 2007 Morphology and ornamentation in male magnificent frigatebirds: variation with age class and mating status. *Am. Nat.* **169**, S93–S111. (doi:10.1086/510096)
106. Liu F, Yin H, Dong B, Qing Y, Zhao L, Meyer S, Liu X, Zi J, Chen B. 2008 Inconspicuous structural coloration in the elytra of beetles *Chlorophila obscuripennis* (Coleoptera). *Phys. Rev. E* **77**, 012901. (doi:10.1103/PhysRevE.77.012901)
107. Stavenga DG, Wilts BD, Leertouwer HL, Hariyama T. 2011 Polarized iridescence of the multilayered elytra of the Japanese jewel beetle, *Chrysocroa fulgidissima*. *Phil. Trans. R. Soc. B* **366**, 709–723. (doi:10.1098/rstb.2010.0197)
108. Johansen VE, Catón L, Hamidjaja R, Oosterink E, Wilts BD, Rasmussen TS, Sherlock MM, Ingham CJ, Vignolini S. 2018 Genetic manipulation of structural color in bacterial colonies. *Proc. Natl. Acad. Sci. USA* **115**, 2652–2657. (doi:10.1073/pnas.1716214115)
109. Edó S, Okoshi K, Kang S, Tokita M, Watanabe J. 2010 Unique reflection property due to bumpy multilayer structure in elytra of *Rhomboorrhina unicolor*. *Jpn. J. Appl. Phys.* **49**, 047201. (doi:10.1143/JJAP.49.047201)
110. Osorio DC, Ham AD. 2002 Spectral reflectance and directional properties of structural coloration in bird plumage. *J. Exp. Biol.* **205**, 2017–2027.
111. Loyau A, Gomez D, Moureau B, Théry M, Hart NS, Jalme MS, Bennett ATD, Sorci G. 2007 Iridescent structurally based coloration of eyespots correlates with mating success in the peacock. *Behav. Ecol.* **18**, 1123–1131. (doi:10.1093/beheco/arm088)
112. White TE, Zeil J, Kemp DJ. 2015 Signal design and courtship presentation coincide for highly biased

- delivery of an iridescent butterfly mating signal. *Evolution* **69**, 14–25. (doi:10.1111/evo.12551)
113. Brink DJ, van der Berg NG. 2004 Structural colours from the feathers of the bird *Bostrychia hagedash*. *J. Phys. D: Appl. Phys.* **37**, 813–818. (doi:10.1088/0022-3727/37/5/025)
114. Meadows MG, Morehouse NI, Rutowski RL, Douglas JM, McGraw KJ. 2011 Quantifying iridescent coloration in animals: a method for improving repeatability. *Behav. Ecol. Sociobiol.* **65**, 1317–1327. (doi:10.1007/s00265-010-1135-5)
115. Stavenga DG, Leertouwer HL, Marshall NJ, Osorio DC. 2011 Dramatic colour changes in a bird of paradise caused by uniquely structured breast feather barbules. *Proc. R. Soc. B* **278**, 2098–2104. (doi:10.1098/rspb.2010.2293)
116. Rutowski RL, Nahm AC, Macedonia JM. 2010 Iridescent hindwing patches in the pipevine swallowtail: differences in dorsal and ventral surfaces relate to signal function and context. *Funct. Ecol.* **24**, 767–775. (doi:10.1111/j.1365-2435.2010.01693.x)
117. Rutowski RL, Rajaguru PK. 2013 Male-specific iridescent coloration in the pipevine swallowtail (*Battus philenor*) is used in mate choice by females but not sexual discrimination by males. *J. Insect Behav.* **26**, 200–211. (doi:10.1007/s10905-012-9348-2)
118. Waldron SJ, Endler JA, Valkonen JK, Honma A, Dobler S, Mappes J. 2017 Experimental evidence suggests that specular reflectance and glossy appearance help amplify warning signals. *Sci. Rep.* **7**, 257. (doi:10.1038/s41598-017-00217-5)
119. Brink DJ, van der Berg NG, Botha AJ. 2002 Iridescent colors on seashells: an optical and structural investigation of *Helcion pruinosa*. *Appl. Opt.* **41**, 717–722. (doi:10.1364/AO.41.000717)
120. Noh H, Liew SF, Saranathan V, Prum RO, Mochrie SGJ, Dufresne ER, Cao H. 2010 Contribution of double scattering to structural coloration in quasiordered nanostructures of bird feathers. *Phys. Rev. E* **81**, 051923. (doi:10.1103/PhysRevE.81.051923)
121. Eliason CM, Bitton P-P, Shawkey MD. 2013 How hollow melanosomes affect iridescent colour production in birds. *Proc. R. Soc. B* **280**, 20131505. (doi:10.1098/rspb.2013.1505)
122. Wilts BD, Pirih P, Arikawa K, Stavenga DG. 2013 Shiny wing scales cause spec(tacular) camouflage of the angled sunbeam butterfly, *Curetis acuta*. *Biol. J. Linnean Soc.* **109**, 279–289. (doi:10.1111/bij.12070)
123. Doucet SM, Meadows MG. 2009 Iridescence: a functional perspective. *J. R. Soc. Interface* **6**(Suppl. 2), S115–S132. (doi:10.1098/rsif.2008.0395.focus)
124. Simpson RK, McGraw KJ. 2018 Two ways to display: male hummingbirds show different color-display tactics based on sun orientation. *Behav. Ecol.* **29**, 637–648. (doi:10.1093/beheco/ary016)
125. Moyroud E *et al.* 2017 Disorder in convergent floral nanostructures enhances signalling to bees. *Nature* **550**, 469–474. (doi:10.1038/nature24285)
126. Montgomerie R. 2006 Analyzing colors. In *Bird coloration, volume 1: mechanisms and measurements* (eds GE Hill, KJ McGraw), p. 640. Cambridge, MA: Harvard University Press.
127. Gur D, Palmer BA, Leshem B, Oron D, Fratzl P, Weiner S, Addadi L. 2015 The mechanism of color change in the neon tetra fish: a light-induced tunable photonic crystal array. *Angew. Chem. Int. Ed.* **54**, 12426–12430. (doi:10.1002/anie.201502268)
128. Land MF. 1966 A multilayer interference reflector in the eye of the scallop, *Pecten maximus*. *J. Exp. Biol.* **45**, 433–447.
129. Brink DJ, Lee ME. 1998 Thin-film biological reflectors: optical characterization of the *Chrysiridia croesus* moth. *Appl. Opt.* **37**, 4213–4217. (doi:10.1364/AO.37.004213)
130. Kinoshita S, Yoshioka S. 2005 Structural colors in nature: the role of regularity and irregularity in the structure. *ChemPhysChem* **6**, 1442–1459. (doi:10.1002/cphc.200500007)
131. Land MF. 1972 The physics and biology of animal reflectors. *Prog. Biophys. Mol. Biol.* **24**, 75–106. (doi:10.1016/0079-6107(72)90004-1)
132. Parker AR, McKenzie DR, Large MCJ. 1998 Multilayer reflectors in animals using green and gold beetles as contrasting examples. *J. Exp. Biol.* **201**, 1307–1313.
133. Kinoshita S, Yoshioka S, Miyazaki J. 2008 Physics of structural colors. *Rep. Prog. Phys.* **71**, 076401. (doi:10.1088/0034-4885/71/7/076401)
134. Vukusic P, Sambles JR, Lawrence CR, Wootton RJ. 2002 Limited-view iridescence in the butterfly *Ancyluris meliboeus*. *Proc. R. Soc. Lond. B* **269**, 7–14. (doi:10.1098/rspb.2001.1836)
135. Del Hoyo J, Elliott A, Sargatal J, Christie DA, de Juana E. 2017 Handbook of the Birds of the World Alive. See [hbw.com](#).
136. McGuire JA, Witt CC, Remsen JVJ, Corl A, Rabosky DL, Altshuler DL, Dudley R. 2014 Molecular phylogenetics and the diversification of hummingbirds. *Curr. Biol.* **24**, 910–916. (doi:10.1016/j.cub.2014.03.016)
137. Berthier S. 2007 *Iridescences: the physical colors of insects*. New York, NY: Springer.
138. Chen D-M, Goldsmith TH. 1986 Four spectral classes of cone in the retinas of birds. *J. Comp. Physiol. A* **159**, 473–479. (doi:10.1007/BF00604167)
139. Maia R, Eliason CM, Bitton P-P, Doucet SM, Shawkey MD. 2013 Pavo: an R package for the analysis, visualization and organization of spectral data. *Methods Ecol. Evol.* **4**, 906–913. (doi:10.1111/2041-210X.12069)
140. Nakagawa S, Schielzeth H. 2010 Repeatability for Gaussian and non-Gaussian data: a practical guide for biologists. *Biol. Rev.* **85**, 935–956. (doi:10.1111/j.1469-185X.2010.00141.x)
141. Evans SR, Hinks AE, Wilkin TA, Sheldon BC. 2010 Age, sex and beauty: methodological dependence of age- and sex-dichromatism in the great tit *Parus major*. *Biol. J. Linnean Soc.* **101**, 777–796. (doi:10.1111/j.1095-8312.2010.01548.x)
142. Midamegbe A, Grégoire A, Staszewski V, Perret P, Lambrechts MM, Boulinier T, Doutrelant C. 2013 Female blue tits with brighter yellow chests transfer more carotenoids to their eggs after an immune challenge. *Oecologia* **173**, 387–397. (doi:10.1007/s00442-013-2617-8)
143. Charmantier A, Wolak ME, Grégoire A, Fargevieille A, Doutrelant C. 2017 Colour ornamentation in the blue tit: quantitative genetic (co)variances across sexes. *Heredity* **118**, 125–134. (doi:10.1038/hdy.2016.70)
144. Maia R, D'Alba L, Shawkey MD. 2011 What makes a feather shine? A nanostructural basis for glossy black colours in feathers. *Proc. R. Soc. B* **278**, 1973–1980. (doi:10.1098/rspb.2010.1637)
145. Iskandar J-P, Eliason CM, Astrop T, Igic B, Maia R, Shawkey MD. 2016 Morphological basis of glossy red plumage colours. *Biol. J. Linnean Soc.* **119**, 477–487. (doi:10.1111/bij.12810)
146. Hunter RS. 1937 Methods of determining gloss. *J. Res. Natl Bureau Standards* **18**, 19–39. (doi:10.6028/jres.018.006)
147. Prum RO. 2006 Anatomy, physics, and evolution of structural colors. In *Bird coloration, volume 1: mechanisms and measurements* (eds GE Hill, KJ McGraw), p. 640. Cambridge, MA: Harvard University Press.
148. D'Alba L, Kieffer L, Shawkey MD. 2012 Relative contributions of pigments and biophotonic nanostructures to natural color production: a case study in budgerigar (*Melopsittacus undulatus*) feathers. *J. Exp. Biol.* **215**, 1272–1277. (doi:10.1242/jeb.064907)

Preamble

This file contains the necessary code and instructions to reproduce our results published in the paper: “Quantitative characterisation of iridescent colours in biological studies: a novel method using optical theory”.

You can also get the code in a runnable format by downloading the attached rmarkdown (*.Rmd) file.

```
suppressPackageStartupMessages(library(tidyverse))
theme_set(theme_minimal())
```

Detailed walkthrough of the method on one example (*Heliomaster furcifer*)

In this example, we focus on the iridescent feathers of the breast of the hummingbird *Heliomaster furcifer* to demonstrate the method. In this specific example, we obtain good results by using angles up to 45° but as stated in the manuscript, it may be necessary to restrict your analysis to angles lower than 30° in some cases. We did not find any significant difference in parameters values when estimated with angles $\leq 30^\circ$ and $\leq 45^\circ$ for hummingbirds and butterflies in our analysis.

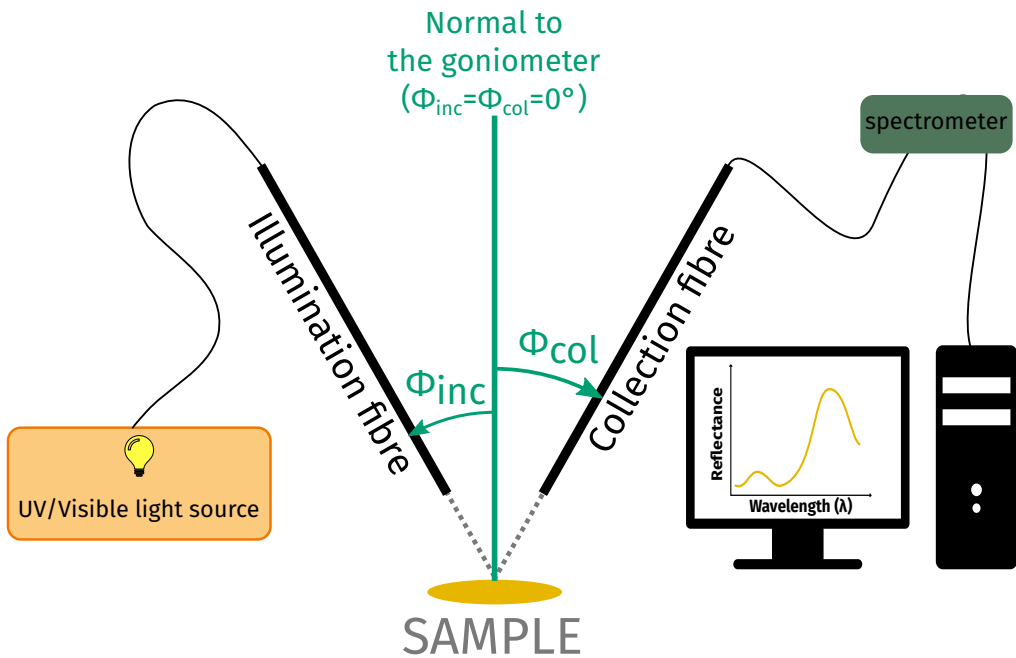


Figure 1: Schematic representation of a goniometer with the illumination and collection fibres and their angle with the normal to the sample Φ_{inc} and Φ_{col} . The sign of Φ_{inc} and Φ_{col} is figured by an arrow pointing towards the positive rotation direction.

This example uses files saved as .jdx using an OceanOptics spectrometer but this code can easily be modified to work with any file format, by using the `lightR` package (<https://github.com/bisaloo/lightR>).

Measurements

We put the measurements for hue and brightness in two different folders named **Hue** and **Brightness** respectively.

Measurements for brightness

As explained in this article, brightness is constant as long as the angle bisector of the two optical fibres of the goniometer remains constant ($\Phi_{inc} - \Phi_{col} = cst$). To estimate the variation of brightness in the

angle space (Φ_{inc}, Φ_{col}) , we thus need to take measurements along the orthogonal axis $\Phi_{inc} + \Phi_{col} = cst.$

1. We move one of the two fibres of the goniometer to find the position where we get a signal of maximal intensity. This position depends on the tilt t of the multilayer and is therefore different for every sample. Once this is done, this means the angle bisector of the two fibres is close to the normal to the multilayer structure. In our case, we get this when the bisector between the fibres is at 18° .
2. We take measurements while keeping the angular span between the two fibres constant (20°) and moving the angle bisector.
3. We name the files according to the following pattern SPECIES_PATCH_PHIINC_PHICOL. All files related to brightness estimation are in a folder named Brightness. So in our case, we get 9 files named

Brightness/HELIFURC_BR_38_-18.jdx,
Brightness/HELIFURC_BR_33_-13.jdx,
Brightness/HELIFURC_BR_28_-8.jdx,
Brightness/HELIFURC_BR_23_-3.jdx,
Brightness/HELIFURC_BR_18_2.jdx,
Brightness/HELIFURC_BR_13_7.jdx,
Brightness/HELIFURC_BR_8_12.jdx,
Brightness/HELIFURC_BR_3_17.jdx,
Brightness/HELIFURC_BR_-2_22.jdx

Measurements for hue

Conversely, hue is constant when the span between the two fibres is constant. To estimate the variation of hue in the angle space, we therefore perform several measurements with different angular spans but the same angle bisector.

1. We know keep the supposed normal of the multilayer as the fibre angle bisector and change the span, producing 8 files
- Hue/HELIFURC_BR_23_-13.jdx,**
Hue/HELIFURC_BR_28_-8.jdx,
Hue/HELIFURC_BR_33_-3.jdx,
Hue/HELIFURC_BR_38_2.jdx,
Hue/HELIFURC_BR_43_7.jdx,
Hue/HELIFURC_BR_48_12.jdx,
Hue/HELIFURC_BR_53_17.jdx,
Hue/HELIFURC_BR_58_22.jdx

White reference measurements

We need to take the same measurements as before but without any tilt, i.e.:

Brightness/WHITE_-20_-20.jdx,
Brightness/WHITE_-15_-15.jdx,
Brightness/WHITE_-10_-10.jdx,
Brightness/WHITE_-5_-5.jdx,
Brightness/WHITE_0_0.jdx,
Brightness/WHITE_-5_5.jdx,
Brightness/WHITE_-10_10.jdx,
Brightness/WHITE_-15_15.jdx,
Brightness/WHITE_-20_20.jdx

and

Hue/WHITE_5_5.jdx,
Hue/WHITE_10_10.jdx,
Hue/WHITE_15_15.jdx,
Hue/WHITE_20_20.jdx,
Hue/WHITE_25_25.jdx,
Hue/WHITE_30_30.jdx,
Hue/WHITE_35_35.jdx,
Hue/WHITE_40_40.jdx

Pre-processing spectral data

We now want to calibrate the spectra using the white reference at the correct angle. Below are a set of functions to perform this step on .ProcSpec files.

For this example, we will work on the files provided in `Data_HelFur.zip`. We must therefore start by decompressing the zip archive

```
unzip("Data_ESM.zip")
```

Here is a helper function modified from R package `lightR` (<https://github.com/bisaloo/lightR>) to output a dataframe with the white reference, the black reference and the raw count data in separate columns (instead of the processed normalised data):

```

parse_jdx <- function(filename) {
  content <- readLines(filename)

  # According to the standard, all blocks must start and end
  # in this way:
  blockstarts <- grep("^##TITLE=", content)[-1]
  blockends   <- grep("^##END=", content)[-4]

  blocktype <- content[blockstarts]
  blocktype <- tolower(gsub(".+: ([[[:alpha:]])+ SPECTRUM$",
                           "\\\1",
                           blocktype))

  get_data <- function(index) {
    # Data is contained in lines that do NOT start with ##
    data <- grep("^##", content[blockstarts[index]:blockends[index]],
                  value = TRUE, invert = TRUE)
    data <- strsplit(data, ",")
    data <- do.call(rbind, data)
  }

  scope_data <- get_data(which(blocktype=="processed"))
  dark_data <- get_data(which(blocktype=="dark"))
  white_data <- get_data(which(blocktype=="reference"))

  data <- cbind(scope_data[,1],
                  dark_data[,2],
                  white_data[,2],
                  scope_data[,2])
  colnames(data) <- c("wl", "dark", "white", "scope")
  data <- data.frame(apply(data, 2, as.numeric))
  data$processed <- with(data, (scope - dark) / (white - dark) * 100)

  return(data)
}

```

Let us pre-process the spectra for brightness parameters estimation first:

```
# List of files that DO NOT start with "W"
specfiles = list.files("Brightness", pattern = "^[^W].*\\".jdx$",
                      full.names = TRUE, recursive = TRUE)

file_phi_inc = sapply(strsplit(specfiles, "[[:punct:]]"),
                      function(x) as.numeric(x[[length(x)-1]]))
file_phi_col = sapply(strsplit(specfiles, "[[:punct:]]"),
                      function(x) as.numeric(x[[length(x)-2]]))
file_norms = (file_phi_inc - file_phi_col) / 2

preprocess_norms = function(file) {

  file_infos = strsplit(file, "/_\\".")[1][1]

  norms = (as.numeric(file_infos[length(file_infos)-1]) -
            as.numeric(file_infos[length(file_infos)-2])) / 2
  species = file_infos[2]

  whitefiles = list.files(path = "Brightness",
                          pattern = "^WHITE", full.names = TRUE)
  white_phi_inc = sapply(strsplit(whitefiles, "[[:punct:]]"),
                         function(x) as.numeric(x[[length(x)-1]]))
  white_phi_col = sapply(strsplit(whitefiles, "[[:punct:]]"),
                         function(x) as.numeric(x[[length(x)-2]]))
  white_norms = (white_phi_inc - white_phi_col) / 2

  specdf = parse_jdx(file)

  whitedf = parse_jdx(whitefiles[which(file_norms==norms)])

  cor = (specdf$scope - specdf$dark) /
    (whitedf$scope - whitedf$dark) * 100

  res = data.frame(wl = specdf$wl, cor)

  write.csv(res, gsub("\\".jdx$", ".csv", file),
```

```

        row.names = FALSE)
}

sapply(specfiles, preprocess_norms)

```

We do the same for files used in estimation of hue parameters

```

specfiles = list.files(path = "Hue", pattern = "^\w+\.jdx",
                       full.names = TRUE, recursive = TRUE)

preprocess_span = function(file) {

  # Match all punct but spaces
  file_infos = strsplit(file, "[/_\\.-]")[[1]]
  span = as.numeric(file_infos[length(file_infos)-1]) +
    as.numeric(file_infos[length(file_infos)-2]) + 180 - 720
  species = file_infos[2]

  whitefiles = list.files(path = "Hue",
                          pattern = "^\w+WHITE", full.names = TRUE)
  white_phi_inc = sapply(strsplit(whitefiles, "[[:punct:]]"),
                         function(x) as.numeric(x[[length(x)-1]]))
  white_phi_col = sapply(strsplit(whitefiles, "[[:punct:]]"),
                         function(x) as.numeric(x[[length(x)-2]]))
  white_spans = white_phi_inc + white_phi_col + 180 - 720

  specdf = parse_jdx(file)

  whitedf = parse_jdx(whitefiles[white_spans == span])

  cor = (specdf$scope - specdf$dark) /
    (whitedf$scope - whitedf$dark) * 100

  res = data.frame(wl = specdf$wl, cor)

  write.csv(res, gsub("\.jdx$", ".csv", file),
            row.names = FALSE)
}

```

```

}

sapply(specfiles, preprocess_span)

```

Iridescence parameters estimation

```

suppressPackageStartupMessages(library(pavo))
library(tidyverse)
theme_set(theme_minimal())

```

This function extracts the colour variables we are going to use (H_1 for hue and B_2 for brightness).

```

get_colvar_folder = function(folder_path, wlim = c(300,700)) {

  spectra_folder = suppressWarnings({
    getspec(folder_path, sep = ",",
            subdir = TRUE, subdir.names = FALSE, lim = wlim)
  })

  spectra_folder = procspec(spectra_folder,
                            opt = "smooth",
                            fixneg = "zero")

  colvar_folder = summary(spectra_folder, subset = c("H1", "B2"))
  colvar_folder$I = sapply(strsplit(rownames(colvar_folder), "_"),
                           function(x) as.numeric(x[length(x)-1]))
  colvar_folder$C = sapply(strsplit(rownames(colvar_folder), "_"),
                           function(x) as.numeric(x[length(x)]))
  colvar_folder$span = 180 + colvar_folder$I + colvar_folder$C - 720
  colvar_folder$halfspan = colvar_folder$span / 2
  colvar_folder$normale = (colvar_folder$I - colvar_folder$C) / 2

  # Hue for black patches is NA
  colvar_folder[colvar_folder$B2 < 8.5, "H1"] = NA
}

```

```

# Remove artefact at the edges
colvar_folder$H1[colvar_folder$H1 %in% c(300,700)] = NA

# Discard large angles
colvar_folder = colvar_folder[colvar_folder$span < 90,]

return(colvar_folder)
}

```

pavo works with base graphics. If we want to plot spectra using ggplot2, we have to define our own function:

```

ggplot_rspec = function(x) {

  rspecdata = as.rspec(x)
  rspecdata_long = tidyrr::gather(rspecdata, name, spec, -wl)

  g = ggplot(data = rspecdata_long,
              aes(x = wl, y = spec, group = name, col = name)) +
    geom_line() +
    ylab("Reflectance (%)") +
    xlab("Wavelength") +
    scale_colour_manual(values = spec2rgb(rspecdata))
  return(g)
}

```

Let's start by having a look at the spectra before estimating any parameters values:

```

helfur_br_h = getspec("Hue", sep = ",", ext = "csv", subdir = TRUE)

##      Length     Class      Mode
##          8 character character

## 8 files found; importing spectra:

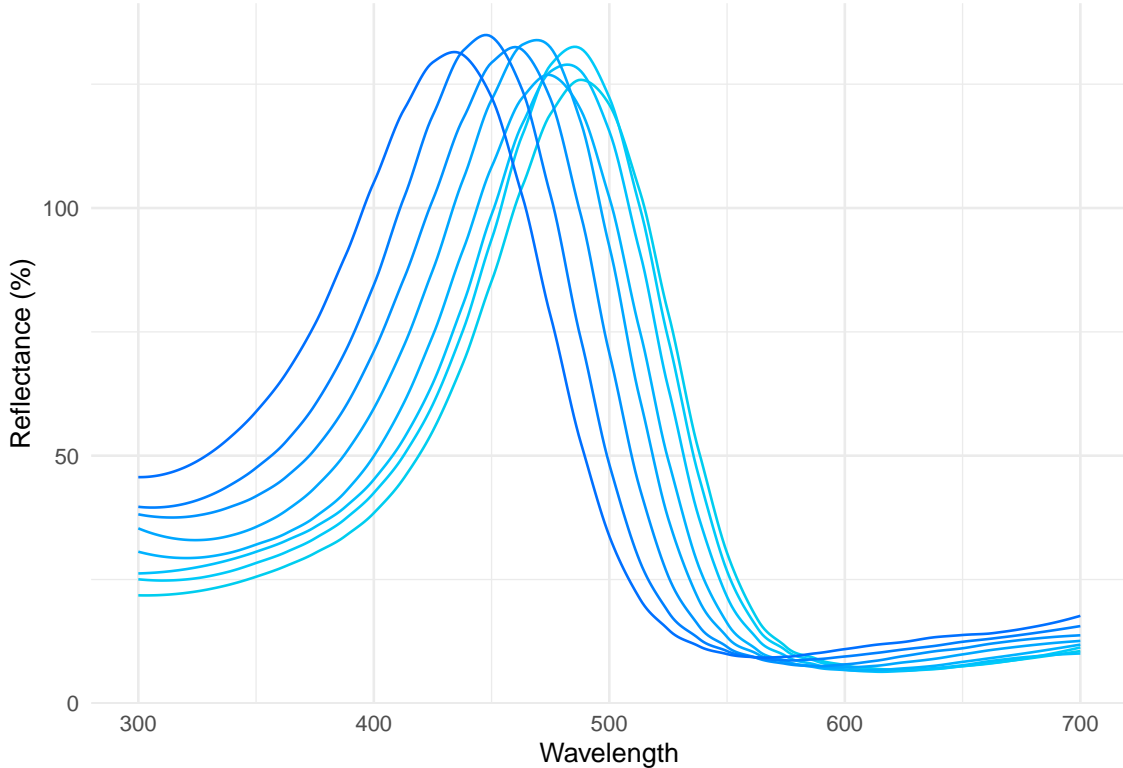
```

```
helfur_br_h = procspec(helfur_br_h, "smooth", "zero")

## processing options applied:
## smoothing spectra with a span of 0.25
## Negative value correction: converted negative values to zero
```

```
ggplot_rspec(helfur_br_h) + theme(legend.position = "none")
```

```
## wavelengths found in column 1
```



```
helfur_br_b = getspec("Brightness", sep = ",", ext = "csv",
                      subdir = TRUE)
```

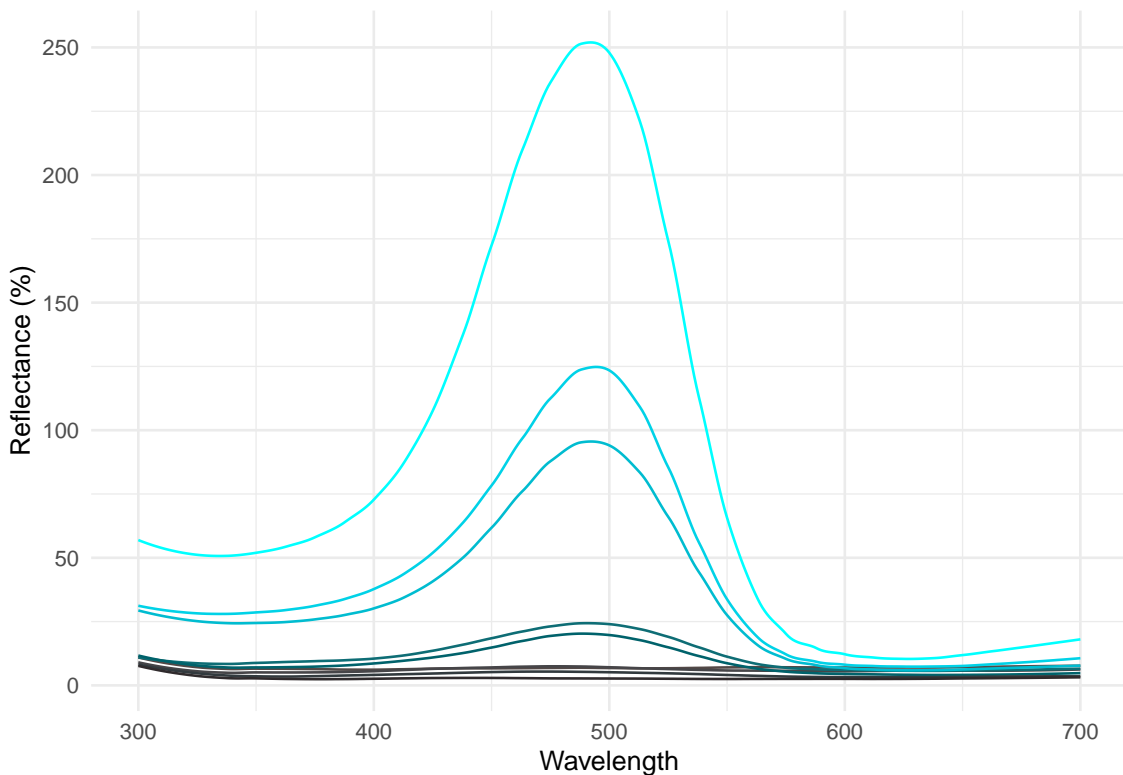
```
##      Length    Class     Mode
##          9 character character

## 9 files found; importing spectra:
```

```
helfur_br_b = procspec(helfur_br_b, "smooth", "zero")
## processing options applied:
## smoothing spectra with a span of 0.25
## Negative value correction: converted negative values to zero
```

```
ggplot_rspec(helfur_br_b) + theme(legend.position = "none")
```

wavelengths found in column 1



Get the values of hue and brightness

```
helfur_br_hvar = get_colvar_folder("Hue")
##      Length     Class      Mode
##      8 character character
```

```

## 8 files found; importing spectra:

## processing options applied:
## smoothing spectra with a span of 0.25
## Negative value correction: converted negative values to zero

helfur_br_hvar$rgb = spec2rgb(helfur_br_h)
helfur_br_bvar = get_colvar_folder("Brightness")

##      Length     Class      Mode
##           9 character character

## 9 files found; importing spectra:
## processing options applied:
## smoothing spectra with a span of 0.25
## Negative value correction: converted negative values to zero

helfur_br_bvar$rgb = spec2rgb(helfur_br_b)

```

We first define the simple normal and cos functions that will be used for brightness and hue.

```

fnorm = function(x, Bmax, t, gammaB) {
  Bmax * exp(-0.5*(x-t)^2/gammaB^2)
}
fcos = function(x, Hmax, gammaH) {
  Hmax * cos(gammaH * x / 180 * pi)
}

```

We then define the functions that find the sets of parameters for brightness and hue optimized in non linear least square method.

```

find_params_nls_normale = function(brightness_folder) {

  maxi = max(brightness_folder$B2)
  norm = brightness_folder$normale[which.max(brightness_folder$B2)]
  sigm = with(brightness_folder, {
    abs(normale[which.min(abs(B2 - exp(-0.5) * maxi))]) - norm)
  })
}

```

```

    })

fit = nls(B2 ~ fnorm(normal, Bmax, t, gammaB),
           data = brightness_folder,
           start = c("Bmax"=maxi, "t"=norm, "gammaB"=sigm),
           lower = c("Bmax"=0, "t"=-50, "gammaB"=0),
           algorithm = "port",
           nls.control(warnOnly = TRUE))

return(summary(fit)$coefficients[,1])
}

find_params_nls_span = function(hue_folder) {

hue_folder = hue_folder[!is.na(hue_folder$H1),]

if (nrow(hue_folder)<2) {
  # If only one measurement, we can't estimate parameters

  return(rep(NA,2))
} else {

  maxi = max(hue_folder$H1)
  s = 0.6

  fit = nls(H1 ~ fcov(halfspan, Hmax, gammaH),
            data = hue_folder,
            start = c("Hmax"=maxi, "gammaH"=s),
            control = nls.control(warnOnly = TRUE))

  return(summary(fit)$coefficients[,1])
}
}
}

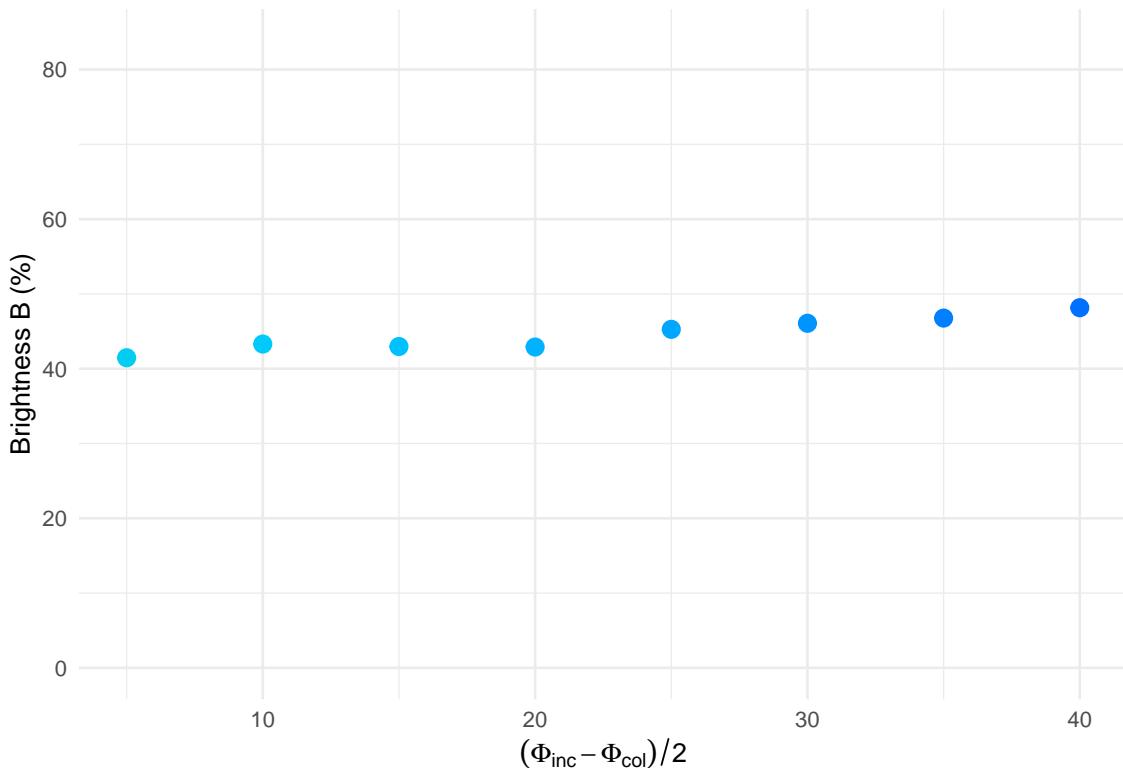
```

We then perform nonlinear least square optimization on our example.

```
helfur_br_bregres = find_params_nls_normale(helfur_br_bvar)
helfur_br_hregres = find_params_nls_span(helfur_br_hvar)
```

We further plot the results, along with the estimated parameter values

```
helfur_br_hvar %>%
  ggplot(aes(x = halfspan, y = B2, col = factor(halfspan))) +
  geom_point(size = 3) +
  xlab(expression((Phi[inc]-Phi[col])/2)) +
  ylim(c(0, max(helfur_br_bvar$B2, helfur_br_hvar$B2))) +
  ylab("Brightness B (%)") +
  scale_color_manual(values = unname(spec2rgb(helfur_br_h))) +
  theme(legend.position = "none")
```

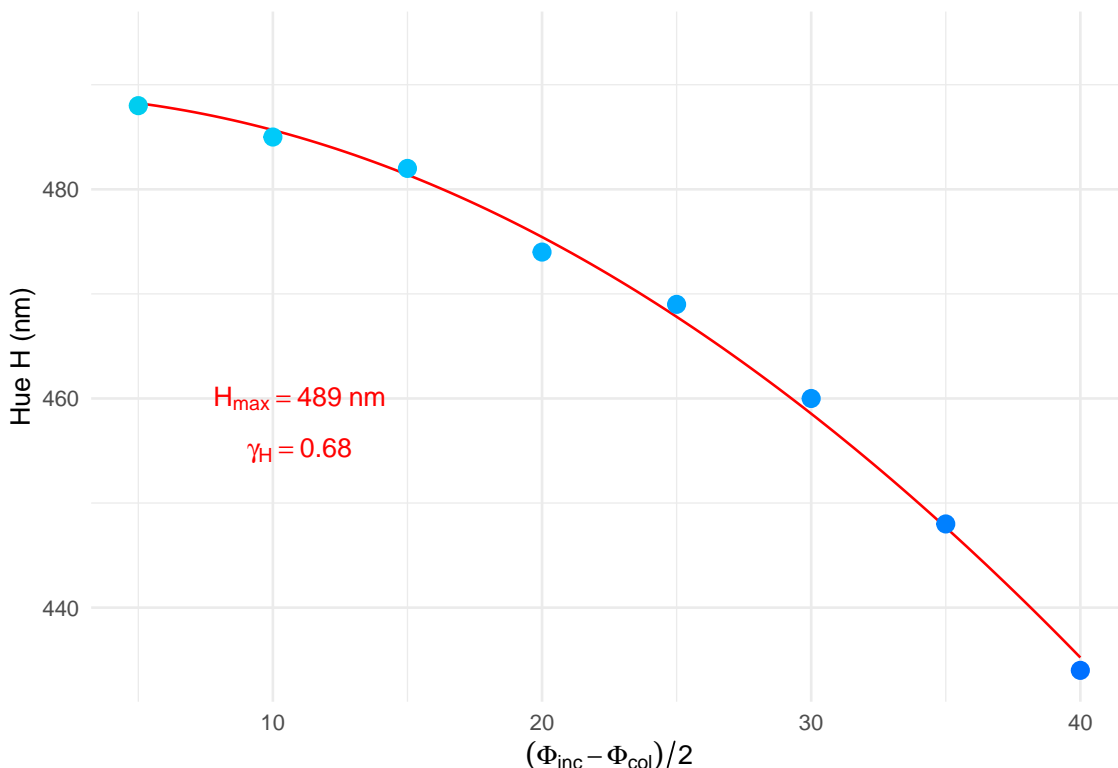


```
helfur_br_hvar %>%
  ggplot(aes(x = halfspan, y = H1, col = factor(halfspan))) +
  xlab(expression((Phi[inc]-Phi[col])/2)) +
```

```

stat_function(fun = fcos, args = helfur_br_hregres, color = "red") +
geom_point(size = 3) +
ylim(range(helfur_br_bvar$H1, helfur_br_hvar$H1, na.rm = TRUE)) +
ylab("Hue H (nm)") +
scale_color_manual(values = unname(spec2rgb(helfur_br_h))) +
theme(legend.position = "none") +
annotate("text", x = 11, y = 460, color = "red",
label = sprintf("Hmax == %.0f nm",
helfur_br_hregres[["Hmax"]]),
parse = TRUE) +
annotate("text", x = 11, y = 455, color = "red",
label = sprintf("γH == %.2f",
helfur_br_hregres[["gammaH"]]),
parse = TRUE)

```

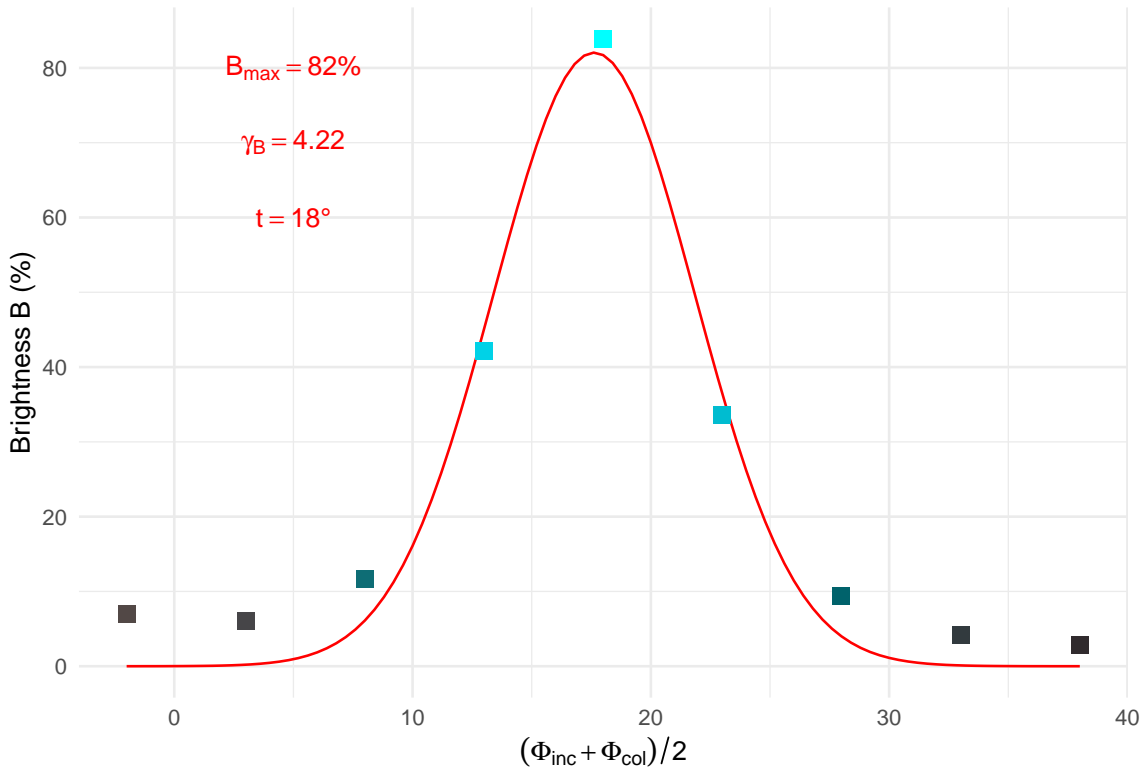


```

helfur_br_bvar %>%
ggplot(aes(x = normale, y = B2, col = factor(normale))) +

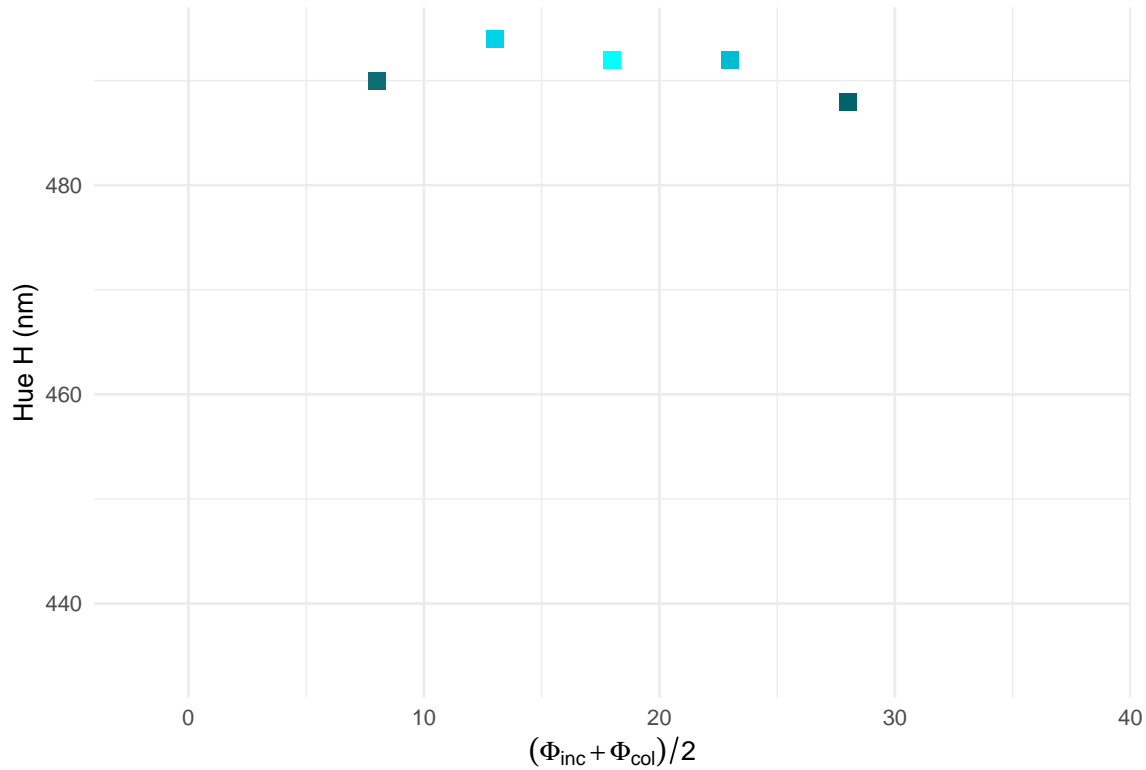
```

```
stat_function(fun = fnorm, args = helfur_br_bregres, color = "red") +
  geom_point(shape = "square", size = 3) +
  xlab(expression((Phi[inc]+Phi[col])/2)) +
  ylim(c(0, max(helfur_br_bvar$B2, helfur_br_hvar$B2))) +
  ylab("Brightness B (%)") +
  scale_color_manual(values = unname(spec2rgb(helfur_br_b))) +
  theme(legend.position = "none") +
  annotate("text", x = 5, y = 80, color = "red",
           label = sprintf("B[max]== %.0f%%", helfur_br_bregres[["Bmax"]]),
           parse = TRUE) +
  annotate("text", x = 5, y = 70, color = "red",
           label = sprintf("gamma[B]== %.2f", helfur_br_bregres[["gammaB"]]),
           parse = TRUE) +
  annotate("text", x = 5, y = 60, color = "red",
           label = sprintf("t== %.0f°", helfur_br_bregres[["t"]]),
           parse = TRUE)
```



```
helfur_br_bvar %>%
  ggplot(aes(x = normale, y = H1, col = factor(normale))) +
  geom_point(shape = "square", size = 3) +
  xlab(expression((Phi[inc]+Phi[col])/2)) +
  ylim(range(helfur_br_bvar$H1, helfur_br_hvar$H1, na.rm = TRUE)) +
  ylab("Hue H (nm)") +
  scale_color_manual(values = unname(spec2rgb(helfur_br_b))) +
  theme(legend.position = "none")
```

```
#> # Warning: Removed 4 rows containing missing values (geom_point).
```



Supplementary figures

Range of parameters estimated for hummingbirds and butterflies

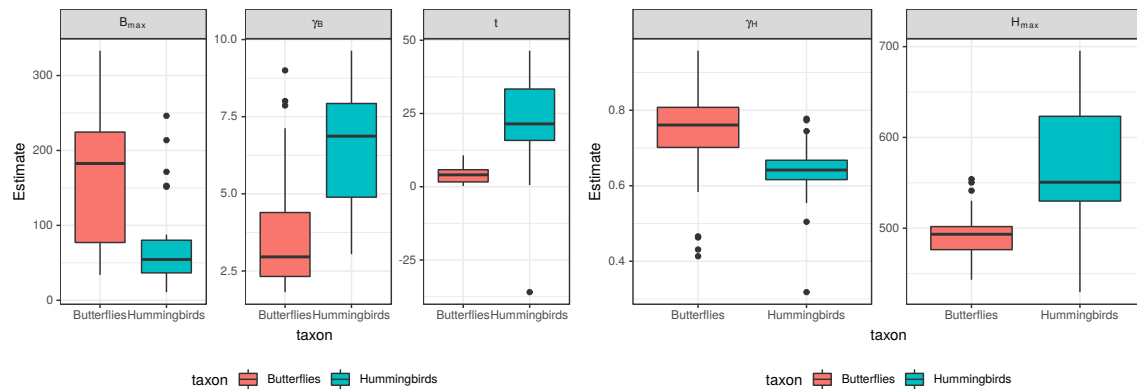


Figure 2: Both hummingbirds and butterflies display a large diversity of hues and brightness, as well as angle dependency in hue and brightness. The butterflies species we measured tend to have multilayer structure parallel to the sample surface (no tilt), which is not the case for hummingbird. The outlier for tilt in hummingbirds is the back of *Aglaeactis cupripennis*.

Tests for correlation between iridescence parameters

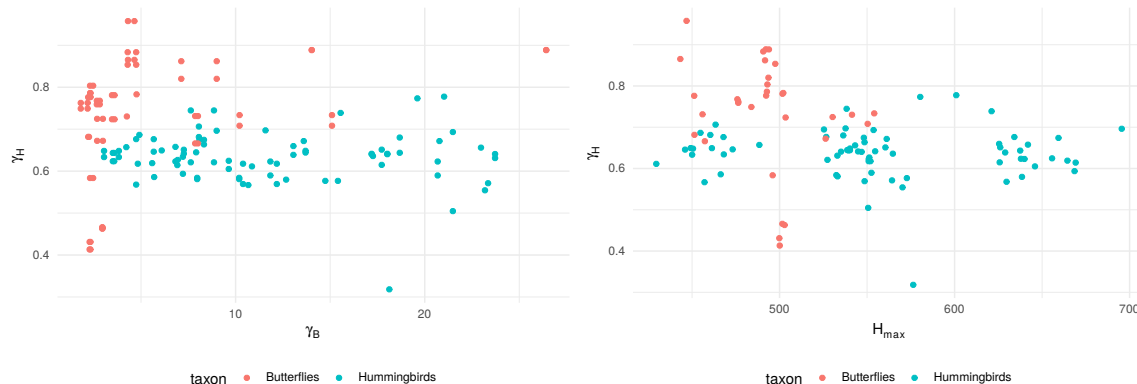


Figure 3: No correlation between hue and brightness angular dependency (γ_H and γ_B respectively) or between hue dependency and hue at a given angle (γ_H and H_{max})

Illustration of the numerical approximations

Fresnel factor is constant for small angles

Let us define functions that compute the value of the Fresnel factor for given values of optical indices n_1 and n_2 and incident angle θ :

```
fresnel_s <- function(n1, n2, theta) {
  theta = theta * pi / 180

  num <- n1*cos(theta) - n2*sqrt(1-(n1*sin(theta)/n2)^2)
  den <- n1*cos(theta) + n2*sqrt(1-(n1*sin(theta)/n2)^2)

  Rs = (num/den)^2

  return(Rs)
}

fresnel_p <- function(n1, n2, theta) {
  theta = theta * pi / 180

  num <- n1*sqrt(1-(n1*sin(theta)/n2)^2) - n2*cos(theta)
  den <- n1*sqrt(1-(n1*sin(theta)/n2)^2) + n2*cos(theta)

  Rp <- (num/den)^2

  return(Rp)
}

fresnel <- function(n1, n2, theta) {

  Rs <- fresnel_p(n1, n2, theta)
  Rp <- fresnel_s(n1, n2, theta)

  R <- 0.5 * (Rp + Rs)

  return(R)
}
```

If we look at the interface between air ($n_{air} = 1$) and melanin ($n_{mel} = 1.8$) for example.

```
n_air=1
n_mel=1.8
```

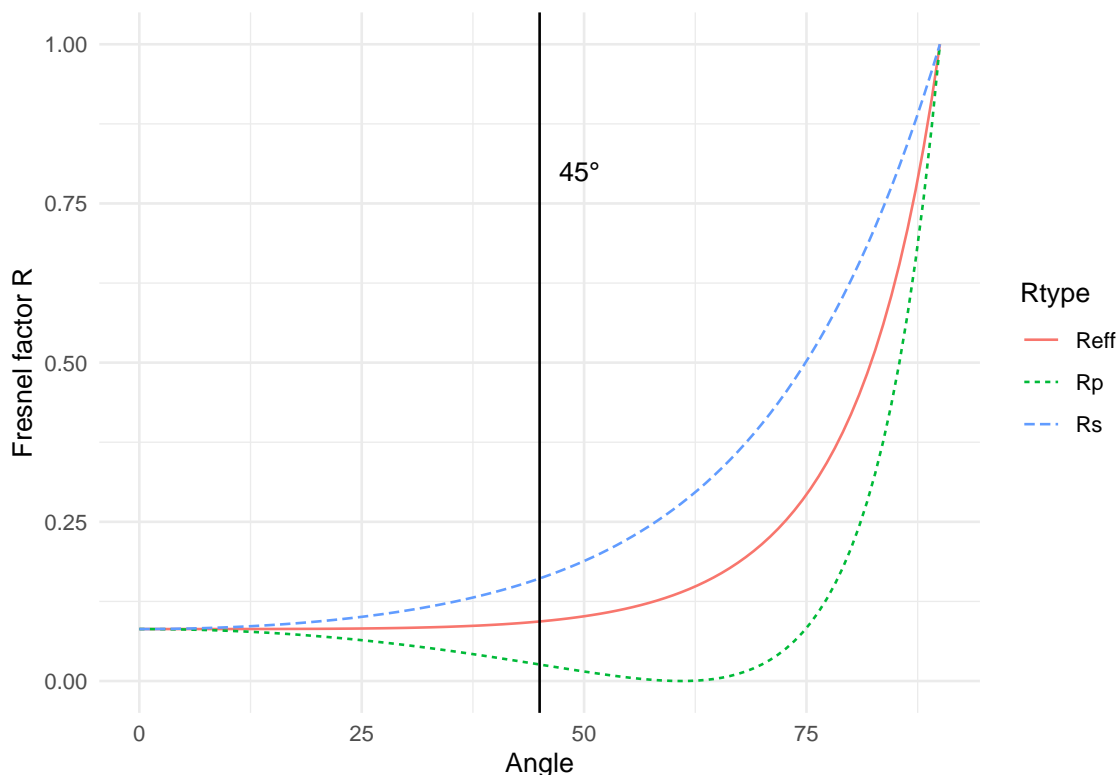
We are focusing on what happens at small angles (assumption 1 in the manuscript):

```
res <- tibble("Angle" = seq(from = 0, to = 90, length.out = 100),
              "Rs" = fresnel_s(n_air, n_mel, Angle),
              "Rp" = fresnel_p(n_air, n_mel, Angle),
              "Reff" = 0.5 * (Rs+Rp))
res <- gather(res, Rtype, "Fresnel factor R", -Angle)
```

where:

- R_s is the amount of reflected light in s polarisation
- R_p is the amount of reflected light in p polarisation
- R_{eff} is the total amount of reflected light, no matter the polarisation

```
ggplot(res, aes(x = Angle, y = Fresnel factor R,
                 col = Rtype, linetype = Rtype)) +
  geom_line() +
  geom_vline(xintercept = 45) +
  annotate(geom = "text", x = 1.1 * 45, y = 0.8, label = "45°")
```



We can notice that at an air/melanin interface, the amount of reflected light (R_{eff}) is relatively constant between 0° and 45° .

Reflectivity in the transfer matrix model for small angles

Simulations can only estimate what happens when the angular span varies. Because the signal reflected out of the specular position is due to the disorder in the alignment of the multilayer, it cannot be properly tested through simulations. It would lead to a circular reasoning where the output is defined in the input.

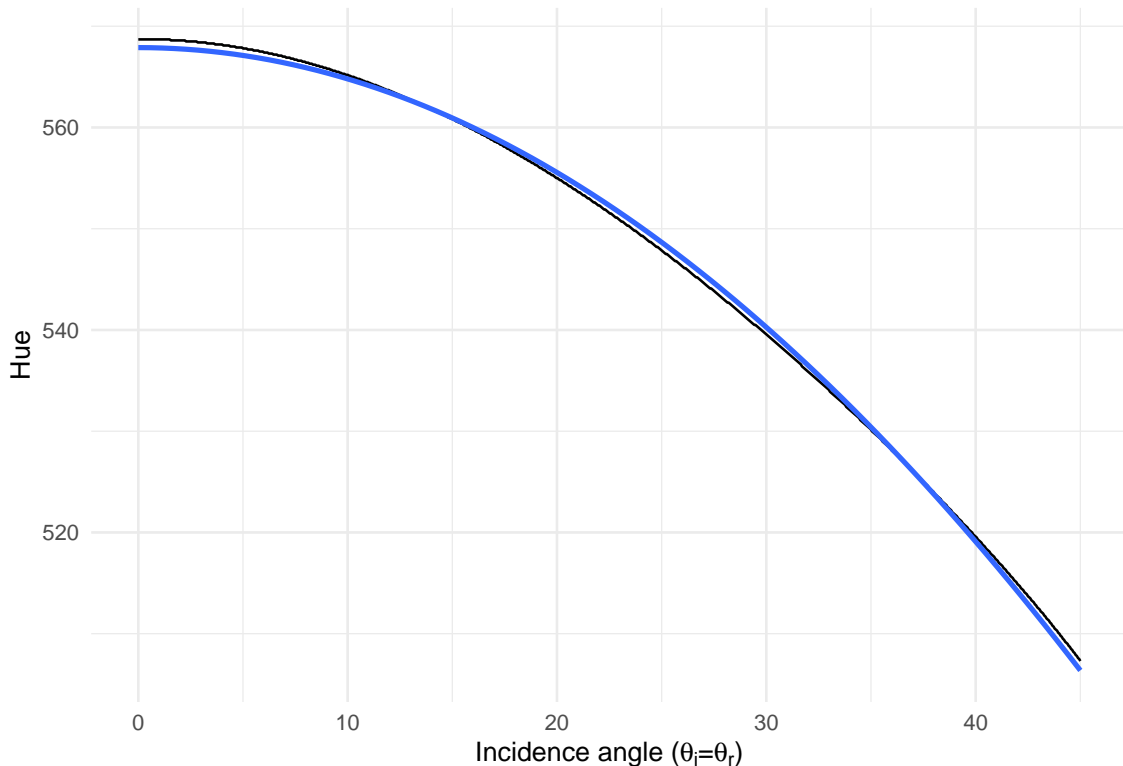
We ran simulations using a transfer matrix model (Yeh 2005) implemented in the python package EMpy (Lbolla 2018; <https://lbolla.github.io/EMpy/>).

Hue

First, we simulated a 10 layers multilayer where each layer was composed of 100nm melanin-100nm air-100nm melanin, separated by 100nm keratin (KK-type in Dürer 1975, that can for example be found in some hummingbirds and starlings iridescent feathers).

```
res_transferrmatrix = read.csv("res_transferrmatrix.csv")

ggplot(res_transferrmatrix, aes(x = Thetas, y = H1_empty)) +
  geom_line() +
  geom_smooth(method = "nls",
    formula = y ~ Hmax * cos(gammaH*x*pi/180),
    method.args = list(start = c(Hmax=570, gammaH=0.6)),
    se = FALSE) +
  ylab("Hue") +
  xlab(expression("Incidence angle ("*theta[i]*"="*theta[r]*")"))
```



The simulation result is in black and the fit by a cosine function is in blue.

Even without an ideal multilayer ($n_1e_1 \neq n_2e_1$ in this simulation), the approximation of the hue depending on the angle by a cosine function is quite good.

```
nls_huecos = nls(H1_empty ~ a * cos(b*Thetas*pi/180),
  res_transferrmatrix,
```

```

start = c(a = 560, b = 0.6)
pred_huecos = predict(nls_huecos, res_transfmatrix$Thetas)

compute_relerror <- function(obs, th) {
  diff = abs(obs-th)
  reldiff = diff/th
  relerror = max(reldiff) * 100

  return(relerror)
}

```

At worst, the error made by this approximation is 0.20%.

Brightness

Here, we test different types of multilayer structures:

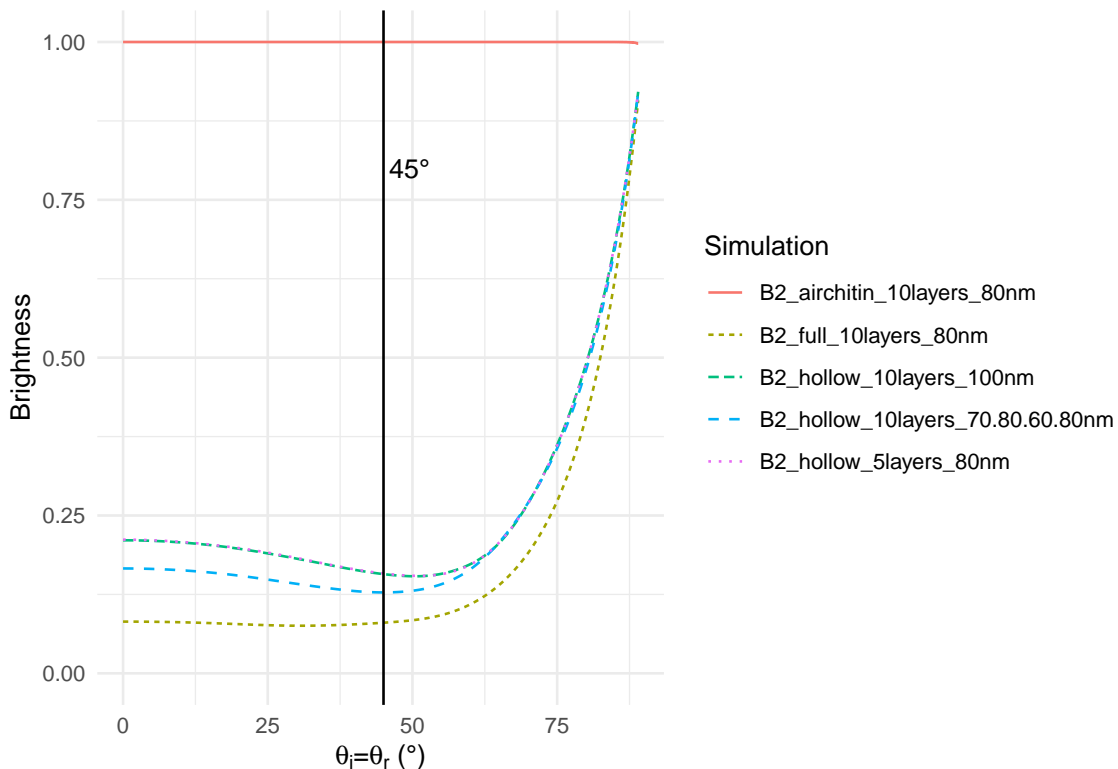
- (100nm keratin / 100nm melanin / 100nm air / 100nm melanin) * 10
- (70nm keratin / 80nm melanin / 60nm air / 80nm melanin) * 10
- (80nm keratin / 80nm melanin / 80nm air / 80nm melanin) * 5
- (80nm keratin / 80nm melanin) * 10
- (80nm air / 80nm chitin) * 10

```

transfmatrix_brightness <- read.csv("merged_brightness.csv") %>%
  gather(Simulation, Brightness, -Theta)

transfmatrix_brightness %>%
  ggplot(aes(x = Theta, y = Brightness,
             col = Simulation, linetype = Simulation)) +
  geom_line() +
  ylim(c(0, 1)) +
  geom_vline(xintercept = 45) +
  annotate(geom = "text", x = 1.1 * 45, y = 0.8, label = "45°") +
  xlab(expression(theta[i] == theta[r] * (°)))

```



```
maxdist2mean = function(vec) {
  max(abs(vec - mean(vec))) * 100
}
maxrelerror = function(vec) {
  max(abs(vec - mean(vec)) / vec) * 100
}
transfermatrix_brightness %>%
  filter(Theta <= 30) %>%
  group_by(Simulation) %>%
  summarise(Maximum relative error = maxrelerror(Brightness),
             Maximum absolute error = maxdist2mean(Brightness)) %>%
knitr::kable()
```

Simulation	Maximum relative error	Maximum absolute error
B2_airchitin_10layers_80nm	0.0000134	0.0000134
B2_full_10layers_80nm	4.9678934	0.3746396

Simulation	Maximum relative error	Maximum absolute error
B2_hollow_10layers_100nm	10.5005369	1.9078967
B2_hollow_10layers_70.80.60.80nm	11.1961421	1.5877553
B2_hollow_5layers_80nm	10.4041522	1.9015925

Approximation of a sum of cosine functions by a single cosine function for small angles

We test the validity of the approximation $\cos(x) + \cos(\alpha x) \approx 2\cos\left(\sqrt{\frac{1+\alpha^2}{2}}x\right)$ (used for the final step in the demonstration of hue equation in the manuscript).

We consider angles between 0° and 90° . More specifically, we are interested in angles smaller than 45° (small angles assumption)

```
ang <- seq(from = 0, to = pi/4, length.out = 100)
```

For biological multilayer structures, $\alpha = \frac{n_1}{n_2}$. This ratio is unlikely to be greater than 2. For example, in the case of an air-melanin interface, $\alpha = \frac{1.8}{1} = 1.8 < 2$. We however test for different values of α between 0 and 2 to test its influence.

```
alpha <- seq(from = 0, to = 2, by = 0.01)
```

Now for the values of the two functions:

```
exact <- outer(ang, alpha, function(x,y) cos(x) + cos(x * y))

approx <- outer(ang, alpha, function(x,y) 2*cos(sqrt((1+y^2)/2)*x))
```

For nice ggplot2 plots, we need to convert exact and approx to data.frames

```
suppressPackageStartupMessages(library(reshape2))
exact_df <- melt(exact,
                  value.name = "exact",
                  varnames = c("ang", "alpha"))
approx_df <- melt(approx,
```

```

            value.name = "approx",
            varnames = c("ang", "alpha"))
final_df <- merge(exact_df, approx_df)
final_df$ang <- ang[final_df$ang]*180/pi

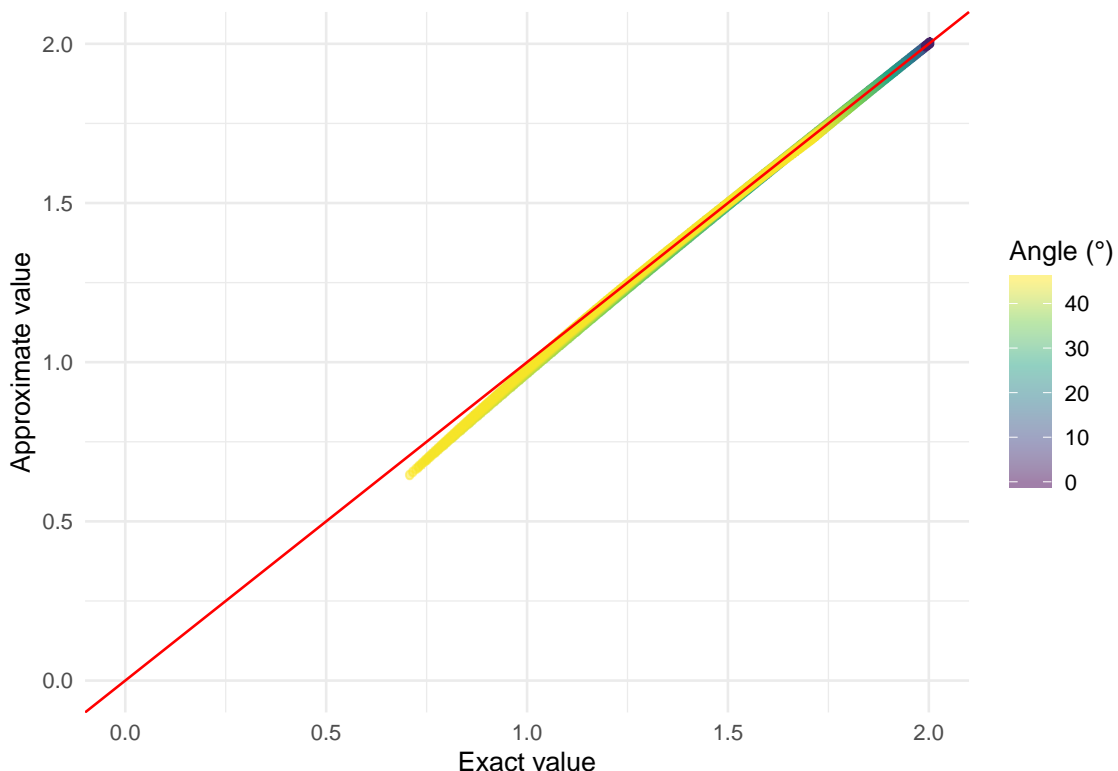
```

Everything is now ready for the plot itself:

```

library(ggplot2)
ggplot(final_df, aes(x = exact, y = approx, col = ang)) +
  geom_point_rast() +
  scale_color_viridis_c(alpha = 0.5) +
  geom_abline(slope = 1, intercept = 0, color = "red") +
  theme_minimal() +
  lims(x = c(0, 2), y = c(0, 2)) +
  xlab("Exact value") +
  ylab("Approximate value") +
  labs(color = "Angle (°)")

```



The data points are along the $x = y$ line (first bissectrice). This means that the numerical approximation is very good for angles smaller than 45° .

Hummingbird iridescence: an unsuspected structural diversity influences colouration at multiple scales

Keywords: Iridescence, Melanosomes, Structural colours, Transfer matrix models, Comparative analyses, Trochilidae.

Manuscript type: Article.

Prepared using the suggested L^AT_EX template for *Am. Nat.*

Abstract

² Iridescent colours are colours that change depending on the angle of illumination or observation. They are produced when light is reflected by multilayer structures or diffracted by gratings.

⁴ While this phenomenon is well understood for simple optical systems, only a limited number of studies have looked at how complex biological structures interact with light to produce iridescence. There are very few comparative studies at interspecific level (often focusing on a single colour patch for each species), resulting in inaccurate and possibly biased estimations

⁶ of structural diversity. Using an interdisciplinary approach combining physics and biology, we here quantify the colour and structure of 36 hummingbirds species evenly distributed across the

¹⁰ phylogeny. We explore at least 2 patches per species, which are assumed to be under different selective regimes. For each patch, we measure structural features (number of layers, layer width,

¹² irregularity, spacing, etc.) of the feathers at different scales using both optical and electron microscopy and we measure colour using a novel approach which encompasses the full complexity

¹⁴ of iridescence, including its angular dependency. We discover an unsuspected diversity of structures producing iridescence in hummingbirds. We also study the effect of several structural

¹⁶ features on the colour of the resulting signal, using both an empirical and modelling approach. Our findings demonstrate the need to take into account multiple patches per species and suggest

¹⁸ possible evolutionary pressures causing the evolutionary transitions from one melanosome type to another.

Introduction

Hummingbirds are famous for their bright and shiny colours which change with the illumination or observation angle: a phenomenon known as iridescence. Iridescent colours are produced by the interaction of light with periodic nanometre-scale structures such as multilayers or diffraction gratings and are widespread among many taxa (Doucet and Meadows, 2009). But few taxa display colours as bright and as saturated as the hummingbirds (Trochilidae family). Most hummingbird species harbour two visually distinct types of iridescent colour patches, as illustrated in fig. S1: *directional* patches, which are only visible at a very narrow angle range (Osorio and Ham, 2002) and are often very bright and saturated, and *diffuse* patches, for which some colour is visible from any angle (Osorio and Ham, 2002) and that are often not as bright as directional patches. Directional patches are often located on facial or ventral patches and thought to be involved in communication while diffuse patches are often located on dorsal patches and thought to be involved in camouflage (Gruson et al., 2019a). Additionally, although all hummingbird species display some degree of iridescence, striking differences can be noticed between the various species and body patches in terms of brightness (describing how much light is reflected by the object), saturation (describing the colour "purity") and directionality (Del Hoyo et al., 2017).

Yet, the structural bases of this intra-individual and interspecific diversity in colour have been poorly explored until now (but see Dorst 1951). In birds, multilayer structures responsible for iridescence are constituted of stacks of nanometre-scale melanin platelets or rods, sometimes hollow (i.e. with a central cavity filled with air) sometimes solid (i.e. entirely made of melanin), called melanosomes (D'Alba and Shawkey, 2018), included in a keratin matrix (Dürrer, 1977) (as illustrated in fig. 1). Although all of the 336 species in the family are iridescent (Del Hoyo et al., 2017), the multilayer structures of only 14 hummingbird species (represented on the hummingbird phylogeny in fig. S2) have been studied to this day (Dürrer, 1977; Greenewalt et al., 1960; Schmidt and Ruska, 1962; Shawkey et al., 2009; Giraldo et al., 2018; Nordén et al., 2019). These fourteen species all had hollow melanin platelets so this type of melanosome was assumed to be present in all hummingbird species (Dürrer, 1977). However, studies in other families, such as

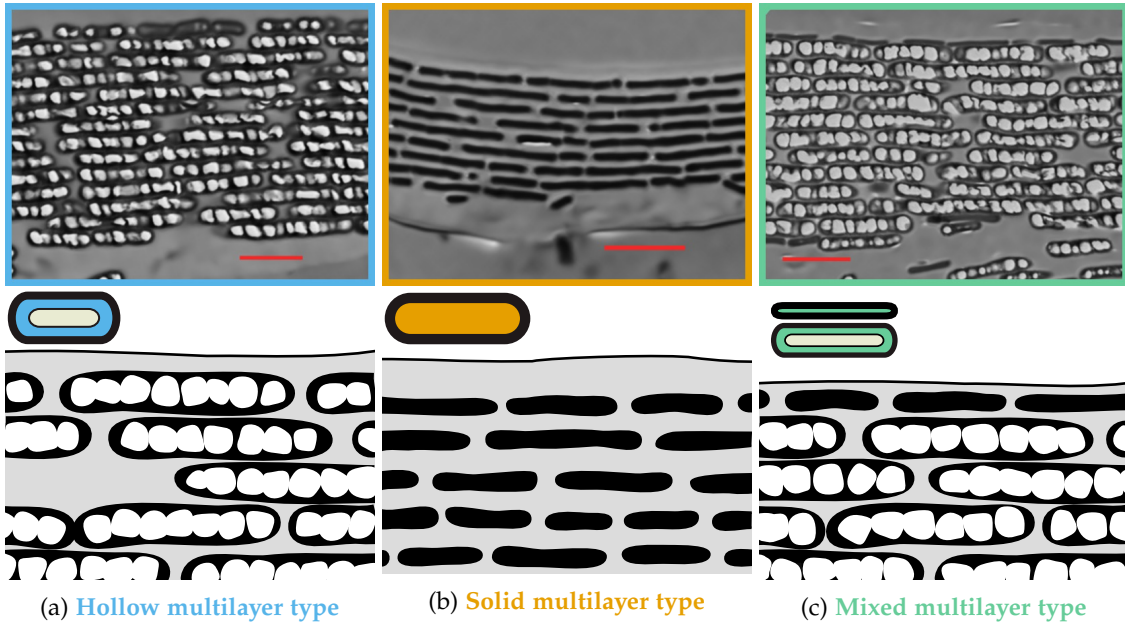


Figure 1: Examples of multilayer structures found in hummingbird barbules (top row) and their schematic representations (bottom row) adapted from Dürrer (1977) with coloured symbols from Maia et al. (2013a). The left panel shows hollow / air-filled platelets found in the breast of *Heliodoxa jacquelineae*, which is the multilayer type that was known before for hummingbirds (Dürrer, 1977; Greenewalt et al., 1960; Schmidt and Ruska, 1962; Shawkey et al., 2009). But we also discover two new types: the middle panel shows solid / melanin-filled platelets found in the back of *Aglaeactis kingi* and the right panel shows a mixed multilayer structure with the outermost layer composed of solid / melanin-filled platelets and the rest of hollow / air-filled platelets, found in the throat of *Chrysolampis mosquitus*. The red bar represents 1 µm.

starlings (Sturnidae), showed that multiple melanosome types can be present in the same family
48 or even the same genus (Dürrer, 1977; Maia et al., 2013a), raising questions about the distribution
of melanosome types and the evolution of iridescence in hummingbirds.

50 In this study, we aim at addressing three fundamental questions for the study of iridescence
in hummingbirds but also in living organisms in general: 1) which type(s) of melanosomes exist
52 in hummingbirds and, if several exist, how are they distributed across hummingbird phylogeny?
2) do the different types result in different colour signals? 3) How do quantitative structural
54 features (e.g. layer thickness, number of layers, etc.) influence the resulting colour?

To answer these questions, we adopted a mixed approach, using both empirical measure-
56 ments on hummingbird iridescent feathers and transfer matrix optical simulations. We sampled

one diffuse and one directional patch in 36 hummingbird species evenly distributed across the
58 phylogeny (species position in the phylogeny shown in fig. S2).

Diffuse and directional patches are thought to be under different selection regimes and we
60 accordingly formulate the following predictions: we predict that directional patches, which are
often located on body areas involved in communication, should reflect overall more light, and
62 produce more saturated colours than diffuse patches, as these characteristics are often important
in mate choice and quality advertising (Hill, 1990; Loyau et al., 2007; Kemp, 2007, 2008). On the
64 other hand, we predict that diffuse patches, which are often located on body area involved in
camouflage should display a lower angle dependency of hue. Indeed, changes in colouration
66 may cause "colour flashes" and alert a potential predator of the bird presence.

Additionally, hummingbirds present sickle-like shaped barbules (Dorst, 1951; Dürrer, 1977),
68 illustrated in figs S3 and S4. We predict that this unusual shape may produce brighter colours.
Indeed, it may allow for a better interlocking of adjacent barbules and thus a higher spatial
70 coherence, leading to a stronger interference pattern and ultimately brighter colours.

The detailed structural features of the multilayers for each patch were determined using
72 Transmission Electron Microscopy (TEM) observations. For each patch, we also took colour mea-
surements using a new method described in Gruson et al. (2019b) that allows the quantification of
74 all iridescence characteristics, including angular dependency of hue and brightness. All analyses
were performed by taking into account the phylogeny (comparative analyses), so as to prevent
76 pseudo-replication due to shared ancestry between species (Felsenstein, 1985).

Methods

Colour measurements

We selected 36 species of hummingbirds evenly distributed across the phylogeny (see fig. S2;
78 phylogeny data from Jetz et al. (2012)). For each species (excluding species that only had diffuse
patches; see fig. 2), we sampled feathers on two patches, one diffuse (colour visible at many
82 angles; often on dorsal patches) and one directional (colour visible over a small angle range;

often on facial patches) from specimens from the collection of the Muséum National d'Histoire
84 Naturelle, in Paris. Feathers were carefully cut using surgical scissors and were only manipulated
85 using tweezers, so as not to remove or deposit any grease on the sample or modify barb
86 arrangement.

Iridescence was quantified using the method published in Gruson et al. (2019b). Briefly, we
88 used a purpose-built goniometer to precisely quantify hue and brightness angular dependency
89 in all directions. Using this method, brightness and its angular dependency can be summarised
90 by two parameters: the maximum brightness B_{max} and the angular dependency of brightness γ_B
91 while hue and hue angular dependency are defined by two parameters: the maximum hue H_{max}
92 (reached when the observer and the incoming light are in the same direction) and the angular
93 dependency of hue γ_H . The saturation is expressed by the full width at half maximum (FWHM)
94 of the spectra and does not change with angle (low values of FWHM correspond to saturated
95 colours). We recorded reflectance spectra with a 300 W Xenon lamp and an OceanOptics USB4000
96 spectrometer and two separate optical fibres for illumination and collection. All spectra were
97 taken relative to a diffuse white spectralon standard (WS2 Avantes). Parameters were estimated
98 using Bayesian non linear-regression with the brms R package (Bürkner, 2017; R Core Team,
99 2017), which yielded slightly better results than non-linear least squares. All variables but the hue
100 angular dependency γ_H were repeatable between species, as reported in table S1. We also defined
101 an additional variable called "overall reflectance" which takes into account both the specular and
102 the diffuse reflectance of a sample and which is calculated with the formula $2\sqrt{2\pi}B_{max}\gamma_B$ (Gruson
103 et al., 2019b).

104 *Electronic and optical microscopy image acquisition and analysis*

After colour measurement, we prepared feathers for observation with a Transmission Electron
105 Microscope (TEM). Feathers were first dehydrated and then embedded in SPUR resin (detailed
106 protocol in ESM). We used a Leica ultramicrotome to prepare 70 nm cross-sections of the barbules,
107 where the multilayer structures responsible for iridescence are located (Dürrer, 1977). We photograped
108 the resulting cross-section with an optical microscope, which allowed us to measure

¹¹⁰ the angle of the barbule (an measure of barbule shape), the overlap between adjacent barbules,
¹¹² and the variance in the alignment of consecutive barbules (two measures of the interlocking be-
tween adjacent barbules). We then measured structural features at the scale of the multilayer
¹¹⁴ such as the number of layers and their thickness using a TEM microscope (Hitachi HT-7700 TEM
set at 60 keV).

¹¹⁶ Measurements on optical microscopy images were performed manually using the ImageJ
¹¹⁸ computer software while TEM images were analysed using a custom python script, available
in electronic supplementary materials (ESM), relying on the OpenCV python library (201, 2017;
¹²⁰ Python Software Foundation). Briefly, we smoothed the grayscale images using Gaussian blur
and a denoising algorithm. Resulting images were converted to binary black and white images
¹²² using adaptive thresholding, then rotated using automatic contour detection, so as to orientate
the multilayer along the vertical direction. Finally, the number of transitions and the distance
¹²⁴ between them (layer thickness) in the rectangular function were determined for each row of the
image matrix and the most common value was estimated using the mean of a fitted Gaussian
function.

Optical simulations

¹²⁶ We used optical simulations to explore a wider combination of parameter values. The interest is
twofold: 1) increase our limited sample size and 2) remove possible correlations (possibly due to
¹²⁸ evolutionary constraints) between structural parameters.

¹³⁰ We used the EMpy python library (Python Software Foundation; Bolla, 2017), which im-
plements the transfer matrix method described in Yeh (2005) to simulate the reflected specular
spectrum of a multilayer structure. The script used for the simulations is also provided in ESM.

¹³² Because of the large array of parameters influencing the resulting reflectance spectrum (com-
plex refractive index of each layer, layer thicknesses, angle of the incoming light ray, number of
¹³⁴ layers), it was not possible to systematically study the effect of each parameter. To overcome this
issue, we ran 500 iterations of Monte Carlo simulations, for each multilayer type, with structural
¹³⁶ parameters randomly drawn from an interval of biologically relevant values. This interval was

determined from the TEM images (95 % variation interval for each parameter, irrespective of the
138 multilayer type). We had several images for each species and patch combination, which allowed us to ensure that all estimated structural variables were repeatable (table S1).

140 Because there is no disorder in the layer alignment, the brightness in the simulations corresponds to the overall reflectance (diffuse + specular reflectance) in the empirical measurements
142 (computed with the formula $2\sqrt{2\pi}B_{max}\gamma_B$).

144 The results are presented in SI with only the mean and the standard deviation of the parameter influence on the response variable, as appropriate for simulations (because the possibly infinite sample size allows for arbitrary low p-values). Additionally, significance of the effect of
146 a given parameter for a sample size of 72, to match the sample size of empirical data, is shown in table 1, using Cohen's d effect size index.

148 We also analysed the resulting spectra as seen by the hummingbirds using Stoddard and Prum (2008) model, implemented in Maia et al. (2013b, 2019). The gamut of each multilayer
150 type was computed as the volume of the convex hull of the set of points in the tetrahedron representing bird colour space, as in (Stoddard and Prum, 2008).

152 *Predictions*

We can formulate a set of predictions for correlations between colour variables and structural
154 parameters, as well as among colour variables, based on two factors: (i) predictions informed by optical theory and the laws of interferences from multilayers (ii) predictions informed by
156 previous research on colours as a communication channel in animals.

In particular, based on the equation computing the wavelengths at which reflected light rays
158 interfere constructively the most, $mH_{max} = 2(n_1e_1 + n_2e_2)$, we predict that hue (H_{max}) and the angular dependency of hue (γ_H) should depend on layer thickness ($e_1; e_2$) and chemical composition ($n_1; n_2$), as well as interference order (m). The angular dependency of brightness γ_B should only depend on the misalignment between consecutive layers or multilayer, because a
160 perfectly aligned multilayer should reflect all light in a single direction ($\gamma_B = 0$), as detailed in Gruson et al. (2019b). Total reflectance ($2\sqrt{2\pi}B_{max}\gamma_B$) is expected to be positively correlated
162

¹⁶⁴ to the number of layers (because more light is reflected and more rays interfere), the chemical
¹⁶⁵ composition (melanin layers absorb more light) and the spatial coherence of adjacent multilayers
¹⁶⁶ (influenced by the barbule shape and the amount of overlap between adjacent barbules). Finally,
¹⁶⁷ saturation should depend on the variability in layer thicknesses (because it produces a mix of
¹⁶⁸ wavelengths that constructively interfere), the misalignment of consecutive layers, as well as the
¹⁶⁹ number of layers and the chemical content (because selective absorbance of some wavelengths
¹⁷⁰ would increase saturation).

We do not study maximum brightness B_{max} separately as we have shown before that it is
¹⁷¹ strongly correlated with γ_B because of structural reasons (Gruson et al. 2019b; illustrated also in
fig. S9).

¹⁷⁴ Additional predictions are due to the putative function of iridescent colours in humming-
birds: colour on directional patches should be highly saturated and reflect overall more light
¹⁷⁵ than on diffuse patches, as directional patches are thought to be involved in communication
and high brightness and saturation are common quality indicators (Hill, 1990; Loyau et al., 2007;
¹⁷⁶ Kemp, 2007, 2008). In other words, we predict a negative correlation between γ_B and the FWHM
(measure of desaturation, opposite of saturation) as well as overall reflectance.

¹⁸⁰ *Correlations between structure and colour using phylogenetic comparative
analyses*

¹⁸² The different multilayer structures studied in this article are not independent samples from a sta-
tistical point of view. Indeed, all samples come from species that share a common evolutionary
¹⁸³ history. This shared history, represented by species phylogeny, must be taken into account using
phylogenetic comparative analyses (Felsenstein, 1985). However, classic phylogenetic compara-
¹⁸⁴ tive methods do not consider multiple data points per species. Since we measured two patches
per species, we used the Bayesian framework implemented in the R package MCMCglmm (Hadfield,
¹⁸⁵ 2010; R Core Team, 2018), which allows analysing such data (see Delhey et al. (2013) for another
example). Multiple studies have shown that results from comparative analyses are more reliable
¹⁸⁶ when performed on multiple trees drawn from the posterior distribution instead of a consensus

	Variable 1	Variable 2	Empirical	Simulations
Colour/structure	Hue at coincident geometry (H_{max})	Layer thickness	yes	yes
	Hue at coincident geometry (H_{max})	Multilayer type	yes	no
	Overall reflectance ($2\sqrt{2\pi}\gamma_B B_{max}$)	Number of layers	no	no
	Overall reflectance ($2\sqrt{2\pi}\gamma_B B_{max}$)	Multilayer type	yes	yes
	Overall reflectance ($2\sqrt{2\pi}\gamma_B B_{max}$)	Barbule shape	yes	NA
	Directionality ($1/\gamma_B$)	Barbule shape	yes	NA
	Directionality ($1/\gamma_B$)	Multilayer type	yes	NA
	Desaturation (FWHM)	Multilayer type	yes	yes
	Desaturation (FWHM)	Barbule shape	no	NA
	Desaturation (FWHM)	Layer thickness variance	no	NA
Colour/Colour	Desaturation (FWHM)	Number of layers	no	yes
	Desaturation (FWHM)	Layer thickness	NA	no
	Hue shift	Multilayer type	NA	yes
	Hue at coincident geometry (H_{max})	Overall reflectance ($2\sqrt{2\pi}\gamma_B B_{max}$)	yes	no
	Overall reflectance ($2\sqrt{2\pi}\gamma_B B_{max}$)	Directionality ($1/\gamma_B$)	yes	NA
	Overall reflectance ($2\sqrt{2\pi}\gamma_B B_{max}$)	Desaturation (FWHM)	yes	yes
	Desaturation (FWHM)	Directionality ($1/\gamma_B$)	no	NA
	Hue at coincident geometry (H_{max})	Desaturation (FWHM)	yes	yes

Table 1: Predicted correlations between colour variables and structural parameters and the outcome from comparative analyses and simulations for these correlations. The correlations can be due to either the optics governing iridescence and to evolution. As mentioned in the methods, it is possible to get an arbitrary low p-value in simulations by increasing the sample size. To prevent this issue and to be able to compare empirical and simulations results, we chose the same sample size for both (72) and counted a result as significant only when $p < 0.05$ (for simulations) or when the credibility interval did not include 0 (for empirical data). Some correlations could not be tested in the simulations and are marked as NA in the table. If results from the empirical data and the simulation output the same result, it is likely due to the optics governing iridescence but in case of mismatch, it reveals the influence of evolutionary constraints.

tree (Pagel and Lutzoni, 2002; de Villemereuil et al., 2012). To account for such phylogenetic uncertainty, we ran models using the `mulTree` R package (R Core Team, 2018; Guillerme and Healy, 2014) on a set of 100 trees downloaded from [birdtree.org](#) (Jetz et al., 2012). Each model was tested with 3 independent MCMC chains, with 200 000 iterations each, including a 1000 burn-in and a thinning factor of 10 to reduce auto-correlation and memory consumption of the program. Convergence was assessed both visually and using the Gelman-Rubin index. Levels of a factor were deemed significantly different when the estimate of one did not overlap with the credibility interval of the other.

Phylogenetic signal for the type of multilayer on the throat and the back was computed using the δ Bayesian approach for discrete characters described in Borges et al. (2019). Larger values of δ express a higher level stronger phylogenetic signal, i.e. a stronger influence of the evolutionary history on the observed trait values. δ values can be arbitrarily large and significance is evaluated by bootstrapping after shuffling the trait value on the phylogeny.

204

Results

Correlations between colour variables in hummingbird iridescent feathers

206 Preliminary study of correlation between colour parameters, without investigating yet the underlying structural variable, reveals a positive correlation between maximum brightness B_{max} and 208 saturation table S2. Directional patches (low γ_B) also tend to reflect overall more light than diffuse colours (table S3). On the other hand and contrary to our predictions, we find no correlation 210 between γ_B (related to directionality) and saturation (table S2). We also find that long wavelength hues (i.e. red colours) are associated with brighter (table S2) but less saturated colours (table S3).

Iridescence in hummingbirds is produced by several different multilayer types

212 Observations of barbule cross-sections with a Transmission Electron Microscope (TEM) confirm 214 that some hummingbird multilayers contain only hollow melanosomes (left panel in fig. 1). But we also discover that some species have multilayers with solid melanosomes (central panel in

²¹⁶ fig. 1). Additionally, we find a highly unusual multilayer structure in some species, where the
²¹⁸ outermost layer is composed of solid melanosomes while the rest of the multilayer is composed
²²⁰ of hollow melanosomes (right panel in fig. 1). We refer to this multilayer structure type as the
mixed multilayer type in the rest of this article. Lastly and importantly, our observations show for
the first time that a single hummingbird species can have different multilayer types depending
on the patch location on the body as shown in fig. 2 and fig. S5.

²²² The thickness of the melanin layer is very similar between hollow and solid melanosomes
(fig. S6). However, because solid melanosomes contain only one layer of melanin (versus two
²²⁴ layers of melanin surrounding one layer of air for hollow melanosomes), they are overall much
smaller than hollow melanosomes. Hollow melanosome thicknesses range from 130 nm to 228 nm
²²⁶ with the air void filling on average 44 % of the total thickness, while solid melanosomes measure
between 29 nm and 80 nm. The total number of melanin layers (2 per hollow melanosomes vs 1
²²⁸ per solid melanosomes) does not significantly differ between the multilayer types (fig. S6). More
detailed data, including variation intervals, relative standard deviations and repeatabilities for
²³⁰ each parameter, is presented in table S1 and fig. S6.

Location on the bird body and optical effects of the different types of multilayers

²³² We find that diffuse patches contain multilayers with only hollow melanosomes more often than
directional patches. At the same time, directional patches contain mixed multilayers more often
²³⁴ than diffuse patches ($\chi^2(2) = 6.8138, p = 0.033$; fig. S10).

²³⁶ There is also a strong phylogenetic signal for the multilayer type on the back ($\delta = 11.03$,
 $p = 0.008$) but not on the throat ($\delta = 1.37, p = 0.067$).

²³⁸ Using phylogenetic comparative analyses, we also find that multilayer structures with only
hollow melanosomes reflect overall more light (diffuse + specular reflectance; table S8) but less
²⁴⁰ saturated colours (i.e. larger FWHM, table S11) than structures with solid melanosomes. Mixed
multilayers have intermediate values compared to solid and hollow multilayer types for both
brightness and saturation. This result is confirmed by transfer matrix simulations, which allow
²⁴² us to explore a much wider range of parameters and ensure this pattern is not caused by a

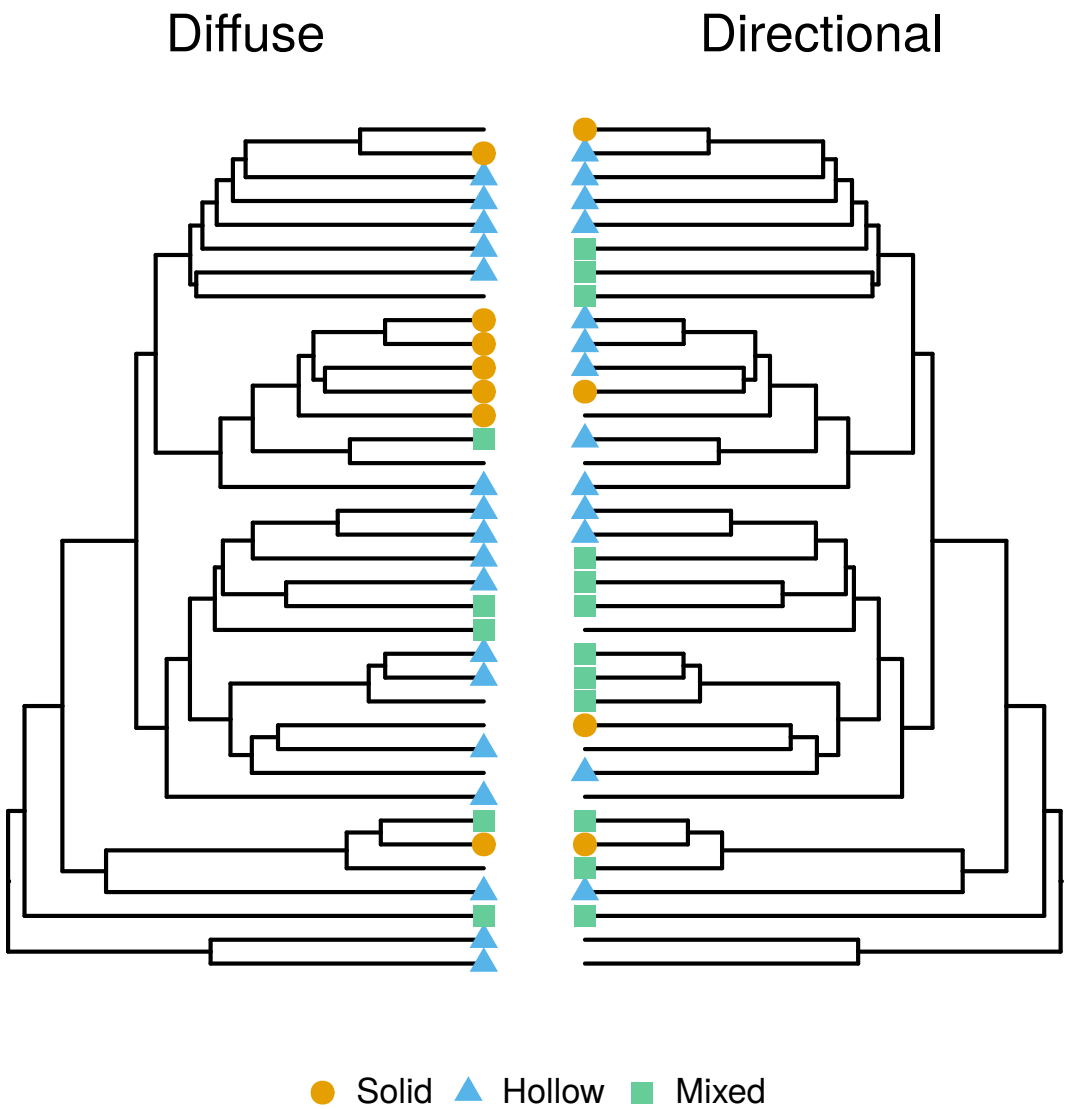


Figure 2: Some hummingbird species use different types of multilayer structures on different patches. For each species, we had one diffuse (left) and one directional (right) patch (diffuse and directional *sensu* Osorio and Ham (2002)). Each tip is a species and tips are in the same order for both trees. Missing data are either species that do not have directional patches (e.g. *Patagona gigas* or species from the Hermit clade) or species that could not be measured due to technical issues. A more detailed version of this figure, with the type of multilayer for each patch and species names is available in SI (fig. S5).

confounding effect (fig. S12 and tables S4 and S5).

²⁴⁴ The different multilayer types also produce different hues, with the mixed type producing the
²⁴⁵ largest diversity of hues in the bird visual space, using simulations based on biologically relevant
²⁴⁶ layer sizes (fig. S13).

²⁴⁷ Finally, the different multilayer structures also differed in their level of iridescence, i.e. how
²⁴⁸ much hue shifts with a change in the angle of illumination or observation, with the hollow
²⁴⁹ type having a larger shift in hue than the solid and the mixed types in the simulations (fig. S11
²⁵⁰ and table S7). This could not be verified on empirical data with hummingbird feathers as this
variable was not repeatable (table S1).

²⁵² *Optical effects of structural features*

²⁵³ At the multilayer level, the number of layers has no effect on overall reflectance in phylogenetic
²⁵⁴ comparative analyses based on empirical data from hummingbird feathers (table S8). Simula-
tions similarly reveal a very weak correlation between the number of layers and brightness
²⁵⁵ (fig. S12 and table S4). On the other hand, a larger number of layers did increase saturation for
both hollow and solid multilayer types but not for the mixed type in the simulations (fig. S12
²⁵⁶ and table S5). Variability in the thickness of melanin, keratin or air layers of a given multilayer
²⁵⁷ did not seem to significantly impact the saturation of the resulting signal (table S5).

²⁵⁸ We show that hue at a given angle configuration (H_{max}) depends on the thickness of the lay-
ers, no matter their chemical composition (air, keratin or melanin), in simulations (table S6) but
²⁵⁹ we only find a significant effect of the thickness of the melanin layer in empirical data (table S10).
²⁶⁰ However, we also find that thicknesses of melanin, keratin and air layer within a given multi-
²⁶¹ layer structure are strongly correlated, as shown in fig. 3, which might hinder our analysis on
²⁶² empirical data. This correlation is not simply due to phylogenetic inertia and the shared history
²⁶³ between species as it remains significant even after taking into account the species phylogenetic
²⁶⁴ relationships (tables S12 to S14). Additionally, the confidence interval of the slope of the correla-
²⁶⁵ tion between the optical thicknesses (thickness times refractive index) of the consecutive layers is
²⁶⁶ often close to 1 but does not contain 1, as shown in fig. 3.

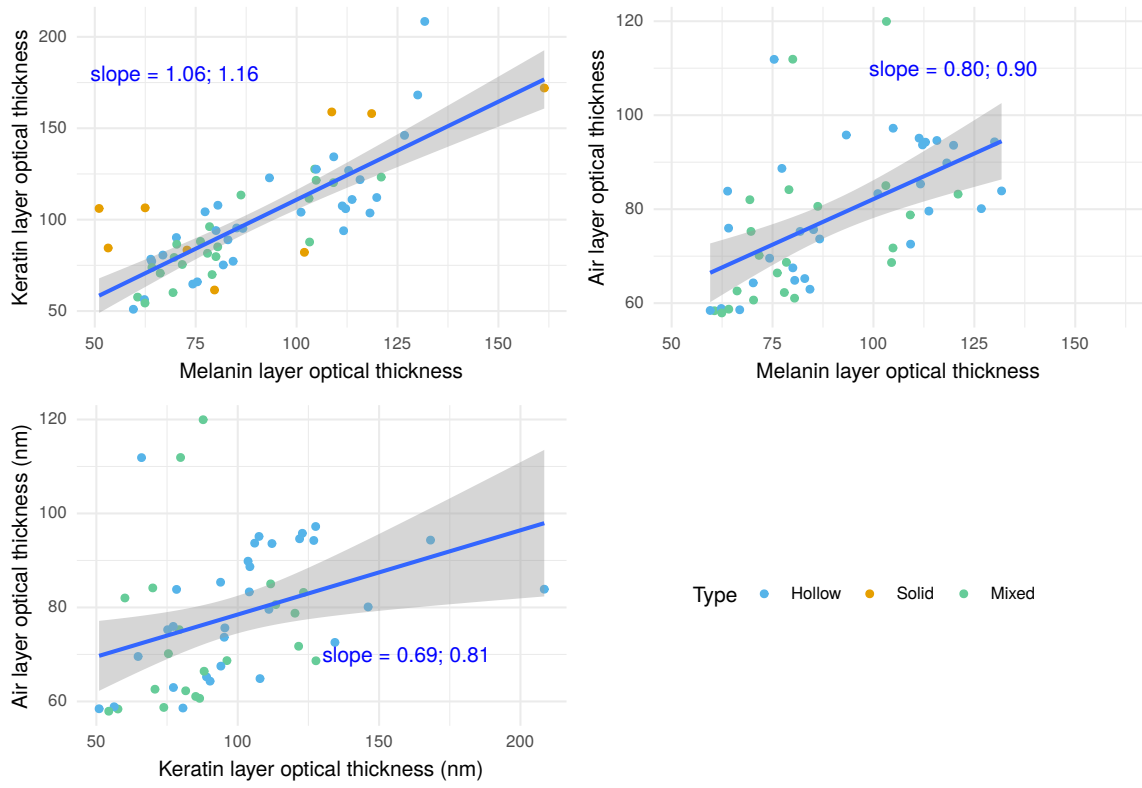


Figure 3: Optical thickness of melanin, keratin and air layers are correlated in hummingbird multilayer structures. Each dot is a multilayer from a given species/patch combination. Correlations are tested by linear models (blue lines on the present figure. Confidence interval of the slopes is in blue as well.) which do not take into account species relatedness, and by comparative phylogenetic analyses using MCMCglmm (tables S12 to S14). There is no data for air layer thickness in solid multilayer types because they do not contain any air.

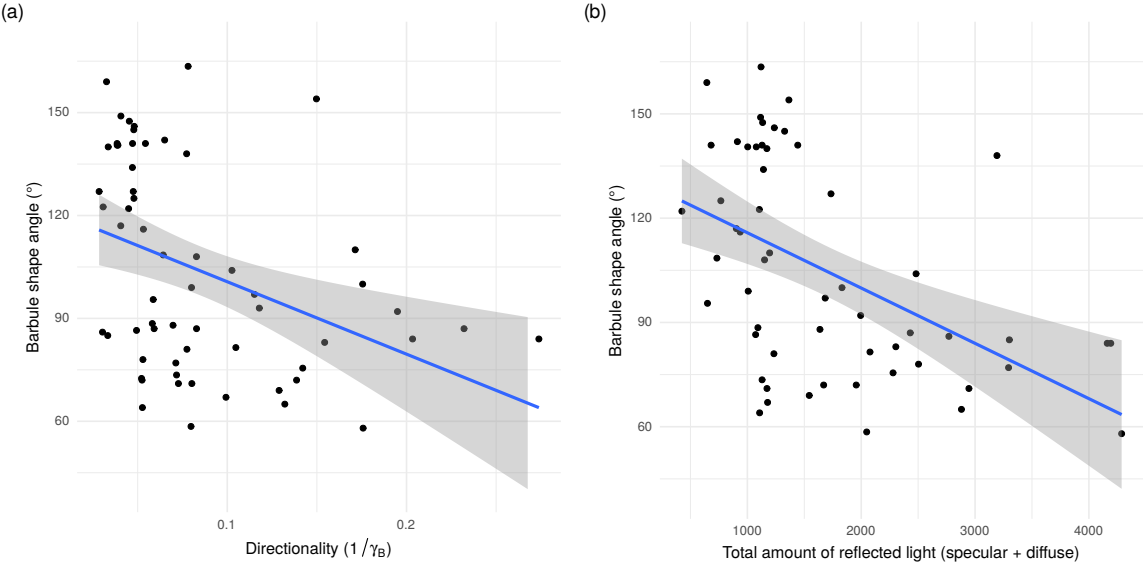


Figure 4: Link between the barbule shape angle and (a) the directionality $1/\gamma_B$ or (b) the total amount of reflected light (specular + diffuse reflected light; computed with the formula $2\sqrt{2\pi}B_{\max}\gamma_B$ from Gruson et al. (2019b)). Barbules with a sickle shape (lower barbule shape angle) produce on average colours which are more directional (lower value of γ_B) and reflect overall more light (taking into account both diffuse and specular reflection). Regression line in blue and the related 95 % confidence interval in grey are fitted by a linear model and only have an illustrative function. Phylogenetic comparative analyses which take into account phylogenetic inertia are presented in table S8.

270 At the barbule level, we find that barbules with a sickle shape (i.e. with a smaller barbule
 271 shape angle, as shown in fig. S4) produce colours that reflect overall more light (taking into
 272 account both diffuse and specular reflection), as illustrated in fig. 4b and table S8. Additionally,
 273 in agreement with our predictions, we show that barbules with a sickle shape also produce more
 274 directional and more saturated colours (fig. 4a and tables S9 and S11). Conversely, variability in
 barbule alignment from the same barb also produces less saturated colours (table S11).

Discussion

Correlations and general characteristics of hummingbird iridescent colours

278 We find many correlations between descriptors of iridescent colours in hummingbirds. In partic-
 279 ular, saturation was negatively correlated with hue (table S2), as expected for interferences from
 280 a multilayer structure. For long wavelength colours, a wider range of wavelengths will indeed
 281 (partially) constructively interfere and contribute to the resulting signal, thereby producing less
 282 saturated colours. Our framework did not allow us to discriminate whether evolutionary con-
 283 straints could also play an additional role in the correlation (i.e. is there a selective pressure for
 284 blue colours to be more saturated than red colours in hummingbirds?)

We nonetheless found additional correlations that are not explained by the physical nature of
 285 hummingbird colours. For example and in accordance with our prediction, we found a positive
 286 correlation between saturation and total reflectance, as could be expected from patches involved
 287 in quality advertising and mate choice (Hill, 1990; Loyau et al., 2007; Kemp, 2007, 2008).

Finally, we showed a correlation positive correlation between hue and overall brightness,
 288 meaning that red colours are on average brighter than blue colours. Two non-mutually exclu-
 289 sive hypotheses can explain this pattern: (i) red colours are often used for communication in
 290 hummingbirds due to a pre-existing sensory bias (Rodríguez-Gironés and Santamaría, 2004) and
 291 communication is often associated with brighter colours, or (ii) blue colours are not as bright
 292 because melanin and keratin absorb more in short wavelengths than in long wavelengths (Leer-
 293 touwer et al., 2011; Stavenga et al., 2015).

Hummingbirds display an unsuspected multilayer diversity

In this study, we discover that hummingbirds do not only have hollow (air-filled) melanosomes
 297 but also solid (melanin-filled) melanosomes. They also sometimes combine both types into a
 298 very unusual multilayer structure that has never been described in any other family, where
 299 the outermost layer is formed by solid melanosomes while the following layers contain hollow

melanosomes.

302 We also discovered that a single species can use different types of multilayer structures at
303 different patch locations on its body (fig. 2 and fig. S5). This means that the type of multilayer
304 found on one patch is not representative of the multilayer type found on all patches for a given
305 species. This finding calls for more careful investigation into the results of previous comparative
306 analyses of bird melanosomes and iridescent colours, as most of them have observed only one
307 patch per species (Dürrer, 1977; Maia et al., 2013a).

308 We also show that the different types of multilayers are not randomly distributed on the
309 bird's body: diffuse patches contained multilayers composed exclusively of hollow or solid
310 melanosomes more often than directional patches. On the other hand directional patches con-
311 tained mixed multilayers more often than diffuse patches (fig. 2 and fig. S10). We find a strong
312 phylogenetic signal for the type of multilayer structure on the back but not on the throat, sug-
313 gesting that the distribution of the multilayer type is mainly due to the phylogeny on the back
314 but likely more strongly influenced by additional selective pressures on the throat.

This suggests that the different multilayer types produce different kinds of colours that are
316 selected in different contexts: mixed types may produce colours that are generally more efficient
for communication while hollow or solid types produce colours more efficient for camouflage.

318 *Different multilayer types produce different colours*

For hue, and in conformity with our prediction that diffuse patches should contain multilayer
320 structures that minimise the angle dependency of hue, we found that diffuse patches contained
the solid multilayer type more often than directional patches, which leads to a lower hue shift
322 in simulations (fig. S11 and table S7). We could not verify this prediction with empirical data as
 γ_H was too similar across species to yield repeatable measurements. This lower hue shift could
324 reduce colour flashes that may alert a potential predator of the presence of the bird. On the other
hand, diffuse patches have most commonly hollow melanosomes, which can lead to the highest
326 hue shift (fig. S11 and table S7). This partial mismatch with our prediction could be explained by
the findings of Kjernsmo et al. (2018), where the authors found that iridescence could improve

328 camouflage by impairing predators' ability to discern target shape. Alternatively, the difference
329 in hue shift among the different multilayer types could be low enough to not be under strong
330 selective pressure.

We also found with simulations that the mixed multilayer type can produce the highest di-
332 versity of hues (fig. S13), while the solid type has the lowest diversity. It does however seem
333 that the full range of possible hues is not explored in hummingbirds. This is probably in part
334 due to our non-exhaustive sampling of hummingbird species but also likely reflects evolutionary
constraints, either on the structures themselves or on the resulting colour (Gruson et al., 2019a).

336 For brightness, previous studies predicted based on optical theory that hollow melanosomes
should produce brighter colours than solid melanosomes (Prum, 2006; Eliason et al., 2013).
338 The simulations in the present study confirm that multilayers with hollow melanosomes re-
flect more light overall (specular + diffuse reflectance) than multilayers with solid melanosomes.
340 Mixed multilayer types have intermediate values between multilayers with only solid or hollow
melanosomes (table S8). However, the multilayer type is likely to have a minimal effect on ef-
342 fective brightness at a given angle. The bright colours of hummingbirds are indeed not caused
by an increase of the total amount of reflected light but rather by a very high directionality of
344 the reflected signal, meaning that all reflected light is focused within a narrow angular sector, as
found by Osorio and Ham (2002); Gruson et al. (2019b) and shown for our study in fig. S9.

346 On the other hand, we find that, in both empirical data and simulations, hollow multilayers
produce less saturated colours than multilayer structures with solid melanosomes or mixed mul-
348 tilayers, as shown in table S11 and fig. S12 and table S5 respectively. However, the mixed multi-
layer type had the highest interaction value with the number of layers (fig. S12 and table S5). This
350 means that mixed multilayers have the highest potential to create highly saturated colours when
composed of a large number of layers, which could explain that they were positively selected in
352 directional patches.

Our results describing the influence of the multilayer type on brightness and saturation are
354 also in line with the detailed study of Giraldo et al. (2018) on the throat feathers of Anna's
hummingbird (*Calypte anna*): using optical simulations, they found that the exclusion of the

356 thinner outermost layer in their simulations produced brighter but less saturated colours.

From a macro-evolutionary point of view, the evolution of new types of multilayer structures
358 might also be responsible for the rapid diversification rate of hummingbirds (McGuire et al.,
2014), playing the role of key innovations that allow them to quickly fill up previously unexplored
360 regions of the phenotypic space (more specifically, new hues and more saturated colours, as
mentioned above), as was previously described in iridescent starlings by Maia et al. (2013a).

362 *Multilayer structures in hummingbirds are not very regular but often close to
ideality*

364 We found a very high intra-multilayer variability for the structural characteristics of melanosomes,
as expressed by the high relative standard deviation values reported in table S1. These values are
366 close to previous values reported in the literature for hummingbird multilayers (Nordén et al.,
2019), and they likely reflect actual biological variability rather than measurement uncertainty.
368 For example, Greenewalt et al. (1960) found that layer thickness generally varied between 20-30 %
within species. The thickness we measured for hollow melanosomes (95 % variation interval =
370 130 nm to 231 nm) was also well within the range of what was estimated in the past on a smaller
species sample (100 nm to 220 nm, with a mode of 150 nm for Greenewalt et al. (1960) and be-
372 tween 200 nm and 250 nm for Dorst (1951) with a photonic microscope).

We also observe strong correlations between the thickness values of the different layers, as
374 shown in fig. 3. In other words, melanosomes with a thicker layer of melanin were also spaced
by thicker layers of keratin. This correlation could explain the above mentioned fact that realised
376 hues are much less diverse than possible theoretical hues for each multilayer type using sim-
ulations with biologically relevant ranges for layer thicknesses. This correlation is not caused
378 by the phylogenetic relationships between species and remains significant even when the phy-
logeny is taken into account (tables S12 to S14). This suggests the existence of selective pressures,
380 or developmental constraints, that maintain this correlation. This may be due to selection for
ideal multilayers, where the optical thickness (defined as refractive index times layer thickness
382 $n_i e_i$) of the successive layers is constant (Land, 1966). This hypothesis is supported by the fact

that slopes of the correlations between optical thicknesses of successive layers are close to 1
384 (fig. 3). Ideal multilayers are found in many organisms such as the butterfly *Chrysiridia rhipheus*
(Brink and Lee, 1998), *Sapphirina* copepods (Chae and Nishida, 1999) or the Japanese jewel beetle
386 *Chrysochroa fulgidissima* (Stavenga et al., 2011a) where they are thought to be selected because
they produce brighter, more saturated colours (Land, 1966).

388 Because the wavelength (i.e. hue) reflected by a multilayer depends on the thickness of the
layers, variability in thickness may produce a mix of numerous wavelengths, and thus less sat-
390 urated colours. This prediction is however not supported by our results (table S11), which suggests
that saturation is not significantly explained by variability in layer thickness.

392 *Multilayer types correlate with other structural features that enhance
conspicuousness*

394 We found little or no effect of the number of layers on brightness, in both simulations (table S4)
and comparative analyses (table S8). This result is in agreement with what Eliason et al. (2015)
396 found in melanosome rods from dabbling ducks and could be partly explained by the fact that
brightness quickly reaches a plateau when the number of layers increases (Land, 1966, 1972; Ki-
398 noshita et al., 2008). Indeed, multilayer theory predicts that brightness increases exponentially
towards its maximum with the number of layers (Yeh, 2005). For example, Giraldo et al. (2018)
400 found that 10 layers created a spectrum that was close to saturation in their modelling investi-
gation of the pink throat feathers from Anna's hummingbird (*Calypte anna*). Similarly, Stavenga
402 et al. (2018) reported that 5 layers were sufficient to reach the maximum brightness in their study
on magpie (*Pica pica*) hollow melanin rods while Berthier et al. (2006) wrote that less than 10
404 layers achieved maximum brightness in an ideal chitin-air multilayer.

However, the multilayers found in hummingbirds have at least 5 layers, with a median of 12
406 layers and a maximal number of layers sometimes over 25, well beyond the theoretical number of
layers needed to reach maximum reflectance. Indeed, an increasing number of layers did increase
408 saturation (i.e. decrease FWHM) in simulations (fig. S12 and table S5). This result echoes
the findings of Xiao et al. (2014) on the common bronzewing *Phaps chalcoptera* and suggests an

⁴¹⁰ explanation for the unusually high number of layers in hummingbird feathers, and especially on
⁴¹¹ directional patches. As we mentioned earlier, more saturated colours are often positively selected
⁴¹² in the context of communication. Selection for higher saturation could then be the driving force
⁴¹³ for the evolution towards a higher number of layers in patches used in communication, even
⁴¹⁴ though brightness does not significantly increase.

We found that the sickle shape of hummingbird barbules is correlated with more reflective
⁴¹⁶ (table S8, more saturated (table S11) and more directional colours (table S9). It remains unclear
⁴¹⁷ whether barbule shape has an optical role at the level of the barbule itself as is the case for
⁴¹⁸ example in the triangular barbules from the breast of the bird of paradise *Parotia lawesi* (Stavenga
et al., 2011b; Wilts et al., 2014). However, it is unlikely that this shape contributes directly to the
⁴²⁰ interference pattern because the position of the lower part of the "sickle" (also called *velum*) does
not reflect light rays in the same direction as the upper part (also called *speculum*) (Giraldo et al.,
⁴²² 2018). However, multiple studies have suggested that barbule organisation nonetheless influences
the resulting signal (see for example Schmidt and Ruska (1962) on the hummingbird *Helianzelus*
⁴²⁴ *strophianus* or Dürrer and Villiger (1970) on the golden cuckoo *Chrysococcyx cupreus*). Indeed,
more packed barbules produce brighter colours because the light reflected from each multilayer
⁴²⁶ also interferes at the level of the barb or even the whole feather. This peculiar sickle shape
could then have been selected because it allows for a better interlocking of adjacent barbules,
⁴²⁸ leading to a greater spatial coherence across scales, causing signals reflected by each barbule
to interfere more constructively and ultimately produce brighter, more saturated colours. This
⁴³⁰ stronger interlocking could also have an effect on processes other than colour generation, such as
producing more waterproof feathers, or increasing lift during flight by limiting air gaps between
⁴³² barbules, which may be especially important for the stationary flight of hummingbirds (Sick,
1937). Dorst (1951) suggests that mechanics (for flight) and optics (for colour) benefit from the
⁴³⁴ same modification and selection likely acts on both jointly.

There are other structural parameters we could not measure with our present experimental
⁴³⁶ setup but that could influence the resulting colour; namely the angle between the barbules and
the parent barb in the plane of the feather (named 'barbular angle' in Greenewalt (1991) and

⁴³⁸ represented in fig. S4), the angle between barbules and the barb axis in a cross section of the barb
(named 'vanular angle' in Greenewalt (1991) and represented in fig. S4). However, Dorst (1951)
⁴⁴⁰ found no effect of the barbular angle on the visual appearance of the feathers in his investigation
of 15 hummingbird species.

Conclusion

⁴⁴² The present study sheds a new light on the evolution of iridescence, in hummingbirds, and
⁴⁴⁴ more generally in all other organisms, with several major findings: (i) hummingbirds display
much more diverse multilayer structures than previously expected, with even a type of structure
⁴⁴⁶ unknown thus far, (ii) a single species may display multiple types of multilayer at different
location on its body, and (iii) structural features at both the level of the multilayer and the level
⁴⁴⁸ of the whole feather interact in the production of iridescent colours.

Literature Cited

- ⁴⁵⁰ S. M. Doucet and M. G. Meadows. Iridescence: a functional perspective. *Journal of The Royal Society Interface*, 6(Suppl 2):S115–S132, Apr. 2009. doi: 10.1098/rsif.2008.0395.focus.
- ⁴⁵² D. C. Osorio and A. D. Ham. Spectral reflectance and directional properties of structural coloration in bird plumage. *Journal of Experimental Biology*, 205(14):2017–2027, July 2002.
- ⁴⁵⁴ H. Gruson, M. Elias, J. L. Parra, C. Andraud, S. Berthier, C. Doutrelant, and D. Gomez. Distribution of iridescent colours in hummingbird communities results from the interplay between selection for camouflage and communication. *bioRxiv*, page 586362, Apr. 2019a. doi: 10.1101/586362.
- ⁴⁵⁸ J. Del Hoyo, A. Elliott, J. Sargatal, D. A. Christie, and E. de Juana. Handbook of the Birds of the World Alive. hbw.com, 2017.
- ⁴⁶⁰ J. Dorst. *Recherches sur la structure des plumes des trochilidés*. PhD thesis, Université de Paris, Paris, 1951. OCLC: 14220401.

- ⁴⁶² L. D'Alba and M. D. Shawkey. Melanosomes: Biogenesis, Properties, and Evolution of an Ancient Organelle. *Physiological Reviews*, 99(1):1–19, Sept. 2018. doi: 10.1152/physrev.00059.2017.
- ⁴⁶⁴ H. Dürrer. *Schillerfarben der Vogelfeder als Evolutionsproblem*. PhD thesis, Medizinischen Fakultät der Universität Basel, 1977.
- ⁴⁶⁶ C. H. Greenewalt, W. Brandt, and D. D. Friel. Iridescent colors of hummingbird feathers. *Journal of the Optical Society of America*, 50(10):1005–1013, Oct. 1960. doi: 10.1364/JOSA.50.001005.
- ⁴⁶⁸ W. J. Schmidt and H. Ruska. Über das schillernde Federmelanin bei *Heliangelus* und *Lophophorus*. *Zeitschrift für Zellforschung und Mikroskopische Anatomie*, 57(1), 1962. doi: 10.1007/BF00338926.
- ⁴⁷⁰ M. D. Shawkey, N. I. Morehouse, and P. Vukusic. A protean palette: colour materials and mixing in birds and butterflies. *Journal of The Royal Society Interface*, 6(Suppl 2):S221–S231, 2009. doi: 10.1098/rsif.2008.0459.focus.
- ⁴⁷² M. A. Giraldo, J. L. Parra, and D. G. Stavenga. Iridescent colouration of male Anna's hummingbird (*Calypte anna*) caused by multilayered barbules. *Journal of Comparative Physiology A*, 204 (12):965–975, Dec. 2018. doi: 10.1007/s00359-018-1295-8.
- ⁴⁷⁶ K. K. Nordén, J. W. Faber, F. Babarović, T. L. Stubbs, T. Selly, J. D. Schiffbauer, P. P. Štefanić, G. Mayr, F. M. Smithwick, and J. Vinther. Melanosome diversity and convergence in the evolution of iridescent avian feathers—Implications for paleocolor reconstruction. *Evolution*, 73(1): 15–27, 2019. doi: 10.1111/evo.13641.
- ⁴⁸⁰ R. Maia, D. R. Rubenstein, and M. D. Shawkey. Key ornamental innovations facilitate diversification in an avian radiation. *Proceedings of the National Academy of Sciences*, 110(26):10687–10692, June 2013a. doi: 10.1073/pnas.1220784110.
- ⁴⁸⁴ G. E. Hill. Female house finches prefer colourful males: sexual selection for a condition-dependent trait. *Animal Behaviour*, 40(3):563–572, Sept. 1990. doi: 10.1016/S0003-3472(05)80537-8.

- 486 A. Loyau, D. Gomez, B. Moureau, M. Théry, N. S. Hart, M. S. Jalme, A. T. D. Bennett, and
G. Sorci. Iridescent structurally based coloration of eyespots correlates with mating success in
488 the peacock. *Behavioral Ecology*, 18(6):1123–1131, Nov. 2007. doi: 10.1093/beheco/arm088.
- 490 D. J. Kemp. Female butterflies prefer males bearing bright iridescent ornamentation. *Proceedings
of the Royal Society of London B: Biological Sciences*, 274(1613):1043–1047, Apr. 2007. doi: 10.1098/
rspb.2006.0043.
- 492 D. J. Kemp. Female mating biases for bright ultraviolet iridescence in the butterfly *Eurema hecabe*
(Pieridae). *Behavioral Ecology*, 19(1):1–8, Jan. 2008. doi: 10.1093/beheco/arm094.
- 494 H. Gruson, C. Andraud, W. Daney de Marcillac, S. Berthier, M. Elias, and D. Gomez. Quantitative
characterization of iridescent colours in biological studies: a novel method using optical theory.
496 *Interface Focus*, 9(1):20180049, Feb. 2019b. doi: 10.1098/rsfs.2018.0049.
- 498 J. Felsenstein. Phylogenies and the comparative method. *The American Naturalist*, 125(1):1–15,
Jan. 1985. doi: 10.1086/284325.
- 500 W. Jetz, G. H. Thomas, J. B. Joy, K. Hartmann, and A. O. Mooers. The global diversity of birds in
space and time. *Nature*, 491(7424):444–448, Nov. 2012. doi: 10.1038/nature11631.
- 502 P.-C. Bürkner. brms: an R package for Bayesian multilevel models using Stan. *Journal of Statistical
Software*, 80(1):1–28, 2017. doi: 10.18637/jss.v080.i01.
- 504 R Core Team. R: A Language and Environment for Statistical Computing, 2017.
- 506 opencv: Open Source Computer Vision Library. OpenCV, 2017.
- Python Software Foundation. Python Language Reference.
- 508 L. Bolla. EMpy - ElectroMagnetic Python, 2017.
- P. Yeh. *Optical waves in layered media*. Wiley series in pure and applied optics. Wiley-Interscience,
Hoboken, NJ, 2005. ISBN 978-0-471-73192-4. OCLC: 255155115.

- M. C. Stoddard and R. O. Prum. Evolution of avian plumage color in a tetrahedral color space:
510 a phylogenetic analysis of New World buntings. *The American Naturalist*, 171(6):755–776, June
2008. doi: 10.1086/587526.
- 512 R. Maia, C. M. Eliason, P.-P. Bitton, S. M. Doucet, and M. D. Shawkey. pavo: an R package for
the analysis, visualization and organization of spectral data. *Methods in Ecology and Evolution*,
514 4(10):906–913, Oct. 2013b. doi: 10.1111/2041-210X.12069.
- 516 R. Maia, H. Gruson, J. A. Endler, and T. E. White. pavo 2: New tools for the spectral and
spatial analysis of colour in R. *Methods in Ecology and Evolution*, 10(7):1097–1107, 2019. doi:
10.1111/2041-210X.13174.
- 518 J. D. Hadfield. MCMC Methods for Multi-Response Generalized Linear Mixed Models: The
MCMCglmm R Package. *Journal of Statistical Software*, Feb. 2010. doi: 10.18637/jss.v033.i02.
- 520 R Core Team. R: A Language and Environment for Statistical Computing, 2018.
- 522 K. Delhey, M. Hall, S. A. Kingma, and A. Peters. Increased conspicuousness can explain the
match between visual sensitivities and blue plumage colours in fairy-wrens. *Proceedings of the
Royal Society B: Biological Sciences*, 280(1750):20121771, Jan. 2013. doi: 10.1098/rspb.2012.1771.
- 524 M. Pagel and F. Lutzoni. Accounting for phylogenetic uncertainty in comparative studies of
evolution and adaptation. In M. Lässig and A. Valleriani, editors, *Biological Evolution and
Statistical Physics*, volume 585 of *Lecture Notes in Physics*. Springer Berlin Heidelberg, Berlin,
526 Heidelberg, 2002. ISBN 978-3-540-43188-6. doi: 10.1007/3-540-45692-9.
- 528 P. de Villemereuil, J. A. Wells, R. D. Edwards, and S. P. Blomberg. Bayesian models for compar-
ative analysis integrating phylogenetic uncertainty. *BMC Evolutionary Biology*, 12(1):102, June
530 2012. doi: 10.1186/1471-2148-12-102.
- 532 T. Guillerme and K. Healy. mulTree: a package for running MCMCglmm analysis on multiple
trees. Zenodo, Nov. 2014.

- R. Borges, J. P. Machado, C. Gomes, A. P. Rocha, and A. Antunes. Measuring phylogenetic signal
534 between categorical traits and phylogenies. *Bioinformatics*, 35(11):1862–1869, June 2019. doi:
10.1093/bioinformatics/bty800.
- 536 M. A. Rodríguez-Gironés and L. Santamaría. Why are so many bird flowers red? *PLOS Biology*,
2(10):e350, Oct. 2004. doi: 10.1371/journal.pbio.0020350.
- 538 H. L. Leertouwer, B. D. Wilts, and D. G. Stavenga. Refractive index and dispersion of butterfly
chitin and bird keratin measured by polarizing interference microscopy. *Optics Express*, 19(24):
540 24061–24066, Nov. 2011. doi: 10.1364/OE.19.024061.
- D. G. Stavenga, H. L. Leertouwer, D. C. Osorio, and B. D. Wilts. High refractive index of melanin
542 in shiny occipital feathers of a bird of paradise. *Light: Science & Applications*, 4(1):e243, Jan.
2015. doi: 10.1038/lsa.2015.16.
- 544 K. Kjernsmo, J. R. Hall, C. Doyle, N. Khuzayim, I. C. Cuthill, N. E. Scott-Samuel, and H. M.
Whitney. Iridescence impairs object recognition in bumblebees. *Scientific Reports*, 8(1):8095,
546 May 2018. doi: 10.1038/s41598-018-26571-6.
- R. O. Prum. Anatomy, physics, and evolution of structural colors. In G. E. Hill and K. J. McGraw,
548 editors, *Bird Coloration, Volume 1: Mechanisms and Measurements*, volume 1 of *Bird Coloration*,
page 640. Harvard University Press, Feb. 2006. ISBN 978-0-674-01893-8.
- 550 C. M. Eliason, P.-P. Bitton, and M. D. Shawkey. How hollow melanosomes affect iridescent colour
production in birds. *Proc. R. Soc. B*, 280(1767):20131505, Sept. 2013. doi: 10.1098/rspb.2013.1505.
- 552 J. A. McGuire, C. C. Witt, J. V. J. Remsen, A. Corl, D. L. Rabosky, D. L. Altshuler, and R. Dudley.
Molecular phylogenetics and the diversification of hummingbirds. *Current Biology*, 24(8):910–
554 916, Apr. 2014. doi: 10.1016/j.cub.2014.03.016.
- M. F. Land. A multilayer interference reflector in the eye of the scallop, *Pecten maximus*. *Journal
556 of Experimental Biology*, 45(3):433–447, Dec. 1966.

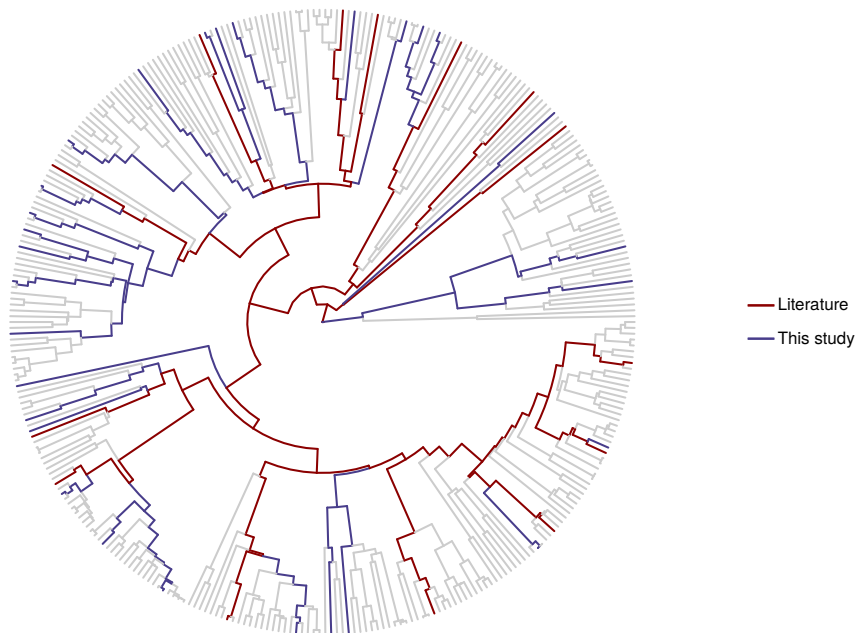
- D. J. Brink and M. E. Lee. Thin-film biological reflectors: optical characterization of the *Chrysiridia croesus* moth. *Applied Optics*, 37(19):4213–4217, July 1998. doi: 10.1364/AO.37.004213.
- J. Chae and S. Nishida. Spectral patterns of the iridescence in the males of *Sapphirina* (Copepoda: Poecilostomatoida). *Journal of the Marine Biological Association of the United Kingdom*, 79(3):437–443, June 1999. doi: 10.1017/S0025315498000563.
- D. G. Stavenga, B. D. Wilts, H. L. Leertouwer, and T. Hariyama. Polarized iridescence of the multilayered elytra of the Japanese jewel beetle, *Chrysochroa fulgidissima*. *Philosophical Transactions of the Royal Society B: Biological Sciences*, 366(1565):709–723, Mar. 2011a. doi: 10.1098/rstb.2010.0197.
- C. M. Eliason, R. Maia, and M. D. Shawkey. Modular color evolution facilitated by a complex nanostructure in birds. *Evolution*, 69(2):357–367, Feb. 2015. doi: 10.1111/evo.12575.
- M. F. Land. The physics and biology of animal reflectors. *Progress in Biophysics and Molecular Biology*, 24:75–106, Jan. 1972. doi: 10.1016/0079-6107(72)90004-1.
- S. Kinoshita, S. Yoshioka, and J. Miyazaki. Physics of structural colors. *Reports on Progress in Physics*, 71(7):076401, 2008. doi: 10.1088/0034-4885/71/7/076401.
- D. G. Stavenga, H. L. Leertouwer, and B. D. Wilts. Magnificent magpie colours by feathers with layers of hollow melanosomes. *Journal of Experimental Biology*, 221(4):jeb174656, Feb. 2018. doi: 10.1242/jeb.174656.
- S. Berthier, E. Charron, and J. Boulenguez. Morphological structure and optical properties of the wings of Morphidae. *Insect Science*, 13(2):145–158, 2006. doi: 10.1111/j.1744-7917.2006.00077.x.
- M. Xiao, A. Dhinojwala, and M. Shawkey. Nanostructural basis of rainbow-like iridescence in common bronzewing Phaps chalcoptera feathers. *Optics Express*, 22(12):14625–14636, June 2014. doi: 10.1364/OE.22.014625.
- D. G. Stavenga, H. L. Leertouwer, N. J. Marshall, and D. C. Osorio. Dramatic colour changes in a bird of paradise caused by uniquely structured breast feather barbules. *Proceedings of the Royal*

- 582 *Society of London B: Biological Sciences*, 278(1715):2098–2104, July 2011b. doi: 10.1098/rspb.2010.
2293.
- 584 B. D. Wilts, K. Michielsen, H. D. Raedt, and D. G. Stavenga. Sparkling feather reflections of a bird-of-paradise explained by finite-difference time-domain modeling. *Proceedings of the National
586 Academy of Sciences*, 111(12):4363–4368, Mar. 2014. doi: 10.1073/pnas.1323611111.
- H. Dürrer and W. Villiger. Schillerradien des Goldkuckucks (*Chrysococcyx cupreus* (Shaw)) im
588 Elektronenmikroskop. *Zeitschrift für Zellforschung und Mikroskopische Anatomie*, 109(3):407–413,
Sept. 1970. doi: 10.1007/BF02226912.
- 590 H. Sick. Morphologisch-funktionelle Untersuchungen über die Feinstruktur der Vogelfeder. *Journal
für Ornithologie*, 85(2):206–372, Apr. 1937. doi: 10.1007/BF01905702.
- 592 C. H. Greenewalt. *Hummingbirds*. Dover Publications, New York, Feb. 1991. ISBN 978-0-486-
26431-8.
- 594 S. Nakagawa and H. Schielzeth. Repeatability for Gaussian and non-Gaussian data: a practical
guide for biologists. *Biological Reviews*, 85(4):935–956, Nov. 2010. doi: 10.1111/j.1469-185X.2010.
00141.x.

Appendix A: Supplementary Figures



Supplementary figure 1: Picture of the same *Calypte anna* individual at different angles. Modified from a video taken by Mick Thompson (<https://www.flickr.com/photos/mickthompson/27991602299/>), CC-BY-NC, special authorisation to use it in this article. The directional throat and crown patches contrast with the diffuse greenish belly patch.



Supplementary figure 2: Consensus phylogeny of the hummingbirds reconstructed using the Maximum Clade Credibility tree from a distribution of 4999 trees downloaded from <http://birdtree.org> (Jetz et al., 2012). The red lineages show the 14 species whose structures had been previously studied in the literature (Dürrer, 1977; Greenewalt et al., 1960; Schmidt and Ruska, 1962; Shawkey et al., 2009; Nordén et al., 2019) while blue lineages show species we studied for the first time in this study.

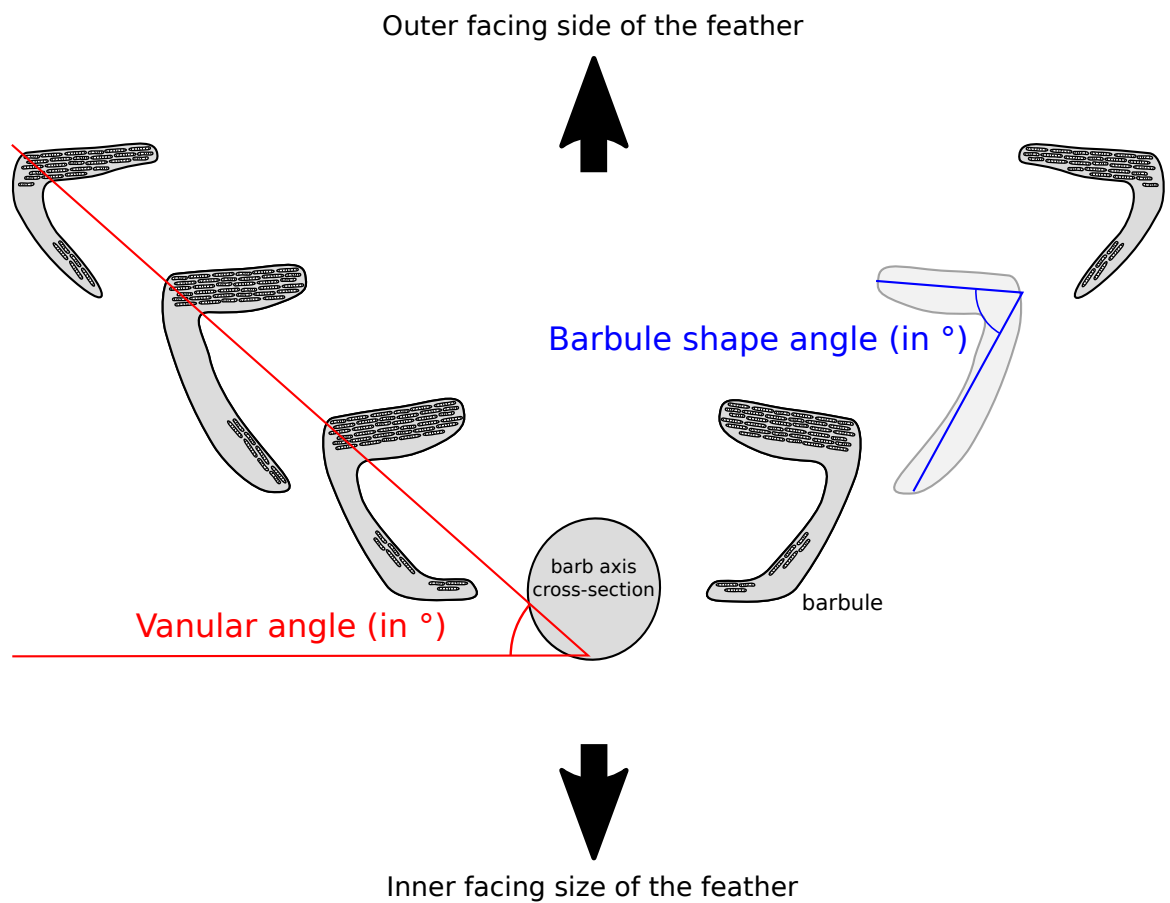


session_3_bloc15_ocreatus_underwoodii_throat_005_Mag_700
session_3_bloc15_ocreatus_underwoodii_throat
16:41:09 6/16/2017
TEM Mode: Imaging
Microscopist: hugo

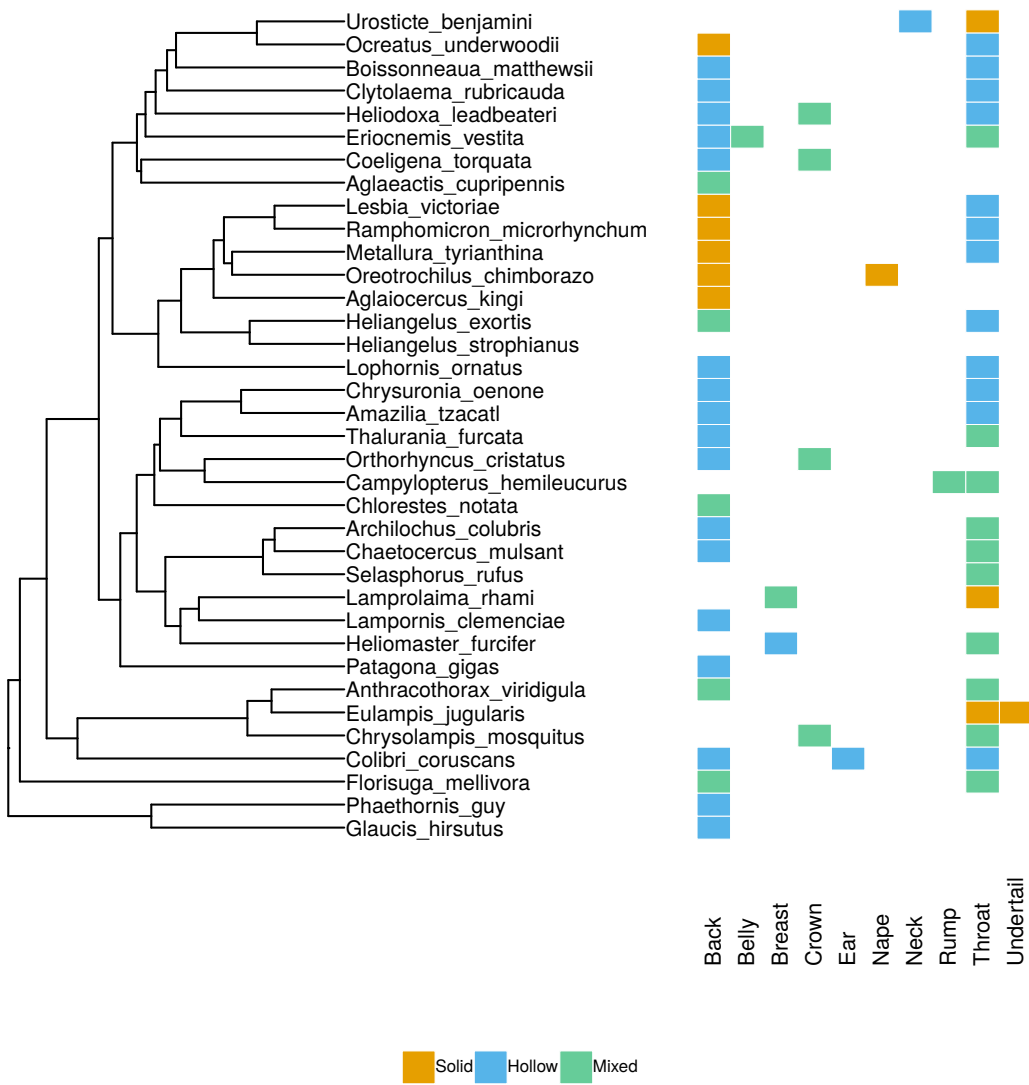
Camera: XR81VwrkGBH77, Exposure(ms): 1600 Gain: 32, Bin: 1
Gamma: 1.00, No Sharpening, Normal Contrast

6 μm
HV=60.0kV
Direct Mag: 700x
X:57.5 Y: -59.
Tilt: 1.0
AMT Camera System

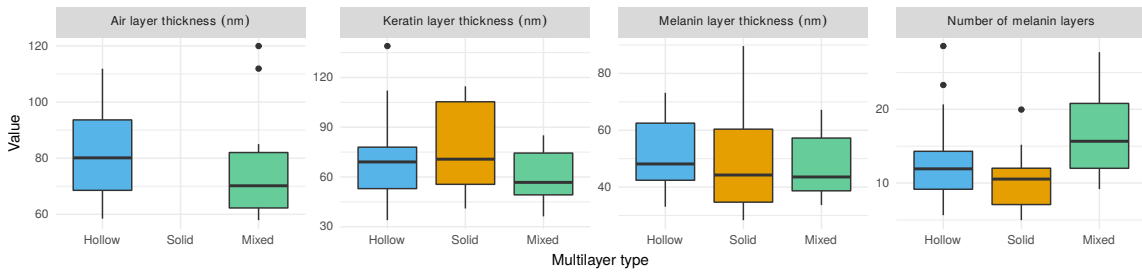
Supplementary figure 3: Unedited TEM photograph of the cross section of 5 consecutive barbules from the same barb of the throat of *Ocreatus underwoodi*.



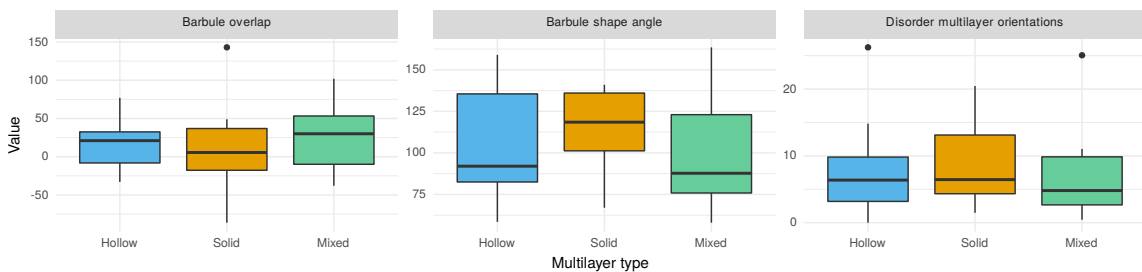
Supplementary figure 4: Cross section of a barb and its barbules. Barbule shape angle is displayed in blue and vanular angle in red. Barbules with a large barbule shape angle tend to be flat while barbules with a low barbule shape angle tend to have a sickle shape.



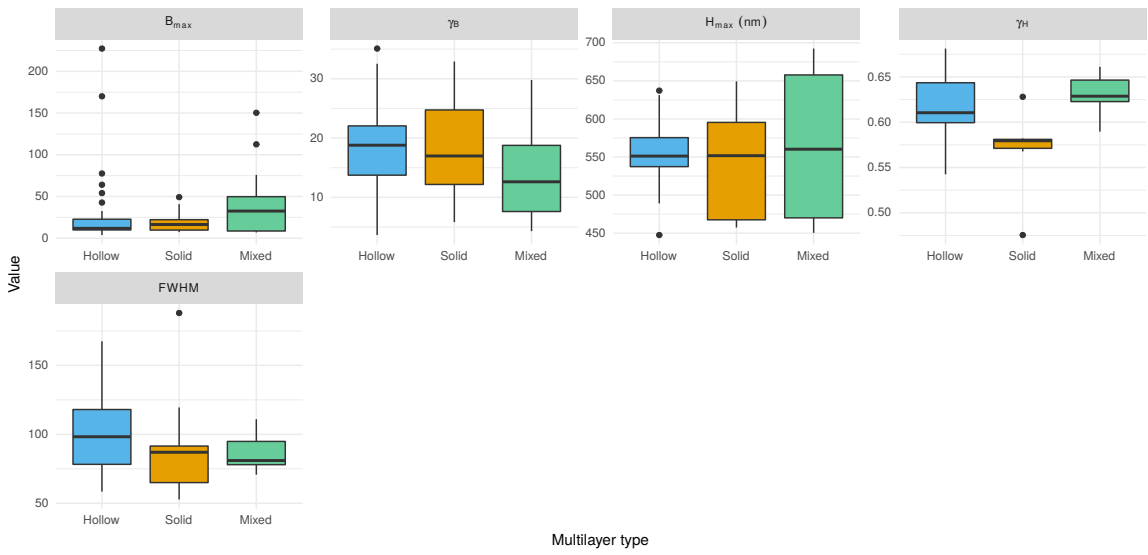
Supplementary figure 5: Type of melanosomes on the different patches we measured for each species. The sampling was dependent on which patch was iridescent (and diffuse / directional) for each species. Different patches of the same species can have different types of multilayer structures and patches such as the throat had more often the outer type than patches such as the back.



Supplementary figure 6: Range of variation of structural parameters for each type of multilayer, estimated on TEM photographs using an automated python script based on OpenCV (201, 2017).



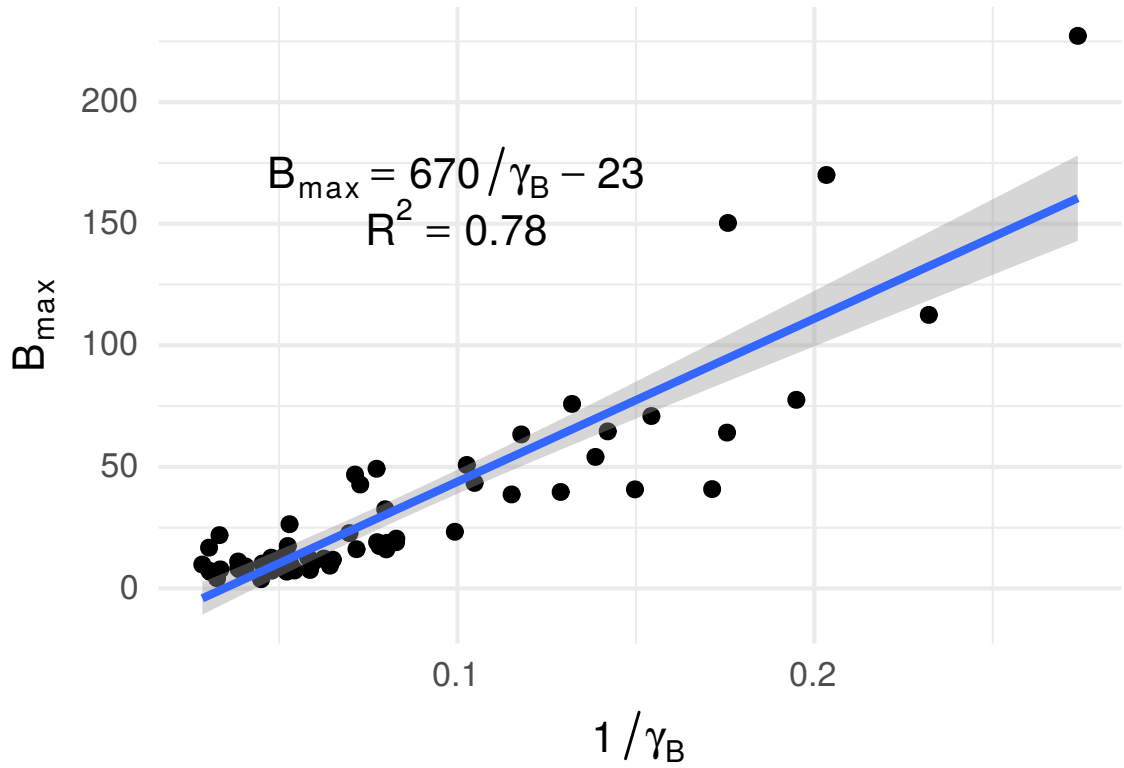
Supplementary figure 7: Range of variation of structural parameters for each type of multilayer, estimated on photonic microscopy photographs. The barbule overlap describes how much adjacent barbules overlap and represents how packed and well-organised the barbules are. The barbule shape angle is illustrated in fig. S4. The disorder in the multilayer orientations describe how parallel adjacent multilayers are.



Supplementary figure 8: Range of variation of all iridescence parameters for each type of multilayer. The parameters are detailed in Gruson et al. (2019b): B_{max} and γ_B characterise brightness with B_{max} being the maximum brightness (reached when the illumination coincides with the observer) and γ_B the angle dependency of brightness. Similarly, H_{max} quantifies the maximum hue (reached when the illumination and the observer are in symmetrical positions relative to the multilayer normal) and γ_H the angle dependency of hue. Finally, FWHM describe the saturation (constant with the angle) with higher values corresponding to less saturated colours.

Variable	RSD (%)	ICC	p (permutation)	p (likelihood)
H_{\max}	0.25	1.00	0.00	< 0.0001
γ_H	2.46	0.17	0.21	0.2396
B_{\max}	16.03	0.89	0.04	< 0.0001
γ_B	23.05	0.71	0.01	0.0087
FWHM	2.27	0.66	0.00	< 0.0001
Number of layers	19.77	0.54	0.00	< 0.0001
Melanin layer thickness	10.79	0.54	0.00	< 0.0001
Keratin layer thickness	15.53	0.64	0.00	< 0.0001
Air layer thickness	8.95	0.77	0.00	< 0.0001
Variability in air layer thickness	14.44	0.77	0.00	< 0.0001
Variability in keratin layer thickness	29.28	0.41	0.00	< 0.0001
Variability in melanin layer thickness	17.37	0.45	0.00	< 0.0001
Barbule shape angle	7.07	0.91	0.00	< 0.0001
Barbule overlap	19.72	0.50	0.02	< 0.0001

Supplementary table 1: Iridescence variables (related to the visual signal) and structure characteristics are repeatable within our sample. Repeatability is measured as the intra-class coefficient (ICC) and p-values are estimated by two methods: permutation (p permutation) and likelihood ratio (p likelihood). All repeatability calculations are performed using the rptR R package (Nakagawa and Schielzeth, 2010). Measurement error is also estimated using relative standard deviation (RSD, also called coefficient of variation CV) which compares the standard deviation of several measurements of the same feature to its average.



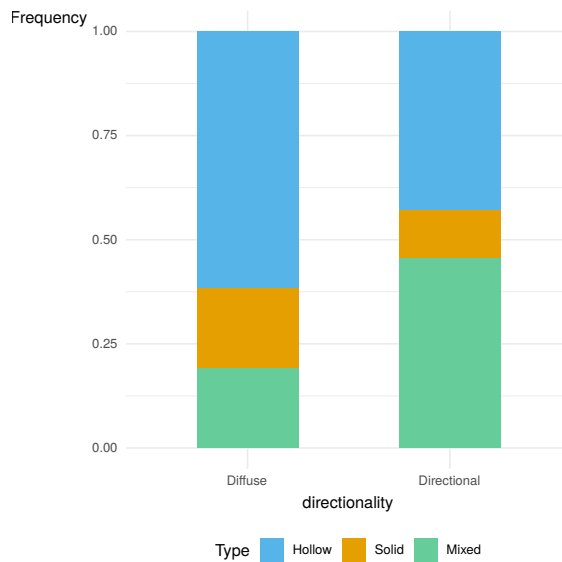
Supplementary figure 9: Correlation between B_{\max} (maximum brightness, reached when the two fibres are in specular position relative to the multilayer structure) and $1/\gamma_B$ (directionality *sensu* Osorio and Ham (2002)). This is an example of correlation between optical characteristics because of physics (as shown in Gruson et al. (2019b)).

	Estimates(median)	lower.CI(2.5)	upper.CI(97.5)
(Intercept)	25.84	-42.75	94.49
totalreflect	-0.01	-0.02	0.00
gammaB	0.54	-0.72	1.80
Hmax	0.14	0.00	0.27
phylogenetic.variance	2.27	0.00	264.36
residual.variance	694.73	453.60	1114.18

Supplementary table 2: Correlation between FWHM (opposite of saturation), overall reflectance ($2\sqrt{2\pi}B_{\max}\gamma_B$), γ_B (inversely related to directionality) and H_{\max} in empirical data from hummingbird feathers.

	Estimates(median)	lower.CI(2.5)	upper.CI(97.5)
(Intercept)	-559.55	-2725.62	1609.37
FWHM	-7.12	-16.72	2.47
gammaB	-47.01	-84.28	-9.77
Hmax	6.79	2.76	10.82
phylogenetic.variance	64.10	0.00	156309.83
residual.variance	698401.57	463069.31	1114969.23

Supplementary table 3: Correlation between overall reflectance ($2\sqrt{2\pi}B_{max}\gamma_B$), FWHM (opposite of saturation), γ_B (inversely related to directionality) and H_{max} in empirical data from hummingbird feathers.



Supplementary figure 10: Correlation between multilayer type (hollow, full or mixed) and directionality (diffuse vs directional).

	Mean	Standard deviation
(Intercept)	25.73	21.71
nb_layers	0.02	1.34
typeSolid	-17.08	30.70
typeMixed	-6.31	30.70
nb_layers:typeSolid	-0.05	1.90
nb_layers:typeMixed	0.01	1.90

Supplementary table 4: Influence of structural parameters on brightness. Optical theory predicts that brightness (B_{\max}) is controlled by the number of layers and their refractive index (i.e. the type of melanosomes). We test this on simulated data from Monte Carlo transfer matrix simulations using linear models. We find that brightness in simulated data is indeed influenced by the type of melanosomes and by the number of layers. This result is also illustrated in fig. S1.

	Mean	Standard deviation
(Intercept)	136.85	255.60
nb_layers	-1.21	8.56
typeSolid	-48.01	242.87
typeMixed	-29.25	183.57
melanin_size	0.24	2.14
keratin_size	-0.65	1.23
air_size	0.18	2.02
nb_layers:typeSolid	0.14	10.93
nb_layers:typeMixed	0.83	11.36

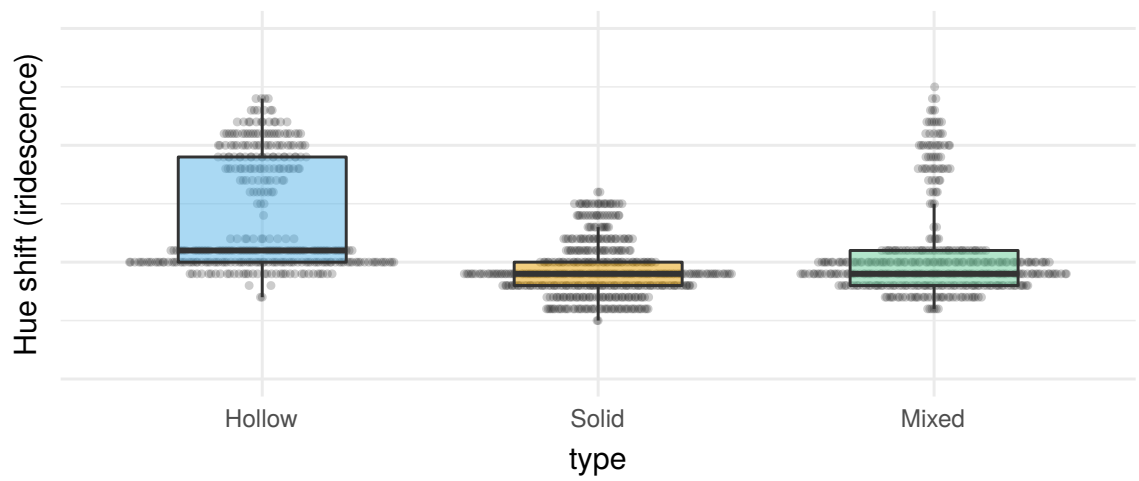
Supplementary table 5: Influence of structural parameters on saturation. Optical theory predicts that FWHM (opposite of saturation) is controlled by the number of layers and their refractive index (i.e. the type of melanosomes), as well as layer thickness. We test this on simulated data from Monte Carlo transfer matrix simulations using linear models. FWHM (opposite of saturation) in simulated data is indeed influenced by the type of melanosomes and by the number of layers for the solid and the mixed type. This result is also illustrated in fig. S2.

	Mean	Standard deviation
(Intercept)	5.26	402.79
melanin_size	3.13	4.40
keratin_size	1.64	2.51
air_size	0.84	2.78
typeSolid	48.13	425.37
typeMixed	74.11	443.55
interference order (m)	330.89	93.11
melanin_size:typeSolid	-0.57	5.55
melanin_size:typeMixed	-0.44	5.71
keratin_size:typeSolid	1.26	2.79
keratin_size:typeMixed	-0.17	3.13
air_size:typeMixed	-0.38	3.88

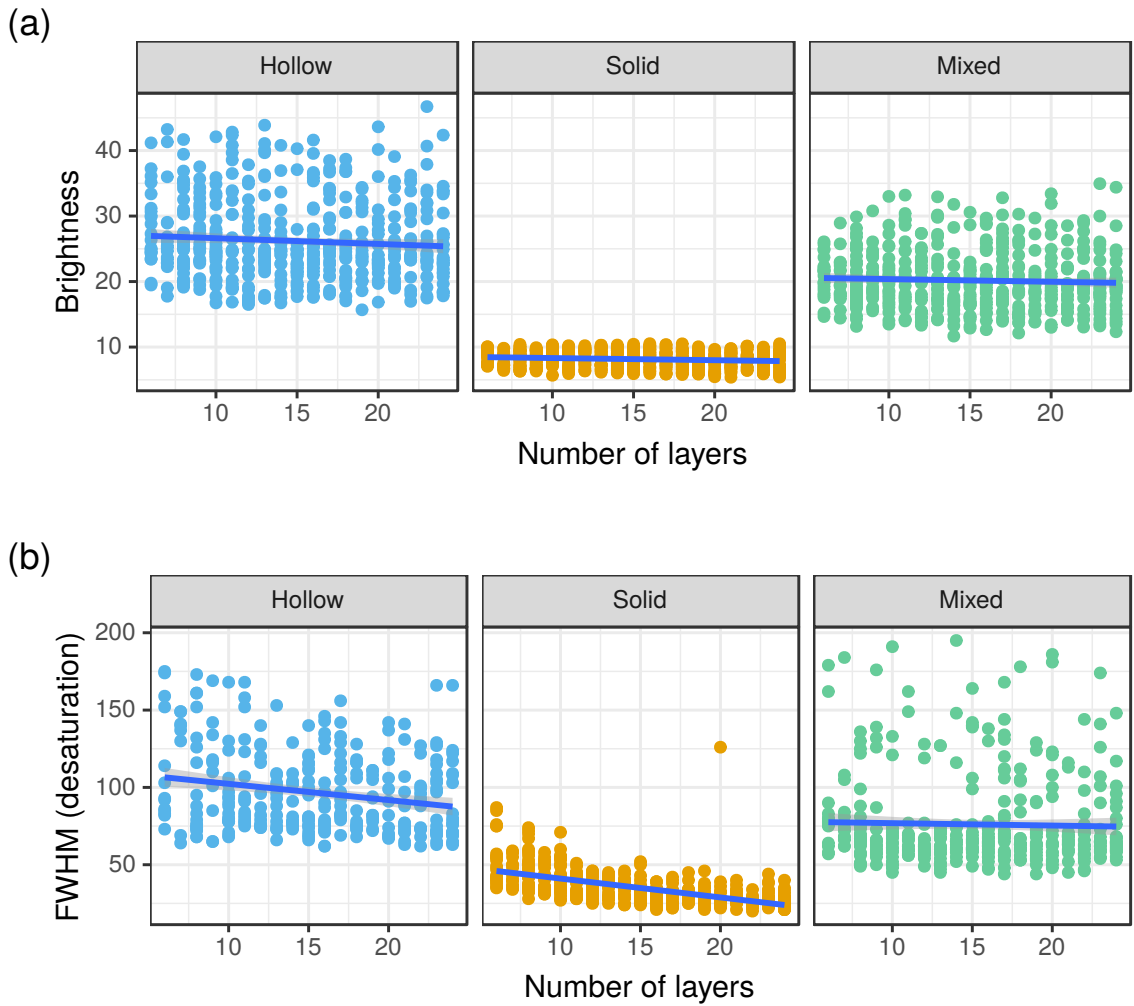
Supplementary table 6: Influence of structural parameters on hue. Optical theory predicts that hue (H_{\max}) is controlled by the thickness of each layer and their refractive index (i.e. the type of melanosomes). We test this on simulated data from Monte Carlo transfer matrix simulations using linear models. Hue in the simulated data indeed depends on the type of melanosomes, the thickness of the layers and the interaction of both.

	Mean	Standard deviation
(Intercept)	14.10	8.02
typeSolid	-4.75	10.57
typeMixed	-3.41	10.89

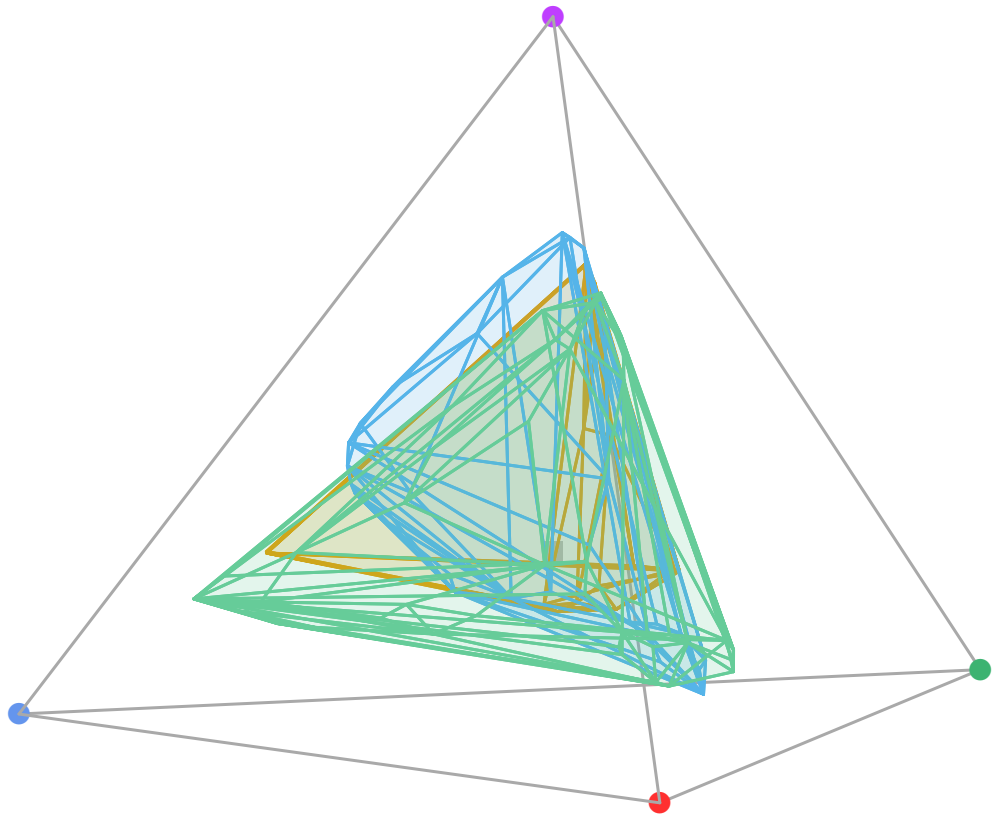
Supplementary table 7: Influence of the multilayer type on hue shift with the change in illumination and observation angle (difference in hue H_1 between specular reflection at 0° and specular reflection at 10° ; strongly related to γ_H , as explained in Gruson et al. 2019b). The linear model was run on simulated data using a transfer matrix model with biologically relevant parameter values.



Supplementary figure 11: Influence of the multilayer type on the hue shift with the angle change (difference in hue H1 between specular reflection at 0° and specular reflection at 10°). The data was produced using a transfer matrix model with biologically relevant parameter values.



Supplementary figure 12: Effect of the number of layers and the type of melanosomes on brightness and FWHM (desaturation). This results from Monte Carlo simulations (500 iterations for each multilayer type) using a transfer-matrix multilayer model. The parameters of each simulation are drawn from a distribution whose range is defined by the analysis of TEM pictures. Statistics analysing the effect of the number of layers and of the multilayer type are presented in tables S4 and S5.



Supplementary figure 13: Colour gamut of the different multilayer types. The gamut was determined by computing the convex hull of the set of points obtained by running the result of the transfer matrix simulations in a avian vision model.

	Estimates(median)	lower.CI(2.5)	upper.CI(97.5)
(Intercept)	2543.30	1138.71	3947.17
nb_layers	14.03	-49.77	77.83
typeSolid	289.10	-1471.37	2050.36
typeMixed	-1012.38	-2523.65	500.18
barbule_shape	-11.05	-19.28	-2.82
barbule_overlap	4.82	-1.63	11.28
nb_layers:typeSolid	-29.11	-173.59	115.25
nb_layers:typeMixed	61.12	-31.97	154.16
phylogenetic.variance	40.21	0.00	84651.91
residual.variance	681879.73	466577.56	1051669.17

Supplementary table 8: Correlation between total brightness and structural parameters. Optical theory predicts that total brightness (proportional to $B_{\max} \gamma_B$) is controlled by the number of layers, their refractive index (i.e. the type of melanosomes) and how packed barbules are (barbule shape and overlap). We test this on empirical data from hummingbird iridescent feathers using MCMCglmm. The first column contains explanatory variables, the second one the estimate of the effect size, and the third and fourth one the lower and higher (respectively) bounds of the 95 % credibility interval for the effect size. Significant effects of explanatory variables are shown with a cyan background. This result is also illustrated in fig. 4b.

	Estimates(median)	lower.CI(2.5)	upper.CI(97.5)
(Intercept)	3.76	-3.72	11.13
barbule_shape	0.12	0.05	0.19
barbule_overlap	-0.05	-0.10	0.01
align_disorder	0.17	-0.21	0.55
phylogenetic.variance	0.52	0.00	16.14
residual.variance	50.48	34.54	76.92

Supplementary table 9: Correlation between directionality and structural parameters. Optical theory predicts that angular dependency of brightness γ_B (inversely proportional to directionality *sensu* Osorio and Ham (2002)) is controlled by how well-arranged barbules are (barbule shape, overlap and alignment). We test this on empirical data from hummingbird iridescent feathers using MCMCglmm. The first column contains explanatory variables, the second one the estimate of the effect size, and the third and fourth one the lower and higher (respectively) bounds of the 95 % credibility interval for the effect size. Significant effects of explanatory variables are shown with a cyan background. This result is also illustrated in fig. 4a.

	Estimates(median)	lower.CI(2.5)	upper.CI(97.5)
(Intercept)	530.52	434.10	628.52
melanin_thickness	-3.95	-6.91	-1.03
keratin_thickness	1.31	-0.15	2.82
air_thickness	1.07	-0.27	2.39
typeSolid	51.99	-83.20	189.78
typeMixed	-48.62	-176.52	83.84
interference order (m)	93.95	67.99	119.55
melanin_thickness:typeSolid	1.92	-2.01	5.79
melanin_thickness:typeMixed	9.64	3.69	15.85
keratin_thickness:typeSolid	-1.09	-3.02	0.87
keratin_thickness:typeMixed	-6.06	-9.56	-2.87
air_thickness:typeMixed	-0.39	-2.32	1.55
phylogenetic.variance	177.48	0.01	2266.77
residual.variance	973.09	297.37	1893.45

Supplementary table 10: Correlation between hue (H_{max}) and structural parameters. Optical theory predicts that hue H_{max} is controlled by layer thickness and refractive index (i.e. multilayer type). We test this on empirical data from hummingbird iridescent feathers using MCMCglmm. The first column contains explanatory variables, the second one the estimate of the effect size, and the third and fourth one the lower and higher (respectively) bounds of the 95% credibility interval for the effect size. Significant effects of explanatory variables are shown with a cyan background.

	Estimates(median)	lower.CI(2.5)	upper.CI(97.5)
(Intercept)	83.79	39.06	128.68
mel_varsizer	-0.56	-2.27	1.18
ker_varsizer	-0.01	-1.09	1.13
air_varsizer	0.45	-0.93	1.80
typeSolid	-54.15	-109.99	-0.41
typeMixed	-37.85	-84.53	8.81
nb_layers	-1.04	-2.73	0.65
align_disorder	1.20	-0.05	2.45
barbule_shape	0.25	0.00	0.50
typeSolid:nb_layers	3.28	-1.80	8.53
typeMixed:nb_layers	1.76	-0.95	4.48
phylogenetic.variance	88.77	0.01	473.16
residual.variance	348.87	176.42	658.59

Supplementary table 11: Correlation between FWHM (opposite of saturation) and structural parameters. Optical theory predicts that saturation is controlled by the variance in layer thickness, the number of layers and their refractive index (i.e. multilayer type) as well as disorder in the alignment of the multilayers. We test this on empirical data from hummingbird iridescent feathers using MCMCglmm. The first column contains explanatory variables, the second one the estimate of the effect size, and the third and fourth one the lower and higher (respectively) bounds of the 95 % credibility interval for the effect size. Significant effects of explanatory variables are shown with a cyan background.

	Estimates(median)	lower.CI(2.5)	upper.CI(97.5)
(Intercept)	15.74	6.72	23.40
keratin_size	0.51	0.41	0.62
phylogenetic.variance	5.41	0.00	70.55
residual.variance	55.64	30.58	87.55

Supplementary table 12: Correlation between melanin and keratin layer thicknesses using MCMCglmm. The first column contains explanatory variables, the second one the estimate of the effect size, and the third and fourth one the lower and higher (respectively) bounds of the 95 % credibility interval for the effect size. Significant effects of explanatory variables are shown with a cyan background.

	Estimates(median)	lower.CI(2.5)	upper.CI(97.5)
(Intercept)	18.21	2.88	34.16
air_thickness	0.41	0.22	0.60
phylogenetic.variance	2.92	0.00	86.14
residual.variance	92.40	53.90	146.26

Supplementary table 13: Correlation between melanin and air layer thicknesses using MCMCglmm. The first column contains explanatory variables, the second one the estimate of the effect size, and the third and fourth one the lower and higher (respectively) bounds of the 95 % credibility interval for the effect size. Significant effects of explanatory variables are shown with a cyan background.

	Estimates(median)	lower.CI(2.5)	upper.CI(97.5)
(Intercept)	32.58	3.19	62.41
air_thickness	0.45	0.11	0.78
phylogenetic.variance	128.86	0.04	416.43
residual.variance	242.14	137.09	448.51

Supplementary table 14: Correlation between keratin and air layer thicknesses using MCMCglmm. The first column contains explanatory variables, the second one the estimate of the effect size, and the third and fourth one the lower and higher (respectively) bounds of the 95 % credibility interval for the effect size. Significant effects of explanatory variables are shown with a cyan background.

Distribution of iridescent colours in hummingbird communities results from the interplay between selection for camouflage and communication.

Aim: Test the phenotypic structure (clustering vs overdispersion) of iridescent colours at the community level on:

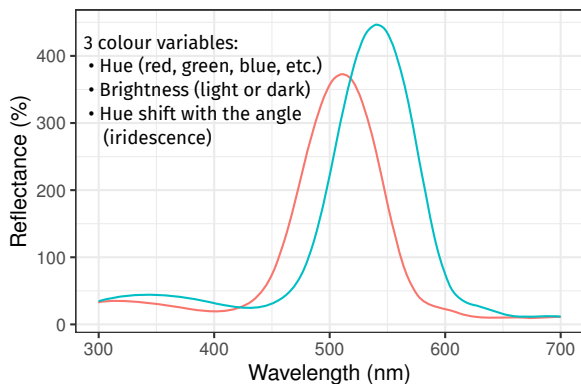
- 112 **hummingbird species**
- spread across **189 local assemblages in Ecuador**



Methods

Iridescent colours measurement

Spectral measurements at two angle configurations with a goniospectrometer:



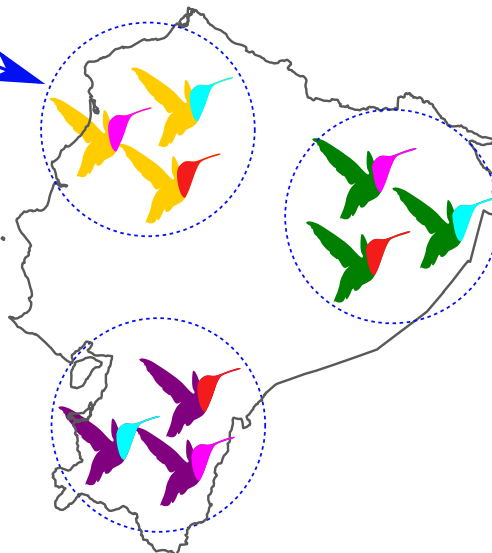
Phenotypic structure quantification

$$\tau_{st} = \frac{\text{global mean trait diversity} - \text{mean trait diversity within a community}}{\text{global mean trait diversity}}$$

↳ $\tau_{st}>0$: phenotypic clustering

↳ $\tau_{st}<0$: phenotypic overdispersion

Results & discussion



- Phenotypic clustering for hue and hue shift on dorsal patches ($\tau_{st}>0$).

↳ likely caused by selection for camouflage

- No phenotypic structure for hue and hue shift on facial patches and rump ($\tau_{st}=0$).

↳ likely caused by balance reproductive interference vs camouflage





Peer Community In Evolutionary Biology

RESEARCH ARTICLE

 Open Access

 Open Peer-Review

 Open Data

 Open Code

Cite as: Hugo G, Marianne E, Juan L. P., Christine A, Serge B, Claire D, and Doris G. Distribution of iridescent colours in hummingbird communities results from the interplay between selection for camouflage and communication. *BioRxiv* 586362, v5 peer-reviewed and recommended by *PCI Evolutionary Biology* (2019). DOI: 10.1101/586362

Posted: 15th November 2019

Recommender:
Sébastien Lavergne

Reviewers:
XXX

Correspondence:
hugo.gruson@normalesup.org

Distribution of iridescent colours in hummingbird communities results from the interplay between selection for camouflage and communication

Hugo Gruson¹, Marianne Elias², Juan L. Parra³, Christine Andraud⁴, Serge Berthier⁵, Claire Doutrelant¹, & Doris Gomez^{1,5}

¹ CEFÉ, Univ Montpellier, CNRS, Univ Paul Valéry Montpellier 3, EPHE, IRD, Montpellier, France

² ISYEB, CNRS, MNHN, Sorbonne Université, EPHE, 45 rue Buffon CP50, Paris, France

³ Grupo de Ecología y Evolución de Vertebados, Instituto de Biología, Universidad de Antioquia, Medellín, Colombia

⁴ CRC, MNHN, Ministère de la Culture et de la Communication, CNRS, Paris, France

⁵ INSP, Sorbonne Université, CNRS, Paris, France

This article has been peer-reviewed and recommended by
Peer Community In Evolutionary Biology

Abstract

Identification errors between closely related, co-occurring, species may lead to misdirected social interactions such as costly interbreeding or misdirected aggression. This selects for divergence in traits involved in species identification among co-occurring species, resulting from character displacement. On the other hand, predation may select for crypsis, potentially leading co-occurring species that share the same environment and predators to have a similar appearance. However, few studies have explored how these antagonistic processes influence colour at the community level. Here, we assess colour clustering and overdispersion in 189 hummingbird communities, tallying 112 species, across Ecuador and suggest possible evolutionary mechanisms at stake by controlling for species phylogenetic relatedness. In hummingbirds, most colours are iridescent structural colours, defined as colours that change with the illumination or observation angle. Because small variations in the underlying structures can have dramatic effects on the resulting colours and because iridescent structures can produce virtually any hue and brightness, we expect iridescent colours to respond finely to selective pressures. Moreover, we predict that hue angular dependence – a specific aspect of iridescent colours – may be used as an additional channel for species recognition. In our hummingbird assemblages in Ecuador, we find support for colour overdispersion in ventral and facial patches at the community level even after controlling for the phylogeny, especially on iridescence-related traits, suggesting character displacement among co-occurring species. We also find colour clustering at the community level on dorsal patches, suspected to be involved in camouflage, suggesting that the same cryptic colours are selected among co-occurring species.

Keywords: Reproductive Character Displacement; Agonistic Character Displacement; Camouflage; Structural Colours; Angle-Dependent Colouration; Community structure; Ecuador

Introduction

Colour is a complex communication channel widespread among various taxa and involved in many ecological and evolutionary processes [7]. It can be described by multiple variables, including hue (colour in its common sense, such as red, green, blue, etc.) and brightness (average level of grey of a colour, i.e. whether the object is light or dark). Colours can be produced by two non-mutually exclusive means: pigmentary colours are produced by the selective absorption of incoming light by pigments, while structural colours are produced by the interaction of incoming light with nanostructures, causing diffraction, interferences or scattering [68]. Among structural colours, iridescent colours are characterised by a shift in hue with changes in illumination or observation angle [88]. Iridescent colours are found

in many bird families such as Anatidae (ducks) Phasianidae (fowls), Sturnidae (starlings), or Trochilidae (hummingbirds), and thought to be involved in numerous adaptations [24]. But evolution of iridescent colours at the community level remains poorly understood. Yet, evolutionary patterns of iridescent colours, which remain poorly studied and understood, may differ from that of non-iridescent colours. Indeed, as opposed to other types of colours, iridescent colours can produce virtually any hue and are expected to respond more readily and finely to selection, because large changes of hue can be achieved by small changes in the underlying structures [72]. They can also result in directional colours only seen at specific angles, as well as highly reflective colours [65].

Because colours are involved in many different ecological processes, they are subject to multiple selection pressures, often with opposite effects [33]. Colour may indeed increase or decrease detectability of an animal depending on the colour contrast with its surroundings. In particular, colour can reduce predation risk via crypsis or aposematism or serve as a means of species identification. In this case, two opposite evolutionary forces act on colours: (i) On the one hand, species living in the same environment are likely experiencing similar selective pressures, such as predation. The environment is characterised by ambient light and vegetation, which both influence greatly which colours are poorly detectable and which colours are highly detectable [29, 32]. We thus expect co-occurring species to harbour the same, poorly detectable, colours as this would decrease the risk of being detected by predators, thereby causing a clustering pattern in colouration at the community level, all else being equal. This colour clustering can result from convergence between sympatric species (evolutionary process), from environmental filtering (ecological process), i.e. species sorting locally according to the traits they harbour, or a mixture of the two (detailed in table 1). (ii) On the other hand, sympatric closely-related species are more likely to face problems of species recognition, eventually resulting in reproductive interference - a phenomenon where an individual courts or mates with individuals of another species, producing no offspring or low fertility hybrids, leading to costly interbreeding [38]. Species misidentification can also lead to misdirected aggression and costly fighting when individuals compete over resources or territories. Hence, any feature that would enhance species recognition is expected to be selected for. In this context, closely related species living in sympatry should be under strong selective pressure to diverge in traits involved in communication, if divergence enhances species recognition. Divergence can result from a process called character displacement (RCD for reproductive character displacement, ACD for agonistic character displacement; evolutionary process) [8, 9, 37] or from species sorting (ecological process). For ACD, it is worth noting that traits are expected to diverge only in case of moderate ecological competition, whereas they should converge in case of high competition [37, 86]. Multiple empirical studies have shown character displacement for songs (e.g. Gerhardt [31] in frogs and Grant and Grant [35] in birds), or olfactory signals [3]. However, fewer studies have looked at divergence in colour patterns (but see Doutrelant, Paquet, Renoult, Grégoire, Crochet, and Covas [25], Hemmingson, Cowman, Hodge, and Bellwood [44], Lukhtanov, Kandul, Plotkin, Dantchenko, Haig,

and Pierce [50], Martin, Montgomerie, and Lougheed [53], Naisbit, Jiggins, and Mallet [61], and Sætre, Moum, Bureš, Král, Adamjan, and Moreno [74]). Almost all these studies were at the species level, and at best involved comparison between closely related species. Many of them also did not use objective spectrometry measurements and instead relied on human vision, which did not allow them to analyse colours as perceived by the intended receiver, in the case of this study: birds [6, 16, 27, 59].

In birds, it has been shown that colouration is under different selective pressures depending on the body patch location: dorsal patches, which are exposed to aerial predators, are mainly involved in camouflage while ventral and facial patches are mainly involved in communication [21, 33]. In this study, we test this hypothesis for iridescent colours at the community level by looking at phenotypic structure in hummingbird local assemblages across different body parts. Hummingbirds are an interesting study system to test this hypothesis as various published accounts of sexual displays and aggressive encounters among hummingbirds have made clear that certain feather patches such as the crown and throat are consistently used during these displays [46, 75–78]. On the other hand, colours displayed on the dorsal side of hummingbirds tend to resemble background colours and thus have been suggested to be cryptic [70]. Accordingly, we predict that co-occurring hummingbird species should display similar hues on dorsal patches, leading to phenotypic clustering of hues (i.e. co-occurring species are more similar than expected by chance, prediction 1) and different hues on ventral patches, resulting in a phenotypic overdispersion pattern (i.e. co-occurring species are more dissimilar than expected by chance, prediction 2). For brightness, we can formulate two alternative predictions: on the one hand, it might evolve in the same way as hue, also because of reproductive character displacement and selection for camouflage, leading to the same outcome as for hue (prediction 3, equivalent to predictions 1 and 2 but for brightness). On the other hand, because brightness level positively correlates with signal conspicuity, poorly detectable signals have similar brightness, and highly detectable signals have similar brightness. Hence, we may instead expect that species co-occurring should converge for brightness on all patches (prediction 3bis) if the same patches are involved in the same ecological process (communication or camouflage).

Compared to other types of colouration, iridescent colours might enable species recognition on another dimension in the sensory space. Two species can have the same hue or brightness at a given angle but can differ at another angle, via an additional variable we call "hue shift". Because hue shift cannot be seen at long distances, it may allow species to diverge without interfering with camouflage against predators [24, 90]. Accordingly, we predict overdispersion for hue shift not only on ventral patches, but also on dorsal patches (prediction 4). However, hue shift is often highly correlated with hue due to the optics underlying iridescence (Dakin and Montgomerie [17] for example reported $R^2 \geq 0.95$ for the correlation between hue and hue shift). We test this correlation with the data from this article and discuss how it may impact our results.

At the community level, we predict that community colour volume (also known as func-

tional richness FRic in functional ecology [87]) and brightness range increase with species richness more than expected in a random species assemblage (null model) because co-occurring species would use different colours (hue or brightness) (prediction 5).

Here we test our five predictions by quantifying both iridescent and non-iridescent colours of 189 hummingbird assemblages in Ecuador that include 112 species and span a large variety of habitats, and by assessing the phenotypic structure (clustering, random distribution, overdispersion of colours) and investigate the underlying processes by taking into account species phylogenetic relatedness within these assemblages. Comparing the uncorrected and the phylogenetically-corrected phenotypic structure of hummingbird communities will allow us to identify which mechanisms (character displacement, species sorting with mutual exclusion of similar species, environmental filtering; as detailed in table 1) underlie the community structure of iridescent colours in hummingbirds.

Materials and methods

All scripts and data used to produce the results and figures from this article are available at <https://doi.org/10.5281/zenodo.3355444>.

Community data

Hummingbirds are particularly suited as a study system to explore the possible effect of reproductive character displacement on iridescent colours because (i) they display a large variety of hues [20] and all species harbour some iridescent patches, many of which have a very strong angular dependence, rapidly shifting from e.g. pink to green or black [22, 26] (but note that many hummingbird species also have non-iridescent, pigmentary, patches), (ii) they belong to a very speciose family whose phylogeny is well established and readily available [48, 55], (iii) they live only in the Americas, especially in the tropics where numerous species can coexist locally [20] (iv) there is an extensive documentation of hybridisation between co-occurring species (see for example [36, 79] for our region of interest), which creates the perfect opportunity to study reproductive interference and (v) almost all species are available in museum collections and their colour can be objectively measured using spectrometric measurements [23].

Presence/absence data for hummingbird assemblages at 189 sites in Ecuador (see map in fig. S3) were compiled from data in peer-reviewed papers and reports from environmental organisations [34]. These sites cover a large variety of elevation ranges (fig. S3) and habitats [34, 69]. This dataset was previously thoroughly reviewed by comparing the observations with the known elevational and geographical ranges of each species [69] and includes observations of 112 of the 132 hummingbird species found in Ecuador [73].

Colour measurements and analyses

For each one of the 112 species, we borrowed one adult male in good condition from either the Muséum National d'Histoire Naturelle (MNHN) in Paris or the Musée des Confluences, in Lyon (full list in Online Supplementary Information). Previous studies show that even low sampling per species can accurately capture colour characteristics of the species [18]. Additionally, preliminary analyses on an independent dataset of 834 points across 18 hummingbird species, with up to 5 individuals measured by species, showed that intraspecific coefficient of variation (standard deviation divided by the average) of hue is very low (1.69 %) but could be higher for brightness (23.18 %) (detailed values for each species in table S3). When comparing intra- to interspecific variation, intraspecific however always remains negligible compared to interspecific variation (intraclass coefficient reported in table S3). We ensured that the specimen colouration was representative of the other specimens available in the collections to the human eye. When multiple subspecies were living in the area where presence was recorded, we randomly picked one of them. Whenever possible, we picked specimens collected in Ecuador (88 % of the cases), or when not available in neighbouring countries, such as Colombia or North Peru (11 % of the cases), as to minimise the effect of regional variability in colour.

We consistently took spectral reflectance measurements on the eight following patches (described in fig. S1): crown, back, rump, tail, throat, breast, belly, wing. We also made additional measurements on patches that visually differed in colouration from these eight main ones, as in Gomez and Théry [33] and Doutrelant, Paquet, Renault, Grégoire, Crochet, and Covas [25].

We measured reflectance using a setup similar to Meadows, Morehouse, Rutowski, Douglas, and McGraw [57], relying on the use of two separate optical fibres. Light was conducted from an Oceanoptics DH-2000 lamp emitting over the 300-700 nm range of wavelengths to which birds are sensitive [11] to the sample through an illuminating FC-UV200-2-1.5 x 100 optical fibre (named illumination fibre). Light reflected by the sample was then collected by a second identical optical fibre (named collection fibre) and conducted toward an Oceanoptics USB4000 spectrophotometer (used with the SpectraSuite 2.0.162 software). This setup allows for a precise independent rotation of the illumination and the collection fibres, necessary for the measurement of iridescent colours [65]. For more details about the measurement conditions as recommended in White, Dalrymple, Noble, O'Hanlon, Zurek, and Umbers [89], see the supplementary materials (ESM).

For every patch, we recorded a first reflectance spectrum at the position of the fibres which maximised total reflectance. To measure hue angle dependency (iridescence), we then moved both fibres 10° away from the previous position and recorded a second spectrum, as in Meadows, Roudybush, and McGraw [58]. More recent measurement methods revealed that it would be more accurate to keep the angular span between the illumination and collection fibres constant [39]. We however confirmed that this did not impact our results by run-

ning our analyses once with all data and once with only data at a given angular span (which represented 94 % of the total data). All measurements were performed in a dark room with temperature control. Recorded spectra were normalised by an Avantes WS-1 white standard and a measurement with the lamp shut down (dark reference) and integration times were determined for each sample as to maximise the intensity of the signal without saturating the spectrometer. Final values were averaged over five consecutive measurements and spectra were smoothed using a loess algorithm and interpolated every 1 nm and negative values were set to zero using the R package pavo [52].

We analysed spectra using Endler and Mielke [30] model with relative quantum catches Q_i (without Fechner's law). All birds are tetrachromats and can see light with wavelengths from 300 to 700 nm, which includes ultra-violet light (UV) [66]. But different bird species vary in their sensitivity [63]: some are UV-sensitive (UVS) while others are violet-sensitive (VS). Literature on colour vision in hummingbirds suggests that both types are found within the family (see Chen and Goldsmith [11] and Herrera, Zagal, Diaz, Fernández, Vielma, Cure, Martinez, Bozinovic, and Palacios [45] for UVS species and Ödeen and Håstad [64] for VS species). Because we did not have enough information to compute ancestral states and vision type for all species in our study and because it was found to have little influence in previous studies [21, 33], we ran our analyses as if all species were VS, using the spectral sensitivities of a typical VS bird, *Puffinus pacificus* [43], whose photoreceptor absorbances match closely those reported for hummingbirds [64]. We used different illuminants defined in Endler [29], depending on the habitat of the species described in Stotz, Fitzpatrick, Parker III, and Moskovits [83] (detailed in SI): "large gaps" illumination was used for species living in the canopy while "forest shade" was used for species living in the understory. Hue was a tridimensional variable defined by the position (x , y and z) of the reflectance spectrum in the tetrahedron representing bird colour vision space [30] and brightness was defined as in Endler and Mielke [30] (perceived intensity of colour, also sometimes referred to as luminance). We ensured that all indices were repeatable (table S1) by measuring twice the same individual and patch on 20 patches and computing the intra-class coefficient (ICC) with the rptR R package [82]. We add another variable to describe iridescence: hue shift, defined as the difference between hue at maximum reflectance and hue at 10° away from maximum reflectance, in a similar fashion to Dakin and Montgomerie [17]. Because it is the difference of two tridimensional variables (hue at the position where reflectance was maximum and hue at 10° away), hue shift is tridimensional as well. Dakin and Montgomerie [17] found a high correlation between hue and hue shift at the intraspecific level in the peacock *Pavo cristatus*, we also report a high correlation at the interspecific level in hummingbirds by performing a linear regression in \mathbb{R}^3 between hue and hue shift ($R^2 = 0.51$, $F(3; 1372) = 469.7$, $p < 0.0001$). New measurement methods have since been developed and propose a new definition for hue shift which is not correlated to hue but they were not available at the time of this study [39].

We analysed the colour volume for each species by measuring the convex hull volume of all colour patches on the bird, as suggested in Stoddard and Prum [81]. We compared the re-

lationship between the colour volume of a community and the number of species within this community relative to a null model (prediction 5) obtained by creating random assemblages from a species pool containing all species from all communities. In other words, actual assemblages are compared to fictional assemblages with exactly the same number of species but no abiotic or biotic constraints on the species composition.

However, the colour volume does not take into account the patch location on the bird body, raising several concerns. First, two species could use the same colour but at different places on their body. They would then look different to an observer but not identified as such in this analysis. Additionally, we expect different evolutionary signals on different patches, that could even each other out, and blur the outcome at the bird level. For these reasons, we also performed our analyses separately for each one of the following eight patches: crown, back, rump, tail, throat, breast, belly, wing (locations shown in fig. S1).

Trochilidae phylogeny and comparative analyses

A distribution of 100 phylogenetic trees of the Trochilidae family was downloaded from birdtree.org [48] to take into account phylogenetic uncertainty in the comparative analyses [67]. The 112 species included in this study constitute a fairly even sampling of the hummingbird phylogeny (fig. S2).

We used the method developed by Hardy and Senterre [42] and Baraloto, Hardy, Paine, Dexter, Cruaud, Dunning, Gonzalez, Molino, Sabatier, Savolainen, and Chave [5] to analyse respectively the phylogenetic (Π_{ST}) and phenotypic (τ_{ST}) structures of the hummingbird communities of Ecuador (clustering or overdispersion). This method relies on computing indices inspired by the Simpson index and the fixation index F_{ST} , comparing the observed diversity within and between communities. For phylogeny, Π_{ST} can reveal phylogenetic clustering ($\Pi_{ST} > 0$) or phylogenetic overdispersion ($\Pi_{ST} < 0$) within communities. Likewise, for phenotypic traits, τ_{ST} can reveal phenotypic clustering ($\tau_{ST} > 0$) or phenotypic overdispersion ($\tau_{ST} < 0$) within communities. Statistical significance of overdispersion or clustering is obtained from comparing the observed value to that obtained for the same patch location from 1000 random communities (created by drawing from the total species pool, using algorithm 1s from Hardy [41], which keeps the local species richness per site constant). This approach compares the phenotypic structure to what would be expected by chance.

To disentangle the relative effect of ecological (species sorting) and evolutionary mechanisms (selection), we also perform our analyses by taking into account the phylogenetic relationships between species. If the species in the community are more clustered or overdispersed than expected given their phylogenetic relationships, this is taken as evidence that the trait has not evolved in a Brownian fashion (detailed in table 1). To this end, we used the `decouple` function [19], which returns phylogenetically predicted and residual trait values by performing a linear regression of individual trait values explained by the phylogeny. We computed the value of τ_{ST} on trait values decoupled from the phylogeny. This value is hereafter

denoted $d\tau_{ST}$. Similarly to the classical τ_{ST} , the sign of $d\tau_{ST}$ indicates phenotypic clustering ($d\tau_{ST} > 0$) or overdispersion ($d\tau_{ST} < 0$) once the effect of the phylogenetic structure of the communities has been decoupled.

Analyses performed on a tree distribution (Π_{ST} and $d\tau_{ST}$) with n trees return a distribution of n statistics values and n p-values p_i . We summarised this information by computing the median of the statistics and the overall p-value p by using Jost's formula [4]:

$$p = k \sum_{i=0}^{n-1} \frac{(-\ln(k))^i}{i!} \quad \text{where } k = \prod_{i=1}^n p_i \quad (1)$$

Results

We find a strong phylogenetic clustering within communities ($\Pi_{ST} = 0.062 > 0$, $p < 0.0001$), indicating that co-occurring species are more closely related than expected by chance.

Phenotypic structure of the communities (predictions 1 - 4)

When looking at the bird entire body (when all patches are included simultaneously) by computing the overlap of the colour volumes, we did not find any phenotypic structure.

When the different major patches (crown, back, rump, tail, throat, breast, belly and wing) are examined separately (table 2 and table S2), we find clustering ($\tau_{ST} > 0$) in hue and hue shift on the back, rump, tail, belly and wing. Once we decouple the effect of the shared evolutionary history, we find clustering on the crown and the back ($d\tau_{ST} > 0$) but overdispersion on the belly for both hue and hue shift ($d\tau_{ST} < 0$). Hue shift is also overdispersed on the rump and the tail ($d\tau_{ST} < 0$). There is no phenotypic structure on the throat, breast or wing for hue and hue shift nor on the rump or the tail for hue.

We find no phenotypic structure (neither clustering nor overdispersion) for brightness on any patches before phylogenetic correction. After phylogenetic correction, brightness values for the throat, breast and belly are clustered among co-occurring species ($d\tau_{ST} > 0$) but show no phenotypic structure for the crown, the back, the wing and the tail.

Effect of community species richness on colour characteristics (prediction 5)

We found that the brightness range within a community increased in the same way as a null model built from random species assemblages (fig. 1b). For colour volume, we find some outliers with a higher colour volume than expected for community with the same number of species (fig. 1a).

$\tau_{ST} < 0$	$\tau_{ST} = 0$	$\tau_{ST} > 0$	
Phenotypic overdispersion		No community structure	Phenotypic clustering
$d\tau_{ST} < 0$	Co-occurring species are less similar than expected by chance because of character displacement.	Co-occurring species are more similar than expected by chance despite character displacement because closely related species co-occur more often than expected at random (phylogenetic clustering ; $\Pi_{ST} > 0$).	Co-occurring species are more similar than expected by chance despite character displacement because closely related species co-occur more often than expected at random (phylogenetic clustering ; $\Pi_{ST} > 0$).
$d\tau_{ST} = 0$	Brownian trait evolution	Competitive exclusion: co-occurring species are more dissimilar than expected by chance because distantly-related (and therefore dissimilar) species co-occur more often than expected at random (phylogenetic overdispersion ; $\Pi_{ST} < 0$).	Environmental filtering: co-occurring species are more similar than expected by chance because closely-related (and therefore similar) species co-occur more often than expected at random (phylogenetic clustering ; $\Pi_{ST} > 0$).
$d\tau_{ST} > 0$	Evolutionary convergence : co-occurring species are more similar than expected given their phylogenetic relationships, which means they evolved towards similarity in their colours.	Co-occurring species are neither more nor less similar than expected by chance despite evolutionary because distantly-related species co-occur more often than expected at random (phylogenetic overdispersion ; $\Pi_{ST} < 0$).	Co-occurring species are more similar than expected by chance because of evolutionary convergence.

Table 1. Summary of the different evolutionary and ecological scenarios and their results in terms of values of τ_{ST} and decoupled $d\tau_{ST}$.

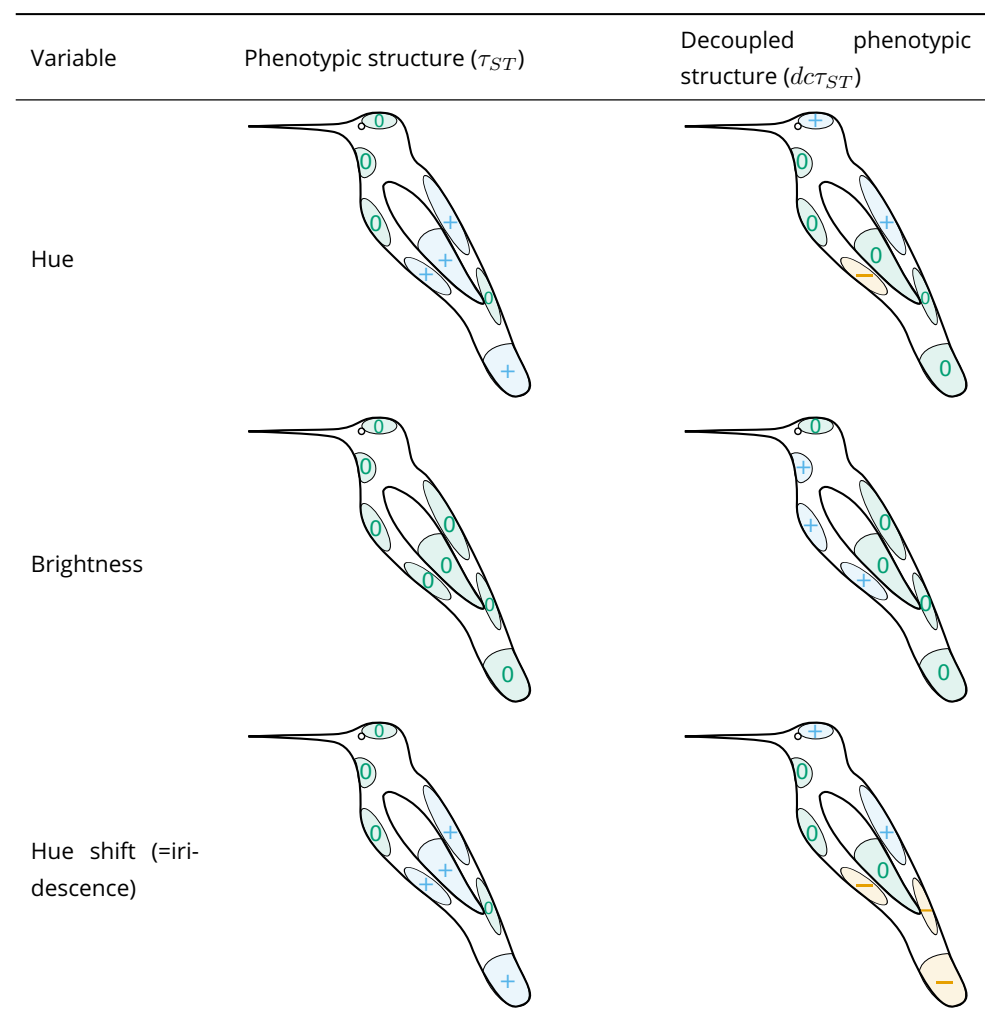


Table 2. Phenotypic structure of hummingbird communities for different variables (hue, brightness and hue shift) on the patches studied (crown, back, rump, tail, throat, breast, belly, wing; names and locations illustrated in fig. S1). Hue is a tridimensional variable defined by the reflectance spectrum position x , y and z in the tetrahedron representing avian colour space. Blue plus signs + indicate significant phenotypic clustering (τ_{ST} or $d\tau_{ST} > 0$), orange minus signs - indicate significant phenotypic overdispersion (τ_{ST} or $d\tau_{ST} < 0$), and green zeros 0 represent the absence of phenotypic structure. The left column shows the raw phenotypic structure of the community (columns in table 1), which may be influenced by the phylogenetic structure while the right column shows the phenotypic structure of the community, decoupled from all effects caused by the phylogeny (rows in table 1). By comparing the values of τ_{ST} and $d\tau_{ST}$ for each trait colour variable (hue, brightness and hue shift), we can assume a probable evolutionary scenario for each patch, based on the explanation in table 1. Exact values for the statistics are available in table S2.

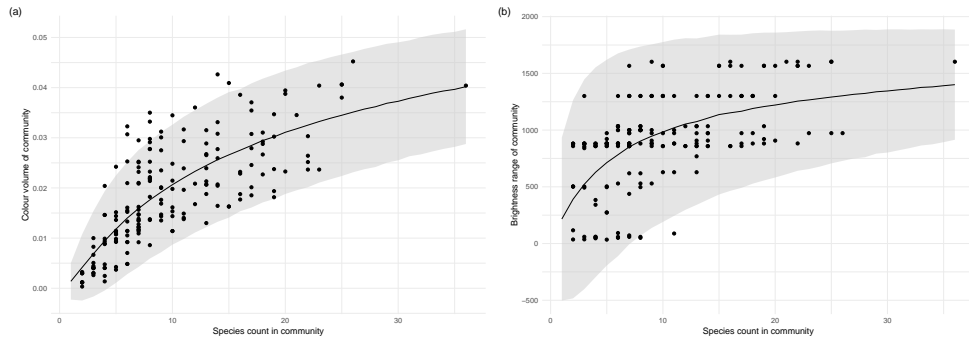


Figure 1. (a) Community total colour volume and (b) brightness range increase with the number of species within the community. Each point is a community. The black solid line represents the mean value of (a) colour volume or (b) brightness range from 10 000 random communities with a given species count (null model) and the gray ribbon represents two standard deviations from the mean of the null model.

Discussion

Our findings are consistent with our hypothesis that colour structure within hummingbird communities likely results from the interplay between two selective pressures, acting in opposite directions: selection by the local environment (e.g. camouflage from predators, leading to phenotypic clustering on dorsal patches, and selection for species recognition, leading to phenotypic overdispersion on ventral and facial patches. We also discuss other possible effects that might have contributed to the observed pattern.

Evidence for different evolutionary scenarios depending on patch location

At the entire bird level (i.e. when pooling together all patches), we did not find any phenotypic structure. But as mentioned earlier, this was expected since different locations on the birds are thought to be under different selection regimes [21, 33].

In accordance with our prediction 5, community colour volume (as estimated by the convex hull of hue and brightness range within a community) increases slightly faster with the number of species in the community than predicted by a null model. This suggests that co-occurring species in these communities tend to use more similar colours than expected by chance. However, this is not the case for the majority of communities, where co-occurring species do not use more nor less similar colours than expected by chance. This is further confirmed by the absence of phenotypic structure on the colour volume and the brightness when the effect of the phylogeny is not decoupled.

This could be the consequence of similar selective pressures between the communities we studied, leading colours in all assemblages to be randomly determined. This is however not very likely because the communities we studied differ a lot in both their vegetation background and therefore in the pressure for crypsis [34] and in their species composition. A more likely hypothesis is that co-occurring species tend to use the same colours but not necessarily on the same patches, which would also explain the absence of phenotypic structure when we pool all patches without taking into account their location. This is confirmed by our analysis patch by patch, where we find either clustering or overdispersion depending on the location of the patch.

Selection for convergence and phenotypic clustering

In accordance with our first two predictions, co-occurring hummingbird species tend to have similar hues on patches more likely dedicated to camouflage (back, rump, tail, wing; prediction 1) but not on patches more likely used in communication (crown, throat, breast; prediction 2), as shown in table 2 and table S2. This new result for iridescent colours matches what has been previously described for non-iridescent colours [21, 33]. The phenotypic clustering observed for hue on the rump, the tail and the wing vanishes after decoupling the clustering effect due to phylogenetic structure. This suggests that phenotypic clustering of hue on the rump, the tail and the wing is not caused by convergent evolution of co-occurring species but by environmental filtering, leading related, similar-looking species to live in the same area (as explained in table 1). This is confirmed by the high value of phylogenetic clustering. This sign of phylogenetic clustering complements the results from Graham, Parra, Rahbek, and McGuire [34] on the same dataset. We showed that intra-community species relatedness is high compared to inter-community species relatedness (Π_{ST}), while they showed that intra-community species relatedness (Net Relatedness Index) is higher than expected from random assemblages in 71 % of the cases [34]. This phylogenetic clustering may be caused by a strong niche conservatism but our study cannot discriminate whether such niche conservatism involves colour or other ecological traits. Our data does not allow us to assert with certainty the evolutionary history from the pattern we observe but the predominance of green and brown hues on the back and the wing respectively, as shown in fig. S4, hints to a role in camouflage. Alternatively, this phylogenetic clustering could be caused by hummingbirds' costly hovering flight at high elevation due to weaker lift caused by the decreasing atmospheric pressure [1, 2, 84], high foraging specialisation [49] or low dispersal ability, but this last hypothesis remains quite unlikely as the rare studies on this topic have shown that different hummingbird species display a wide variation in their dispersal ability [10, 60].

Contrary to our prediction 2, we also find clustering of hue on the belly before the use of the `decouple` function. However, the fact that it turns into overdispersion after the use of the `decouple` function, and not simply into a random phenotypic structure (as opposed to the rump, the tail and the wing mentioned just before), suggests this initial clustering (right

column in table 1) is mainly caused by environmental filtering on another trait but that hue on the belly is still under selection for divergence (first row in table 1). This other trait may be the colour of another patch or other ecological traits, as we explained previously.

We found a significant clustering of brightness on the throat, breast and belly after controlling for the phylogeny, indicating that brightness on those patches is more similar than expected given the phylogeny among co-occurring species (prediction 3bis). This suggests that the same patches have been selected to be involved either in communication or in camouflage among species living in the same environment. This is seen after controlling for the phylogeny and it is therefore not caused by the phylogenetic relatedness of co-occurring species. This is not surprising as many studies showed the paramount importance of the throat in the courtship display of many hummingbird species [46, 75–78] Two main hypotheses can explain why co-occurring species tend to communicate (or camouflage themselves) using the same patches: (i) There may be selective pressures for the use of specific patches in camouflage in a given environment (e. g., patches that are more exposed to predators' sight). (ii) Convergence in patches used in communication may be selected because it improves competitor identification in the case of a strong ecological niche overlap (convergence by agonistic character displacement as shown in Grether, Losin, Anderson, and Okamoto [37] and Tobias, Planqué, Cram, and Seddon [85]).

All those results suggest a strong effect of the environment in the evolution of colour in agreement with McNaught and Owens [56] who found that bird plumage colour was due to the light environment and not to reproductive character displacement in Australian birds. However, we do not find clustering on all patches, which suggests that, for some patches, the effect of habitat pressure is somehow limited or counterbalanced by reproductive or agonistic character displacement. On the contrary, for some patches, we found patterns that are likely the result of character displacement.

Character displacement and phenotypic overdispersion

In agreement with our prediction 2, after decoupling the effect of the phylogeny, there is overdispersion of hue on the belly, likely caused by character displacement (table 1). At a completely different taxonomic scale, focusing on a single hummingbird genus (*Coeligena*) with 11 species, Parra [70] also found that the belly was always involved in the difference in hue between subspecies. It was sometimes even the only patch causing those differences, as for example between *Coeligena torquata fulgidigula* and *Coeligena torquata torquata*. This suggests that the interspecific divergence we found on the belly at the community level on the whole Trochilidae family can be observed at different geographic and taxonomic scales, and even between subspecies of the same species.

As predicted, we also find more phenotypic overdispersion for hue shift than hue after decoupling the effect of the phylogeny, for example, on the rump and on the tail (prediction 4). It is possible that hue shift is less sensitive to selection for convergence because it may

vary without disturbing camouflage efficacy. However, we did not find the expected relaxing of clustering on hue shift on patches such as the back. This is likely caused by the fact that hue shift is highly correlated with hue, as found in this study and in Dakin and Montgomerie [17], who used the same indices to quantify iridescence. This correlation is due to the optics controlling iridescence, meaning that species that display similar hues should also display the same hue shift if they use the same underlying multilayer structures. The fact that the correlation is not perfect and that we nonetheless get different phenotypic patterns for hue and hue shift on some patches suggests that co-occurring species use different multilayer structures (as recently confirmed by [40]), which can produce different iridescent effects while displaying the same hue (functional convergence on hue).

Against our prediction 2, we did not find phenotypic overdispersion on any of the colour variables on patches such as the throat or the crown, that are thought to be sexually selected and often used in courtship displays [15, 78]. Several hypotheses can explain this fact: (i) The overdispersion on some patches (hue on the belly and hue shift on the rump and tail) is sufficient to enable species recognition. (ii) The current phenotypic structure, which is neither overdispersed nor clustered, on those patches is sufficient to enable species recognition. Indeed, the absence of phenotypic overdispersion does not mean that species look the same. It simply means that colour differences between species living in the same community and species in different communities occur in similar ranges. This difference may be sufficient to relax the selective pressure towards reproductive character displacement. (iii) The pressure towards overdispersion is balanced by habitat filtering (for both ventral and dorsal patches), resulting in no apparent phenotypic structure. The latter hypothesis was also a candidate explanation of the pattern found by Martin, Montgomerie, and Lougheed [53], where sympatric closely related species are more divergent than allopatric ones, but only when the range overlap is limited. They suggested that local adaptation could hinder divergence when species ranges were exactly the same. (iv) Species recognition is achieved by additional means and divergence occurs on other traits, such as modified feathers [28], song [51, 54] or non-vocal noises [12–14] and size. Notably, different species of hummingbirds can have very different courtship behaviour: leks for hermits [71, 80], dives and shuttle displays for bees [13, 47, 77], for instance.

Taken together, our results suggest that hummingbird iridescent colours are determined by different evolutionary mechanisms depending on their location. Within a community, co-occurring hummingbird species tend to display the same hues on dorsal patches which is what we expect if colour on these patches is mainly driven by selective pressures related to the local environment, such as selection for crypsis by predators, causing phenotypic clustering at the community level. This phenotypic clustering does not seem to be caused by adaptive convergence on colours but rather by environmental filtering perhaps linked to other ecological traits such as elevation tolerance or flight ability. In spite of this suspected environmental filtering, there is overdispersion for hue on the belly and hue shift on the rump and the tail. This suggests a possible role of character displacement, which could mean that

iridescence could be used a way to enable species recognition without affecting camouflage efficacy of birds, by opening up a new dimension in the sensory space: hue shift.

Data accessibility

Data are available online: <https://doi.org/10.5281/zenodo.3355443>

Acknowledgments

This project heavily relied on museum specimens which were made available by the work of collection curators: Patrick Boussès, Anne Previato, and Jérôme Fuchs (Muséum National d'Histoire Naturelle), Cédric Audibert and Harold Labrique (Musée des Confluences). J.L.P was funded by a Colombian Administrative Department for Science and Technology – Colciencias Grant code 111571250482 – contract number 248-2016. We also thank PCI recommender Sébastien Lavergne and two anonymous reviewers for their comments which helped us improve this manuscript. Version 5 of this preprint has been peer-reviewed and recommended by Peer Community In Evolutionary Biology (<https://doi.org/10.24072/pci.evolbiol.100086>).

Conflict of interest disclosure

The authors of this preprint declare that they have no financial conflict of interest with the content of this article. Marianne Elias is part of the managing board of PCIevoBiol and is one of the PCIevoBiol recommenders.

References

- [1] Altshuler DL, Dudley R, and McGuire JA. Resolution of a paradox: Hummingbird flight at high elevation does not come without a cost. *Proceedings of the National Academy of Sciences* 101 (2004), 17731–17736. doi: 10.1073/pnas.0405260101. pmid: 15598748.
- [2] Altshuler DL, Stiles FG, and Dudley R. Of hummingbirds and helicopters: hovering costs, competitive ability, and foraging strategies. *The American Naturalist* 163 (2004), 16–25. doi: 10.1086/380511. pmid: 14767833.
- [3] Bacquet PMB, Brattström O, Wang HL, Allen CE, Löfstedt C, Brakefield PM, and Nieberding CM. Selection on male sex pheromone composition contributes to butterfly reproductive isolation. *Proceedings of the Royal Society B: Biological Sciences* 282 (2015), 20142734. doi: 10.1098/rspb.2014.2734. pmid: 25740889.

- [4] Balasubramanian VN, Chakraborty S, and Panchanathan S. Conformal predictions for information fusion. *Annals of Mathematics and Artificial Intelligence* 74 (2015), 45–65. doi: 10.1007/s10472-013-9392-4.
- [5] Baraloto C, Hardy OJ, Paine CET, Dexter KG, Cruaud C, Dunning LT, Gonzalez MA, Molino JF, Sabatier D, Savolainen V, and Chave J. Using functional traits and phylogenetic trees to examine the assembly of tropical tree communities. *Journal of Ecology* 100 (2012), 690–701. doi: 10.1111/j.1365-2745.2012.01966.x.
- [6] Bennett ATD, Cuthill IC, and Norris KJ. Sexual selection and the mismeasure of color. *The American Naturalist* 144 (1994), 848–860. doi: 10.1086/285711.
- [7] Bradbury JW and Vehrenamp SL. *Principles of animal communication*. 2. ed. Sunderland, Mass: Sinauer Associates, 2011. 697 pp. isbn: 978-0-87893-045-6.
- [8] Brown WL and Wilson EO. Character displacement. *Systematic Biology* 5 (1956), 49–64. doi: 10.2307/2411924.
- [9] Butlin R. Speciation by reinforcement. *Trends in Ecology & Evolution* 2 (1987), 8–13. doi: 10.1016/0169-5347(87)90193-5.
- [10] Céspedes LN, Pavan LI, Hazlehurst JA, and Jankowski JE. The behavior and diet of the Shining Sunbeam (*Aglaeactis cupripennis*): A territorial high-elevation hummingbird. *The Wilson Journal of Ornithology* 131 (2019), 24–34. doi: 10.1676/18-79.
- [11] Chen DM and Goldsmith TH. Four spectral classes of cone in the retinas of birds. *Journal of Comparative Physiology A* 159 (1986), 473–479. doi: 10.1007/BF00604167.
- [12] Clark CJ. Wing, tail, and vocal contributions to the complex acoustic signals of courting Calliope hummingbirds. *Current Zoology* 57 (2011), 187–196. doi: 10.1093/czoolo/57.2.187.
- [13] Clark CJ, Elias DO, and Prum RO. Aeroelastic flutter produces hummingbird feather songs. *Science* 333 (2011), 1430–1433. doi: 10.1126/science.1205222. pmid: 21903810.
- [14] Clark CJ and Feo TJ. The Anna's hummingbird chirps with its tail: a new mechanism of sonation in birds. *Proceedings of the Royal Society of London B: Biological Sciences* 275 (2008), 955–962. doi: 10.1098/rspb.2007.1619. pmid: 18230592.
- [15] Clark CJ, Feo TJ, and Escalante I. Courtship displays and natural history of scintillant (*Selasphorus scintilla*) and volcano (*S. flammula*) hummingbirds. *The Wilson Journal of Ornithology* 123 (2011), 218–228. doi: 10.1676/10-076.1.
- [16] Cuthill IC, Bennett ATD, Partridge JC, and Maier Ej. Plumage reflectance and the objective assessment of avian sexual dichromatism. *The American Naturalist* 153 (1999), 183–200. doi: 10.1086/303160.
- [17] Dakin R and Montgomerie R. Eye for an eyespot: how iridescent plumage ocelli influence peacock mating success. *Behavioral Ecology* 24 (2013), 1048–1057. doi: 10.1093/beheco/art045.

- [18] Dalrymple RL, Hui FKC, Flores-Moreno H, Kemp DJ, and Moles AT. Roses are red, violets are blue – so how much replication should you do? An assessment of variation in the colour of flowers and birds. *Biological Journal of the Linnean Society* 114 (2015), 69–81. doi: 10.1111/bij.12402.
- [19] De Bello F, Šmilauer P, Diniz-Filho JAF, Carmona CP, Lososová Z, Herben T, and Götzenberger L. Decoupling phylogenetic and functional diversity to reveal hidden signals in community assembly. *Methods in Ecology and Evolution* 8 (2017), 1200–1211. doi: 10.1111/2041-210X.12735.
- [20] Del Hoyo J, Elliott A, Sargatal J, Christie DA, and de Juana E. *Handbook of the Birds of the World Alive*. 2017. url: hbw.com.
- [21] Delhey K. Revealing the colourful side of birds: Spatial distribution of conspicuous plumage colours on the body of Australian birds. *Journal of Avian Biology* (2019). doi: 10.1111/jav.02222.
- [22] Dorst J. Recherches sur la structure des plumes des trochilidés. Paris: Université de Paris, 1951. 260 pp.
- [23] Doucet SM and Hill GE. Do museum specimens accurately represent wild birds? A case study of carotenoid, melanin, and structural colours in long-tailed manakins *Chiroxiphia linearis*. *Journal of Avian Biology* 40 (2009), 146–156. doi: 10.1111/j.1600-048X.2009.03763.x.
- [24] Doucet SM and Meadows MG. Iridescence: a functional perspective. *Journal of The Royal Society Interface* 6 (Suppl 2 2009), S115–S132. doi: 10.1098/rsif.2008.0395.focus. pmid: 19336344.
- [25] Doutrelant C, Paquet M, Renault JP, Grégoire A, Crochet PA, and Covas R. Worldwide patterns of bird colouration on islands. *Ecology Letters* 19 (2016), 537–545. doi: 10.1111/ele.12588.
- [26] Dürrer H. Schillerfarben der Vogelfeder als Evolutionsproblem. Medizinischen Fakultät der Universität Basel, 1977.
- [27] Eaton MD. Human vision fails to distinguish widespread sexual dichromatism among sexually “monochromatic” birds. *Proceedings of the National Academy of Sciences* 102 (2005), 10942–10946. doi: 10.1073/pnas.0501891102. pmid: 16033870.
- [28] Eliason CM, Shawkey MD, and Clarke JA. Evolutionary shifts in the melanin-based color system of birds. *Evolution* 70 (2016), 445–454. doi: 10.1111/evo.12855. pmid: 26044706.
- [29] Endler JA. The color of light in forests and its implications. *Ecological Monographs* 63 (1993), 1–27. doi: 10.2307/2937121.
- [30] Endler JA and Mielke PW. Comparing entire colour patterns as birds see them. *Biological Journal of the Linnean Society* 86 (2005), 405–431. doi: 10.1111/j.1095-8312.2005.00540.x.

- [31] Gerhardt HC. Reproductive character displacement of female mate choice in the grey treefrog, *Hyla chrysoscelis*. *Animal Behaviour* 47 (1994), 959–969. doi: 10.1006/anbe.1994.1127.
- [32] Gomez D and Théry M. Influence of ambient light on the evolution of colour signals: comparative analysis of a Neotropical rainforest bird community. *Ecology Letters* 7 (2004), 279–284. doi: 10.1111/j.1461-0248.2004.00584.x.
- [33] Gomez D and Théry M. Simultaneous crypsis and conspicuousness in color patterns: comparative analysis of a neotropical rainforest bird community. *The American Naturalist* 169 (2007), S42–S61. doi: 10.1086/510138.
- [34] Graham CH, Parra JL, Rahbek C, and McGuire JA. Phylogenetic structure in tropical hummingbird communities. *Proceedings of the National Academy of Sciences* 106 (Supplement 2 2009), 19673–19678. doi: 10.1073/pnas.0901649106. pmid: 19805042.
- [35] Grant BR and Grant PR. Songs of Darwin's finches diverge when a new species enters the community. *Proceedings of the National Academy of Sciences* 107 (2010), 20156–20163. doi: 10.1073/pnas.1015115107. pmid: 21048082.
- [36] Graves GR and Zusi RL. An intergeneric hybrid hummingbird (*Heliodoxa leadbeateri* × *Helianzelus amethysticollis*) from Northern Colombia. *The Condor* 92 (1990), 754–760. doi: 10.2307/1368695.
- [37] Grether GF, Losin N, Anderson CN, and Okamoto K. The role of interspecific interference competition in character displacement and the evolution of competitor recognition. *Biological Reviews* 84 (2009), 617–635. doi: 10.1111/j.1469-185X.2009.00089.x. pmid: 19681844.
- [38] Gröning J and Hochkirch A. Reproductive interference between animal species. *The Quarterly Review of Biology* 83 (2008), 257–282. doi: 10.1086/590510.
- [39] Gruson H, Andraud C, Daney de Marcillac W, Berthier S, Elias M, and Gomez D. Quantitative characterization of iridescent colours in biological studies: a novel method using optical theory. *Interface Focus* 9 (2019), 20180049. doi: 10.1098/rsfs.2018.0049.
- [40] Gruson H, Elias M, Andraud C, Djediat C, Berthier S, Doutrelant C, and Gomez D. Hummingbird iridescence: an unsuspected structural diversity influences colouration at multiple scales. *bioRxiv* (2019). in revision, 699744. doi: 10.1101/699744.
- [41] Hardy OJ. Testing the spatial phylogenetic structure of local communities: Statistical performances of different null models and test statistics on a locally neutral community. *Journal of Ecology* 96 (2008), 914–926. doi: 10.1111/j.1365-2745.2008.01421.x.
- [42] Hardy OJ and Senterre B. Characterizing the phylogenetic structure of communities by an additive partitioning of phylogenetic diversity. *Journal of Ecology* 95 (2007), 493–506. doi: 10.1111/j.1365-2745.2007.01222.x.

- [43] Hart NS. Microspectrophotometry of visual pigments and oil droplets in a marine bird, the wedge-tailed shearwater *Puffinus pacificus*: topographic variations in photoreceptor spectral characteristics. *Journal of Experimental Biology* 207 (2004), 1229–1240. doi: 10.1242/jeb.00857. pmid: 14978063.
- [44] Hemingson CR, Cowman PF, Hodge JR, and Bellwood DR. Colour pattern divergence in reef fish species is rapid and driven by both range overlap and symmetry. *Ecology Letters* 22 (2019), 190–199. doi: 10.1111/ele.13180.
- [45] Herrera G, Zagal JC, Diaz M, Fernández MJ, Vielma A, Cure M, Martinez J, Bozinovic F, and Palacios AG. Spectral sensitivities of photoreceptors and their role in colour discrimination in the green-backed firecrown hummingbird (*Sephanoides sephaniodes*). *Journal of Comparative Physiology A* 194 (2008), 785. doi: 10.1007/s00359-008-0349-8. pmid: 18584181.
- [46] Hogan BG and Stoddard MC. Synchronization of speed, sound and iridescent color in a hummingbird aerial courtship dive. *Nature Communications* 9 (2018), 5260. doi: 10.1038/s41467-018-07562-7.
- [0] Hugo G, Marianne E, Juan L. P, Christine A, Serge B, Claire D, and Doris G. Distribution of iridescent colours in hummingbird communities results from the interplay between selection for camouflage and communication. *BioRxiv* 586362, v5 peer-reviewed and recommended by PCI Evolutionary Biology (2019). doi: 10.1101/586362.
- [47] Hurly TA, Scott RD, and Healy SD. The function of displays of male rufous hummingbirds. *The Condor* 103 (2001), 647–651. doi: 10.1650/0010-5422(2001)103[0647:TFODOM]2.0.CO;2.
- [48] Jetz W, Thomas GH, Joy JB, Hartmann K, and Mooers AO. The global diversity of birds in space and time. *Nature* 491 (2012), 444–448. doi: 10.1038/nature11631. pmid: 23123857.
- [49] Lindberg AB and Olesen JM. The fragility of extreme specialization: *Passiflora mixta* and its pollinating hummingbird *Ensifera ensifera*. *Journal of Tropical Ecology* 17 (2001), 323–329. doi: 10.1017/S0266467401001213.
- [50] Lukhtanov VA, Kandul NP, Plotkin JB, Dantchenko AV, Haig D, and Pierce NE. Reinforcement of pre-zygotic isolation and karyotype evolution in *Agrodiaetus* butterflies. *Nature* 436 (2005), 385–389. doi: 10.1038/nature03704.
- [51] Luther D. The influence of the acoustic community on songs of birds in a neotropical rain forest. *Behavioral Ecology* 20 (2009), 864–871. doi: 10.1093/beheco/arp074.
- [52] Maia R, Gruson H, Endler JA, and White TE. pavo 2: New tools for the spectral and spatial analysis of colour in R. *Methods in Ecology and Evolution* 10 (2019), 1097–1107. doi: 10.1111/2041-210X.13174.

- [53] Martin PR, Montgomerie R, and Lougheed SC. Color patterns of closely related bird species are more divergent at intermediate levels of breeding-range sympatry. *The American Naturalist* 185 (2015), 443–451. doi: 10.1086/680206.
- [54] Matyjasik P. Birds associate species-specific acoustic and visual cues: recognition of heterospecific rivals by male blackcaps. *Behavioral Ecology* 16 (2005), 467–471. doi: 10.1093/beheco/ari012.
- [55] McGuire JA, Witt CC, Remsen JVJ, Corl A, Rabosky DL, Altshuler DL, and Dudley R. Molecular phylogenetics and the diversification of hummingbirds. *Current Biology* 24 (2014), 910–916. doi: 10.1016/j.cub.2014.03.016. pmid: 24704078.
- [56] McNaught MK and Owens IPF. Interspecific variation in plumage colour among birds: species recognition or light environment? *Journal of Evolutionary Biology* 15 (2002), 505–514. doi: 10.1046/j.1420-9101.2002.00431.x.
- [57] Meadows MG, Morehouse NI, Rutowski RL, Douglas JM, and McGraw KJ. Quantifying iridescent coloration in animals: a method for improving repeatability. *Behavioral Ecology and Sociobiology* 65 (2011), 1317–1327. doi: 10.1007/s00265-010-1135-5. pmid: 876.
- [58] Meadows MG, Roudybush TE, and McGraw KJ. Dietary protein level affects iridescent coloration in Anna's hummingbirds, *Calyptra anna*. *Journal of Experimental Biology* 215 (2012), 2742–2750. doi: 10.1242/jeb.069351. pmid: 22837446.
- [59] Montgomerie R. Analyzing colors. In: *Bird Coloration, Volume 1: Mechanisms and Measurements*. Ed. by Hill GE and McGraw KJ. Vol. 1. 2 vols. Bird Coloration. Harvard University Press, 2006, p. 640. isbn: 978-0-674-01893-8.
- [60] Moore RP, Robinson WD, Lovette IJ, and Robinson TR. Experimental evidence for extreme dispersal limitation in tropical forest birds. *Ecology Letters* 11 (2008), 960–968. doi: 10.1111/j.1461-0248.2008.01196.x.
- [61] Naisbit RE, Jiggins CD, and Mallet J. Disruptive sexual selection against hybrids contributes to speciation between *Heliconius cydno* and *Heliconius melpomene*. *Proceedings of the Royal Society of London B: Biological Sciences* 268 (2001), 1849–1854. doi: 10.1098/rspb.2001.1753. pmid: 11522205.
- [62] Nakagawa S and Schielzeth H. Repeatability for Gaussian and non-Gaussian data: a practical guide for biologists. *Biological Reviews* 85 (2010), 935–956. doi: 10.1111/j.1469-185X.2010.00141.x. pmid: 20569253.
- [63] Ödeen A and Håstad O. Complex distribution of avian color vision systems revealed by sequencing the SWS1 opsin from total DNA. *Molecular Biology and Evolution* 20 (2003), 855–861. doi: 10.1093/molbev/msg108. pmid: 12716987.
- [64] Ödeen A and Håstad O. Pollinating birds differ in spectral sensitivity. *Journal of Comparative Physiology A* 196 (2010), 91–96. doi: 10.1007/s00359-009-0474-z.

- [65] Osorio DC and Ham AD. Spectral reflectance and directional properties of structural coloration in bird plumage. *Journal of Experimental Biology* 205 (2002), 2017–2027. pmid: 12089207.
- [66] Osorio DC and Vorobyev M. A review of the evolution of animal colour vision and visual communication signals. *Vision Research*. Vision Research Reviews 48 (2008), 2042–2051. doi: 10.1016/j.visres.2008.06.018. pmid: 18627773.
- [67] Pagel M and Lutzoni F. Accounting for phylogenetic uncertainty in comparative studies of evolution and adaptation. In: *Biological Evolution and Statistical Physics*. Ed. by Lässig M and Valleriani A. Vol. 585. Lecture Notes in Physics. Berlin, Heidelberg: Springer Berlin Heidelberg, 2002. isbn: 978-3-540-43188-6. doi: 10.1007/3-540-45692-9.
- [68] Parker AR. 515 million years of structural colour. *Journal of Optics A: Pure and Applied Optics* 2 (2000), R15–R28. doi: 10.1088/1464-4258/2/6/201.
- [69] Parra JL, McGuire JA, and Graham CH. Incorporating clade identity in analyses of phylogenetic community structure: an example with hummingbirds. *The American Naturalist* 176 (2010), 573–587. doi: 10.1086/656619. pmid: 20849270.
- [70] Parra JL. Color evolution in the hummingbird genus *Coeligena*. *Evolution* 64 (2010), 324–335. doi: 10.1111/j.1558-5646.2009.00827.x. pmid: 19703221.
- [71] Pizo MA. Lek behavior of the plovercrest (*Stephanoxis lalandi*, Trochilidae). *The Wilson Journal of Ornithology* 124 (2012), 106–112. doi: 10.1676/11-055.1.
- [72] Prum RO. Anatomy, physics, and evolution of structural colors. In: *Bird Coloration, Volume 1: Mechanisms and Measurements*. Ed. by Hill GE and McGraw KJ. Vol. 1. 2 vols. Bird Coloration. Harvard University Press, 2006, p. 640. isbn: 978-0-674-01893-8.
- [73] Ridgely RS and Greenfield PJ. *The birds of Ecuador: status, distribution and taxonomy*. Ithaca, NY: Cornell University Press, 2001. 880 pp. isbn: 978-0-8014-8720-0.
- [74] Sætre GP, Moum T, Bureš S, Král M, Adamjan M, and Moreno J. A sexually selected character displacement in flycatchers reinforces premating isolation. *Nature* 387 (1997), 589–592. doi: 10.1038/42451. pmid: 847.
- [75] Simpson RK and McGraw KJ. Experimental trait mis-matches uncover specificity of evolutionary links between multiple signaling traits and their interactions in hummingbirds. *Evolution* 73 (2019), 436–451. doi: 10.1111/evo.13662.
- [76] Simpson RK and McGraw KJ. It's not just what you have, but how you use it: solar-positional and behavioural effects on hummingbird colour appearance during courtship. *Ecology Letters* 21 (2018), 1413–1422. doi: 10.1111/ele.13125.
- [77] Simpson RK and McGraw KJ. Two ways to display: male hummingbirds show different color-display tactics based on sun orientation. *Behavioral Ecology* 29 (2018), 637–648. doi: 10.1093/beheco/ary016.

- [78] Stiles FG. Aggressive and courtship displays of the male Anna's hummingbird. *The Condor* 84 (1982), 208–225. doi: 10.2307/1367674. JSTOR: 1367674.
- [79] Stiles FG and Cortés-Herrera JO. Diagnosis and observations of a hybrid hummingbird (*Metallura tyrianthina* × *Aglaiaocercus kingi*) in the Eastern Andes of Colombia. *Revista de la Academia Colombiana de Ciencias Exactas, Físicas y Naturales* 39 (2015), 481–490. doi: 10.18257/raccefyn.260.
- [80] Stiles FG and Wolf LL. Ecology and evolution of lek mating behavior in the long-tailed hermit hummingbird. *Ornithological Monographs* (1979), iii–78. doi: 10.2307/40166760. JSTOR: 40166760.
- [81] Stoddard MC and Prum RO. Evolution of avian plumage color in a tetrahedral color space: a phylogenetic analysis of New World buntings. *The American Naturalist* 171 (2008), 755–776. doi: 10.1086/587526.
- [82] Stoffel MA, Nakagawa S, and Schielzeth H. rptR: repeatability estimation and variance decomposition by generalized linear mixed-effects models. *Methods in Ecology and Evolution* 8 (2017). Ed. by Goslee S, 1639–1644. doi: 10.1111/2041-210X.12797.
- [83] Stotz DF, Fitzpatrick JW, Parker III TA, and Moskovits DK. *Neotropical birds: ecology and conservation*. Vol. 3. University of Chicago Press, 1996. isbn: 978-0-226-77629-3.
- [84] Suarez RK. Hummingbird flight: sustaining the highest mass-specific metabolic rates among vertebrates. *Experientia* 48 (1992), 565–570. doi: 10.1007/BF01920240.
- [85] Tobias JA, Planqué R, Cram DL, and Seddon N. Species interactions and the structure of complex communication networks. *Proceedings of the National Academy of Sciences* 111 (2014), 1020–1025. doi: 10.1073/pnas.1314337111. pmid: 24395769.
- [86] Tobias JA and Seddon N. Signal design and perception in *Hypocnemis* antbirds: Evidence for convergent evolution via social selection. *Evolution* 63 (2009), 3168–3189. doi: 10.1111/j.1558-5646.2009.00795.x. pmid: 19659594.
- [87] Villéger S, Mason NWH, and Mouillot D. New multidimensional functional diversity indices for a multifaceted framework in functional ecology. *Ecology* 89 (2008), 2290–2301. doi: 10.1890/07-1206.1.
- [88] Vukusic P. Natural photonics. *Physics World* 17 (2004), 35. doi: 10.1088/2058-7058/17/2/34.
- [89] White TE, Dalrymple RL, Noble DW, O'Hanlon JC, Zurek DB, and Umbers KD. Reproducible research in the study of biological coloration. *Animal Behaviour* 106 (2015), 51–57. doi: 10.1016/j.anbehav.2015.05.007.
- [90] Wilts BD, Michielsen K, Kuipers J, De Raedt H, and Stavenga DG. Brilliant camouflage: photonic crystals in the diamond weevil, *Entimus imperialis*. *Proceedings of the Royal Society B: Biological Sciences* 279 (2012), 2524–2530. doi: 10.1098/rspb.2011.2651.

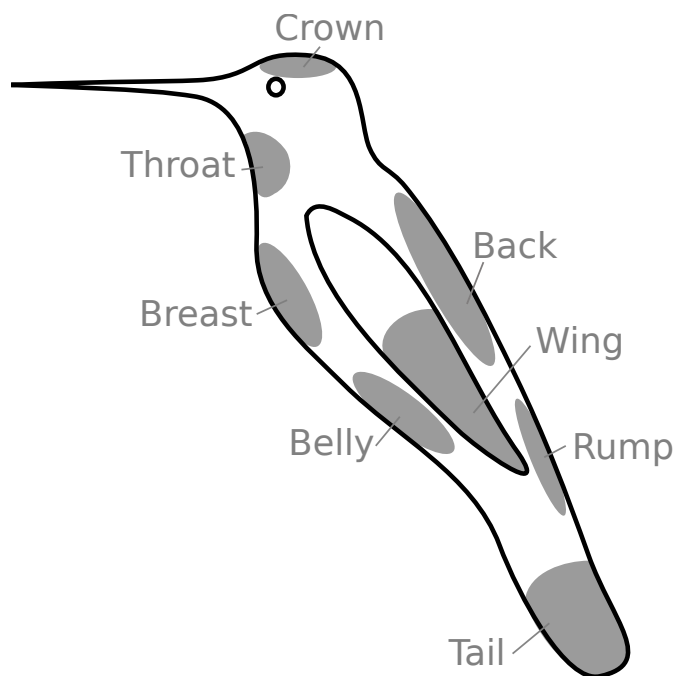
Appendix

Table 3. List of species with their provenance (Confluences = Musée des Confluences, Lyon, France, MNHN = Muséum National d'Histoire Naturelle, Paris, France), strata, and place of collection (when known). Strata data were extracted from Stotz, Fitzpatrick, Parker III, and Moskovits [83] and used in vision models.

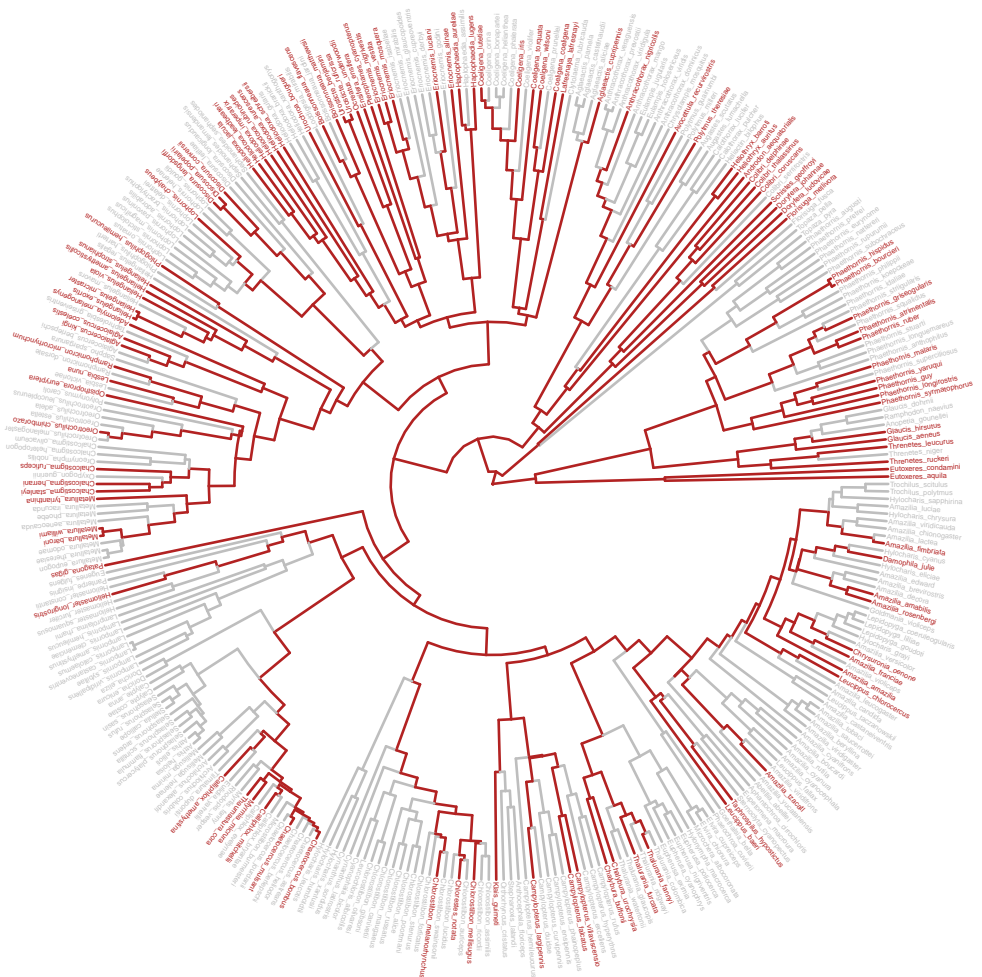
Species	Clade	Provenance	Strata	Location
<i>Adelomyia melanogenys</i>	Coquette	Confluences	Understory	
<i>Aglaeactis cupripennis</i>	Brilliant	MNHN	Canopy	Ecuador
<i>Aglaiocercus coelestis</i>	Coquette	MNHN	Canopy	Ecuador
<i>Aglaiocercus kingi mocoia</i>	Coquette	MNHN	Canopy	Ecuador
<i>Amazilia amabilis</i>	Emerald	MNHN	Understory	Ecuador
<i>Amazilia amazilia</i>	Emerald	MNHN	Understory	Ecuador
<i>Amazilia fimbriata fluvialis</i>	Emerald	MNHN	Canopy	Ecuador
<i>Amazilia franciae</i>	Emerald	MNHN	Canopy	Ecuador
<i>Amazilia grayi meridionalis</i>	Emerald	MNHN	Canopy	Ecuador
<i>Amazilia rosebergi</i>	Emerald	MNHN	Understory	Ecuador
<i>Amazilia sapphirina</i>	Emerald	MNHN	Canopy	Brasil
<i>Amazilia tzacatl jucunda</i>	Emerald	MNHN	Canopy	Ecuador
<i>Androdon aequatorialis</i>	Mangoe	MNHN	Understory	Ecuador
<i>Anthracothorax nigricollis</i>	Mangoe	MNHN	Canopy	Colombia
<i>Avocettula recurvirostris</i>	Mangoe	Confluences	Understory	
<i>Boissonneaua flavescens</i>	Brilliant	MNHN	Canopy	Ecuador
<i>Boissonneaua matthewsii</i>	Brilliant	MNHN	Canopy	Ecuador
<i>Calliphlox amethystina</i>	Bee	MNHN	Canopy	Ecuador
<i>Calliphlox mitchellii</i>	Bee	Confluences	Canopy	
<i>Campylopterus falcatus</i>	Emerald	MNHN	Understory	Colombia
<i>Campylopterus largipennis</i>	Emerald	MNHN	Understory	Peru
<i>Campylopterus villaviscensio</i>	Emerald	MNHN	Understory	Ecuador
<i>Chaetocercus bombus</i>	Bee	MNHN	Canopy	Ecuador
<i>Chaetocercus mulsant</i>	Bee	MNHN	Understory	Ecuador
<i>Chalcostigma herrani</i>	Coquette	MNHN	Canopy	Ecuador
<i>Chalcostigma ruficeps</i>	Coquette	Confluences	Understory	
<i>Chalcostigma stanleyi stanleyi</i>	Coquette	MNHN	Canopy	Ecuador
<i>Chalybura buffonii intermedia</i>	Emerald	Confluences	Understory	
<i>Chalybura urochrysia urochrysia</i>	Emerald	Confluences	Understory	
<i>Chlorestes notata obsoletus-puruensis</i>	Emerald	Confluences	Canopy	
<i>Chlorostilbon melanorhynchus</i>	Emerald	MNHN	Understory	Ecuador
<i>Chlorostilbon mellisugus phoeopygus</i>	Emerald	Confluences	Understory	
<i>Chrysuronia oenone</i>	Emerald	MNHN	Canopy	Ecuador
<i>Coeligena coeligena</i>	Brilliant	MNHN	Understory	Ecuador
<i>Coeligena iris hesperus</i>	Brilliant	MNHN	Understory	Ecuador
<i>Coeligena iris iris</i>	Brilliant	MNHN	Understory	Ecuador
<i>Coeligena lutetiae</i>	Brilliant	MNHN	Understory	Ecuador
<i>Coeligena torquata fulgidigula</i>	Brilliant	MNHN	Understory	Ecuador
<i>Coeligena torquata torquata</i>	Brilliant	MNHN	Understory	Ecuador
<i>Coeligena wilsoni</i>	Brilliant	MNHN	Understory	Ecuador
<i>Colibri coruscans</i>	Mangoe	MNHN	Canopy	Ecuador

Species	Clade	Provenance	Strata	Location
<i>Colibri delphinae</i>	Mangoe	MNHN	Canopy	Ecuador
<i>Colibri thalassinus</i>	Mangoe	MNHN	Canopy	Colombia
<i>Damophila julie</i>	Emerald	MNHN	Understory	Ecuador
<i>Discosura conversii</i>	Coquette	MNHN	Canopy	Ecuador
<i>Discosura langsdorffi</i>	Coquette	Confluences	Canopy	
<i>Discosura popelairii</i>	Coquette	MNHN	Canopy	Ecuador
<i>Doryfera johannae</i>	Mangoe	MNHN	Understory	Ecuador
<i>Doryfera ludoviciae</i>	Mangoe	MNHN	Understory	Ecuador
<i>Ensifera ensifera</i>	Brilliant	MNHN	Understory	Ecuador
<i>Eriocnemis alinae</i>	Brilliant	MNHN	Understory	Ecuador
<i>Eriocnemis luciani</i>	Brilliant	MNHN	Understory	Ecuador
<i>Eriocnemis mosquera</i>	Brilliant	Confluences	Understory	
<i>Eriocnemis nigrivestis</i>	Brilliant	MNHN	Understory	Ecuador
<i>Eriocnemis vestita smaragdinicollis</i>	Brilliant	MNHN	Understory	Ecuador
<i>Eutoxeres aquila</i>	Hermit	MNHN	Understory	Ecuador
<i>Eutoxeres condamini</i>	Hermit	Confluences	Understory	
<i>Florisuga mellivora</i>	Topazes	MNHN	Canopy	Ecuador
<i>Glaucis aeneus</i>	Hermit	MNHN	Understory	
<i>Glaucis hirsutus affinis</i>	Hermit	MNHN	Understory	Peru
<i>Haplophaedia aureliae russata</i>	Brilliant	Confluences	Understory	
<i>Haplophaedia lugens</i>	Brilliant	Confluences	Understory	
<i>Heliangelus amethysticollis laticlavius</i>	Coquette	Confluences	Understory	
<i>Heliangelus exortis</i>	Coquette	MNHN	Understory	Ecuador
<i>Heliangelus micraster</i>	Coquette	MNHN	Understory	Ecuador
<i>Heliangelus strophianus</i>	Coquette	MNHN	Understory	Ecuador
<i>Heliangelus viola</i>	Coquette	MNHN	Understory	Ecuador
<i>Heliodoxa aurescens</i>	Brilliant	MNHN	Understory	Colombia
<i>Heliodoxa imperatrix</i>	Brilliant	MNHN	Understory	Ecuador
<i>Heliodoxa jacula jamesoni</i>	Brilliant	MNHN	Understory	Ecuador
<i>Heliodoxa leadbeateri</i>	Brilliant	MNHN	Understory	Ecuador
<i>Heliodoxa rubinoides aequatorialis</i>	Brilliant	MNHN	Understory	Ecuador
<i>Heliodoxa schreibersii</i>	Brilliant	MNHN	Understory	Ecuador
<i>Heliomaster longirostris</i>	MtGem	MNHN	Canopy	Colombia
<i>Heliothryx auritus</i>	Mangoe	MNHN	Canopy	Ecuador
<i>Heliothryx barroti</i>	Mangoe	MNHN	Canopy	Ecuador
<i>Klais guimeti</i>	Emerald	MNHN	Understory	Ecuador
<i>Lafresnaya lafresnayi gayi</i>	Brilliant	Confluences	Understory	
<i>Lesbia nuna gracilis</i>	Coquette	MNHN	Canopy	Ecuador
<i>Leucippus baeri</i>	Emerald	Confluences	Understory	
<i>Leucippus chlorocercus</i>	Emerald	Confluences	Canopy	
<i>Lophornis chalybeus verreauxi</i>	Coquette	MNHN	Canopy	Colombia
<i>Metallura baroni</i>	Coquette	MNHN	Canopy	Ecuador
<i>Metallura tyrianthina tyrianthina</i>	Coquette	MNHN	Understory	Ecuador
<i>Metallura williami primolina</i>	Coquette	MNHN	Canopy	Ecuador
<i>Myrmia micrura</i>	Bee	MNHN	Canopy	Peru
<i>Ocreatus underwoodii melantherus</i>	Brilliant	MNHN	Understory	Ecuador
<i>Opisthoproraeuryptera</i>	Coquette	Confluences	Understory	
<i>Oreotrochilus chimborazo chimborazo</i>	Coquette	MNHN	Understory	Ecuador
<i>Oreotrochilus chimborazo jamesonii</i>	Coquette	MNHN	Understory	Ecuador

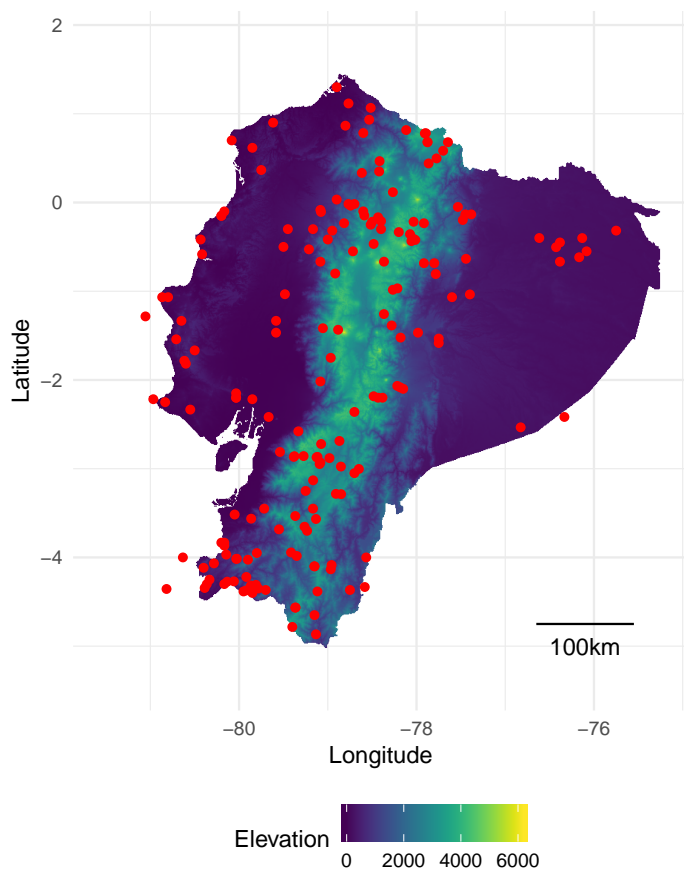
Species	Clade	Provenance	Strata	Location
<i>Patagona gigas</i>	Patagona	MNHN	Canopy	Ecuador
<i>Phaethornis atrimentalis atrimentalis</i>	Hermit	Confluences	Understory	
<i>Phaethornis bouri</i>	Hermit	MNHN	Understory	
<i>Phaethornis griseogularis</i>	Hermit	MNHN	Understory	Ecuador
<i>Phaethornis guy</i>	Hermit	MNHN	Understory	Ecuador
<i>Phaethornis hispidus</i>	Hermit	Confluences	Understory	
<i>Phaethornis longirostris</i>	Hermit	Confluences	Understory	
<i>Phaethornis malaris</i>	Hermit	Confluences	Understory	
<i>Phaethornis ruber</i>	Hermit	Confluences	Understory	
<i>Phaethornis syrmatophorus columbianus</i>	Hermit	MNHN	Understory	Ecuador
<i>Phaethornis yaruqui yaruqui</i>	Hermit	MNHN	Understory	Ecuador
<i>Phlogophilus hemileucurus</i>	Coquette	MNHN	Understory	Ecuador
<i>Polytmus theresiae leucorrhous</i>	Mangoe	MNHN	Understory	Ecuador
<i>Pterophanes cyanopterus</i>	Brilliant	MNHN	Understory	Ecuador
<i>Ramphomicron microrhynchum</i>	Coquette	MNHN	Canopy	Ecuador
<i>Schistes geoffroyi</i>	Mangoe	MNHN	Understory	Ecuador
<i>Taphrospilus hypostictus</i>	Emerald	MNHN	Understory	Ecuador
<i>Thalurania fannyi verticeps</i>	Emerald	MNHN	Understory	Ecuador
<i>Thalurania furcata viridispectus</i>	Emerald	MNHN	Understory	
<i>Thaumastura cora</i>	Bee	Confluences	Canopy	
<i>Threnetes leucurus cervinicauda</i>	Hermit	Confluences	Understory	
<i>Threnetes ruckeri</i>	Hermit	MNHN	Understory	Ecuador
<i>Urochroa bougueri</i>	Brilliant	Confluences	Understory	
<i>Urochroa bougueri leucura</i>	Brilliant	Confluences	Understory	
<i>Urosticte benjamini</i>	Brilliant	MNHN	Understory	Ecuador
<i>Urosticte ruficrissa</i>	Brilliant	Confluences	Understory	



Supplementary figure 1. Locations and names of the 8 patches measured on all species. Additional patches were measured for each species as soon as they differed from one of the 8 patches listed here for a human observer, as detailed in the methods section and as in Gomez and Théry [33].



Supplementary figure 2. Phylogenetic coverage of the *Trochilidae* family in our dataset (species and lineages in red).



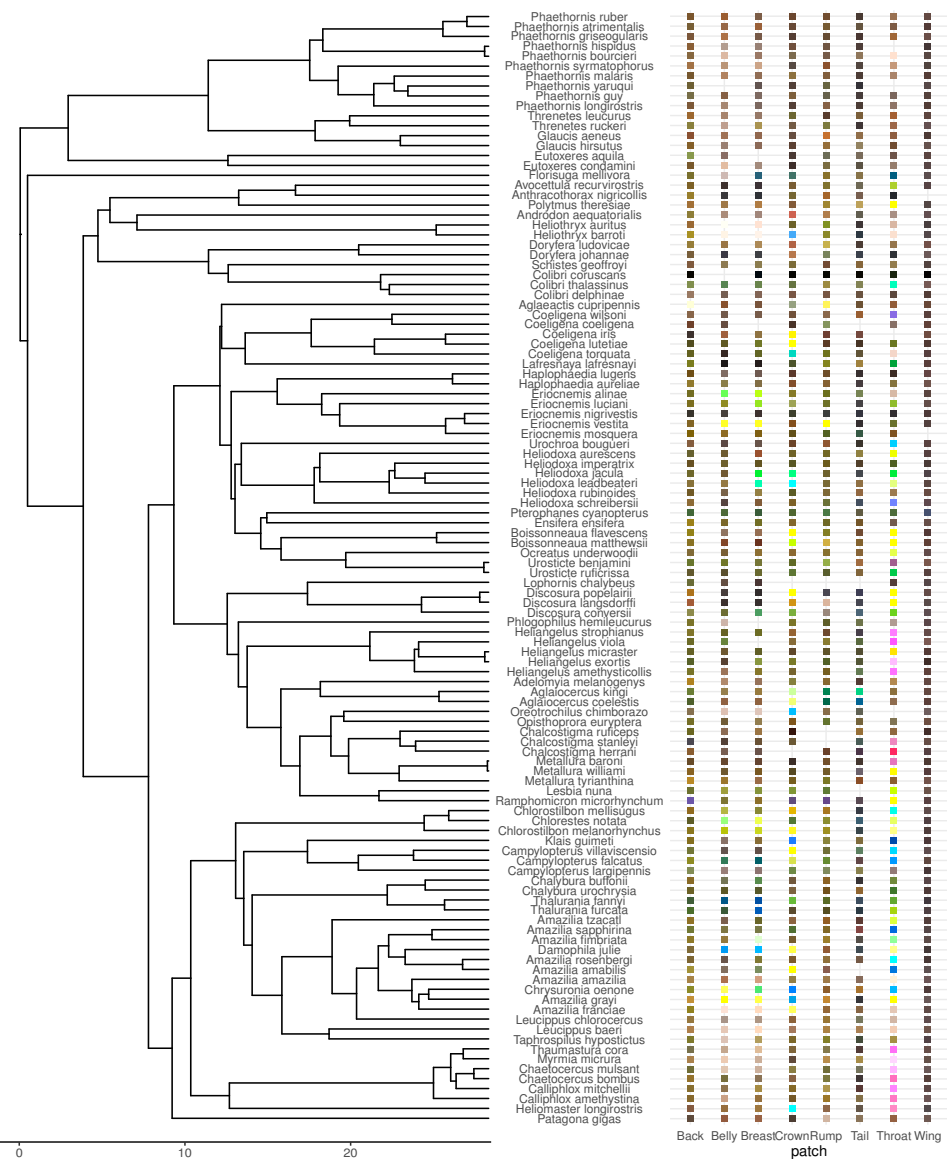
Supplementary figure 3. Study site locations (red dots) plotted on an altitudinal map of Ecuador. Communities outside the borders of the map are on islands or close enough to Ecuador borders to be taken into account in our study.

Table 4. Measurement of intraspecific variability for brightness (B2) and hue (H1) by computing the coefficient of variation (standard deviation divided the average) on an independent dataset of hummingbirds living in French Guiana (Gomez *et al*, unpublished data), in which between 2 and 5 males (last column) were measured for each species. The measurement protocol differs slightly from the one used in this study, because we used a bifurcated probe at 45°, which may increase the intraspecific variability in brightness. In spite of the apparently high values of the coefficient of variation for brightness, it remains highly repeatable as estimated by the intra-class coefficient [62]: $R = 0.809, p < 0.0001$ for brightness and $R = 0.661, p < 0.0001$ for hue.

Species	CV brightness (%)	CV_hue (%)	n
<i>Anthracothorax nigricollis</i>	20.57	2	3
<i>Calliphlox amethystina</i>	24.37	1.13	5
<i>Campylopterus largipennis</i>	17.43	0.1	2
<i>Chlorestes notatus</i>	19.79	1.96	5
<i>Discosura longicauda</i>	26.27	2.51	5
<i>Florisuga mellivora</i>	22.41	2.1	5
<i>Glaucis hirsuta</i>	33.75	0	4
<i>Heliomaster longirostris</i>	26.88	2.26	4
<i>Heliothryx aurita</i>	22.82	1.26	5
<i>Hylocharis cyanus</i>	29.75	2.55	3
<i>Hylocharis sapphirina</i>	23.32	3.36	4
<i>Lophornis ornatus</i>	23.38	1.55	5
<i>Phaethornis longuemareus</i>	18.59	0.15	4
<i>Phaethornis malaris</i>	21.44	0.1	2
<i>Phaethornis superciliosus</i>	27.88	0.1	5
<i>Thalurania furcata</i>	84.13	12.4	2
<i>Threnetes niger</i>	16.42	0.1	2
<i>Topaza pella</i>	23.04	1.83	5

Variable	Diffuse		Directional		Both		
	R	p-value	R	p-value	R	p-value	
Hue	x y z	0.734 0.923 0.780	0.002 <0.0001 0.0006	0.877 0.785 0.880	<0.0001 0.0006 <0.0001	0.925 0.951 0.940	<0.0001 <0.0001 <0.0001
Brightness		0.411	0.090	0.055	0.48	0.373	0.04

Supplementary table 1. We quantified the repeatability R (intra-class coefficient ICC) and the related p-value by bootstrapping using the `rptR` R package [62] of indices used in this study by performing the same measurements twice on two patches for 12 species (*Coeligena torquata*, *Colibri coruscans*, *Doryfera ludovicae*, *Helianzelus strophianus*, *Heliodoxa jamesonii*, *Heliothryx barroti*, *Juliamyia julie*, *Lesbia nuna*, *Metallura tyrianthina*, *Ramphomicron microrhynchum*, *Schistes albogularis*, *Urosticte benjamini*). Patches were selected to be of similar hue from a human point of view.



Supplementary figure 4. Colour of the 8 main patches for each species in our dataset. The colour corresponds to the colour in the human visual system (CIE10). The x-axis on the phylogeny is in millions years.

variable	value	Crown	Back	Rump	Tail	Throat	Breast	Belly	Wing
Hue	τ_{st}	-0.0073	0.055	0.055	0.044	0.027	0.03	0.05	0.058
	$p_{\tau_{st}<0}$	0.4	1	1	1	0.9	0.9	1	1
	$p_{\tau_{st}>0}$	0.6	0.01	0.01	0.03	0.09	0.06	0.005	0.006
	$d\tau_{st}$	0.0099	0.026	-0.0021	0.0034	-0.0021	-0.0032	-0.01	0.00073
	$p_{\tau_{st}<0}$	1	1	0.8	1	0.9	0.3	< 0.0001	1
	$p_{\tau_{st}>0}$	<0.0001	<0.0001	1	0.2	1	1	1	1
Brightness	τ_{st}	-0.021	0.0078	0.0032	-0.0064	0.00015	0.0041	-0.0031	0.0091
	$p_{\tau_{st}<0}$	0.1	0.7	0.6	0.5	0.5	0.6	0.5	0.6
	$p_{\tau_{st}>0}$	0.9	0.3	0.4	0.5	0.5	0.4	0.5	0.4
	$d\tau_{st}$	-0.0014	0.0028	0.00037	0.00068	0.013	0.023	0.007	-0.0058
	$p_{\tau_{st}<0}$	0.3	1	0.9	1	1	1	1	0.2
	$p_{\tau_{st}>0}$	0.8	0.7	0.7	0.8	< 0.0001	< 0.0001	0.002	1
Hue shift	τ_{st}	-0.007	0.051	0.052	0.043	0.027	0.029	0.049	0.058
	$p_{\tau_{st}<0}$	0.4	1	1	1	0.9	0.9	1	1
	$p_{\tau_{st}>0}$	0.6	0.01	0.01	0.03	0.08	0.06	0.006	0.006
	$d\tau_{st}$	0.0087	0.0059	-0.0068	-0.006	-0.0033	0.0023	-0.0098	-0.0018
	$p_{\tau_{st}<0}$	1	1	0.005	0.01	0.6	1	< 0.0001	1
	$p_{\tau_{st}>0}$	<0.0001	0.03	1	1	1	0.9	1	1

Supplementary table 2. Numerical values for τ_{st} and decoupled τ_{st} (denoted $d\tau_{st}$). P-values were computed by comparison of the actual value with the null distribution (obtained by randomisation of the communities using method 1s of Hardy [41]). Significant p-values are in bold and green. Positive values of $d\tau_{st}$ indicate phenotypic clustering whereas negative values indicate overdispersion.



Digest: Disentangling plumage and behavior contributions to iridescent signals*

Hugo Gruson^{1,2} 

¹CEFE, CNRS, Univ Montpellier, Univ Paul Valéry, Montpellier 3, EPHE, IRD, Montpellier, France

²E-mail: hugo.gruson@normalesup.org

Received December 20, 2018

Accepted January 16, 2019

To what extent do plumage properties and behavior interact to produce visual signals? Simpson and McGraw (2018) propose an elegant and novel experimental set-up to dissociate behavior and color and assess their relative effects in the resulting iridescent signal. They find that modification of either component leads to a modification of the resulting signal as seen by the receiver, suggesting that sexual selection acts simultaneously on both signal components.

Hummingbirds are famous for their bright colors that change rapidly with the angle of observation or illumination, a phenomenon known as iridescence (Doucet and Meadows 2009). This angle-dependency of color may produce flashes that are particularly conspicuous on feather patches such as the throat or the crown (Osorio and Ham 2002). Color as seen by the receiver (e.g., by a female during a male's courtship display) therefore results from both the intrinsic properties of the feather, and the orientation of the male during display. However, studying iridescent signals by taking into account both the feather properties and behavioral displays, and looking at how those two components might interact, has proven incredibly difficult. It requires a detailed knowledge of the courtship display behavior and a precise quantification of the iridescent color angle-dependency as seen in the receiver's visual system—birds, for example, can see ultraviolet colors.

In this study, Simpson and McGraw (2018) used data from their previous works at the intraspecific level to investigate how behavior and iridescent plumage interact in five hummingbird species from the “bee” clade (tribe: Mellisugini). These five bee hummingbird species recently diverged (McGuire et al. 2014) and have the same kind of courtship behavior (called a “shuttle display”), in which males fly back and forth in front of the female, while at the same time erecting their shiny throat feathers (Clark 2011).

*This article corresponds to Simpson, R. K., and K. J. McGraw. 2018. Experimental trait mismatches uncover specificity of evolutionary links between multiple signaling traits and their interactions in hummingbirds. *Evolution*, <https://doi.org/10.1111/evo.13662>.

Simpson and McGraw (2018) proposed an elegant and novel experimental set-up: they used plucked throat feathers and camera recordings of the display behavior, which allowed them to experimentally recreate the iridescent signal of a species during a display (top row of Fig. 1, also referred to as “**natural color appearance**¹” in the original article). To disentangle the relative effects of the plumage properties and courtship behavior on the resulting iridescent signal, they then created **mismatches**, where the plucked throat feathers and the display behavior came from different species (bottom row of Fig. 1).

The researchers measured two iridescent signal variables: **average color appearance** (color characteristics averaged for all positions during the display) and **percent change in color appearance** (the sum of differences in color characteristics between each position during the display; also called “**flashiness**”). Those two variables were features of what the authors refer to as **color appearance during display** (Fig. 1).

They found that mismatches between plumage and display behavior (i.e., when feathers and display behavior did not come from the same species) led to a different **average color appearance** and a different **flashiness** for the receiver. For example, throat feathers from all species changed more during display (higher **flashiness** value) when used in the shuttle display from the black-chinned hummingbird than when they were used in shuttle displays by other species (even their own). This suggests that

¹See Simpson and McGraw (2018) Table 1 for a full list of definitions of bolded words.

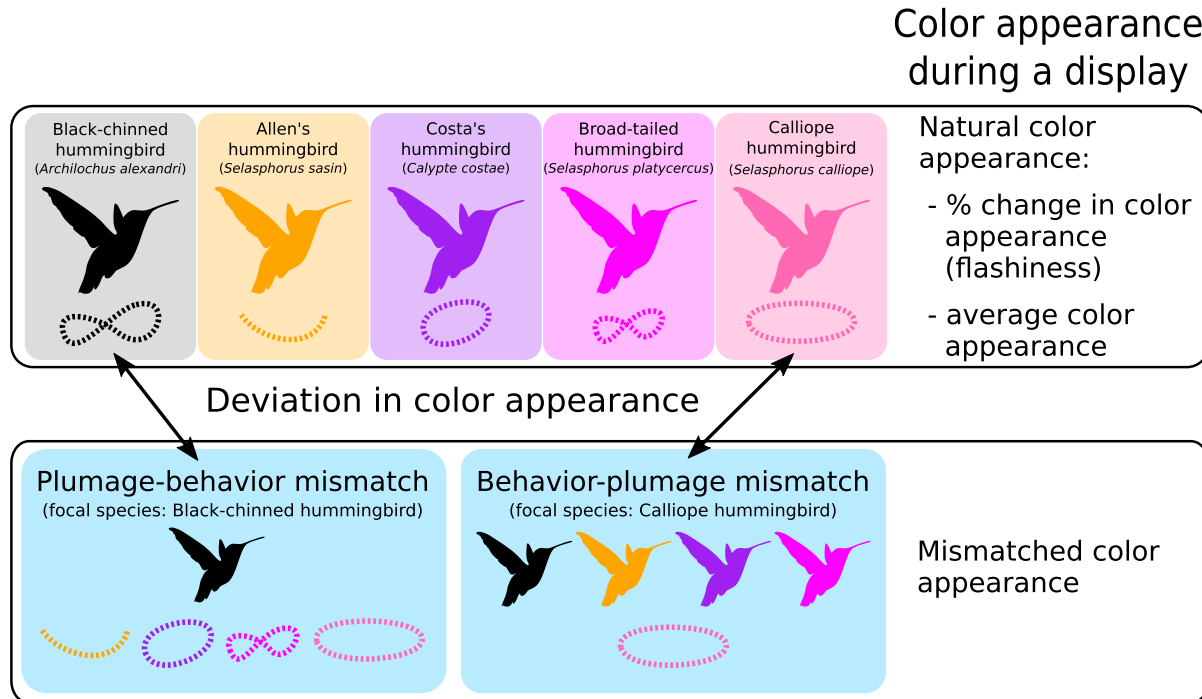


Figure 1. Summary of the protocol used in Simpson and McGraw (2018). Dashed paths represent shuttle display behavior of each species. The authors looked at deviations in color appearance during display (average color appearance and flashiness) between natural color appearance (feather and shuttle display from the same species, top block in this figure) and mismatched color appearance (feather and shuttle display from different species, bottom block in this figure). Colors for each species match those used in the original paper (Simpson and McGraw 2018, Fig. 4).

sexual selection acts simultaneously on intrinsic plumage characteristics and courtship behavior, and that both components play an important role in the resulting iridescent signal within each species.

The authors also investigated the relative contributions of both plumage and shuttle behavior to the resulting iridescent signal. They found that the overall color appearance and changes in hue during a display were mainly influenced by behavior rather than plumage characteristics. On the contrary, changes in luminescence during a display were correlated to throat patch size.

This article provides the first attempt to study a signal by evaluating and manipulating multiple signal components at the same time (behavior and feather properties) and by working at the interspecific level. In doing so, this study provides an interesting and reproducible experimental set-up that may be used to study other parts of courtship displays in bee hummingbirds (e.g., dives; Tamm et al. 1989) or in different species with complex colors and/or displays (e.g., birds-of-paradise; Stavenga et al. 2011). Future studies should also investigate the ecological and evolutionary drivers of the interspecific divergence in color and courtship behavior in bee hummingbirds. In particular, it remains unclear which specific signal features female prefer and use to select their mates.

LITERATURE CITED

- Clark, C. J. 2011. Wing, tail, and vocal contributions to the complex acoustic signals of courting Calliope hummingbirds. *Curr. Zool.* 57:187–196.
- Doucet, S. M., and M. G. Meadows. 2009. Iridescence: a functional perspective. *J. R. Soc. Interface* 6:S115–S132.
- McGuire, J. A., C. C. Witt, J. V. J. Remsen, A. Corl, D. L. Rabosky, D. L. Altshuler, and R. Dudley. 2014. Molecular phylogenetics and the diversification of hummingbirds. *Curr. Biol.* 24:910–916.
- Osorio, D. C., and A. D. Ham. 2002. Spectral reflectance and directional properties of structural coloration in bird plumage. *J. Exp. Biol.* 205:2017–2027.
- Simpson, R. K., and K. J. McGraw. 2018. Experimental trait mismatches uncover specificity of evolutionary links between multiple signaling traits and their interactions in hummingbirds. *Evolution*, <https://doi.org/10.1111/evo.13662>
- Stavenga, D. G., H. L. Leertouwer, N. J. Marshall, and D. C. Osorio. 2011. Dramatic colour changes in a bird of paradise caused by uniquely structured breast feather barbules. *Proc. R. Soc. Lond. B Biol. Sci.* 278:2098–2104.
- Tamm, S., D. P. Armstrong, and Z. J. Tooze. 1989. Display behavior of male Calliope hummingbirds during the breeding season. *The Condor* 91:272–279.

Associate editor: K. Moore
Handling Editor: Mohamed A. F. Noor

¹ RESEARCH ARTICLE

² **Running head:** COLOUR VOLUME ESTIMATION WITH α -SHAPES

³ Estimation of colour volumes as concave hypervolumes using
⁴ α -shapes

⁵ Hugo Gruson

⁶ hugo.gruson@normalesup.org

⁷ CEFE, Univ Montpellier, CNRS, Univ Paul Valéry Montpellier 3, EPHE, IRD, Montpellier,
France

⁸ **Keywords:** α -shapes, Colour volume, Colourfulness, Concave Hull, Convex Hull, Hyper-
volumes, Functional Richness, Morphospace

¹⁰ **Abstract**

- 11 1. Organisms often display multiple colours patches and for many analyses, it may be useful
12 to take into account all these patches at the same time, and reconstruct the colour volume
13 of the organisms. Stoddard and Prum (2008) proposed to use convex hulls to reconstruct
14 the colour volume of a species. Convex hull volume has since then often been used as an
15 index of colourfulness, and the intersection of multiple convex hulls is used to study the
16 colour similarity between two objects.
- 17 2. In this article, I outline the limitations of convex hulls in this context. In particular,
18 multiple studies have reported that the convex hull overestimates the actual colour volume.
19 I argue for the use of a more general tool, developed as a more flexible extension of the
20 convex hulls: α -shapes. Depending on the parameter α , α -shapes can reconstruct concave
21 (i.e. non-convex) volumes with voids or pockets, that are better suited for the estimation
22 of colour volumes.
- 23 3. To determine the optimal value of the parameter α , I point out two properties of multidimensional trait spaces and I propose technical tools to identify the α value satisfying these
24 two properties. Using colour data from the whole bird community from the biological
25 station of the Nouragues, French Guiana, I show that using α -shapes rather than convex
26 hulls results in possibly major differences in the estimation of the colour volume.
- 27 4. I discuss possible future developments of this new framework in both colour science, as well
28 as other areas of ecology dealing with multidimensional trait spaces, such as community
29 ecology where α -shape volumes could serve as a replacement for the functional richness
30 FRic, or morphometrics.

³² **Introduction**

³³ Colour is a communication channel widespread among a wide range of taxa (Bradbury and
³⁴ Vehrencamp, 2011; Schaefer, 2010). Many organisms do not display a single colour but rather
³⁵ an assemblage of colours on their body and it may be relevant to study all colour patches at the
³⁶ same time, instead of running independent analyses for each patch (Endler and Mielke, 2005).
³⁷ To allow the study of all the different colours in a single integrative analysis, Stoddard and
³⁸ Prum (2008) defined the *colour volume*, which they described as a measure of colour diversity

39 of an individual or a species (Stoddard and Prum, 2008). This colour volume was computed by
40 building the minimal **convex set** (terms in bold are defined in the glossary at the end of this
41 manuscript), also called **convex hull**, containing all data points (fig. 1a). An intuitive definition
42 of a convex set is that it must contain all line segments connecting any pair of points. In 2011,
43 this metric was extended by Stoddard and Stevens to compare colours between entire organisms
44 or objects (such as eggs from nest parasites versus hosts) using vision models by computing the
45 overlap between the convex hulls of the two objects.

46 The convex hull may seem like an obvious choice for this task. It is commonly used in many
47 areas of biological sciences to build a volume from a set of data points because it has many
48 computational (efficient algorithms such as those presented in Graham 1972; Barber, Dobkin
49 and Huhdanpaa 1996; Kirkpatrick and Seidel 1986; Chan 1996) and mathematical (uniqueness,
50 conservation of convexity by projection or intersection, etc.) benefits. It is for example known as
51 a measure for functional richness (often denoted **FRic**) in community ecology (Cornwell, Schwilke
52 and Ackerly, 2006; Villéger, Mason and Mouillot, 2008), as a tool to evaluate species distributions
53 (Burgman and Fox, 2003), body mass from skeletons in palaeontology (Sellers et al., 2012) or
54 morphospaces (Kotrc and Knoll, 2015; Nordén et al., 2019). However no study has hitherto
55 discussed the biological and evolutionary relevance of convex volumes to describe the colour
56 space that can be produced by a taxon. Convexity is indeed a strong mathematical property
57 that has been criticised in other areas of ecology (Galton and Duckham, 2006; Burgman and
58 Fox, 2003). On the contrary, if we relax the convexity hypothesis, we get concave volumes which
59 are defined as the absence of convexity and do therefore not make any assumption on the nature
60 of the data. Some criticisms against convex hulls for colour volumes already emerged because
61 it could not properly fit datasets that were obviously concave, as reported by Delhey (2015) in
62 his study on Australian birds colour, and often led to an overestimation of the actual volume.
63 Additionally, as reported previously (Worton, 1995; Blonder, Lamanna, Viole and Enquist,
64 2014; Delhey, 2015; Kotrc and Knoll, 2015; Eliason, Shawkey and Clarke, 2016; Stournaras
65 et al., 2013; Renoult, Kelber and Schaefer, 2017; Maia and White, 2018), convex polygons (such
66 as the convex hull) are strongly influenced by outliers, which can cause errors in errors of volume
67 or shape estimation. It is worth noticing that the original authors, Stoddard and Prum (2008)
68 already highlighted these weaknesses in their founding article and alerted readers about the
69 possible dangers in the interpretation of colour volumes, when used with no additional metrics.
70 In spite of those criticisms, no alternative has been proposed yet and convex hull volumes are

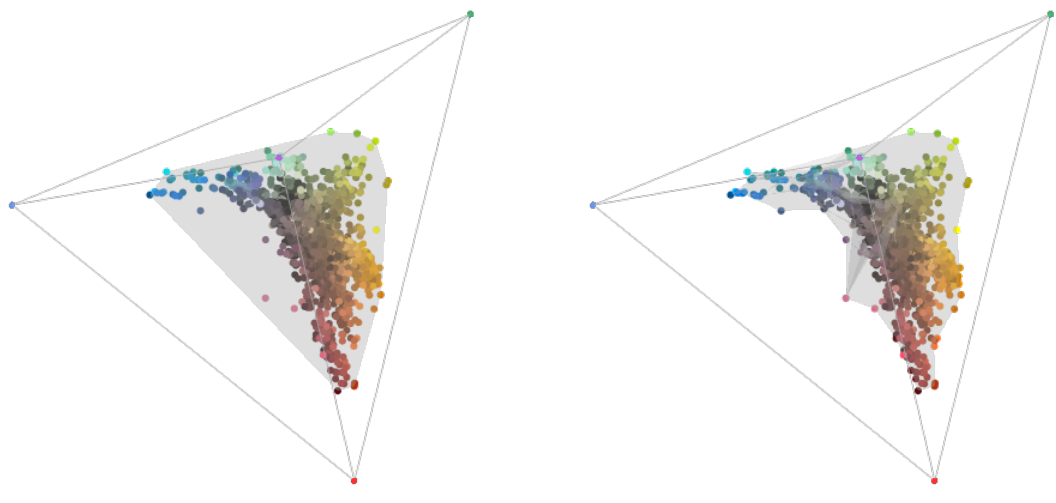


Figure 1: Comparison of the fits with (a) a convex hull (plotted with the `vol()` function from the R package `pavo`) and (b) an α -shape with the optimal α^* value determined in this study, plotted with the new `tetraShape()` function available in ESM. Each point is the colour of one patch from birds living in the Nouragues rainforest, in French Guiana, represented in the colour space of an average VS bird species, under ideal illumination. The colour of the points corresponds to the colour of the data points as seen in human colour vision.

71 still routinely used in colour science (Stoddard and Prum, 2011; Langmore et al., 2011; Stod-
72 dard, 2012; Prum, LaFountain, Berro, Stoddard and Frank, 2012; Spottiswoode and Stevens,
73 2012; Ödeen, Pruett-Jones, Driskell, Armenta and Håstad, 2012; Galván, Negro, Rodríguez and
74 Carrascal, 2013; Hanley, Stoddard, Cassey and Brennan, 2013; Pérez i de Lanuza, Font and
75 Monterde, 2013; Renoult, Courtiol and Schaefer, 2013; Stournaras et al., 2013; Burd, Stayton,
76 Shrestha and Dyer, 2014; Muchhal, Johnsen and S. D. Smith, 2014; Delhey, 2015; Ornelas,
77 González, Hernández-Baños and García-Moreno, 2016; Doutrelant et al., 2016; Bukovac et al.,
78 2017; Enbody, Lantz and Karubian, 2017; White, Dalrymple, Herberstein and Kemp, 2017;
79 Dalrymple et al., 2018; Merwin, B. T. Smith and Seeholzer, 2018).

80 In this article, I propose the use of a new mathematical tool to estimate colour volumes and
81 colour volumes overlap, that works even for non-convex set of points: **α -shapes** (Edelsbrunner,
82 Kirkpatrick and Seidel, 1983; Edelsbrunner and Mücke, 1994). α -shapes are a generalisation
83 of convex hulls which aims at proposing a mathematical definition to the intuitive concept of
84 shape of a set of points. They also present multiple benefits compared to other concave hulls
85 (discussed in more details later on): (i) they can work in an arbitrary number of dimensions,
86 and efficient algorithms exist for either 2 or 3-dimensional data (algorithmic time complexity of
87 $O(n \log n)$ in 2D; Edelsbrunner, Kirkpatrick and Seidel 1983; Edelsbrunner and Mücke 1994), (ii)
88 they are already used in other areas of ecology and evolution (Burgman and Fox, 2003; Brassey
89 and Gardiner, 2015), meaning there are readily available and well tested tools to compute them
90 (Pateiro-López and Rodríguez-Casal, 2010; Lafarge and Pateiro-López, 2017; Matlab 2018), (iii)
91 when alpha is large enough, the α -shape algorithm gives the same output as the convex hull
92 (Edelsbrunner, Kirkpatrick and Seidel, 1983), which means both the current Stoddard and Prum
93 (2011)'s and the new approach described here can be thought of as using α -shapes, only with
94 different choices of α .

95 Methods

96 Definition of α -shapes and algorithm

97 An intuitive definition of α -shapes is illustrated in fig. 2 and stems from the close proximity
98 between α -shapes and another geometrical object: **α -hulls**. Edelsbrunner, Kirkpatrick and
99 Seidel (1983) and Edelsbrunner and Mücke (1994) present α -hulls using an analogy with the
100 eraser tool from image editing softwares (the "eraser intuition"). An α -hull is what remains

101 once you have cleared everything possible without erasing any data point using your eraser tool
102 which has the shape of a ball (a disc in 2D) of radius α . The α -shape is obtained from the α -hull
103 by linking points at the edge of the α -hull with straight lines, as illustrated in fig. 2.

104 The algorithm to build α -shapes derives from an alternative but equivalent definition: α -shapes
105 are **simplicial complexes**, whose simplicial components are obtained from the **Delaunay**
106 **triangulation**, removing the simplices (edges, triangles, tetrahedra, etc.) whose circumcircle
107 has radius greater or equal to α (Edelsbrunner, Kirkpatrick and Seidel, 1983; Edelsbrunner and
108 Mücke, 1994). The algorithm can then be summarised in two simple steps:

- 109 1. Compute the Delaunay triangulation of the set of points
- 110 2. Remove all Delaunay simplices whose circumcircle has radius greater or equal to α or
111 contains any data point

112 From this definition follow two important properties of α -shapes (Edelsbrunner, Kirkpatrick and
113 Seidel, 1983):

114 **Property 1.** *The length of edges of an α -shape is at most 2α .*

115 **Property 2.** *For α large (i.e. $\alpha \rightarrow +\infty$), the α -shape is the convex hull (Edelsbrunner, Kirk-
116 patrick and Seidel, 1983; Edelsbrunner and Mücke, 1994).*

117 Characteristics of colour spaces

118 Although the method presented here can be generalised to more general multidimensional niches
119 and trait spaces, I will focus mostly on the case of colour spaces, which present several charac-
120 teristics which simplify slightly the problem at hand.

121 Colour spaces are multidimensional polygons that contain all colours that an organism can
122 perceive. The most common colour spaces are chromaticity diagrams. Chromaticity diagrams
123 are regular $(n - 1)$ -simplices where n is the number of photoreceptors from the species of interest.
124 For example, in the case of trichomat species, the chromaticity diagram is Maxwell's triangle
125 and in the case tetrachromat species, it is a tetrahedron (Endler and Mielke, 2005; Stoddard
126 and Prum, 2008).

127 The coordinates of the chromaticity diagram vertices and thus the total possible volume have
128 no real biological significance and are based on arbitrary conventions (Renoult, Kelber and
129 Schaefer, 2017). Because of this, independently derived visual models may have different vertices

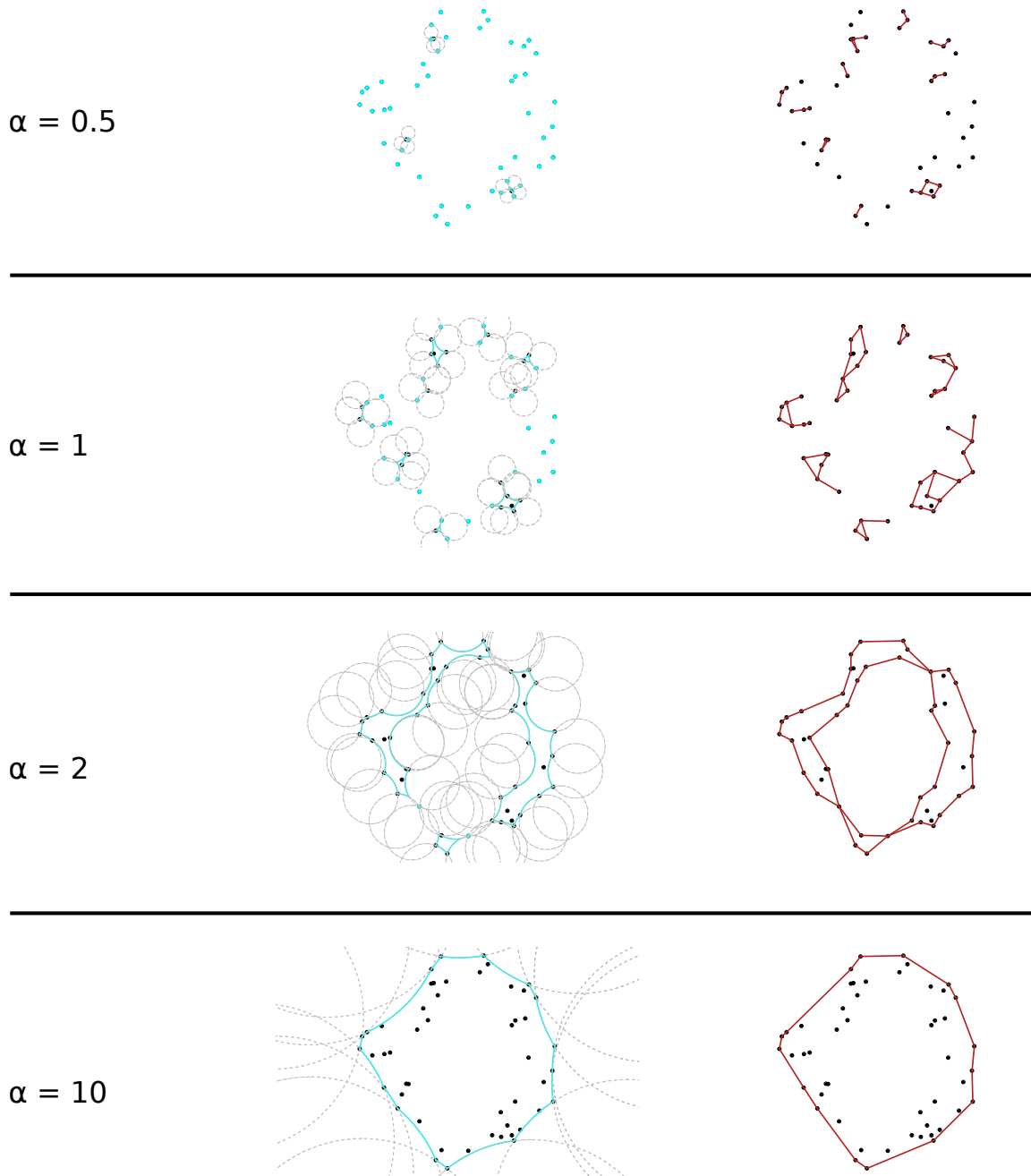


Figure 2: Illustration of α -hull (cyan; left panel) and α -shape (red; right panel) for different alpha values on a fictive dataset. α -hull is what is left once circles of radius alpha has been dug out without removing any points ("eraser intuition"). The α -shape can be derived from the α -hull by drawing straight lines instead of curves (" α -neighbours").

coordinates and total possible volume. For example, for tetrachromatic chromaticity diagrams (represented in a tetrahedron), which are used for bird vision, two systems of vertices coordinates leading to two different total possible volumes co-exist in the literature: the one from Kelber, Vorobyev and Osorio (2003), with total volume of $1/3$ and the one from Endler and Mielke (2005) and Stoddard and Prum (2008), with total volume of $\sqrt{3}/8 \approx 0.2165$. For this reason, colour volume should always be reported as a proportion of the total possible volume (using for example `rel.c.vol` column from `pavo`'s R package `summary.colspace()` output) instead of an absolute value.

Reporting colour volumes as proportion of the total possible volume also allows to compare it between different organisms, even when they have different numbers of photoreceptors (e.g. colour volume in the trichromatic human colour space vs colour volume in the tetrachromatic bird colour space). On the opposite, comparing volumes across dimensions for multidimensional niches or trait spaces in the general case (not colour spaces) does not make sense.

Another property of chromaticity diagrams simplifies the exploration of α -shapes in the present studies: chromaticity diagrams are isotropic, which means all directions have the same properties and distance unit. On the opposite, general multidimensional trait spaces used in functional ecology may be anisotropic (e.g. a 2D space with home range and longevity as axes). In this case, a distance of one unit does not have the same meaning depending on the direction. I discuss later in the article how this issue can be mitigated.

Example data: bird colours from the Nouragues rainforest

The present article uses two types of data to demonstrate the strengths of α -shapes over convex hulls: (i) Simulated data, (ii) Empirical data of quantum catches from the entire bird community from the Nouragues rainforest, in French Guiana, as seen by a UVS bird viewer under ideal illumination (constant reflectance for all wavelengths). Reflectance measurements were using a deuterium-halogen light source, a bifurcated optic probe at 45° and a spectrophotometer calibrated relative to a dark reference and a white spectralon standard to ensure that measurements were independent of the light source and spectrometer used.

Implementation of α -shapes in colour analysis toolbox `pavo`

I have developed a series of scripts available in supplementary data to easily compute and plot colour volumes with α -shapes in R (R Core Team, 2019). The α -shape computation itself is

performed thanks to existing R packages (Pateiro-López and Rodríguez-Casal, 2010; Lafarge and Pateiro-López, 2017). R is a free and open-source programming language and widely used in ecology and evolution, making it a good target for large and rapid dissemination of this method. These functions are also readily compatible with the pavo R package, a widely used toolbox in colour science (Maia, Eliason, Bitton, Doucet and Shawkey, 2013; Maia, Gruson, Endler and White, 2018), and provide the `tetrareshape()` and `tcsshape()` functions as drop-in replacements for pavo's function which plot convex hulls (`vol()` and `tcsvol()` respectively). These functions alongside a detailed example showing how to use them are available in ESM.

Results and discussion

Determination of optimal α value

Most studies using α -shapes in other fields do not offer guidance on the choice of the value α and instead recommend the choice is made based on *a posteriori* visual evaluation of the fit. But for colour volumes (and more generally, for multidimensional niches or trait spaces), there is no theoretical reason to prefer one fit compared to the other (as the general shape of the colour volume is not known) and the *a posteriori* visual evaluation entirely relies on the user subjective judgement, possibly resulting in biased choices that would better conform to their predictions and expectations.

On the contrary, we want to define an optimal value of α based on minimal assumptions about the colour volume. Because of property 1, there is no "magic" value for α that will work for all data sets. This value can only be defined in the context of a given set on points.

But in all cases, we want to satisfy the two following conditions:

Condition 1. *All data points should contribute to the final volume. In other words, there should be no isolated n-simplex (points and lines in 2D; points, lines and triangles in 3D) because their volume is zero, everything happens as if the related data points were discarded from the estimation of the trait volume.*

Condition 2. *The shape should fit the data points as closely as possible (following the parsimony principle). In other words, the volume should be minimised given the data points.*

The α value which meets these two conditions is the α^* used in Cholewo and Love (1999). It also corresponds to the value returned by the `criticalAlpha()` function in MATLAB2014b (or

189 following versions) when used with the option "all-points" and the default value to build 2D
190 α -shape with the `alphaShape()` function. I also provide in ESM an R script to compute the 3D
191 α -shapes matching these two criteria.

192 **Effect of subsampling and outliers**

193 Convex hulls have been criticised for being highly sensitive to outliers (Renoult, Kelber and
194 Schaefer, 2017; Maia and White, 2018), and this problem worsens as the number of dimensions
195 of the colour space increases.

196 For similar reasons to those developed by Reem (2011) about the related mathematical concept
197 of **Voronoi diagrams**, α -shapes benefit from a relative local stability property. Let us imagine
198 that one data point is removed from the data set. In the best case scenario, it is an interior point
199 and this removal does not affect that resulting α -shape. In the worst case scenario, this point is
200 a regular vertex linked to the furthest possible α -neighbours, which each lie at a distance α . This
201 area of the removed Delaunay k-simplex is then $\frac{\sqrt{k+1}}{k!\sqrt{2^k}}\alpha^k$. We notice that the change in colour
202 volume with the removal of one point increases with α . Therefore, the change in colour volume
203 with the framework proposed here is smaller than the change with a convex hull (α large).

204 For the same reason, measurement errors or noise in the data will only have an effect on the α -
205 neighbours, and will cause overall an error in the estimation of the volume that directly depends
206 on the value of α . The error will thus be smaller in the case of α -shapes than in the case of
207 convex hulls.

208 **Comparison of α -shapes versus convex hulls for the computation of the volume**

209 Because of property 2 and the fact that the volume of α -shapes increases with α (Edelsbrunner,
210 Kirkpatrick and Seidel, 1983), we can deduce that α -shapes will always result in a lower colour
211 volume than convex hulls. The difference in the estimation of the volume will depend on the
212 data set. Unsurprisingly, the effect is larger in data set with holes or concave data sets.

213 For example, the colour volume of the Nouragues bird community has large empty areas when
214 fitted by a convex hull (fig. 1), in a very similar fashion to what Delhey (2015) found for the bird
215 community of Australia. These empty areas inflate the colour volume of the Nouragues natural
216 reserve to 25 % (relative to the total volume of the tetrahedron). When fitted by an α -shape
217 with the optimal α parameter ($\alpha \approx 0.111$ for this example), the resulting colour volume is very
218 different and represents only 8.6 % of the total volume of the tetrahedron (fig. 3).

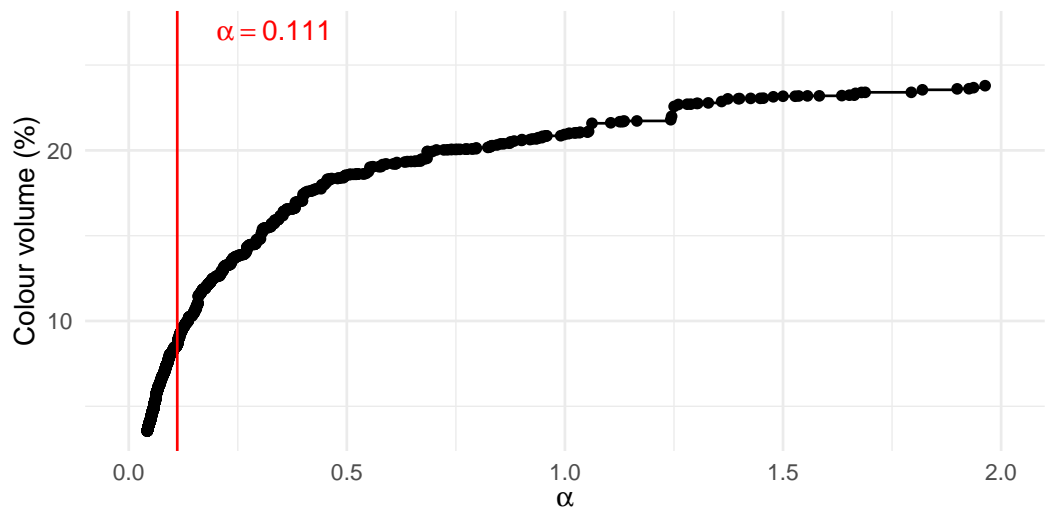


Figure 3: Effect of the value α on the volume of the resulting α -shapes, or colour volume, for the Nouragues rainforest bird community. The optimal α (≈ 0.111) value for this dataset, identified thanks to the two criteria listed previously, is marked with a red line. The convex hull volume is 25 %.

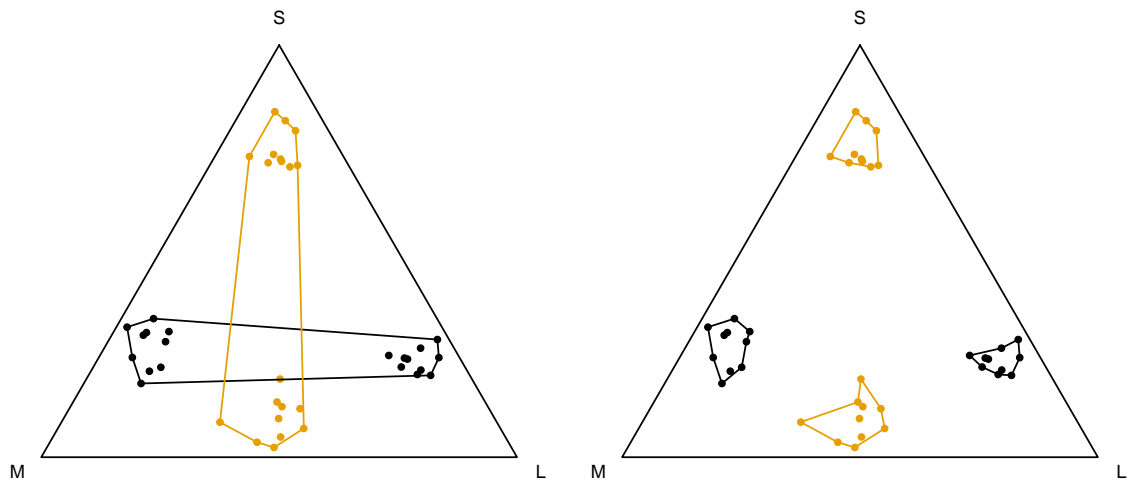
219 **Comparison of α -shapes versus convex hulls for the computation of the overlap**

220 One of the criticisms against convex hulls is that they can create spurious overlap values. This is
221 actually due to the fact that convex hulls can include large areas with no data points. α -shapes,
222 because they more closely fit the data points (especially if you use the α value recommended in
223 this study), should not suffer as much from this weakness. This difference between convex hulls
224 and α -shapes is illustrated on a example with simulated data for a trichromat viewer in fig. 4.
225 There is currently no exact algorithm to compute the intersection of concave polygons, such
226 as α -shapes, in an arbitrary number of dimensions (but see `st_intersect()` function from
227 the `sf` R package for 2D; Pebesma 2018). A computationally efficient method is then to use a
228 Monte Carlo approach, as was done in Stoddard and Prum (2008) and Blonder, Lamanna, Viole
229 and Enquist (2014). An example for α -shapes in 3D is given in ESM (`overlap3d()`, drop-in
230 replacement for `pavo::voloverlap()`).

231 **Comparison of α -shapes versus other concave hull fitting methods**

232 α -shapes have interesting unique properties compared to other types of concave hulls used in
233 the literature and in other areas of ecology and evolution:

- 234 • Concaveman, described in Park and Oh (2012), is an algorithm that builds possibly concave
235 hulls by removing edges larger than a given threshold value from the convex hull. However,
236 current implementations only work in 2D (Gombin, Vaidyanathan and Agafonkin, 2017),
237 which is not suitable for tetrachromat and pentachromat viewer, as well as for its use to
238 describe a multidimensional niche or trait space in a more general case.
- 239 • The `hypervolume` R package provides a method based on multidimensional kernel density
240 estimation (KDE) to construct possibly concave hypervolumes from data points, even
241 in a high number of dimensions (Blonder, Lamanna, Viole and Enquist, 2014; Blonder,
242 Morrow et al., 2018). It has met a large success for the description of multidimensional
243 niches but the probabilistic approach makes it more difficult to formally derive general
244 properties of the niche or the intersection of niches. The KDE and the α -shape approaches
245 also fundamentally differ in the way extreme points are considered. Depending on the
246 parameters, the KDE approach used in the `hypervolume` approach will mainly focus on
247 the areas with high point density and may leave extreme points outside of the niche
248 (depending on the threshold value). On the opposite, the α -shape approach presented



(a) Colour volume intersection with convex hull (b) Colour volume intersection with α -shapes.
 $(\alpha \rightarrow +\infty)$.

Figure 4: Overlaps of colour volumes in the chromaticity diagram of a trichromat, estimated with (a) a convex hull or (b) an α -shape. Two different species are figured with different colours. The estimation with the convex hull can create spurious non-zero overlap values even in the case when the two species do not share any common colours. This is not the case for α -shapes.

in this article will include all points in the resulting niche. Depending on the biological question, either of these two approaches may be preferred to the other. Interestingly, in high dimensions, the only computationally tractable way to use this KDE method is to use a rectangular function kernel and the **hypervolume** and the α -shape approaches then become highly related from the mathematical point of view, as detailed in ESM.

254 **Perspectives: α -shapes in other domains of ecology and evolution**

255 α -shapes could also be used in other fields where the use of convex hulls gives rise to growing
256 criticism. However, caution is required to transpose the approach we describe here. As
257 mentioned before, the colour space is known *a priori* and is isotropic (i.e. all directions have
258 the same properties). Conversely, in functional ecology or in morphometrics for example, trait
259 spaces may be composed by binary, discrete, or continuous traits, meaning all directions are not
260 equivalent and one unit of dimension does not have the same meaning in every direction. To
261 solve this issue, data must be normalised beforehand, as already reported in previous studies
262 about other types of concaves volumes (Blonder, Lamanna, Viole and Enquist, 2014).

263 As of today, the main limit to use α -shapes in other fields lies in the fact that current software
264 to compute α -shapes only work in two or three dimensions, mainly because of a lack of interest
265 (most applications focus on reconstructing 3D objects, such as proteins). However, α -shapes
266 can easily be generalised to higher dimensions (Edelsbrunner, Kirkpatrick and Seidel, 1983;
267 Edelsbrunner and Mücke, 1994) and the current limitation is purely a computational limitation,
268 with the most computationally intensive step being the Delaunay triangulation (Edelsbrunner
269 and Mücke, 1994). But new, efficient algorithms for the Delaunay triangulation have been
270 developed recently (Hornus and Boissonnat, 2008) and could allow the use of α -shapes for
271 animals with more than four classes of photoreceptors (Pike, 2012).

272 **Acknowledgments**

273 I would like to thank Doris Gomez for her valuable comments on an earlier version of this
274 manuscript and the Eco-Evo Mathématiques team at the IBENS for insightful discussions about
275 α -shapes and multidimensional niches.

276 **References**

- 277 Barber, C. B., Dobkin, D. P. and Huhdanpaa, H. (1996). ‘The Quickhull Algorithm for Convex
278 Hulls’. *ACM Trans. Math. Softw.* 22.4, pp. 469–483. DOI: 10.1145/235815.235821.
- 279 Blonder, B., Lamanna, C., Violle, C. and Enquist, B. J. (2014). ‘The N-Dimensional Hyper-
280 volume’. *Global Ecology and Biogeography* 23.5, pp. 595–609. DOI: 10.1111/geb.12146.
- 281 Blonder, B., Morrow, C. B. et al. (2018). ‘New Approaches for Delineating N-Dimensional Hy-
282 pervolumes’. *Methods in Ecology and Evolution* 9.2. Ed. by S. McMahon, pp. 305–319. DOI:
283 10.1111/2041-210X.12865.
- 284 Bradbury, J. W. and Vehrencamp, S. L. (2011). *Principles of Animal Communication*. 2. ed.
285 OCLC: 759797180. Sunderland, Mass: Sinauer Associates. 697 pp. ISBN: 978-0-87893-045-6.
- 286 Brassey, C. A. and Gardiner, J. D. (2015). ‘An Advanced Shape-Fitting Algorithm Applied to
287 Quadrupedal Mammals: Improving Volumetric Mass Estimates’. *Royal Society Open Science*
288 2.8, p. 150302. DOI: 10.1098/rsos.150302.
- 289 Bukovac, Z., Shrestha, M., Garcia, J. E., Burd, M., Dorin, A. and Dyer, A. G. (2017). ‘Why
290 Background Colour Matters to Bees and Flowers’. *Journal of Comparative Physiology A*
291 203.5, pp. 369–380. DOI: 10.1007/s00359-017-1175-7.
- 292 Burd, M., Stayton, C. T., Shrestha, M. and Dyer, A. G. (2014). ‘Distinctive Convergence in Aus-
293 tralian Floral Colours Seen through the Eyes of Australian Birds’. *Proc. R. Soc. B* 281.1781,
294 p. 20132862. DOI: 10.1098/rspb.2013.2862. pmid: 24573847.
- 295 Burgman, M. A. and Fox, J. C. (2003). ‘Bias in Species Range Estimates from Minimum Con-
296 vex Polygons: Implications for Conservation and Options for Improved Planning’. *Animal*
297 *Conservation* 6.1, pp. 19–28. DOI: 10.1017/S1367943003003044.
- 298 Chan, T. M. (1996). ‘Optimal Output-Sensitive Convex Hull Algorithms in Two and Three Di-
299 mensions’. *Discrete & Computational Geometry* 16.4, pp. 361–368. DOI: 10.1007/BF02712873.
- 300 Cholewo, T. and Love, S. (1999). ‘Gamut Boundary Determination Using Alpha-Shapes’.
- 301 Cornwell, W. K., Schwilk, D. W. and Ackerly, D. D. (2006). ‘A Trait-Based Test for Hab-
302 itat Filtering: Convex Hull Volume’. *Ecology* 87.6, pp. 1465–1471. DOI: 10.1890/0012-
303 9658(2006)87[1465:ATTFHF]2.0.CO;2.
- 304 Dalrymple, R. L. et al. (2018). ‘Abiotic and Biotic Predictors of Macroecological Patterns in
305 Bird and Butterfly Coloration’. *Ecological Monographs* 88.2, pp. 204–224. DOI: 10.1002/
306 ecm.1287.

- 307 Delhey, K. (2015). ‘The Colour of an Avifauna: A Quantitative Analysis of the Colour of Aus-
308 tralian Birds’. *Scientific Reports* 5, p. 18514. DOI: 10.1038/srep18514.
- 309 Doutrelant, C., Paquet, M., Renault, J. P., Grégoire, A., Crochet, P.-A. and Covas, R. (2016).
310 ‘Worldwide Patterns of Bird Colouration on Islands’. *Ecology Letters* 19.5, pp. 537–545. DOI:
311 10.1111/ele.12588.
- 312 Edelsbrunner, H. (1995). ‘The Union of Balls and Its Dual Shape’. *Discrete & Computational
313 Geometry* 13.3, pp. 415–440. DOI: 10.1007/BF02574053.
- 314 Edelsbrunner, H., Kirkpatrick, D. G. and Seidel, R. (1983). ‘On the Shape of a Set of Points
315 in the Plane’. *IEEE Transactions on Information Theory* 29.4, pp. 551–559. DOI: 10.1109/
316 TIT.1983.1056714.
- 317 Edelsbrunner, H. and Mücke, E. P. (1994). ‘Three-Dimensional Alpha Shapes’. *ACM Trans.
318 Graph.* 13.1, pp. 43–72. DOI: 10.1145/174462.156635.
- 319 Eliason, C. M., Shawkey, M. D. and Clarke, J. A. (2016). ‘Evolutionary Shifts in the Melanin-
320 Based Color System of Birds’. *Evolution* 70.2, pp. 445–454. DOI: 10.1111/evo.12855. pmid:
321 26044706.
- 322 Enbody, E. D., Lantz, S. M. and Karubian, J. (2017). ‘Production of Plumage Ornaments
323 among Males and Females of Two Closely Related Tropical Passerine Bird Species’. *Ecology
324 and Evolution* 7.11, pp. 4024–4034. DOI: 10.1002/ece3.3000.
- 325 Endler, J. A. and Mielke, P. W. (2005). ‘Comparing Entire Colour Patterns as Birds See Them’.
326 *Biological Journal of the Linnean Society* 86.4, pp. 405–431. DOI: 10.1111/j.1095-8312.
327 2005.00540.x.
- 328 Galton, A. and Duckham, M. (2006). ‘What Is the Region Occupied by a Set of Points?’ In:
329 *Geographic Information Science*. Ed. by M. Raubal, H. J. Miller, A. U. Frank and M. F.
330 Goodchild. Lecture Notes in Computer Science. Springer Berlin Heidelberg, pp. 81–98. ISBN:
331 978-3-540-44528-9.
- 332 Galván, I., Negro, J. J., Rodríguez, A. and Carrascal, L. M. (2013). ‘On Showy Dwarfs and
333 Sober Giants: Body Size as a Constraint for the Evolution of Bird Plumage Colouration’.
334 *Acta Ornithologica* 48.1, pp. 65–80. DOI: 10.3161/000164513X670007.
- 335 Gombin, J., Vaidyanathan, R. and Agafonkin, V. (2017). *Concaveman: A Very Fast 2D Concave
336 Hull Algorithm*. Version 1.0.0. URL: <https://CRAN.R-project.org/package=concaveman>
337 (visited on 14/03/2018).

- 338 Graham, R. L. (1972). ‘An Efficient Algorithm for Determining the Convex Hull of a Finite Planar
339 Set’. *Information Processing Letters* 1.4, pp. 132–133. DOI: 10.1016/0020-0190(72)90045-
340 2.
- 341 Hanley, D., Stoddard, M. C., Cassey, P. and Brennan, P. L. (2013). ‘Eggshell Conspicuousness
342 in Ground Nesting Birds: Do Conspicuous Eggshells Signal Nest Location to Conspecifics?’
343 *Avian Biology Research* 6.2, pp. 147–156. DOI: 10.3184/175815513X13617279883973.
- 344 Hornus, S. and Boissonnat, J.-D. (2008). *An Efficient Implementation of Delaunay Triangula-
345 tions in Medium Dimensions*. report. INRIA, p. 15. URL: <https://hal.inria.fr/inria-00343188/document> (visited on 20/02/2019).
- 347 Kelber, A., Vorobyev, M. and Osorio, D. (2003). ‘Animal Colour Vision — Behavioural Tests and
348 Physiological Concepts’. *Biological Reviews* 78.1, pp. 81–118. DOI: 10.1017/S1464793102005985.
- 349 Kirkpatrick, D. G. and Seidel, R. (1986). ‘The Ultimate Planar Convex Hull Algorithm?’ *SIAM
350 Journal on Computing* 15.1, pp. 287–299. DOI: 10.1137/0215021.
- 351 Kotrc, B. and Knoll, A. H. (2015). ‘A Morphospace of Planktonic Marine Diatoms. I. Two Views
352 of Disparity through Time’. *Paleobiology* 41.1, pp. 45–67. DOI: 10.1017/pab.2014.4.
- 353 Lafarge, T. and Pateiro-López, B. (2017). *Alphashape3d: Implementation of the 3D Alpha-Shape
354 for the Reconstruction of 3D Sets from a Point Cloud*. Version 1.3. URL: <https://CRAN.R-project.org/package=alphashape3d> (visited on 14/11/2018).
- 356 Langmore, N. E., Stevens, M., Maurer, G., Heinsohn, R., Hall, M. L., Peters, A. and Kilner, R. M.
357 (2011). ‘Visual Mimicry of Host Nestlings by Cuckoos’. *Proceedings of the Royal Society B:
358 Biological Sciences* 278.1717, pp. 2455–2463. DOI: 10.1098/rspb.2010.2391.
- 359 Maia, R., Eliason, C. M., Bitton, P.-P., Doucet, S. M. and Shawkey, M. D. (2013). ‘Pavo: An
360 R Package for the Analysis, Visualization and Organization of Spectral Data’. *Methods in
361 Ecology and Evolution* 4.10, pp. 906–913. DOI: 10.1111/2041-210X.12069.
- 362 Maia, R., Gruson, H., Endler, J. A. and White, T. E. (2018). ‘Pavo 2.0: New Tools for the
363 Spectral and Spatial Analysis of Colour in R’. *bioRxiv*, p. 427658. DOI: 10.1101/427658.
- 364 Maia, R. and White, T. E. (2018). ‘Comparing Colors Using Visual Models’. *Behavioral Ecology
365* 29.3, pp. 649–659. DOI: 10.1093/beheco/ary017.
- 366 Matlab (2018). Version 2018b. Natick, Massachusetts, United States: The Mathworks, Inc.
- 367 Merwin, J. T., Smith, B. T. and Seeholzer, G. F. (2018). ‘Macroevolutionary Bursts and Con-
368 straints Generate a Rainbow in a Clade of Tropical Birds’. *bioRxiv*, p. 489419. DOI: 10.1101/
369 489419.

- 370 Muchhala, N., Johnsen, S. and Smith, S. D. (2014). ‘Competition for Hummingbird Pollination
371 Shapes Flower Color Variation in Andean Solanaceae’. *Evolution* 68.8, pp. 2275–2286. DOI:
372 [10.1111/evo.12441](https://doi.org/10.1111/evo.12441). pmid: 24766107.
- 373 Nordén, K. K. et al. (2019). ‘Melanosome Diversity and Convergence in the Evolution of Irides-
374 cent Avian Feathers—Implications for Paleocolor Reconstruction’. *Evolution* 73.1, pp. 15–
375 27. DOI: [10.1111/evo.13641](https://doi.org/10.1111/evo.13641).
- 376 Ödeen, A., Pruitt-Jones, S., Driskell, A. C., Armenta, J. K. and Håstad, O. (2012). ‘Multiple
377 Shifts between Violet and Ultraviolet Vision in a Family of Passerine Birds with Associated
378 Changes in Plumage Coloration’. *Proceedings of the Royal Society B: Biological Sciences*
379 279.1732, pp. 1269–1276. DOI: [10.1098/rspb.2011.1777](https://doi.org/10.1098/rspb.2011.1777). pmid: 21976683.
- 380 Ornelas, J. F., González, C., Hernández-Baños, B. E. and García-Moreno, J. (2016). ‘Molecular
381 and Iridescent Feather Reflectance Data Reveal Recent Genetic Diversification and Phenotypic
382 Differentiation in a Cloud Forest Hummingbird’. *Ecology and Evolution* 6.4, pp. 1104–
383 1127. DOI: [10.1002/ece3.1950](https://doi.org/10.1002/ece3.1950).
- 384 Park, J.-S. and Oh, S.-J. (2012). ‘A New Concave Hull Algorithm and Concaveness Measure for
385 N-Dimensional Datasets’. *Journal of Information Science and Engineering*, p. 14.
- 386 Pateiro-López, B. and Rodríguez-Casal, A. (2010). ‘Generalizing the Convex Hull of a Sample:
387 The R Package Alphahull’. *Journal of Statistical Software* 34.1, pp. 1–28. DOI: [10.18637/jss.v034.i05](https://doi.org/10.18637/jss.v034.i05).
- 389 Pebesma, E. (2018). ‘Simple Features for R: Standardized Support for Spatial Vector Data’. *The R Journal* 10.1, pp. 439–446. URL: <https://journal.r-project.org/archive/2018/RJ-2018-009/index.html> (visited on 15/03/2019).
- 392 Pérez i de Lanuza, G., Font, E. and Monterde, J. L. (2013). ‘Using Visual Modelling to Study
393 the Evolution of Lizard Coloration: Sexual Selection Drives the Evolution of Sexual Dichro-
394 matism in Lacertids’. *Journal of Evolutionary Biology* 26.8, pp. 1826–1835. DOI: [10.1111/jeb.12185](https://doi.org/10.1111/jeb.12185).
- 396 Pike, T. W. (2012). ‘Generalised Chromaticity Diagrams for Animals with N-Chromatic Colour
397 Vision’. *Journal of Insect Behavior* 25.3, pp. 277–286. DOI: [10.1007/s10905-011-9296-2](https://doi.org/10.1007/s10905-011-9296-2).
- 398 Prum, R. O., LaFountain, A. M., Berro, J., Stoddard, M. C. and Frank, H. A. (2012). ‘Molecu-
399 lar Diversity, Metabolic Transformation, and Evolution of Carotenoid Feather Pigments in
400 Cotingas (Aves: Cotingidae)’. *Journal of Comparative Physiology B* 182.8, pp. 1095–1116.
401 DOI: [10.1007/s00360-012-0677-4](https://doi.org/10.1007/s00360-012-0677-4).

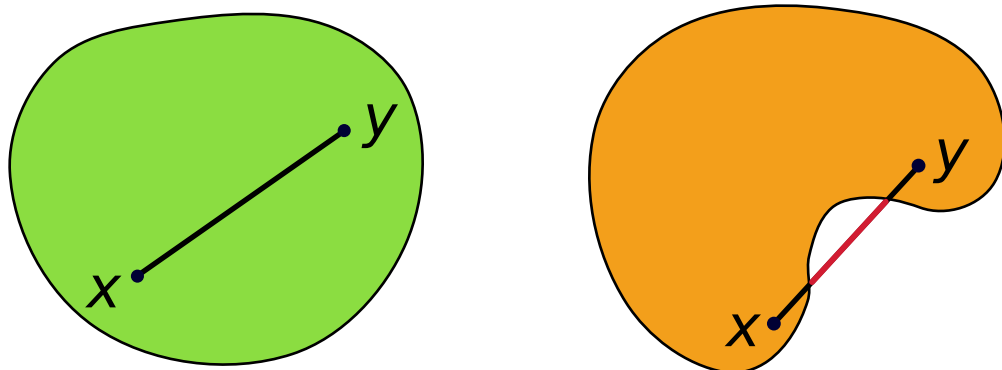
- 402 R Core Team (2019). *R: A Language and Environment for Statistical Computing*. Version 3.5.
403 URL: <https://www.r-project.org/>.
- 404 Reem, D. (2011). ‘The Geometric Stability of Voronoi Diagrams with Respect to Small Changes
405 of the Sites’. In: *Proceedings of the Twenty-Seventh Annual Symposium on Computational
406 Geometry*. (Paris, France). SoCG ’11. New York, NY, USA: ACM, pp. 254–263. ISBN: 978-
407 1-4503-0682-9. DOI: 10.1145/1998196.1998234.
- 408 Renoult, J. P., Courtiol, A. and Schaefer, H. M. (2013). ‘A Novel Framework to Study Colour
409 Signalling to Multiple Species’. *Functional Ecology* 27.3, pp. 718–729. DOI: 10.1111/1365-
410 2435.12086.
- 411 Renoult, J. P., Kelber, A. and Schaefer, H. M. (2017). ‘Colour Spaces in Ecology and Evolutionary
412 Biology’. *Biological Reviews* 92.1, pp. 292–315. DOI: 10.1111/brv.12230.
- 413 Schaefer, H. M. (2010). ‘Visual Communication: Evolution, Ecology, and Functional Mechanisms’.
414 In: *Animal Behaviour: Evolution and Mechanisms*. Ed. by P. Kappeler. Berlin, Heidelberg:
415 Springer Berlin Heidelberg, pp. 3–28. ISBN: 978-3-642-02624-9. DOI: 10.1007/978-3-
416 642-02624-9_1. URL: https://doi.org/10.1007/978-3-642-02624-9_1 (visited on
417 22/03/2019).
- 418 Sellers, W. I., Hepworth-Bell, J., Falkingham, P. L., Bates, K. T., Brassey, C. A., Egerton, V. M.
419 and Manning, P. L. (2012). ‘Minimum Convex Hull Mass Estimations of Complete Mounted
420 Skeletons’. *Biology Letters*, rsbl20120263. DOI: 10.1098/rsbl.2012.0263. pmid: 22675141.
- 421 Spottiswoode, C. N. and Stevens, M. (2012). ‘Host-Parasite Arms Races and Rapid Changes in
422 Bird Egg Appearance.’ *The American Naturalist* 179.5, pp. 633–648. DOI: 10.1086/665031.
- 423 Stoddard, M. C. (2012). ‘Mimicry and Masquerade from the Avian Visual Perspective’. *Current
424 Zoology* 58.4, pp. 630–648. DOI: 10.1093/czoolo/58.4.630.
- 425 Stoddard, M. C. and Prum, R. O. (2008). ‘Evolution of Avian Plumage Color in a Tetrahedral
426 Color Space: A Phylogenetic Analysis of New World Buntings.’ *The American Naturalist*
427 171.6, pp. 755–776. DOI: 10.1086/587526.
- 428 — (2011). ‘How Colorful Are Birds? Evolution of the Avian Plumage Color Gamut’. *Behavioral
429 Ecology* 22.5, pp. 1042–1052. DOI: 10.1093/beheco/arr088.
- 430 Stoddard, M. C. and Stevens, M. (2011). ‘Avian Vision and the Evolution of Egg Color Mimicry
431 in the Common Cuckoo’. *Evolution* 65.7, pp. 2004–2013. DOI: 10.1111/j.1558-5646.2011.
432 01262.x.

- 433 Stournaras, K. E. et al. (2013). ‘How Colorful Are Fruits? Limited Color Diversity in Fleshy
 434 Fruits on Local and Global Scales’. *New Phytologist* 198.2, pp. 617–629. DOI: 10.1111/nph.
 435 12157.
- 436 Villéger, S., Mason, N. W. H. and Mouillot, D. (2008). ‘New Multidimensional Functional Di-
 437 versity Indices for a Multifaceted Framework in Functional Ecology’. *Ecology* 89.8, pp. 2290–
 438 2301. DOI: 10.1890/07-1206.1.
- 439 White, T. E., Dalrymple, R. L., Herberstein, M. E. and Kemp, D. J. (2017). ‘The Perceptual
 440 Similarity of Orb-Spider Prey Lures and Flower Colours’. *Evolutionary Ecology* 31.1, pp. 1–
 441 20. DOI: 10.1007/s10682-016-9876-x.
- 442 Worton, B. J. (1995). ‘A Convex Hull-Based Estimator of Home-Range Size’. *Biometrics* 51.4,
 443 p. 1206. DOI: 10.2307/2533254.

444 Supplementary information

445 Glossary

- 446 • Convex set: a set of points in space is convex if a segment between any 2 points of this set
 is within the set. The opposite of convex is concave.



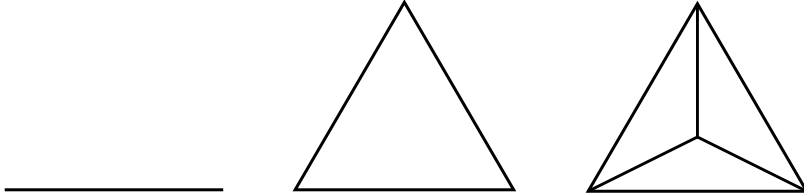
- (l) A segment between any points of the green set (l) The segment between x and y , two points of the
 (such as x and y) is contained in the green set itself. orange set, is not contained is the orange set itself.
 The green set is thus convex. The orange set is thus not convex, and is said to be
 concave.

Supplementary figure 1: Illustration of a convex (green; left) and concave (orange; right) set.
 Illustrations modified from Wikipedia user CheCheDaWaff (CC-by-sa).

447

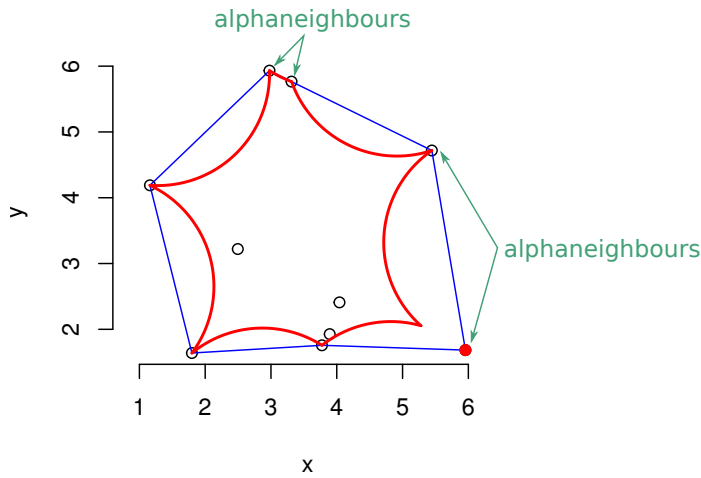
- 448 • Convex hull: minimal convex set. Convex set which surrounds all data points while
 449 minimising its volume.

- 450 • Simplex: generalisation of the notion a triangle in 2D or tetrahedron in 3D to an arbitrary
 451 number of dimension. A point is a 0-simplex, a line is a 1-simplex, a triangle is a 2-simplex,
 452 a tetrahedron is a 3-simplex, etc.



Supplementary figure 2: Example of simplices. Left to right: 1-simplex (line), 2-simplex (triangle) and 3-simplex (tetrahedron).

- 453 • α -shape: attempt at a formal, mathematical definition of the intuitive concept of shape by
 454 Edelsbrunner, Kirkpatrick and Seidel (1983). It is a multidimensional polygon (= poly-
 455 tope) whose vertices are data points and which can be either convex or concave depending
 456 on the value of the parameter α . When $\alpha \rightarrow \infty$, the α -shape is the convex hull.
 457 • α -hull: similar to the α -shape excepted that edges are not straight line but arcs between
 458 the vertices.
 459 • α -neighbour: α -neighbours are adjacent vertices in the α -shape or α -hull.



Supplementary figure 3: Illustration of the α -shape (blue), α -hull (red) and α -neighbour (green) on a set of points.

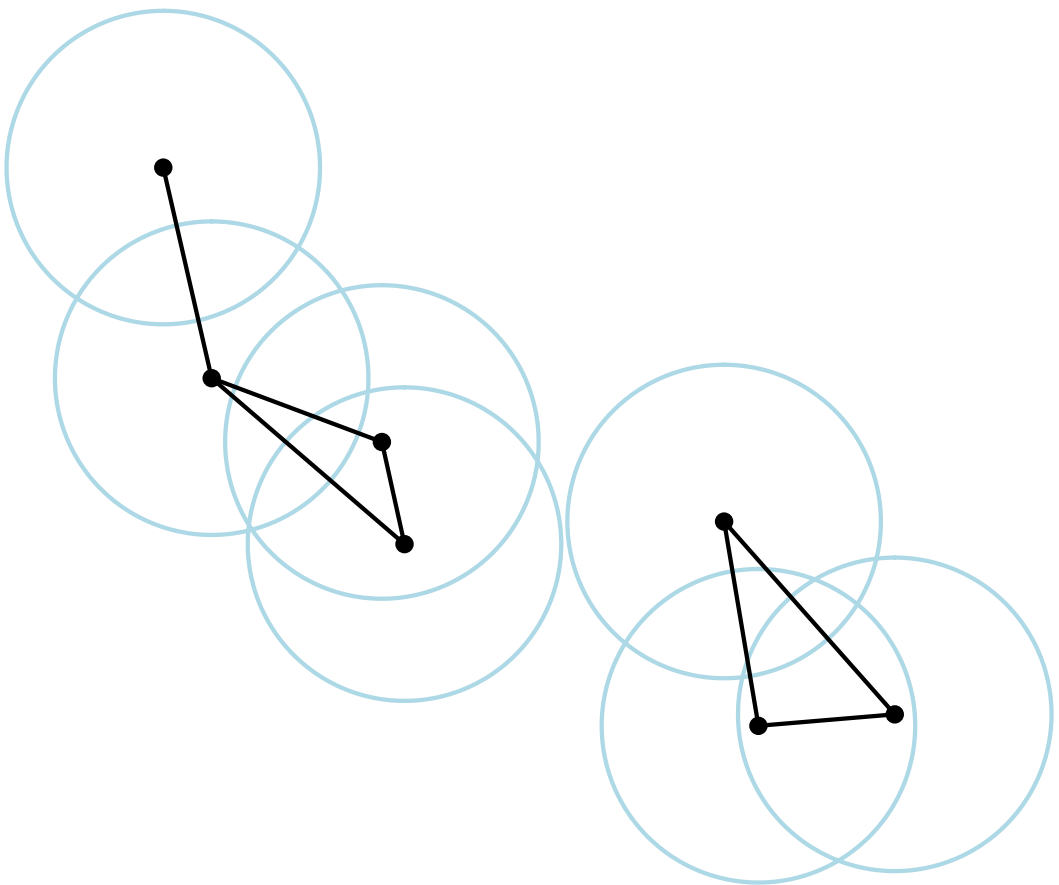
- 460 • Triangulation: a triangulation is a partitioning of the space with simplices whose vertices
 461 are the data points. For a given set of points, the Delaunay triangulation is one specific
 462 triangulation which is unique and has several other properties I do not detail here.

- 463 • Voronoi diagram: a Voronoi diagram is a specific partitioning of the space into regions
464 depending on the closest data point. It has a strong mathematical relationship to the
465 Delaunay triangulation (duality).

466 **Link between α -shapes and hypervolumes with rectangular function kernels**

467 When the kernel used in the KDE approach implemented in the `hypervolumes` R package by
468 Blonder, Morrow et al. (2018) is a rectangular function, the result is a geometrical object with
469 a strong relationship to α -shapes. An alternative definition of α -shapes is indeed that they are
470 the nerve of the intersection between union of balls of radius α centered on the data points with
471 the voronoi cells of the data set (Edelsbrunner, 1995).

472 This means that α -shapes is the nerve of the intersection between hypervolume obtained by the
473 KDE method and the Voronoi cells of the data set, as illustrated in fig. S4.



Supplementary figure 4: Illustration of the link between α -balls (in blue) and α -shapes (in black). α -balls are balls (or discs in 2D) of radius α centered on the data points. α -shapes are the nerve of the union of α -balls. In the case of a rectangular kernel, each α -balls is also the density estimated around a given point by the **hypervolume** approach.

Scientific publication in the technological era

The publishing industry started in 1665 with Philosophical Transactions of the Royal Society, which detailed its mission in an editorial (“[An introduction to this tract](#)” 1667):

“Whereas there is nothing more necessary for promoting the improvement of Philosophical Matters, than the communicating to such, as apply their studies and endeavours that way, such things as are discovered or put in practise by others.”

This need for the dissemination of studies remains today but science practices, public expectations and the research communities have changed since the beginning of scientific publication. This requires a reflection on how the publishing industry must evolve to follow these changes. In this chapter, I detail some of the issues I (and many other fellow scientists) encountered during my PhD, the current proposals to tackle these issues and how my work integrates with said proposals.

2.1 Introduction: The dire state of science

The publishing industry started as a way to disseminate scientific work. Its centralised nature meant that advances and discovery could more efficiently reach a much larger amount of people. But it has slowly strayed away from this original goal and what was initially a means to communicate, became an end for many scientists. Evaluation processes and hiring committees focus on the number of publications and the impact factor of the journal in which they are published. This puts pressure on research teams to produce articles as fast as possible (a trend dubbed “publish or perish”; Neill 2008), sometimes at the expense of quality and robustness. Some institutions even go as far as setting their employee salaries based on the number of publications in a given year or hand out prize money for publications in high impact journals (Nature Publishing Group, 2017; Abritis, McCook, and Watch, 2017) or for each citation (Abritis, McCook, and Watch, 2017). This contributes to the reproducibility crisis observed in many fields (Pashler and Wagenmakers, 2012; Baker, 2016), with problems ranging from bad methods reporting and poorly designed experiments, to outright unethical practices such as

plagiarism (including self-plagiarism) or fabricated results (Steen, 2011b; Steen, 2011a; Bik, Casadevall, and Fang, 2016; Bik, 2016).

Even among honest studies, few results are successfully reproduced. Indeed, scientists are faced with an ever increasing mathematical, statistical, technical and computational complexity but lack proper training (Barraquand et al., 2014). Additionally, accepted articles are biased towards attractive sounding, positive results (Schekman, 2013). Little space is left for replication studies or negative results (Nosek, Spies, and Motyl, 2012). This creates a biased picture of the current state of the art in a given topic. For one study which found a significant effect, many others which did not find such effect might not have been published. This trend has become worse in the last decades, as reported by Fanelli (2012) based on a sample of 4.600 articles from various fields, published between 1990 and 2007. Additionally, the peer review system, which is supposed to detect mistakes and methodological weaknesses (and correct them whenever possible) rely entirely on volunteer work from already overworked scientists, even in the case of for-profit journals.

Community initiatives exist to try and solve this issue. For example, PubPeer (<https://pubpeer.org/>) provides a platform where anyone can anonymously comment on a published article (as long as it has a DOI). Even though it accepts all kind of comments (positive or negative), it has quickly become a place to report scientific misconduct such as figure manipulation or gel splicing. But even articles with fabricated results do not always get retracted (Ravindranath, 2019), and when they do, it might take a very long time and readers are not always clearly informed when an article is retracted (Steen, 2011a). In the meantime, other teams may be misled by the results and use them as the basis of their own research, as attested by the fact that retracted articles still get cited (Budd, Sievert, and Schultz, 1998; Budd et al., 1999; Redman, Yarandi, and Merz, 2008; Bar-Ilan and Halevi, 2017). Additionally, even articles which eventually get retracted can leave a long-lasting misconception in public opinion (see for example the effect of the Wakefield study, now retracted for fraud, on vaccine hesitancy, as reported in Sansonetti 2018). On a positive note, I would like to acknowledge the great work of RetractionWatch (<https://retractionwatch.org>) in partnership with the bibliography software Zotero which now prominently warns users when they have a retracted article in their library (Dan Stillman, 2019), as shown in fig. 2.22.

All of this contributes to the ever growing public confidence crisis (Haerlin and Parr, 1999; Nadelson and Hardy, 2015). A possible way out lies in a better communication and accessibility of scientific discoveries: open science (Grand et al., 2012).

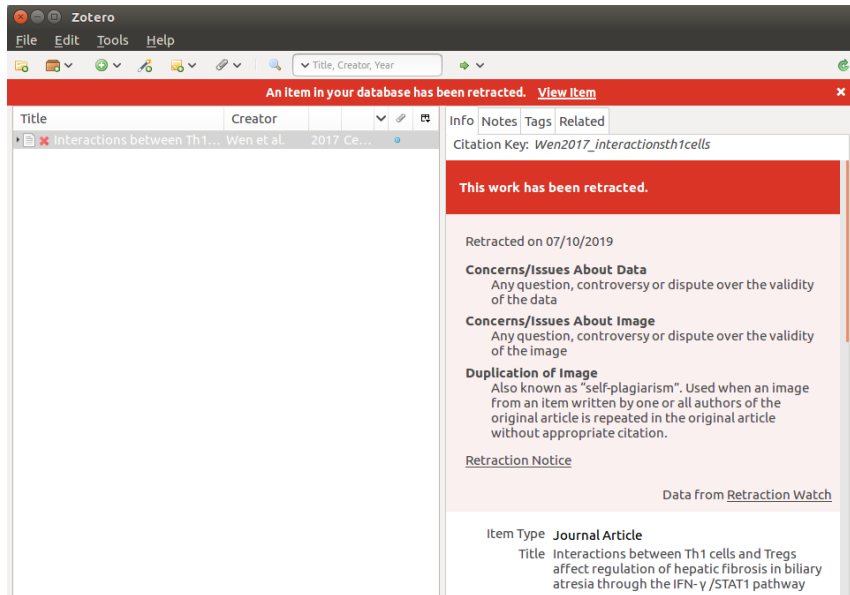


Figure 2.22: Screenshot of Zotero retraction warning feature.

2.2 New publishing practices and community initiatives

Green open access

One facet of open science is open access, i.e. making the content of the article accessible to everybody free of charge. There are several categories of open access but the most common and widely accepted definitions are:

- Gold open access: the journal provides the article free of charge for readers but authors have to pay a fee (named article processing charges, or APC), often justified by journals as a necessity to cover the costs associated with publication (but see García et al. 2019).
- Green open access: the full text of the article is uploaded to an institutional archive (such as the government-sponsored French repository HAL, <https://hal.archives-ouvertes.fr>) by the authors.

Many articles have talked about the ethics (Alizon, 2018) and the dangers (Bohannon, 2013) of each of the two systems and my work has mainly focused on the practical side of things. During my PhD, I provided guidance and tools to increase the uptake of green open access, including its legal aspects to researchers from my institution, the CEFÉ, as well as workshops to guide them through the archival of an article in HAL. During this workshop, we presented SHERPA/RoMEO, a database which lists open access policies for all journals and details the green open access conditions: right to deposit a pre-print (unreviewed) version of the manuscript in an institutional archive, right to deposit the post-print (reviewed but unformatted) version, right to deposit the publisher version (reviewed and typeset), as well as respec-

tive embargoes for each case. After this day, we decided with Matthias Grenié to write the R package `rromeo` which provides access to the SHERPA/RoMEO data from R, thereby allowing researchers in meta-research and bibliometrics to conveniently analyse trends in open access policies. The code of this R package was reviewed by rOpenSci (see after for more information about this) and we wrote a blog post to detail its genesis: [rromeo: Access publisher copyright & self-archiving policies via the 'SHERPA/RoMEO' API](#) (published on rOpenSci blog; Grenié and Gruson 2019).

Low cost publishing

Historically, the major reason for the high cost of publication (whether it be supported by subscriptions or not) was due to technical reasons: copy-editing, printing and shipping was indeed costly. But for electronic publication, the printing and shipping costs are lifted to be replaced by hosting. But it is not as expensive as some would make it out to be (García et al., 2019). This is best demonstrated by preprint servers, which manage to host thousands of articles each month, with costs estimated at around \$10 per article. The Journal of Open Source Software (JOSS; ISSN 2475-9066) also published a detailed blog post about the costs of open source publishing and estimate the actual current costs at \$3.54 per article (Katz et al., 2019). They go on saying that if they did not get any grant support and if they were a for-profit initiative with 30-35% profit margin, this would only raise the article processing charges (APC) to \$140, which remains much lower than most journals' APC (Solomon and Björk, 2012).

To achieve such low APC, most community and non-profit systems rely on existing infrastructure to host articles and/or the review process. For example:

- JOSS (Journal of Open Source Software; ISSN 2475-9066) and JOSE (Journal of Open Source Education; ISSN 2577-3569) are presented as 'open journals'. In other words, they are journals that rely entirely on open source tools, perform open, transparent reviews and publish the final articles in open access (CC-BY license). To achieve this while staying free of charge for everybody (both authors and readers), they use GitHub issues for the open review process and to host articles and article formatting is achieved thanks to a simple markdown template.
- Peer Community In (PCI; <https://peercommunityin.org>) is a community initiative started by scientists and stemming for the realisation that most tasks necessary to the publication of articles are already performed free of charge by scientists themselves. They propose a service to peer review articles posted on pre-prints servers by providing a platform to put in contact editors (called 'recommenders') and reviewers with the authors. They are free of charge for both authors and readers as well by leveraging pre-print servers such as bioRxiv (<https://biorxiv.org>) to host the article and providing a `LATEX` and a `.docx` templates for article formatting.

Breaking down the publishing process

While these projects focus on cost and convenience of submission, other initiatives choose to focus on other faulty steps of the process. In particular, other issues I mentioned earlier are the lack of reproducibility and the bias towards positive results. To prevent this, several organisations and journals have made a push for the adoption of pre-registration studies (also called registered reports) (Chambers, 2013; Nosek et al., 2018). In short, authors send a first version of the manuscript presenting the theoretical background, their predictions and the methods they plan on using to test these predictions. This first version of the manuscript goes through peer-review and if the science is deemed robust, it is published. The authors then go on and actually run the experiments and analyses and then report back to the journal. This process has multiple benefits compared to the traditional publication process:

1. The article is not judged on the nature of its results (positive or negative) but on the robustness of the methods and analyses to get these results.
2. All analyses and subsequent results are supported by theoretical background or *a priori* expectations (e.g. in the case of medical trials where the mechanism of a drug is not yet fully understood), thus preventing post-hoc explanations to possibly spurious correlations (Cornell, 1997) (dubbed "postdictions" by Nosek et al. 2018).

Yet, pre-registration studies remain scarce. One possible explanation in ecology and evolution may be the lack of journals and the prohibitive costs of those that accept pre-registration studies. To my knowledge, in this field, only Royal Society Open Science (ISSN 2054-5703) and BMC Ecology (ISSN 1472-6785) have an explicit policy regarding pre-registration studies. But PCI has recently launched PCI registered reports, which offer free and open peer review of registered reports posted on pre-print servers. Additionally, some advocacy groups, such as the centre of open science, try to encourage replication studies by offering grants (Center for Open Science, 2019; Dutch Research Council (NWO), 2016), which may provide a financial incentive, and alleviate the APC costs.

Some projects propose to split the publication process into even smaller steps. In particular, Octopus is a project sponsored by Mozilla and eLife, which proposes to publish separately each of the following parts: problem, hypothesis, protocol, data, analysis, interpretation (Freeman, 2019). This approach has the same benefits as registered reports and it also speeds up the dissemination of scientific theories, data and results, allowing multiple teams to test the same hypothesis with different experiments at the same time, run the same experiment in different labs, or even propose different way to analyse the same data.

2.3 The danger of proprietary, closed-source software in science

The downsides and dangers of proprietary software have long been discussed by activists and organisations such as the Free Software Foundation (FSF; <https://www.fsf.org/>). In this thesis, I would like to focus more precisely on the importance of free, open-source software in research.

When software acts without your knowledge

One of the most dangerous issues related to proprietary software in science is its 'black box' nature: without access to the code, users have no way of telling what the software does or if it actually does what it claims. This is surprising because the science process (e.g. in publications) asks for tangible proofs when it comes to trust experimental results (western blot gels, microscopy photographs, etc.) Yet, many scientists accept that proprietary software performs operations without their knowledge. One of the cases I know best is software for spectrophotometry, that I used during my PhD to measure colour in an objective way (see [box 1](#)). These programs save spectral reflectance (or transmittance) data and related metadata in custom, non-standard, formats and then offer a feature to export these formats into plain text csv tables. But during this conversion process, some programs modify the data. For example, spectral data is interpolated and pruned to one value every nm. But the user does not know the exact algorithm to perform this interpolation and pruning step, and cannot use another algorithm should they want to. Similarly, proprietary software sometimes change their underlying algorithms, without publishing detailed release notes, which can lead to the perplexing situation where scientific results cannot be reproduced but without any indication why.

During my PhD, I have developed the `lightr` R package, which is open source and released under a free license (GPLv2+), and which allows users to import the proprietary formats in a completely transparent way. The code was also peer-reviewed by rOpenSci and the detailed work was published in JOSS (Gruson, T. E. White, and Maia, [2019](#)).

The difficulty of software maintenance over time

Most scientific software is developed by scientists themselves, many of whom never had any formal training in software development (Hannay et al., [2009](#)). Many underestimate the work needed to simply maintain a piece of software, even once feature maturity has been achieved. Breakage can happen anytime, even when everything was previously working fine, because of upstream bug fixes or breaking changes in operating software or in third-party libraries.

Yet, there is little incentive for good quality software development and even less for maintenance, as detailed in [section 2.5](#), and in the hyper-competitive world of research, most researchers prefer devoting their time to tasks which can lead to the production of scientific articles. If the software

is proprietary and its developer stops maintaining it, correcting bugs and making sure it still works, it inevitably become unusable after a couple of years, and turns into what is called "abandonware" (Jaffe, 2004).

On the contrary, if the software is free and open source, someone else can freely take over and update it to fix the issues. This is what I did during my PhD with François Bienvenu, Guilhem Doulcier and Maxime Woringer, on software initially developed by Stéphane Legendre (ULM Legendre and Clobert 1995; available at <https://www.biologie.ens.fr/~legendre/ulm/ulm.html> and ZEN), which did not work anymore on Linux, macOS and on newer versions on Windows. Our first step was to contact the initial developer (Stéphane Legendre), point out the current limitations of his software and the practical benefits, as well as the ethical premises of free and open source software. We helped him pick a free license, which was in line with his goals and values (in this case, the GNU Public License version 3). He then uploaded the code source online (<https://gitlab.com/ecoevomath/ulm>), and each one of us worked on issues they felt most qualified to tackle. This operation was a huge success as it quickly attracted an external contributor who none of us knew before this, which helped us on issues relating to a specific operating system (macOS), thereby demonstrating the interest of opening the sources.

Thomas White did something similar for pavo (Maia et al., 2019). Endler (2012)'s scripts were coded in the proprietary programming language Matlab, without any explicit license and were only "available upon request". With the release of pavo 2 (Maia et al., 2019), this method is now freely available to everybody, with no need for request to the author or for expensive proprietary software.

Lock-in

Finally, the use of proprietary software in research is highly problematic because research is incremental: current and future studies build upon past ones. It is important that future generations of researchers can access our data. From a more practical point of view, non-free software can be very expensive and they put themselves in a monopoly situation by preventing users to open their own data via other software (Beel, 2013): a phenomenon called lock-in. For example, in 2018, the proprietary bibliography management software Mendeley, edited by Elsevier, updated its database format, which prevents users from exporting their bibliography and use other bibliography management software (Zotero Documentation, 2019).

This issue does not exist with free software, because even if it is abandoned and it becomes non-free, anyone can download the last available free version and take over from there (a process named a *fork* in the free software world), as explained in the previous section. Additionally, developers are now encouraged to deposit their source code in long-term archives such as Zenodo (E. P. White, 2015) (<https://zenodo.org>) or Software Heritage (Di Cosmo and Zacchiroli, 2017) (<https://www.softwareheritage.org/>).

2.4 Leveraging technology to reduce human workload

I believe we are still far from being replaced by machines in research but software can help in menial tasks, leaving just the most stimulating and exciting part to humans.

Helpers for bibliography search

Bibliography is perhaps the domain where technology has eased the daily tasks of researchers the most, and it makes a good example of how software can improve science. Many tools now offer article recommendations directly in the user email inbox, or their twitter feed. This can be done by watching certain keywords, certain topics, or certain authors (feature available on Google Scholar, Web of Science, PubMed, Semantic Scholar). But some services go even further by proposing new articles or keyword selections based on your current bibliography (Mendeley) or your current alerts (Google Scholar).

New tools have also emerged to better characterise the citation relationships between articles. Until now, we could only know that one article was citing another one (but even this was often incomplete as it often relied on non-public data). With these tools, it is now possible to assess how influential an article was to another one (Semantic Scholar) and to know whether the citing articles are in agreement or disagreement (scite.ai).

However, most of these tools rely on proprietary software and belong to private for-profit companies, which creates important issues described earlier in this manuscript. Additionally, for more advanced tools which use machine learning, multiple examples have shown the possible dangers of biased training data, as I explain in the last paragraph of this section.

Automated checks

The use of some computer software to automate tedious tasks is now part of our everyday life. For example, most computer programs and text editing software now include an automatic spellchecker and the squiggly red line has become a widely recognised symbol to represent a mistake in a text. It has also now become commonplace to see on-the-fly validation when one fills out online forms. Similarly, programs to auto-detect possible plagiarism are now integrated on most e-teaching platforms (e.g. moodle), and students assignments are checked upon submission and flagged for manual review by the teacher in case of plagiarism suspicions (Butakov and Scherbinin, 2009).

In the same manner, the last few years have seen the rise of continuous integration systems in software development. These systems automatically run predetermined tasks after a specific trigger. For example, one common use is regression tests: a set of tasks to accomplish and to compare to an expected output which runs after each code modification, to ensure that the code still produces

correct results. Yet, these checks are painfully missing in many cases for scientific software, which have dramatic consequences. A recent article detected a code error in python code for chemistry (Bhandari Neupane et al., 2019), contributed by an earlier article from another research group. This error led to different results depending on the user operating system and went undetected for 5 years, even though the code was re-used and cited in more than 150 articles. Another use of continuous integration would be to automatically deploy a website with an updated documentation that matches the latest version of the code (e.g. if you add a new argument to a function, the online documentation is automatically updated to reflect this change). I implemented both of these types of continuous integration in pavo (Maia et al., 2019).

These tests are also run on submission to authoritative platforms such as the Comprehensive R Archive Network (CRAN) which is the default repository from which GNU R package are installed (via the `install.packages()` command).

Yet, this type of automated check still lacks in the submission process to scientific journals. It is most obvious when one looks at places where community post-publication review takes place, such as non-specific social networks (e.g. twitter) or specific, dedicated, websites (e.g. PubPeer). In these places, users have developed computer programs ('bots'), which automatically check some aspects of the publications. Here are some of them:

- Statcheck (Nuijten et al., 2016), which scanned about 700,000 papers in psychology and found 50,000 with errors in the reported statistical values (as of 2016) (Chawla, 2016).
- Colormap bot (Rampin, 2018), which would praise users when their articles use the new, perceptually uniform "viridis" colourmap ([A better default colormap for Matplotlib | SciPy 2015](#) 2015; Berkeley Institute for Data Science, 2017) and advised them to change when they used the problematic "jet" colourmap. "Jet" has indeed long been criticised because it has perceptual discontinuities, which can lead to erroneous interpretation of figures.

But all of this happens after article publication, when it is difficult to fix mistakes (especially mostly benign mistakes which do not warrant an official correction) or to retract the article (as mentioned earlier). These checks need to be integrated to the journal publishing process, ideally even before the manuscript is sent to reviewers. One example of such checks could precisely be a software which scans the references in the manuscript and warns the handling editor and possibly the authors if the references include a retracted article. The only journals I know of which have implemented such checks are the Journal of Open Source Software (JOSS) or Journal of Open Source Education (JOSE). They use a bot on GitHub as their editorial management system and this bot can perform automated checks such as checking if every reference includes a digital object identifier (DOI) and if this DOI is valid. [dataseer.io](#) is another possible candidate for automated checks. It is still in development

but aims at being integrated in the publication process, right after acceptance. This software scans articles and identify sentences referring to datasets and confirms with the author that the relevant datasets are shared in appropriate long-term archives.

Limits and caveats

I took the example of online forms which check if the input is valid on the fly as an example of powerful checks. Yet, everybody knows the pain of badly programmed form validations, which prevent submission even when the input is actually valid. The aforementioned checks in publication systems should never cause the automatic rejection of a manuscript or prevent its submission. No software is not perfect and mistakes can happen. It should not act as a all-powerful judge but should simply flag potential problems in manuscript. The editor can then make an informed decision and choose whether this is an actual issue or a false positive.

This is even more important if such checks start relying on so called 'artificial intelligence' (AI), which uses algorithms trained for a specific task based on an initial annotated dataset. But if the training data is biased, it can have dramatic effects because biases are amplified by this kind of tool. Famous popular culture examples of AI fails are 'Tay', a twitter robot that learned from their interactions with users of the platform, and quickly started to post racist messages (Hunt, 2016) or Google Translate, which reinforced gender stereotypes in its translation of job names (Sonnad, 2017) (e.g. with nurse being often translated as 'female nurse' and mechanic as 'male mechanic' in many languages).

2.5 Software and data as valid research outputs

Initiatives and incentives for high quality scientific software

Complex software becomes more and more necessary in many fields. Yet, most researchers do not have formal training in formal development (Hannay et al., 2009). And even among those who do, there is no incentive to invest time in it. Research is very competitive and currently, the only valid currency to get grants or a position are publications. In this context, it seems counterproductive from a career point of view to spend time on developing software. This creates a practical problem, as some methods absolutely require complex code and some teams do not have the means to achieve this. This is for example what happens with the colour pattern analyses method I mentioned in the first part of this manuscript. I was lucky enough to work on `pavo`, a R package to analyse colour, during my PhD. As detailed in our article "pavo 2", Thomas White spent a lot of time implementing new methods, to prepare for `pavo` 2 release. During this time, I mainly worked on simplifying existing code and adding unit tests. This was slightly unusual because this huge work took place even though `pavo` had already been published (Maia et al., 2013) and it was unlikely to get a second publication. Yet, surprisingly,

pavo 2 was accepted in Methods in Ecology and Evolution (Maia et al., 2019), with the following words from the associate editor, Chris Grieves:

"I think this may be the first 'version 2' paper considered for publication in MEE (but I haven't looked very hard). It's been a bit of a balancing act between MEE's selectivity and requirement of novelty and our desire to support continued work on software. The article makes a good case that this version adds new functionality and is worthy of publication, and the reviewers and I agree. However, to meet that bar for novelty ([with regards to] the previous paper and software) the standards for software quality have to raise slightly."

Similarly, the Journal of Open Source Software (JOSS) publishes articles about software, with the following introduction on their website:

"[...] in a perfect world we'd rather papers about software weren't necessary but we recognize that for most researchers, papers and not software are the currency of academic research and that citations are required for a good career."

I mentioned how a huge benefit of free open source software was the fact that anybody could look at the code and figure out whether it was actually doing what it claimed. Yet, this point is moot if nobody actually looks at the code. If scientific software is going to be widely used, it also needs to be reliable and journals can play a part in this. For example, Methods in Ecology and Evolution provides peer review for the code linked to the articles they publish. In the case of *pavo*, it was to our knowledge the first time that reviewers used rOpenSci review checklist, as reported in [When standards go wild - software review for a manuscript](#). rOpenSci is an initiative to review the code from R package used in science Ram et al., 2019. They provide reviewers and editors with a checklist to ensure the code is of highest quality: enough unit tests, extensive documentation, clear and commented code, use of the current best practices. In [rromeo: Access publisher copyright & self-archiving policies via the 'SHERPA/RoMEO' API](#), Matthias Grenié and I talk about our experience going through the process of review for the *rromeo* R package.

Collaborative databases with unified interfaces

Similarly, as mentioned in the first part, we are lacking incentives to build databases. For example, the information about hummingbird predation exists but it is scattered all across the web. And even if someone built this database for their own study, most of the time, they would not publish it alongside their results. Some journals are tackling this issue by focusing on publishing only datasets, thereby providing a way to credit author with "research currency": articles and citations (as explained in [section 2.1](#)).

But then, it is also important that datasets are easily discoverable, and easy to download through a unified interface. An example I faced during my PhD was digital catalogues of museum collections. Some museums did not manage to digitalise the entirety of the collections yet. Yet digital collections

are a very valuable tools for researchers because they can browse through the catalogue, find out if the museum has the resources they need, and then make the decision to travel or not. But even when museums provide a complete online catalogue, it can be very challenging to find out which museum owns the resources you need. A possible solution would be to build a centralised repository which access all individual catalogues.

Another example I encountered during my PhD where discoverability and ease of use could be improved is for phylogenies. As I explained in the first part of this thesis, two different phylogenies exist for hummingbirds. Yet, the one from McGuire et al. (2014) is not readily available and anyone who wants to use it must email the authors. On the opposite, Jetz et al. (2012) built a website (<https://birdtree.org>) where users can download a tree distribution from a list of species they provide (Rubolini et al., 2015). It could still be improved by offering an API (application programming interface), i.e. a way to do this without using the web user interface but programmatically. API often lead to the development of packages or libraries in various languages by motivated users (this is for example what we did in the case of [rromeo: Access publisher copyright & self-archiving policies via the 'SHERPA/RoMEO' API](#)), which, ultimately, makes it even easier to use the data (e.g. users could directly download the phylogeny from R by giving their list of species, without the need to go on the web interface <https://birdtree.org>).

2.6 My future projects in this area

During my thesis, I have been largely confronted to these issues, either as a user, or as a developer. In the future, I plan on working more on this topic. More specifically, I am currently collaborating on emerging projects to collate spectral data for bird from all taxa all over the world, and information about vision (number of photoreceptors, density, visual acuity, etc.) for all organisms. Currently, this information is spread out over thousands of articles, not always completely openly accessible, and stored in a large variety of not always suitable formats. Collating this data will allow us to answer large scale questions about the evolution of vision or the evolution of colours in birds and it will centralise the information for researchers interested in more precise questions in a focal group.

I will also continue to contribute to rOpenSci, as I have been doing during this PhD by submitting two R packages for review (`lightr` and `rromeo`), but also by contributing to dozens of their packages (sometimes just correcting typos, sometimes more time consuming and valuable contributions). I also plan on providing guidance to scientists interested in Open Science, either by organising information day and workshops, as we did for the Open Access day, or by direct mentoring, as we did with Stéphane Legendre for his software.

References

- A better default colormap for Matplotlib | SciPy 2015 (2015). In collab. with Smith, N. and van der Walt, S. URL: <https://www.youtube.com/watch?v=xAoljeRJ3lU> (cit. on p. 235).
- Abritis, A., McCook, A., and Watch, R. (2017). “Cash incentives for papers go global”. *Science* 357.6351, pp. 541–541. <https://doi.org/10.1126/science.357.6351.541>. pmid: 28798113 (cit. on p. 227).
- Alizon, S. (2018). “Inexpensive Research in the Golden Open-Access Era”. *Trends in Ecology & Evolution* 33.5, pp. 301–303. <https://doi.org/10.1016/j.tree.2018.02.005>. pmid: 29625710 (cit. on p. 229).
- “An introduction to this tract” (1667). *Philosophical Transactions of the Royal Society of London* 1.1, pp. 1–2. <https://doi.org/10.1098/rstl.1665.0002> (cit. on p. 227).
- Baker, M. (2016). “1,500 scientists lift the lid on reproducibility”. *Nature News* 533.7604, p. 452. <https://doi.org/10.1038/533452a> (cit. on p. 227).
- Bar-Ilan, J. and Halevi, G. (2017). “Post retraction citations in context: a case study”. *Scientometrics* 113.1, pp. 547–565. <https://doi.org/10.1007/s11192-017-2242-0> (cit. on p. 228).
- Barraquand, F., Ezard, T. H. G., Jørgensen, P. S., Zimmerman, N., Chamberlain, S., Salguero-Gómez, R., Curran, T. J., and Poisot, T. (2014). “Lack of quantitative training among early-career ecologists: a survey of the problem and potential solutions”. *PeerJ* 2, e285. <https://doi.org/10.7717/peerj.285> (cit. on p. 228).
- Beel, J. (2013). *What makes a bad reference manager?* URL: <https://www.scss.tcd.ie/joeran.beel/blog/2013/10/14/what-makes-a-bad-reference-manager/> (cit. on p. 233).
- Berkeley Institute for Data Science (2017). *matplotlib colormaps*. URL: <https://bids.github.io/colormap/> (cit. on p. 235).
- Bhandari Neupane, J., Neupane, R. P., Luo, Y., Yoshida, W. Y., Sun, R., and Williams, P. G. (2019). “Characterization of leptazolines A–D, polar oxazolines from the cyanobacterium *Leptolyngbya* sp., reveals a glitch with the “Willoughby–Hoye” scripts for calculating NMR chemical shifts”. *Organic Letters*. <https://doi.org/10.1021/acs.orglett.9b03216> (cit. on p. 235).
- Bik, E. M. (2016). *Image duplication quartet*. URL: <https://microbiomedigest.com/2016/06/10/image-duplication-quartet/> (cit. on p. 228).
- Bik, E. M., Casadevall, A., and Fang, F. C. (2016). “The prevalence of inappropriate image duplication in biomedical research publications”. *mBio* 7.3, e00809–16. <https://doi.org/10.1128/mBio.00809-16>. pmid: 27273827 (cit. on p. 228).
- Bohannon, J. (2013). “Who’s afraid of peer review?” *Science* 342.6154, pp. 60–65. <https://doi.org/10.1126/science.342.6154.60>. pmid: 24092725 (cit. on p. 229).

- Budd, J. M., Sievert, M., Schultz, T. R., and Scoville, C. (1999). "Effects of article retraction on citation and practice in medicine." *Bulletin of the Medical Library Association* 87.4, pp. 437–443. pmid: [10550028](#) (cit. on p. 228).
- Budd, J. M., Sievert, M., and Schultz, T. R. (1998). "Phenomena of retraction: Reasons for retraction and citations to the publications". *JAMA* 280.3, pp. 296–297. <https://doi.org/10.1001/jama.280.3.296> (cit. on p. 228).
- Butakov, S. and Scherbinin, V. (2009). "The toolbox for local and global plagiarism detection". *Computers & Education* 52.4, pp. 781–788. <https://doi.org/10.1016/j.compedu.2008.12.001> (cit. on p. 234).
- Center for Open Science (2019). *Opening influenza research*. URL: <https://cos.io/our-services/research/flulab/> (cit. on p. 231).
- Chambers, C. D. (2013). "Registered reports: A new publishing initiative at Cortex". *Cortex* 49.3, pp. 609–610. <https://doi.org/10.1016/j.cortex.2012.12.016> (cit. on p. 231).
- Chawla, A. D. S. (2016). *Here's why more than 50,000 psychology studies are about to have PubPeer entries*. URL: <https://retractionwatch.com/2016/09/02/heres-why-more-than-50000-psychology-studies-are-about-to-have-pubpeer-entries/> (cit. on p. 235).
- Cornell, D. G. (1997). "Post hoc explanation is not prediction. Commentary on J. Archer". *American Psychologist* 52.12, pp. 1380–1380. <https://doi.org/10.1037/0003-066X.52.12.1380.a> (cit. on p. 231).
- Dan Stillman (2019). *Retracted item notifications with Retraction Watch integration*. URL: <https://www.zotero.org/blog/retracted-item-notifications/> (cit. on p. 228).
- Di Cosmo, R. and Zacchiroli, S. (2017). "Software Heritage: Why and how to preserve software source code". In: *iPRES 2017 - 14th International Conference on Digital Preservation*. Kyoto, Japan, pp. 1–10 (cit. on p. 233).
- Dutch Research Council (NWO) (2016). *NWO makes 3 million available for Replication Studies pilot*. URL: <https://www.nwo.nl/en/news-and-events/news/2016/nwo-makes-3-million-available-for-replication-studies-pilot.html> (cit. on p. 231).
- Endler, J. A. (2012). "A framework for analysing colour pattern geometry: adjacent colours". *Biological Journal of the Linnean Society* 107.2, pp. 233–253. <https://doi.org/10.1111/j.1095-8312.2012.01937.x> (cit. on p. 233).
- Fanelli, D. (2012). "Negative results are disappearing from most disciplines and countries". *Scientometrics* 90.3, pp. 891–904. <https://doi.org/10.1007/s11192-011-0494-7> (cit. on p. 228).
- Freeman, A. (2019). *Innovator story: Wrestling the Octopus*. URL: <https://elifesciences.org/labs/9fdd6f3c/innovator-story-wrestling-the-octopus> (cit. on p. 231).

- García, J. A., Rodriguez-Sánchez, R., Fdez-Valdivia, J., and Chamorro-Padial, J. (2019). "The author's ignorance on the publication fees is a source of power for publishers". *Scientometrics*. <https://doi.org/10.1007/s11192-019-03231-8> (cit. on pp. 229, 230).
- Grand, A., Wilkinson, C., Bultitude, K., and Winfield, A. F. T. (2012). "Open science: A new "trust technology"?" *Science Communication* 34.5, pp. 679–689. <https://doi.org/10.1177/1075547012443021> (cit. on p. 228).
- Grenié, M. and Gruson, H. (2019). *Access publisher copyright & self-archiving policies via the 'SHERPA/Romeo' API*. URL: <https://ropensci.org/blog/2019/06/04/rromeo/> (cit. on p. 230).
- Gruson, H., White, T. E., and Maia, R. (2019). "lightr: import spectral data and metadata in R". *Journal of Open Source Software* 4.43, p. 1857. <https://doi.org/10.21105/joss.01857> (cit. on p. 232).
- Haerlin, B. and Parr, D. (1999). "How to restore public trust in science". *Nature* 400.6744, pp. 499–499. <https://doi.org/10.1038/22867> (cit. on p. 228).
- Hannay, J. E., MacLeod, C., Singer, J., Langtangen, H. P., Pfahl, D., and Wilson, G. (2009). "How do scientists develop and use scientific software?" In: *Proceedings of the 2009 ICSE Workshop on Software Engineering for Computational Science and Engineering*. SECSE '09. Washington, DC, USA: IEEE Computer Society, pp. 1–8. ISBN: 978-1-4244-3737-5. <https://doi.org/10.1109/SECSE.2009.5069155> (cit. on pp. 232, 236).
- Hunt, E. (2016). "Tay, Microsoft's AI chatbot, gets a crash course in racism from Twitter". *The Guardian. Technology* (cit. on p. 236).
- Jaffe, S. (2004). "Scientists abandon their software". *The Scientist* 18.3 (cit. on p. 233).
- Jetz, W., Thomas, G. H., Joy, J. B., Hartmann, K., and Mooers, A. O. (2012). "The global diversity of birds in space and time". *Nature* 491.7424, pp. 444–448. <https://doi.org/10.1038/nature11631>. pmid: 23123857 (cit. on p. 238).
- Katz, D. S., Barba, L. A., Niemeyer, K. E., and Smith, A. M. (2019). *Cost models for running an online open journal*. URL: <https://blog.joss.theoj.org/2019/06/cost-models-for-running-an-online-open-journal> (cit. on p. 230).
- Legendre, S. and Clobert, J. (1995). "ULM, a software for conservation and evolutionary biologists". *Journal of Applied Statistics* 22.5-6, pp. 817–834. <https://doi.org/10.1080/02664769524649> (cit. on p. 233).
- Maia, R., Eliason, C. M., Bitton, P.-P., Doucet, S. M., and Shawkey, M. D. (2013). "pavo: an R package for the analysis, visualization and organization of spectral data". *Methods in Ecology and Evolution* 4.10, pp. 906–913. <https://doi.org/10.1111/2041-210X.12069> (cit. on p. 236).
- Maia, R., Gruson, H., Endler, J. A., and White, T. E. (2019). "pavo 2: New tools for the spectral and spatial analysis of colour in R". *Methods in Ecology and Evolution* 10.7, pp. 1097–1107. <https://doi.org/10.1111/2041-210X.13174> (cit. on pp. 233, 235–237).

- McGuire, J. A., Witt, C. C., Remsen, J. V. J., Corl, A., Rabosky, D. L., Altshuler, D. L., and Dudley, R. (2014). "Molecular phylogenetics and the diversification of hummingbirds". *Current Biology* 24.8, pp. 910–916. <https://doi.org/10.1016/j.cub.2014.03.016>. pmid: 24704078 (cit. on p. 238).
- Nadelson, L. S. and Hardy, K. K. (2015). "Trust in science and scientists and the acceptance of evolution". *Evolution: Education and Outreach* 8.1, p. 9. <https://doi.org/10.1186/s12052-015-0037-4> (cit. on p. 228).
- Nature Publishing Group (2017). "Don't pay prizes for published science". *Nature News* 547.7662, p. 137. <https://doi.org/10.1038/547137a> (cit. on p. 227).
- Neill, U. S. (2008). "Publish or perish, but at what cost?" *The Journal of Clinical Investigation* 118.7, p. 2368. <https://doi.org/10.1172/JCI36371>. pmid: 18596904 (cit. on p. 227).
- Nosek, B. A., Ebersole, C. R., DeHaven, A. C., and Mellor, D. T. (2018). "The preregistration revolution". *Proceedings of the National Academy of Sciences* 115.11, pp. 2600–2606. <https://doi.org/10.1073/pnas.1708274114> (cit. on p. 231).
- Nosek, B. A., Spies, J., and Motyl, M. (2012). *Scientific utopia: II - Restructuring incentives and practices to promote truth over publishability*. SSRN Scholarly Paper ID 2062465. Rochester, NY: Social Science Research Network (cit. on p. 228).
- Nuijten, M. B., Hartgerink, C. H. J., van Assen, M. A. L. M., Epskamp, S., and Wicherts, J. M. (2016). "The prevalence of statistical reporting errors in psychology (1985–2013)". *Behavior Research Methods* 48.4, pp. 1205–1226. <https://doi.org/10.3758/s13428-015-0664-2> (cit. on p. 235).
- Pashler, H. and Wagenmakers, E. (2012). "Editors' introduction to the special section on replicability in psychological science: A crisis of confidence?" *Perspectives on Psychological Science* 7.6, pp. 528–530. <https://doi.org/10.1177/1745691612465253> (cit. on p. 227).
- Ram, K., Boettiger, C., Chamberlain, S., Ross, N., Salmon, M., and Butland, S. (2019). "A Community of practice around peer review for long-term research software sustainability". *Computing in Science Engineering* 21.2, pp. 59–65. <https://doi.org/10.1109/MCSE.2018.2882753> (cit. on p. 237).
- Rampin, R. (2018). A Twitter bot identifying matplotlib colormaps. (Cit. on p. 235).
- Ravindranath, P. (2019). *Manipulation within a photo should always result in a retraction: Elisabeth Bik*. URL: <https://journosdiary.com/2019/07/13/manipulation-photo-retraction-duplication-elisabeth-bik/> (cit. on p. 228).
- Redman, B. K., Yarandi, H. N., and Merz, J. F. (2008). "Empirical developments in retraction". *Journal of Medical Ethics* 34.11, pp. 807–809. <https://doi.org/10.1136/jme.2007.023069>. pmid: 18974415 (cit. on p. 228).
- Rubolini, D., Liker, A., Garamszegi, L. Z., Møller, A. P., and Saino, N. (2015). "Using the BirdTree.org website to obtain robust phylogenies for avian comparative studies: A primer". *Current Zoology* 61.6, pp. 959–965. <https://doi.org/10.1093/czoolo/61.6.959> (cit. on p. 238).

- Sansonetti, P. J. (2018). "Measles 2018: a tale of two anniversaries". *EMBO Molecular Medicine* 10.5, e9176. <https://doi.org/10.15252/emmm.201809176> (cit. on p. 228).
- Schekman, R. (2013). "How journals like Nature, Cell and Science are damaging science". *The Guardian. Opinion* (cit. on p. 228).
- Solomon, D. J. and Björk, B.-C. (2012). "A study of open access journals using article processing charges". *Journal of the American Society for Information Science and Technology* 63.8, pp. 1485–1495. <https://doi.org/10.1002/asi.22673> (cit. on p. 230).
- Sonnad, N. (2017). "A gender-biased poem about "lazy" women, by Google Translate". *Quartz* (cit. on p. 236).
- Steen, R. G. (2011a). "Retractions in the scientific literature: do authors deliberately commit research fraud?" *Journal of Medical Ethics* 37.2, pp. 113–117. <https://doi.org/10.1136/jme.2010.038125>. pmid: 21081306 (cit. on p. 228).
- (2011b). "Retractions in the scientific literature: is the incidence of research fraud increasing?" *Journal of Medical Ethics* 37.4, pp. 249–253. <https://doi.org/10.1136/jme.2010.040923>. pmid: 21186208 (cit. on p. 228).
- White, E. P. (2015). "Some thoughts on best publishing practices for scientific software". *Ideas in Ecology and Evolution* 8.1 (cit. on p. 233).
- Zotero Documentation (2019). *How do I import a Mendeley library into Zotero?* URL: https://www.zotero.org/support/kb/mendeley_import (cit. on p. 233).

Access Publisher Copyright & Self-Archiving Policies via the 'SHERPA/Romeo' API

Matthias Grenié, Hugo Gruson



This blog post has been published on rOpenSci blog and is released under a Creative Commons Attribution 4.0 license

We've been following rOpenSci's work for a long time, and we use several packages on a daily basis for our scientific projects, especially taxize to clean species names, rredlist to extract species IUCN statuses or treeio to work with phylogenetic trees. rOpenSci is a perfect incarnation of vibrant and diverse community where people learn and develop new ideas, especially regarding scientific packages. We've also noticed how much the thorough review process improves the quality of the packages that join the rOpenSci ecosystem. And while we were admiring the dynamics of rOpenSci community, we started to wonder how we could contribute to this ecosystem. And this is how we started our quest to find a project that could fit rOpenSci goals while at the same time teach us new skills.

Open Access is the idea that scientific articles should be available to everyone to favour scientific dissemination, as well as public information. Open Access is rising in the scientific community with more and more public funding agencies requiring funded projects to make their article open access. But several very different models exist under this umbrella term of “Open Access”. One of them is the so-called “green open access”, where the articles are made publicly available by their authors via their deposition in institutional or public repositories, such as bioRxiv or HAL. Scientific journals have different policies regarding green open access: some let you archive various versions of the manuscript right after acceptance, while others ask you to wait an embargo period or forbid entirely the archival of the manuscript. To support green open access, scientists can elect to publish their work in journals that authorize manuscript archival. And this is where SHERPA/RoMEO comes in handy: it offers a publicly available database of open access policies of scientific journals and lists the conditions under which manuscript archival might be allowed.

The SHERPA/RoMEO database is available through an Application Programming Interface (API), which meant that we could build an R client to programmatically access this data. This would allow researchers to more easily select journals based on their manuscript archival policies. An R client would also be a precious tool for bibliometrists who want to get the general picture of open access practices in a particular subfield.

Although we had no prior experience working with web data or scraping APIs for data, we knew several tools existed to interact with APIs in R such as httr or rOpenSci's crul. And as we started the development of rrromeo, we also knew we could use the many examples of R client for APIs available on the CRAN Task View on Web Technologies as models.

SHERPA/RoMEO API

SHERPA/RoMEO has been available through a web interface since at least February 2004 according to the Internet Archive and their API was released in December 2006, making their data available to anyone since then.

There are three versions of the manuscript considered in SHERPA/RoMEO:

1. **pre-print**, which is the manuscript version **before peer review**;
2. **post-print**, which is the manuscript as **accepted after peer review** but not yet typeset as an article in the journal;
3. and **typeset manuscript/publisher's manuscript**, which is the manuscript with the text after peer-review, **fully typeset**, as it appears in the journal.



Figure by Ryan Regier, with Book icon from Benny Forsberg, CC-BY 3.0

Some journals accept the archival only of the pre-print, while others accept both pre-print and post-print, or even accept the archival of all three versions! SHERPA/RoMEO’s API lets you know what is the policy of a journal using its name, or its ISSN, and whether restrictions apply such as embargo periods before publicly archiving different manuscript versions.

But even though the database is still updated, it seems the development of the API stopped in 2013, which means it’s lacking some functionalities and it does not always follow modern web standards. Because of this, we could not always readily use R packages but we often needed to perform small adjustments first. For example, it did not always use valid XML and the character encoding was not declared in the HTTP headers, but in the body of the document. Furthermore, the SHERPA/RoMEO is not RESTful and thus the queries were a little more complex to design. Fortunately, the developers had written a full documentation of all different types of query we could run.

rromeo: an R API client

rromeo lets you access basic information regarding the journal policies in R. You can get the policy of a specific journal with its title using the function `rr_journal_name()`:

```
1 rromeo::rr_journal_name("Methods in Ecology and Evolution")
```

```
1                               title      issn romeocolour preprint
2 1 Methods in Ecology and Evolution 2041-210X      yellow      can
3   postprint    pdf pre_embargo post_embargo pdf_embargo
4 1 restricted cannot          <NA>     12 months      <NA>
```

In this example, we see that “Methods in Ecology and Evolution” allows the archival of pre-print manuscripts, post-print manuscripts (but with restrictions) but it does not allow the archival of the typeset manuscript (`pdf` column). A 12 months embargo is required before the public archival of post-print manuscripts (`post_embargo` column).

You can also fetch the policy of several journals at once by matching the beginning of the title via the argument `qtype = "starts"`:

```
1 rromeo::rr_journal_name("Bird", qtype = "starts")
```

```
1 4 journals match your query terms.
2 Recursively fetching data from each journal. This may take some time...
3                               title      issn romeocolour preprint
4
5 1                               Bird Behavior 0156-1383      blue      cannot
6   cannot
7 2 Bird Conservation International 0959-2709      green      can
8   can
9 3                               Bird Populations 1074-1755      <NA>      <NA>      <
10  NA>
11 4                               Bird Study 0006-3657      green      can
12   can
13   pdf pre_embargo post_embargo pdf_embargo
14 1   can          <NA>          <NA>          <NA>
15 2   cannot        <NA>          <NA>          <NA>
16 3   <NA>          <NA>          <NA>          <NA>
17 4   cannot        <NA>          <NA>          <NA>
```

Finally, rromeo can also retrieve publisher’s information:

```
1 rromeo::rr_publisher_name("Oxford University Press")
```

```
1      romeoid          publisher alias romeocolour preprint
      postprint
2  1      55 Oxford University Press    OUP      yellow      can
      restricted
3      pdf
4  1 unclear
```

which gives you the general policy of the “Oxford University Press” regarding manuscript archival. Some restrictions may apply depending on the precise branch of the publisher you plan to publish with, so you should always double check before archiving your manuscripts.

You can get a full overview of rromeo capabilities by reading the introductory vignette.

Developing an API package: first steps

We had no prior experience working with web technologies within R, and this ended up begin a rich and fruitful experience for us. Our first step was to choose the R package to perform the web requests. We picked httr over rOpenSci’s crul package for its even higher-level of use as httr hides even more details on how it handles the query compared to crul. We made sure to follow the best practices described in its “Building API Packages” vignette. We then naturally turned to the xml2 package to parse the resulting XML file, as recommended in rOpenSci package development book.

We wanted to follow best development practices such as having unit tests to check the behavior of functions in the package. But we didn’t intially know how to run unit tests that required an internet connection. We discovered that the answer is **mocking**: storing locally fake HTTP responses that *mimic* the API and use them to test the functions in our package. Creating these fake responses is not an easy task but fortunately, rOpenSci’s vcr package is exactly suited for this task. vcr records requests and replays them during the tests (learn more about it in the technote about vcr). We used it in all our tests as well as for caching the examples shown in the README file. The companion book on HTTP testing helped us dive into the different options suitable to record our requests.

While working on rromeo, we realized that the level of details offered to the user was a delicate balance: on one side, we ran the risk of not being flexible enough to be useful and on the other side, the complexity of the package would just become untractable. We were greatly inspired by the many packages developed by Scott Chamberlain that sometimes offer two different interfaces for different kind of users (see rredlist for example). This strategy may be useful to offer different kind of granularity of information on details depending on the future use of the API information.

A similar issue lied with the license of the SHERPA/RoMEO data: the API returns a license notice with each request but we didn’t want to flood the user with too much information. We opted to include this information in the [CITATION](#) file of the package accessible with the command `citation("rromeo")`. We since then noticed other strategies in other packages, such as having a [DATA_USE](#) file in the root of the source repository and we are still thinking about what the best choice is here.

Developing an API package: gotchas and lessons learned

We were eager to learn but we made some mistakes in the process. Thankfully, these were caught in the review process before we submitted the package for the first official release on CRAN.

For example, it is good practice to use an API key when working with APIs, to let the owners track usage. `rromeo` provides several ways to set up an API key after registering it: a `key` argument in all functions, setting up an environment variable in the session, using an `.Renvironment` or an `.Rprofile` file. These 4 options are summarized in the API key vignette. Our first explanation on how to setup an API key was difficult to understand and was located in the function help files. We thank both our reviewers, Philipp Ottolinger and Bruna Wundervald, for encouraging us to write a full vignette regarding API keys. Thanks to their comments we also wrote the `rr_auth()` function that writes the key as an environmental variable. There may be room for improvement regarding the security of the API key but the access to the API is probably not very sensitive in our case.

Similar to setting up an API key, setting a user-agent when doing web-scraping is good practice to let the owners of the website/API from which kind of software the requests come from. Bruna Wundervald pointed out that we had forgotten to setup a user-agent even though it was specified in the `httr` best practices vignette. We tweaked our requests using `httr::add_headers("user-agent"= ...)` to add a user-agent with a custom defined string that links to the GitHub page of the package and returns its version number. To check that the user-agent was well defined we used the awesome website <https://httpbin.org/> which is a simple HTTP request & response service. It is very useful to test prototype queries and make sure you get back what you wanted. We used <https://httpbin.org/user-agent> with our custom specified header to make sure we had set up the user-agent correctly. We do recommend using `httpbin.org` services to prototype requests and test the passing of arguments.

Because all packages are in the end made for users, it is always important to think about the interface you want to expose to your users. We first had a single function `rr_journal_name()` with a Boolean argument called `multiple`. Based on the value of this argument, the result of `rr_journal_name()` could be wildly different. Both our reviewers noticed it was unexpected from a naive user point of view and suggested to split the function in two different functions that had consistent output: `rr_journal_name()` would return all the information regarding policies and `rr_journal_find()` would return simply the title as well as the ISSN of the journal if found. The new outlook of independent reviewers helped us take a step back regarding the functions we were exposing to the users.

Giving back to the community

As we mentioned previously, our main source of attraction towards rOpenSci was its thriving community. We've always been convinced that collaboration produced the best scientific output. Because of this, we were glad to notice that our experience with rromeo could have ripple effects and help other projects in the community.

Filing issues when you find a bug is an easy but efficient way to give back to the community. vcr and webmockr are recent rOpenSci packages that have mainly been used by a handful of developers until now, one of them being rOpenSci co-founder Scott Chamberlain. Scott often uses crul in his API packages while we used httr for rromeo. We were able to identify issues with vcr and webmockr when used with httr but they were fixed promptly¹²³.

We also plan to contact the SHERPA/RoMEO API developers to let them know we developed rromeo and have their feedback on the package.

The future

rromeo is both on GitHub and CRAN now and seems quite stable. The SHERPA/RoMEO API offers more data regarding paid open access policies (<http://www.sherpa.ac.uk/romeo/PaidOA.php>) as well as other restrictions on manuscript archival. We are still looking for a suitable format to return this information to users. If you want to get involved, we welcome contributions (look for the issues tagged “help wanted” on GitHub).

We enjoyed the experience of contributing to rOpenSci, benefiting from great recommendations by the editor and reviewers, as well as discovering bugs in lesser used packages along the way.

We are now moving to another package that we plan to submit to rOpenSci. It is also an API package so we'll be using some of the knowledge we got from developing rromeo. We hope to be back soon on the rOpenSci blog to talk about that ;)

Acknowledgements

We would like to thank both of the reviewers Philipp Ottolinger and Bruna Wundervald as well as the editor Scott Chamberlain for their input to improve the documentation and the package. We also want to mention Scott Chamberlain for building so many tools to make the interactions with API within R easier (vcr, webmockr, crul, as well as many API packages that can be used as examples for developing your own API package).

¹<https://github.com/ropensci/vcr/issues/91>

²<https://github.com/ropensci/vcr/issues/92>

³<https://github.com/ropensci/vcr/issues/93>

lightr: import spectral data and metadata in R

Hugo Gruson¹, Thomas White², and Rafael Maia³

¹ CEFÉ, University Montpellier, CNRS, University Paul Valéry Montpellier 3, EPHE, IRD, Montpellier, France ² School of Life and Environmental Sciences, University of Sidney, Sidney, NSW, Australia ³ Department of Ecology, Evolution and Environmental Biology, Columbia University, New York, NY

DOI: [10.21105/joss.01857](https://doi.org/10.21105/joss.01857)

Software

- [Review ↗](#)
- [Repository ↗](#)
- [Archive ↗](#)

Submitted: 31 October 2019

Published: 01 November 2019

License

Authors of papers retain copyright and release the work under a Creative Commons Attribution 4.0 International License ([CC-BY](#)).

Summary

Living organisms wildly differ in their ability to see colours (Osorio & Vorobyev, 2008). For this reason, colour science relies on the use of objective measurements of reflectance, transmittance, or absorbance spectra rather than human vision (Bennett, Cuthill, & Norris, 1994; Cuthill, Bennett, Partridge, & Maier, 1999; Eaton, 2005). These spectra are then used in vision models that allow scientists to predict how a given object is seen through the eyes of a given species (e.g., how a male bird is seen by a potential mate). This is the basis of all studies in for example the study of the evolution of colours of animals and plants as communication signals

Spectrometers record the amount of captured photons at different wavelengths (usually between 300–700 nm for colour science, as many species are sensitive to ultraviolet radiations). However, there is no standard file format for spectrometry data and different scientific instrumentation companies use wildly different formats to store spectral data. This use of non-standard file formats jeopardises scientific reproducibility (Peng, 2009) as other researchers might not have the (paid) tools to open these files, and it makes us dependent on a third-party which might vanish anytime, leaving a trove of scientific data impossible to access. Vendors' proprietary software sometimes have an option to convert those formats into human readable files such as csv but such software are often expensive and they discard most metadata in the process. Yet, those metadata are critical to ensure reproducibility of the measurements, and ultimately of the scientific findings (White, Zeil, & Kemp, 2015).

In this article, we present `lightr`, an R package that aims at offering a unified user-friendly interface for users to read reflectance, transmittance, and absorbance spectra files from various formats in a single line of code. Additionally, it provides for the first time a fully free and open source solution to read proprietary spectra file formats on all operating systems.

`lightr` started as a fork from the popular R package `pavo`, which provides a large suite of colour analysis tools (Maia, Eliason, Bitton, Doucet, & Shawkey, 2013; Maia, Gruson, Endler, & White, 2019).

Package design

`lightr` has been designed to provide two levels on the complexity / customability trade-off:

- Spectral data and metadata for each file format are extracted using specialized parsers. Parsers are also aliased with many different names so that users can often use `lr_parse_<extension>()` where `<extension>` is the file extension of the file to parse. For convenience, we also provide a generic fallback, named `lr_parse_generic()` that

works for many “simple” formats, often derived from `csv` or `tsv`. Specialized parsers should usually be preferred to `lr_parse_generic()` because `lr_parse_generic()` is not able to parse metadata.

- Because spectrometers store each measurement in a separate file, the number of files for a single study can quickly increase. To ensure easy and efficient processing of those files, `lightr` also provides three high-level functions that can recursively find files and process them with a parallelized loop using the `parallel` R package: `lr_get_spec()` and `lr_get_metadata()`, which import respectively spectral data and metadata as `data.frame` in R, as well as `lr_convert_tocsv()`, which converts all spectra files in a given folder as `csv`, with the same filename (minus the file extension).

```
library(lightr)
lr_convert_tocsv(where = "yourfolder", ext = "ProcSpec")
```

Recommended workflow

As mentioned earlier, proprietary spectrometry software can also export spectral data into a human-readable format (usually a kind of tabulation separated values, or `tsv`, with a complex header). `lightr` can read files generated by this export step. We however **do not recommend you use the software's built-in export function**, because it will apply possibly unwanted transformation to your data (interpolation and subsetting) and may discard important metadata.

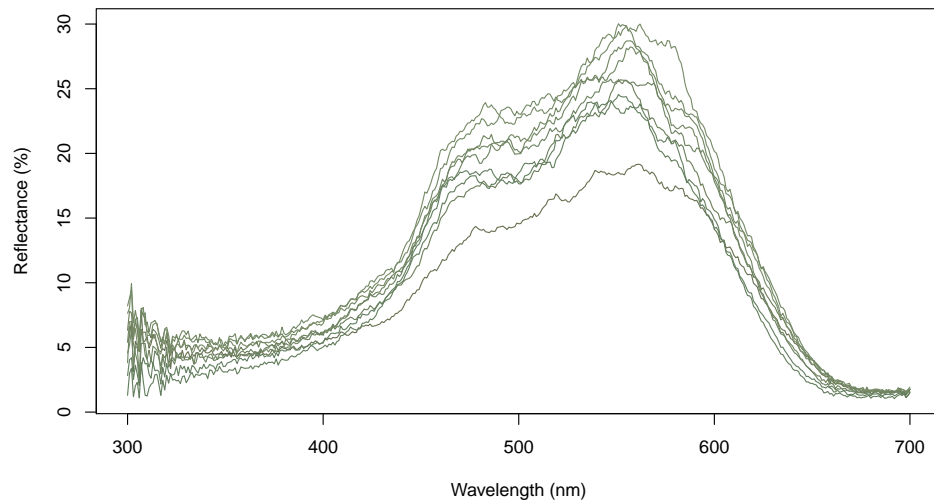
Instead, we recommend you keep the files in the proprietary format (such as Avantes ABS, ROH and TRM, or OceanOptics ProcSpec and `jdx`) and that you use `lightr` to convert them into your preferred file format (such as `csv`).

Usage and future directions

`lightr` can serve as a basis for colour analysis R packages to deal with the file import step. Most of them can only read a limited variety of file formats currently. Future versions of `pavo`, for example, will include `lightr` as a dependency. Below is an illustration of a workflow where `lightr` is used to import the spectral data, which is then analysed with `pavo`:

```
library(lightr)
specs <- lr_get_spec(where = "yourfolder", ext = "ProcSpec")

library(pavo)
plot(specs, col = spec2rgb(specs))
```



```
summary(specs, subset = TRUE)
```

	B2	S8	H1
9.31682	9.31682	1.915661	561
11.26643	11.26643	2.156246	551
12.78053	12.78053	2.128401	557
13.41558	13.41558	2.123076	551
13.44852	13.44852	2.118632	562
12.14774	12.14774	2.210931	557
11.76633	11.76633	2.076845	547
10.62519	10.62519	2.204452	551
10.14280	10.14280	2.272771	547

The first column indicates the brightness (in % relative to a white reference), the second contains the saturation (also called spectral purity) and the last contains the hue (in nm).

`lightr` can also prove useful for developers of other programming languages, providing a free and open source template that can easily be translated to such other languages. We also plan on providing a web application based on shiny (<https://github.com/rstudio/shiny>), which uses `lightr` in the background, and provides users with limited R or technical knowledge with a simple and convenient way to convert all their proprietary files to csv.

Acknowledgements

We thank the two rOpenSci reviewers, Jeroen Ooms and Karthik Ram, for their helpful feedback that improved this package, as well as JOSS editor Daniel S. Katz for his comments on this manuscript.

References

- Bennett, A. T. D., Cuthill, I. C., & Norris, K. J. (1994). Sexual selection and the mismeasure of color. *The American Naturalist*, 144(5), 848–860. doi:[10.1086/285711](https://doi.org/10.1086/285711)
- Cuthill, I. C., Bennett, A. T. D., Partridge, J. C., & Maier, E. J. (1999). Plumage reflectance and the objective assessment of avian sexual dichromatism. *The American Naturalist*, 153(2), 183–200. doi:[10.1086/303160](https://doi.org/10.1086/303160)
- Eaton, M. D. (2005). Human vision fails to distinguish widespread sexual dichromatism among sexually “monochromatic” birds. *Proceedings of the National Academy of Sciences*, 102(31), 10942–10946. doi:[10.1073/pnas.0501891102](https://doi.org/10.1073/pnas.0501891102)
- Maia, R., Eliason, C. M., Bitton, P.-P., Doucet, S. M., & Shawkey, M. D. (2013). Pavo: An R package for the analysis, visualization and organization of spectral data. *Methods in Ecology and Evolution*, 4(10), 906–913. doi:[10.1111/2041-210X.12069](https://doi.org/10.1111/2041-210X.12069)
- Maia, R., Gruson, H., Endler, J. A., & White, T. E. (2019). Pavo 2: New tools for the spectral and spatial analysis of colour in R. *Methods in Ecology and Evolution*, 10(7), 1097–1107. doi:[10.1111/2041-210X.13174](https://doi.org/10.1111/2041-210X.13174)
- Osorio, D. C., & Vorobyev, M. (2008). A review of the evolution of animal colour vision and visual communication signals. *Vision Research, Vision Research Reviews*, 48(20), 2042–2051. doi:[10.1016/j.visres.2008.06.018](https://doi.org/10.1016/j.visres.2008.06.018)
- Peng, R. D. (2009). Reproducible research and biostatistics. *Biostatistics*, 10(3), 405–408. doi:[10.1093/biostatistics/kxp014](https://doi.org/10.1093/biostatistics/kxp014)
- White, T. E., Zeil, J., & Kemp, D. J. (2015). Signal design and courtship presentation coincide for highly biased delivery of an iridescent butterfly mating signal. *Evolution*, 69(1), 14–25. doi:[10.1111/evo.12551](https://doi.org/10.1111/evo.12551)

When Standards Go Wild - Software Review for a Manuscript

Stefanie Butland, Nick Golding, Chris Grieves, Hugo Gruson, Thomas White, Hao Ye



This blog post has been published on rOpenSci and MEE blogs and is released under a Creative Commons Attribution 4.0 license

Stefanie Butland, rOpenSci Community Manager

Some things are just irresistible to a community manager – PhD student Hugo Gruson’s recent tweets definitely fall into that category.

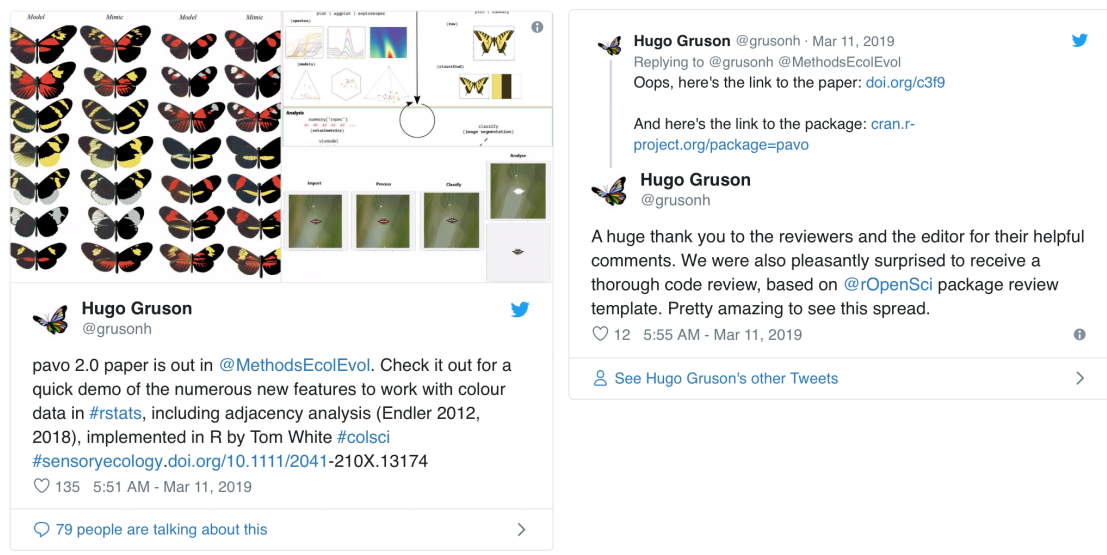


Figure 1: “Pavo tweets”

I was surprised and intrigued to see an example of our software peer review guidelines being used in a manuscript review, independent of our formal collaboration with the journal Methods in Ecology and Evolution (MEE). This is exactly the kind of thing rOpenSci is working to enable by developing a good set of practices that broadly apply to research software.

But who was this reviewer and what was their motivation? What role did the editors handling the manuscript play? I contacted the authors and then the journal and, in less than a week we had everyone on board to talk about their perspectives on the process.

Nick Golding, Associate Editor, Methods in Ecology and Evolution

To me, MEE’s role is to help increase the quality of the methods used in ecology and evolution, and this includes research software. It would be great to reach a point where all the research software used in ecology is at the same high standard as the packages that have been through rOpenSci software peer review.

Not all R packages that we receive at MEE fit in with the rOpenSci package scope, but I'd love to see them go through a similar process. This is where the rOpenSci review checklist comes in. In my view, it's the gold standard for reviewing R packages and I was thrilled to see that Hao (manuscript reviewer) had used it with this paper.

The idea of doing code review as part of reviewing a manuscript is new to a lot of people. Often, invited reviewers decline because they don't think they have the right experience. If you have experience with creating packages though, reviewing code isn't something to be worried about. rOpenSci's guidelines are a great way for people new to reviewing code to become comfortable with the process.

Hao Ye, Manuscript Reviewer

When I was asked to review the code for the pavo 2.0 manuscript¹, I had an initial moment of panic – I had no experience doing formal code review. Luckily, I knew that rOpenSci had a set of reviewing guidelines, and that a few MEE Applications papers had used them. The same guidelines are also used by the Journal of Open Source Software (JOSS). Although this submission wasn't flagged for rOpenSci review, I didn't see a conflict with using their guidelines for my task.

The checklist helped me to organise my review. I started with the basic package review template, and then focused on a detailed look at the primary vignette (which is where I expect most users start). The rOpenSci guidelines encourage the use of some automated tools, like `goodpractice` to facilitate reviewing. The hardest part was providing suggestions to address what the `goodpractice::gp()` function flagged as complex or redundant code. The remainder of the review went pretty smoothly. I'm a fan of task checklists, so I'm glad that the authors found my comments useful. Hopefully the changes will help with the future maintenance of the package.

Thomas White and Hugo Gruson, Manuscript Authors

We were immediately struck by the rigor and thoughtfulness of the reviews and pleasantly surprised to see reference to rOpenSci in Hao's [anonymous] review. It was clear that Hao and two other reviewers had invested significant time in examining not only the manuscript and documentation, but the codebase itself. An uncommon, but welcome experience.

Our package was singularly improved as a result, both for end-users and ourselves. Many of the suggestions that we implemented – such as comprehensive test coverage, explicit styling, greater code safety, executable examples, and contributor guidelines – will persist and guide the development of this (and related) packages into the future.

¹Maia, R., Gruson, H., Endler, J. A., & White, T. E. (2019). pavo 2: new tools for the spectral and spatial analysis of colour in R. *Methods in Ecology and Evolution*. <https://doi.org/10.1111/2041-210X.13174>

We know that software is challenging to review since the overlap of field-specific expertise between developers and biologists is relatively limited. This is where the value of rOpenSci's work in developing tractable standards for reviewers and developers really comes into focus, as well as the willingness of journals such as MEE to encourage their use. We're just grateful for the experience and would be thrilled to see the practice expand in scope and reach where possible.

Chris Grieves, Assistant Editor, *Methods in Ecology and Evolution*

Since the early days of the journal, code and software papers (or Applications articles as we call them) have been really important to MEE. In our Policy on Publishing Code we highlight our commitment to ensuring the quality of code through the peer review process.

We've got a team of dedicated Applications Editors who handle code manuscripts and they do a great job of balancing their comments on the manuscript and the code that goes along with it. Resources like the rOpenSci package review guidelines can really help to take the pressure off these Editors, and they give reviewers confidence to comment on the code. It's great to have the chance to promote them here and we hope that this post will encourage more people to check them out.

We also partner directly with rOpenSci for software peer review. If you have an R package that meets the aims and scope of both MEE and rOpenSci, you can opt for a joint review in which the R package is reviewed by rOpenSci, followed by fast-tracked review of the manuscript by MEE. Manuscripts published through this process are recognized via a mark on both HTML and PDF versions of their paper. We've had two articles published to date as a result of this partnership^{2 3}.

Reflections

Having a manuscript reviewed can often feel like a quite mysterious process. Your work disappears into a black box and comes out with a load of anonymous suggestions for how to improve it. At rOpenSci and *Methods in Ecology and Evolution*, we want to help open up that black box. Thanks to Hugo's tweet of gratitude, and the goodwill of the editors, reviewers and authors of the pavo 2.0 paper, this post provides a glimpse of what is possible. Will you give it a try next time?

²Sciaiani, M., Fritsch, M., Scherer, C., & Simpkins, C. E. (2018). NLMR and landscapetools: An integrated environment for simulating and modifying neutral landscape models in R. *Methods in Ecology and Evolution*, 9(11), 2240-2248. <https://doi.org/10.1111/2041-210X.13076>

³Zizka, A., Silvestro, D., Andermann, T., Azevedo, J., Duarte Ritter, C., Edler, D., ... & Svantesson, S. CoordinateCleaner: Standardized cleaning of occurrence records from biological collection databases. *Methods in Ecology and Evolution*. <https://doi.org/10.1111/2041-210X.13152>



PAVO 2: New tools for the spectral and spatial analysis of colour in R

Rafael Maia¹ | Hugo Gruson² | John A. Endler³ | Thomas E. White⁴

¹Department of Ecology, Evolution and Environmental Biology, Columbia University, New York, NY

²CEFE, University Montpellier, CNRS, University Paul Valéry Montpellier 3, EPHE, IRD, Montpellier, France

³School of Life and Environmental Sciences, Deakin University, Waurn Ponds Campus, Vic., Australia

⁴School of Life and Environmental Sciences, University of Sydney, Sydney, NSW, Australia

Correspondence

Thomas E. White
Email: thomas.white@sydney.edu.au

Handling Editor: Robert B. O'Hara

Abstract

1. Biological coloration presents a canvas for the study of ecological and evolutionary processes. Enduring interest in colour-based phenotypes has driven, and been driven by, improved techniques for quantifying colour patterns in ever-more relevant ways, yet the need for flexible, open frameworks for data processing and analysis persists.
2. Here we introduce `PAVO 2`, the latest iteration of the R package `PAVO`. This release represents the extensive refinement and expansion of existing methods, as well as a suite of new tools for the cohesive analysis of the spectral and (now) spatial structure of colour patterns and perception. At its core, the package retains a broad focus on (a) the organization and processing of spectral and spatial data, and tools for the alternating (b) visualization, and (c) analysis of data. Significantly, `PAVO 2` introduces image-analysis capabilities, providing a cohesive workflow for the comprehensive analysis of colour patterns.
3. We demonstrate the utility of `PAVO` with a brief example centred on mimicry in *Heliconius* butterflies. Drawing on visual modelling, adjacency, and boundary strength analyses, we show that the combined spectral (colour and luminance) and spatial (pattern element distribution and boundary salience) features of putative models and mimics are closely aligned.
4. `PAVO 2` offers a flexible and reproducible environment for the analysis of colour, with renewed potential to assist researchers in answering fundamental questions in sensory ecology and evolution.

KEY WORDS

colour, colourspace, photography, reflectance, sensory ecology, spectra, spectrometry, vision

1 | INTRODUCTION

The study of colour in nature continues to generate fundamental knowledge: from the neurobiology and ecology of information processing (Caves et al., 2018; Schnaitmann et al., 2018; Thoen, How, Chiou, & Marshall, 2014; White & Kemp, 2017), to the evolutionary drivers of life's diversity (Dalrymple et al., 2015, 2018; Endler, 1980; Maia, Rubenstein, & Shawkey, 2013b). Colour is a subjective perceptual experience, however, so our understanding

of the function and evolution of this conspicuous facet of variation depends on our ability to analyse phenotypes in meaningful ways. Excellent progress continues to be made in this area, with emerging techniques now able to quantify and integrate both the spectral (i.e. colour and luminance) and spatial (i.e. the distribution of pattern elements) properties of colour patterns (Endler, 2012; Endler, Cole, & Kranz, 2018; Kemp et al., 2015; Renault, Kelber, & Schaefer, 2017; Troscianko, Skelhorn, & Stevens, 2017; van den Berg et al., in prep). The need remains, however, for tools that

integrate these complex methods into clear, open, and reproducible workflows (White et al., 2015), allowing researchers to retain focus on the exploration of interesting questions.

Here we introduce `PAVO 2`, a major revision and update of the R package `PAVO` (Maia, Eliason, Bitton, Doucet, & Shawkey, 2013a). Since its initial release, the package has provided a cohesive framework for the processing and analysis of spectral data, yet the interceding years have seen the advent of novel analytical methods and the refinement of existing ones. As detailed below, `PAVO 2` has been extensively expanded to incorporate a suite of new tools, with the most significant advance being the inclusion of geometry-based analyses. This allows for the quantification of spectral and spatial properties of colour patterns within a single workflow, thereby minimizing the computational and

cognitive overhead associated with their otherwise fragmented analysis.

2 | THE PAVO PACKAGE, VERSION 2

The conceptual focus of `PAVO` remains centred on three components: (a) data importing and processing, and ongoing feedback between (b) visualization and (c) analysis (Figure 1). The package is available for direct installation through R from CRAN (<https://CRAN.R-project.org/package=pavo>), while the development version is available on Github (<https://github.com/rmaia/pavo>). Comprehensive details and examples of the rich functionality of `PAVO` are available in help files as well as the package vignettes. Indeed, we strongly encourage readers to

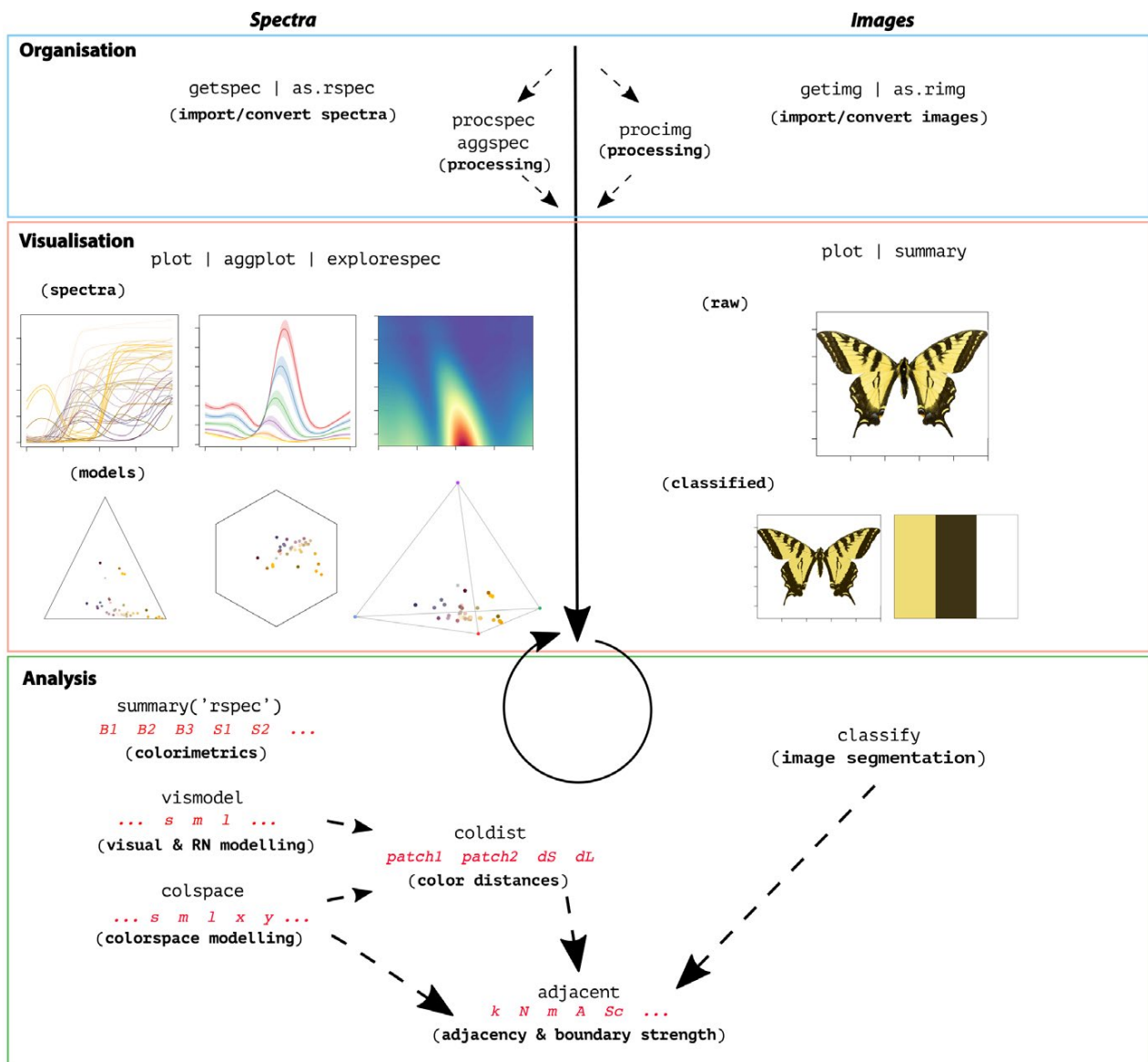


FIGURE 1 A general overview of the colour-pattern analysis workflow in `PAVO` as of version 2, displaying some key functions at each stage

refer to the vignettes as the primary source for information on `PAVO`'s functionality (accessible through `browseVignettes(pavo)`, and at <http://rafaelmaia.net/pavo/>), since they are updated as necessary with every package release.

3 | ORGANIZATION

Images and spectra can be loaded into `PAVO` in bulk through the use of `getimg()` and `getspec()`, respectively. Both are capable of handling multiple data formats, such as jpeg, bmp, and png in the case of images, and over a dozen formats of spectral data, including the diverse and complex proprietary formats of the various spectrometer vendors. Once loaded, the data are stored as objects of an appropriate custom S3 class for use in further functions. Spectral data are of class `rspec`, and inherit methods from `data.frame`, while images are of class `rimg`, and are multidimensional objects (typically 3D, for an RGB image) that inherit methods from `array`. If more than one image is imported in a single call to `getimg()`, then each image is stored as an element of a list. This class system allows for — among other things — the reliable use of generic functions such as `plot()` and `summary()`, which can be called any time to inspect and visualize data.

Several functions then facilitate the initial processing of colour data. It is often desirable to process spectra to remove unwanted noise, modify the spectral range, and/or interpolate the standard wavelength intervals, all of which may be achieved through `procspec()`. For images, `procimg()` offers similar functionality such as the ability to interactively specify the real-world scale of images (in preferred units of measurement), rotate and resize images, or define the boundary between a focal object and the visual background. The scope of image processing in `PAVO 2` is minimalist by design, as much of what might be used during standard image handling are either needs best considered and met by researchers during image capture and data-checking, or are readily achieved within R using existing packages such as `IMAGER` (Barthelme, 2018) and `MAGICK` (Ooms, 2018). Indeed, `PAVO 2` includes convenience functions to convert between image-classes used by `PAVO`, `IMAGER` and `MAGICK`, allowing ready access to extensive image-processing capabilities.

4 | VISUALIZATION

The repeated visualization of spectral and spatial data is an essential step during all stages of analysis, and `PAVO 2` offers numerous tools and publication-ready graphics fit for purpose. Once the package is loaded, the `plot()` function recognizes objects of class `rspec` and `rimg`, as well as `colspace` (the product of visual modelling, detailed below), and becomes the conduit to most visualizations. For raw spectral data, for example, `plot()` will produce a clean plot of the spectra vs. wavelengths (Figure 1, centre-left). Following visual modelling, di-, tri- and tetra-chromatic models can instead be visualized, as well as data from more specialized models,

such as the colour hexagon (Chittka, 1992), CIEXYZ or LAB spaces (Smith & Guild, 1931; Westland, Ripamonti, & Cheung, 2012), categorical space (Troje, 1993), segment analysis (Endler, 1990), the colour-opponent coding space (Backhaus, 1991), or the 'receptor-noise' space (de Ibarra, Giurfa, & Vorobyev, 2001; Pike, 2012). Images can also be plotted, with the result depending on whether and how they have been processed. When given an unprocessed `rimg` object, `plot()` will produce a simple raster-based plot of the image (Figure 1, right). Following the results of `classify()` (discussed below), in which images are segmented into discrete colour-classes (or if a colour-classified image is loaded directly), the plot will use the mean RGB values of each colour-class to plot the now-classified image (Figure 2).

5 | ANALYSIS

Since the perception of colour is a subjective experience, significant progress has been made in representing its reception using ecologically relevant 'visual models' (Kelber, Vorobyev, & Osorio, 2003; Kemp et al., 2015; Renoult et al., 2017), which `PAVO 2` includes in an extended repertoire. The first step in such analyses is a call to `vismodel()`, which models photoreceptor stimulation (quantum-catches, or photon-flux) based on information about the viewer's visual sensitivity and viewing environments. While users are free to use their own spectra, `PAVO` includes a suite of built-in receptor sensitivities, illuminant and transmission data (be it environmental or ocular), and viewing backgrounds, for convenience.

Once quantum catches are estimated the results can be used in a number of models, depending on the question and analytical objective at hand (Kemp et al., 2015; Renoult et al., 2017). General colourspaces are available through a call to `colspace()` which, if provided no further arguments, will model the data in a generalist di-, tri- or tetrachromatic space informed by the dimensionality of the visual system. More specialized colourspaces — which may be informed by specific information about the visual systems of particular species — are also available via `colspace()`. The CIEXYZ, CIELAB and CIELch models (designed and intended exclusively for humans) are available, and `colspace()` will check that the appropriate inputs, such as the human colour-matching function, have been used to model receptor stimulation, as required (Smith & Guild, 1931; Westland et al., 2012). The colour-opponent-coding (Backhaus, 1991) and colour-hexagon (Chittka, 1992) models of bee vision are implemented, as is the 'categorical' model of fly colour-vision detailed by Troje (1993). Plots for every space are accessible through a call to `plot()` which, thanks to the underlying class system, will draw on the appropriate visualization for the model at hand — be it a hexagon, a dichromatic segment, a Maxwell triangle or a three-dimensional tetrahedron.

The receptor-noise limited (RN) model of early-stage (retinal) colour processing has proven exceptionally popular (Vorobyev, Brandt, Peitsch, Laughlin, & Menzel, 2001; Vorobyev & Osorio, 1998), and has been tested to varying degrees in diverse taxa

(Barry, White, Rathnayake, Fabricant, & Herberstein, 2015; Fleishman et al., 2016; Kelber et al., 2003; Olsson, Lind, & Kelber, 2015; White & Kemp, 2016). Following the estimation of receptor stimulation in `vismodel()`, the model incorporates information on relative receptor densities and noise through the function `coldist()`, and estimates either quantum- or neural-noise weighted colour distances. Version 2 of `PAVO` introduces several extensions of this approach, such as the bootstrapped colour distance of `bootcoldist()`, which provides an estimate of the noise-weighted distances (dS 's and/or dL 's) between the centroids of colour samples in multivariate space, with an appropriate measure of error (detailed in Maia & White, 2018). Stimuli can also now be expressed and plotted as coordinates in 'perceptual' (i.e. receptor-noise corrected) space by calling `jnd2xyz()` on the distances calculated in `coldist()` (de Ibarra et al., 2001; Pike, 2012). Notably, these functions now accept n-dimensional data (derived independently, but see Clark, Santer, & Brebner, 2017; Gawryszewski, 2018, for valuable discussion). This allows for the modelling of extreme (Chen, Awata, Matsushita, Yang, & Arikawa, 2016; Cronin & Marshall, 1989, though given the lack of support for traditional opponency in these systems, the RN model may be of limited use here) or entirely hypothetical visual systems. Of course `coldist()` also accepts the results of alternative models – such as the hexagon or CIELAB – and will return colour distances in units appropriate for each space.

Exciting recent advances now allow for the analysis of colour pattern geometry – that is, the spatial structure of colour patches – in conjunction with the comparatively well-developed approaches to the spectral analysis of colour outlined

above (Endler, 2012; Endler et al., 2018; Pike, 2018; Troscianko et al., 2017). The most significant extension of `PAVO` as of version 2 is the introduction of an image-based workflow to allow for the combined analysis of the spectral and spatial structure of colour patterns, currently centred on measures of overall pattern contrast (Endler & Mielke, 2005), the adjacency analysis (Endler, 2012), and its extension, the boundary strength analysis (Endler et al., 2018). In `PAVO` 2, the various steps for such analyses are carried out through calls to `classify()`, which automatically or interactively segments images into discrete colour-classes, and/or `adjacent()`, which performs the adjacency analysis and, if appropriate colour distances are also specified, the boundary strength analysis (discussed in Endler et al., 2018).

Briefly, these analyses entail classifying evenly spaced points within a visual scene into discrete colour classes using spectrometric measurements and/or photography. The column-wise and row-wise colour-class transitions between adjacent points are then tallied, and from this a suite of summary statistics on pattern structure – from simple colour proportions, through to colour diversity and pattern complexity – are estimated (e.g. Endler, Gaburro, & Kelley, 2014; Rojas, Devillechabrolle, & Endler, 2014; Rojas & Endler, 2013; White, 2017). The precise procedure that might be followed by researchers will vary considerably depending on the goal and tools at hand, and `PAVO` 2 is designed to accommodate such flexibility. In relatively simple cases (as in the below example), users may import and calibrate images via `getimg()` and `procimg()`, segment the image via clustering using `classify()`, and combine it with spectrometric

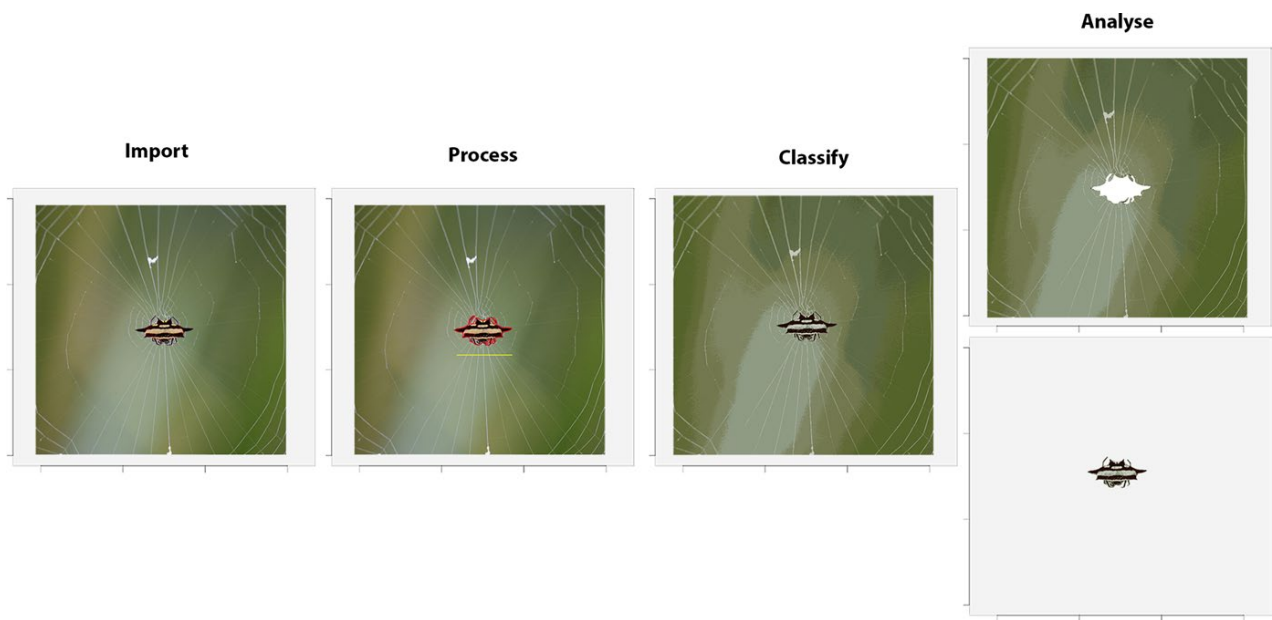


FIGURE 2 A sample workflow for image handling and analysis in `PAVO`, as of version 2. Images are first imported and optionally processed by, for example, setting scales (yellow line) or defining objects and backgrounds (red outline). They may then be colour-classified before being passed to analytical functions, currently centred on the adjacency and boundary-strength analyses. If backgrounds and focal objects are defined then they can be analysed separately, concurrently, or either one can be excluded entirely

measurements and visual modelling of the few discrete colour-classes in a call to `adjacent()`. In more complex cases, such as animals in their natural habitats, users may instead wish to collect spectrometric measurements along a grid-sample of the visual scene, visually model and statistically cluster the results (e.g. using `vismodel()`), then feed the resulting colour-classified grid into `adjacent()` directly (as per 'method 1': Endler, 2012), without the use of images or the `classify()` function at all (see the package vignette for an example).

As alluded to earlier, our goal is to provide a flexible and relatively simple analytical framework for the analysis of a colour pattern's spatial structure using images, with few requirements for specialized photographic equipment or and/or extensive calibration and processing (demonstrated in the colour-plate based

example below). We thus make an analytical and conceptual distinction between the spectral data afforded by spectrometry (i.e. the number and 'colour' of patches), and the spatial data afforded by images (i.e. the size, distribution and arrangement of patches), with the two able to be conveniently combined during latter analyses (Figure 1). This also minimizes the unnecessary duplication of efforts of more general-purpose tools such as `IMAGER` (Barthelme, 2018) and `MAGICK` (Ooms, 2018), and the excellent image analysis toolbox 'mica' for `imageJ` (Troscianko & Stevens, 2015), which offer rich functionality for image processing and (in the latter case) analysis. We emphasize, however, that the convenience of the toolkit provided by `PAVO 2` belies the complexity of the choices demanded of researchers and that every parameter and option requires close consideration and justification. It

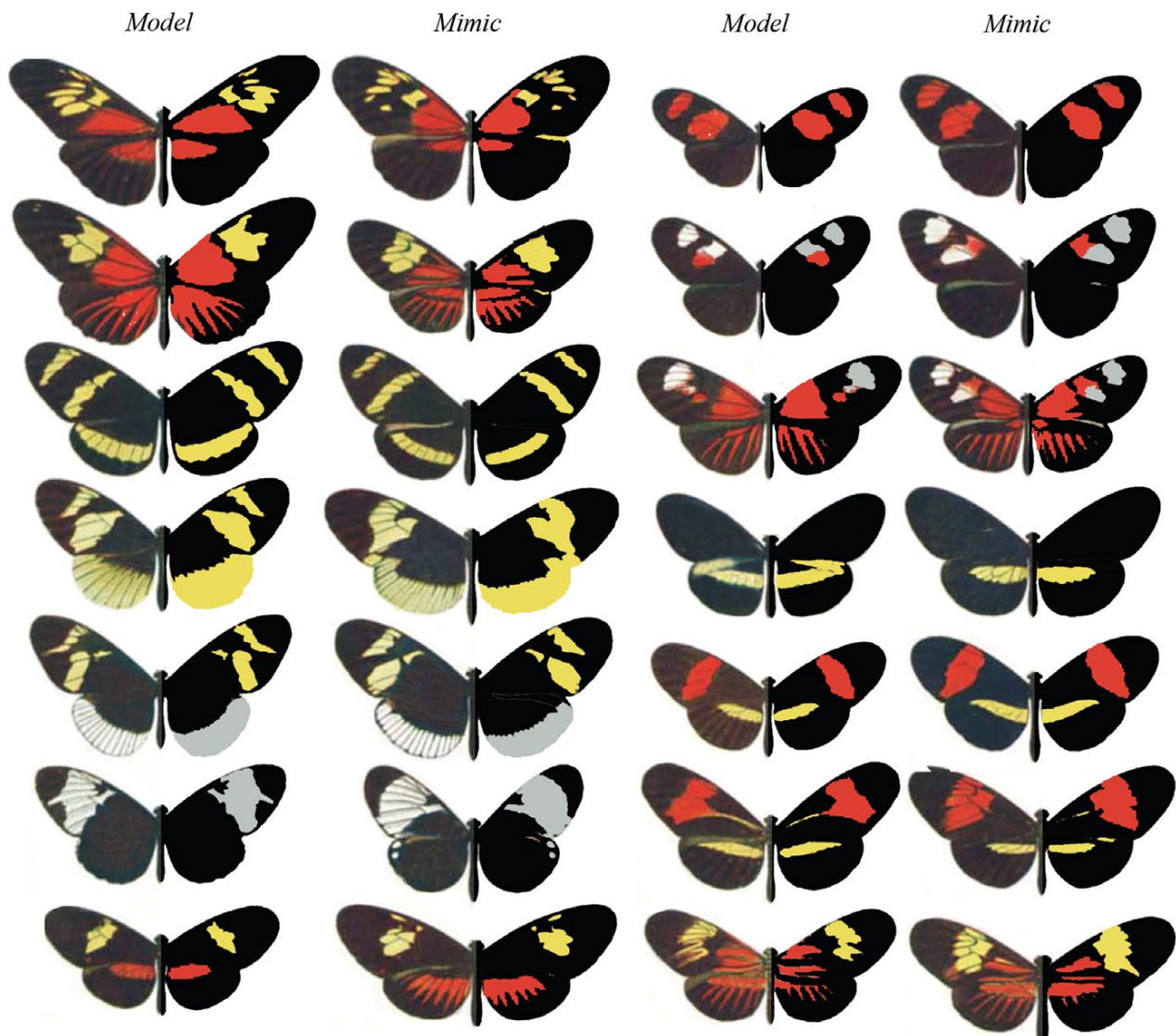


FIGURE 3 A modification of Eltringham's (1916) colour plate of *Heliconius* butterflies, sensu Endler (2012), arranged into putative models and mimics. The left side of each individual is as per the original, while the right half display pattern elements that have been classified into discrete classes via k-means clustering, using the `classify()` function

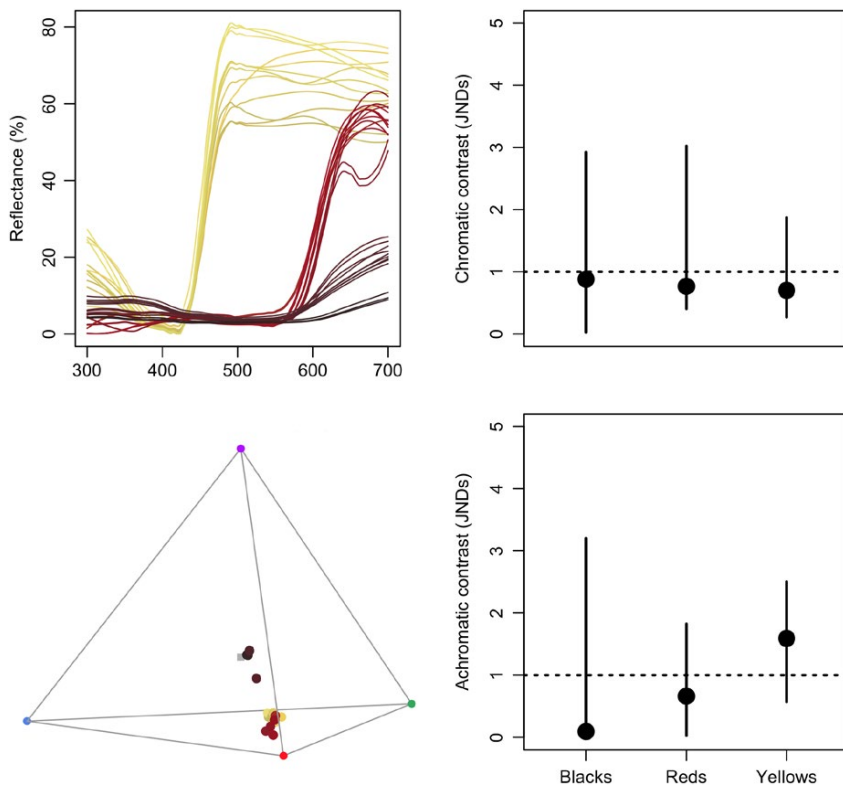


FIGURE 4 Reflectance spectra from black, red, and yellow patches of *Heliconius egeria* and *Heliconius melpomene*, along with their positions in a tetrahedral model of avian vision (left side). The bootstrapped, noise-corrected chromatic and achromatic patch distances between species (right) predicts that the individual colours of this model/mimic pair are likely indistinguishable to avian predators

is rare, for example, that image analyses should be used without any input from visually-modelled spectrometric data, since naive clustering performed on uncalibrated images will offer a poor representation of a visual scene as relevant to non-human animals. For example, even in simple cases, as below, the number of discrete patches present (e.g. the argument `kcols` in `cluster()`) and their approximate distribution is best estimated using spectrometric data in an ecologically relevant model, rather than relying on human-subjective estimates of colour segregation, or the automated clustering of RGB/HSV/Lab image data. Note that this is true across software packages for biological image analysis more generally, which should be used with caution if attempting to estimate ecologically salient measures of colour and/or pattern similarity only using uncalibrated, compressed images clustered using human-based colourspaces. One flexible approach combining spectrometry and image analysis is integrated into the below example, and Endler (2012) details others, such as estimating extant colours within a scene as the number of receptor-noise ellipsoids required to encompass an entire sample of spectra.

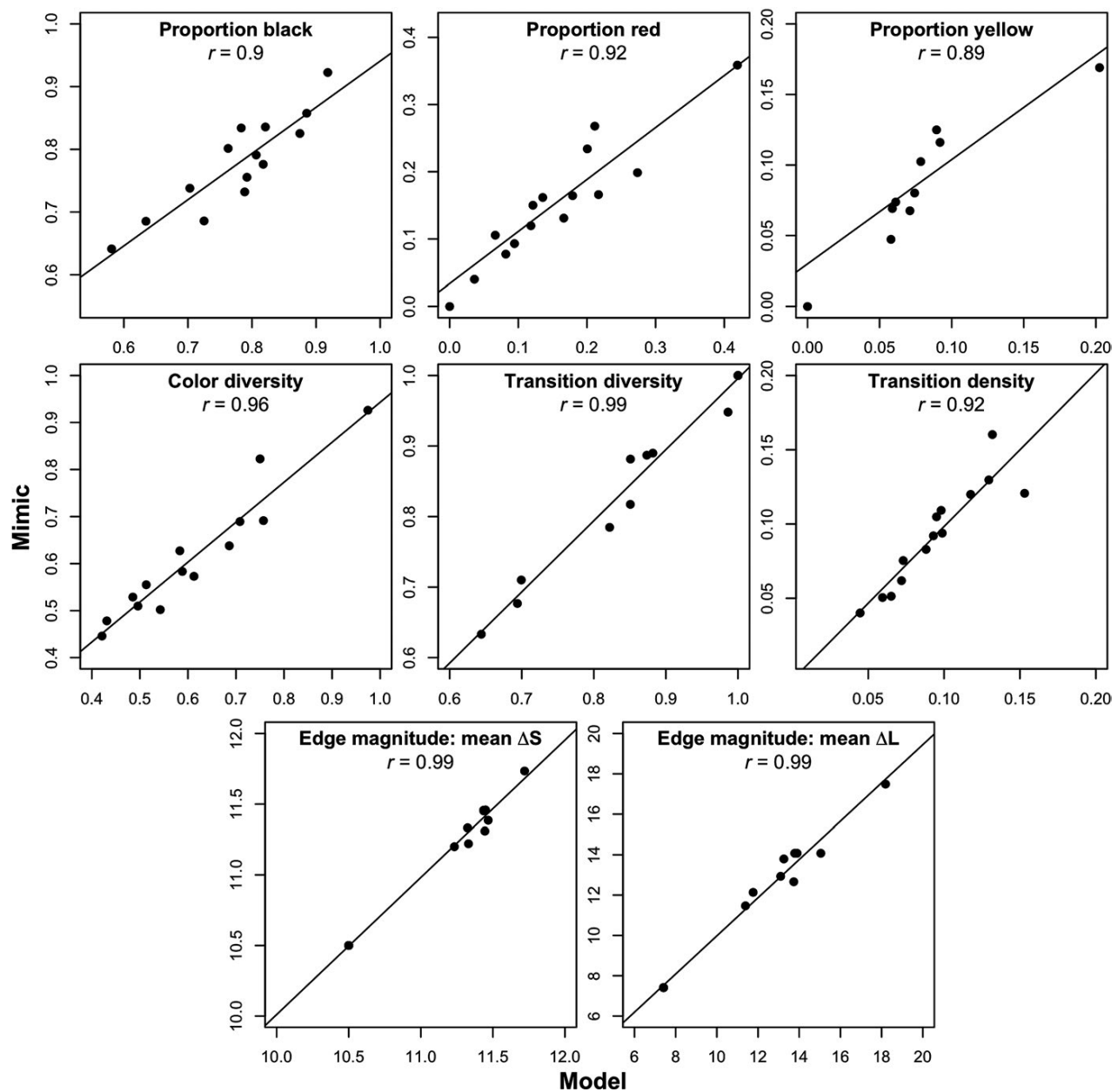
6 | WORKED EXAMPLE: MIMICRY IN *HELICONIUS* spp.

Butterflies of the genus *Heliconius* are widely involved in mimicry and have proven an exemplary system for studies of colour pattern

development, ecology and evolution (Jiggins, 2016). Here we demonstrate some of `pavo` 2's capabilities by briefly examining the visual basis of mimicry in this system, with the objective of quantifying the spectral and spatial (dis)similarity between putative models and mimics. For our spatial analyses, we follow Endler (2012) and use colour plate XII from Eltringham (1916), which is arranged into what he described as model and mimic pairs (Figure 3). For our spectral analyses we collated six reflectance spectra from each of the assumed-discrete 'red', 'yellow' and 'black' patches (confirmed by spectral measurement, below) of the forewings of two species – *H. egeria* and *H. melpomene* (Figure 3, top left pair) – from personal sources and the literature (Bybee et al., 2011; Wilts, Vey, Briscoe, & Stavenga, 2017). For reasons of simplicity and data availability we restrict our visual modelling to these two species, though the below spectral analyses would ideally be repeated for all model/mimic pairs.

6.1 | Spectral analysis

We first focus on the spectral data, both to confirm the assumption that there are discrete colour patches and because some of the results of this work will be drawn on for the latter pattern analyses. We begin by loading the reflectance spectra, which are saved in a single tab-delimited text file along with the image plates (available at the package repository; <https://github.com/rmaia/pavo>, or via figshare; <https://doi.org/10.6084/m9.figshare.7445840>), before



LOESS-smoothing them to remove any minor electrical noise and zeroing spurious negative values.

```
# Load spectra
> heli_specs <- getspec("../data", ext = "txt")

# Smooth spectra and zero negative values
> heli_specs <- procspec(heli_specs,
>   opt = "smooth",
>   fixneg = "zero")
```

A call to `plot(heli_specs, col = spec2rgb(heli_specs))` displays the now-clean spectra, with each line coloured according to how it might appear to a human viewer (Figure 4, top left).

Our interest is in quantifying the fidelity of visual mimicry, so we must consider the perspective of ecologically relevant viewers (the primary selective agents) which, in the case of aposematic *Heliconius*, are avian predators (Benson, 1972; Chai, 1986). We thus use the receptor-noise limited model (Vorobyev & Osorio, 1998;

Vorobyev et al., 2001) to predict whether the black, red and yellow colour patches of a representative model and mimic are distinguishable to avian predators. This first entails estimating the photoreceptor quantum catches of a representative viewer, so we use a built-in average UV-sensitive avian visual phenotype for estimating chromatic distances, and the double-cone sensitivity of the blue tit for luminance distances.

```
> heli_model <- vismodel(heli_specs,
>                         visual = "avg.uv",
>                         achromatic = "bt.dc",
>                         relative = FALSE)
```

At this point we may wish to get a quick sense of the relative distribution of stimuli by converting them to locations in an avian tetrahedral colourspace and plotting the results with `plot(colspace(heli_model))` (Figure 4). With receptor stimulation estimated, we now calculate noise-corrected chromatic and achromatic distances between patches. The `coldist()` function can be used to return the pairwise distances between every spectrum, which might then be averaged to derive a mean distance between species for every patch. This neglects the multivariate structure of such data, however, when the objective is to estimate the separation of groups in colourspace (Maia & White, 2018). We therefore prefer a bootstrapped measure of colour distance using `bootcoldist()`, which provides a robust measure of the separation of our focal samples (i.e. the red, white, and black patches of model vs. mimic), along with a 95% confidence interval, which can be inspected to see if it exceeds the theoretical discrimination threshold of one JND. We specify a relative receptor density of 1:2:2:4 (ultra-violet:short:medium:long wave-length receptors; Maier & Bowmaker, 1993), a signal-to-noise ratio yielding a Weber fraction of 0.1 for both chromatic and achromatic receptors, and assume that noise is proportional to the Weber fraction and independent of the magnitude of receptor stimulation (reviewed in Kelber et al. 2003; Olsson, Lind, & Kelber, 2017).

```
# Calculate the bootstrapped, noise-corrected colour distance
# between groups, using sample names to specify grouping ID's.
> heli_dist <- bootcoldist(heli_model,
>                           by = sub("\\..*", "", rownames(heli_model)),
>                           n = c(1, 2, 2, 4),
>                           weber = 0.1,
>                           weber.achro = 0.1)
```

Inspection of the key comparisons of interest (Figure 4, right) reveals that the 95% CI of all chromatic and achromatic comparisons includes the theoretical threshold of one JND. This predicts that the individual colour pattern elements of putative model and mimic *H. egeria* and *H. melpomene* are indistinguishable, or difficult to discriminate, to avian viewers – the assumed intended recipient of the aposematic signals. As noted above, the analysis of this representative pair can be readily scaled to encompass all species given the necessary data, and we can now use this information to inform our study of the spatial structure of these signals.

6.2 | Pattern analysis

We first load the focal images, which comprise the individual samples from plate XII of Eltringham (1916), saved as jpgs (Figure 3). We then plot one or all of the images to check they are as expected.

```
# Load all images. Here the 28 jpgs are stored in a folder called
# 'butterflies' located within the current working directory.
> heli_images <- getimg("butterflies")
28 files found; importing images.

# Plot the first image in the list only.
> plot(heli_images[[1]])

# Plot all images, which will progress through
# the sequence automatically.
> plot(heli_images)
```

We then segment the image and classify the pixels of all images into discrete colour or luminance categories, in this instance using k-means clustering, to create a colour-classified image matrix. The function `classify()` will carry this out, though there are numerous specific ways in which it may be achieved, including automatically or ‘interactively’, with the option of a reference image as template. Since our images are heterogeneous, it is simplest to use the interactive version of `classify()`, which will cycle through each image and ask the user to manually identify a homologous sample from every discrete colour or luminance class present, which are then used as cluster centres.

```
# Interactively colour-classify all images using k-means clustering.
> heli_class <- classify(heli_images, interactive = TRUE)

# Cycle through plots of the colour-classified images, alongside their
# identified colour palettes.
> summary(heli_class, plot = TRUE)
```

Finally, we use an adjacency analysis to estimate a suite of metrics describing the structure and complexity of the colour pattern geometry of model and mimic *Heliconius*, and by including the visually modelled colour distances estimated above the output will include several measures of the salience of colour patch edges as part of the boundary strength analysis (Endler, 2012; Endler et al., 2018). We will exclude the white background since it is not relevant, simply by specifying the colour-category ID belonging to the homogeneous underlay. If the image was more complex, such as an animal in its natural habitat, we might instead interactively identify and separate the focal animal and background using `procimg()` (e.g. Figure 2, second panel). Alternatively, we might forego the use of images altogether, and instead grid-sample and cluster the spectra across the visual scene and use these in directly in the call to `adjacent()` (sensu ‘method 1’ in Endler, 2012, see package vignette).

```
# Construct and inspect a data.frame of pairwise colour and luminance
# distances between all colour classes, built from the earlier
# receptor-noise modelled estimates. Note that we do not bother
# including colour-class ID 1, since that is the white background
# which is to be excluded from the analysis (see below).
# (Alternatively we could include it, and it would simply be ignored).
> distances <- data.frame(c1 = c(2, 2, 3),
>                         c2 = c(3, 4, 4),
>                         dS = c(10.6, 5.1, 4.4),
>                         dL = c(1.1, 2.5, 3.2))
> distances
```

c1	c2	dS	dL
2	3	10.50	7.41
2	4	11.76	23.40
3	4	13.29	15.99

```
# Calculate adjacency and boundary-strength statistics. We specify a
# scale of 50 mm, and note that the 'white' background, which has the class
# ID of 1 in this case, is to be excluded from the analysis.
# We also include the colour distance between all patches, as estimated above.
> heli_adj <- adjacent(heli_class,
>                       xscale = 50,
>                       bkgID = 1,
>                       exclude = "background",
>                       coldists = distances)

# Inspect a subset of the resulting data.frame. Variable meanings
# are detailed in the function documentation (see ?adjacent),
# or Endler (2012), Endler et al. (2018), and Endler & Mielke (2005).
> head(heli_adj)[, 1:7]
```

k	N	n_off	p_2	p_3	p_4	q_2_2 ...	
mimic_01	3	345522	6547	0.801	0.130	0.067	0.796
mimic_02	2	1018370	4091	0.835	0.164	NA	0.834
mimic_03	3	265278	6155	0.685	0.198	0.116	0.677
...							

We can now inspect the pattern descriptors of particular interest and explore the similarity of models and mimics with respect to their broader colour pattern geometry. As seen in Figure 5, the relative proportions of focal colours (top row), measures of pattern diversity and complexity (centre row), and the salience of patch boundaries (bottom row) are highly correlated between species pairs. This, in conjunction with the above modelling, suggests that the overall colour patterns of putative model and mimic *Heliconius* – both spectrally and spatially – are highly similar, and are thus predicted to be very difficult to discriminate to the intended avian viewers of their aposematic signals, as consistent with theory (Müller, 1879). More interesting questions remain, of course, including the degree to which mimics need resemble models to deceive viewers, and the relative importance of different colour pattern elements (e.g. Figure 5) in mediating the subjective resemblance of species pairs, for which `PAVO 2` is well-suited to help answer.

7 | CONCLUSIONS

The integrative study of biological coloration has borne rich fruit, though its potential to illuminate the structure and function of much of the natural world is not nearly realized (Endler & Mappes, 2017). As we have sought to demonstrate, `PAVO 2` (and beyond) provides a flexible framework to assist researchers studying the physiology, ecology and evolution of colour patterns and visual perception. We appreciate bug reports and suggestions, via email or the Github issue tracker <https://github.com/rmaia/pavo/issues>.

8 | CITATION OF METHODS

Many of the methods applied in `PAVO 2` are described in detail in their original publications – as listed in the documentation for the relevant functions – to which users should refer and cite as appropriate, along with `PAVO` itself, via this publication.

ACKNOWLEDGEMENTS

We thank Kate Umbers, Georgia Binns, and Julia Riley for the rigorous testing of image-based methods. The package and manuscript also greatly benefited from the thoughtful input of an associate editor and three reviewers at MEE, which we appreciate. T.E.W. thanks Elizabeth Mulvenna and Cormac White for their endless support. The authors have no conflicts of interest to declare.

AUTHORS' CONTRIBUTIONS

T.E.W., R.M. and H.G. authored the software and manuscript, J.A.E. developed and assisted in the implementation of methods, and critically revised the manuscript.

DATA ACCESSIBILITY

The current version of the package is available via CRAN <https://CRAN.R-project.org/package=pavo>, while the development version is available on github. All data used in this manuscript are either available from within the package itself, or in the github repository (<https://github.com/rmaia/pavo>).

ORCID

- Rafael Maia  <https://orcid.org/0000-0002-7563-9795>
- Hugo Gruson  <https://orcid.org/0000-0002-4094-1476>
- John A. Endler  <https://orcid.org/0000-0002-7557-7627>
- Thomas E. White  <https://orcid.org/0000-0002-3976-1734>

REFERENCES

- Backhaus, W. (1991). Color opponent coding in the visual system of the honeybee. *Vision Research*, 31, 1381–1397. [https://doi.org/10.1016/0042-6989\(91\)90059-E](https://doi.org/10.1016/0042-6989(91)90059-E)

- Barry, K. L., White, T. E., Rathnayake, D. N., Fabricant, S. A., & Herberstein, M. E. (2015). Sexual signals for the colour-blind: Cryptic female mantids signal quality through brightness. *Functional Ecology*, 29, 531–539. <https://doi.org/10.1111/1365-2435.12363>
- Barthelme, S. (2018) IMAGER: *Image processing library based on CImg*. CRAN. R package version 0.41.1.
- Benson, W. W. (1972). Natural selection for müllerian mimicry in *Heliconius erato* in Costa Rica. *Science*, 176, 936–939. <https://doi.org/10.1126/science.176.4037.936>
- Bybee, S. M., Yuan, F., Ramstetter, M. D., Llorente-Bousquets, J., Reed, R. D., Osorio, D., & Briscoe, A. D. (2011). Uv photoreceptors and uv-yellow wing pigments in *Heliconius* butterflies allow a color signal to serve both mimicry and intraspecific communication. *The American Naturalist*, 179, 38–51.
- Caves, E. M., Green, P. A., Zipple, M. N., Peters, S., Johnsen, S., & Nowicki, S. (2018). Categorical perception of colour signals in a songbird. *Nature*, 560(7718), 365. <https://doi.org/10.1038/s41586-018-0377-7>
- Chai, P. (1986). Field observations and feeding experiments on the responses of rufous-tailed jacamars (*Galbulia ruficauda*) to free-flying butterflies in a tropical rainforest. *Biological Journal of the Linnean Society*, 29, 161–189. <https://doi.org/10.1111/j.1095-8312.1986.tb01772.x>
- Chen, P. J., Awata, H., Matsushita, A., Yang, E. C., & Arikawa, K. (2016). Extreme spectral richness in the eye of the common bluebottle butterfly, *Graphium sarpedon*. *Frontiers in Ecology and Evolution*, 4, 18.
- Chittka, L. (1992). The colour hexagon: A chromaticity diagram based on photoreceptor excitations as a generalized representation of colour opponency. *Journal of Comparative Physiology A*, 170, 533–543.
- Clark, R., Santer, R., & Brebner, J. (2017). A generalized equation for the calculation of receptor noise limited colour distances in n-chromatic visual systems. *Royal Society Open Science*, 4, 170712. <https://doi.org/10.1098/rsos.170712>
- Cronin, T. W., & Marshall, N. J. (1989). A retina with at least ten spectral types of photoreceptors in a mantis shrimp. *Nature*, 339, 137. <https://doi.org/10.1038/339137a0>
- Dalrymple, R. L., Flores-Moreno, H., Kemp, D. J., White, T. E., Laffan, S. W., Hemmings, F. A., ... Moles, A. T. (2018). Abiotic and biotic predictors of macroecological patterns in bird and butterfly coloration. *Ecological Monographs*, 88, 204–224. <https://doi.org/10.1002/ecm.1287>
- Dalrymple, R., Kemp, D., Flores-Moreno, H., Laffan, S., White, T., Hemmings, F., ... Moles, A. (2015). Birds, butterflies and flowers in the tropics are not more colourful than those in higher latitudes. *Global Ecology and Biogeography*, 848–860.
- Eltringham, H. (1916). IV. on specific and mimetic relationships in the genus *Heliconius*, I. *Ecological Entomology*, 64, 101–148.
- Endler, J. A. (1980). Natural selection on color patterns in *Poecilia reticulata*. *Evolution*, 34, 76–91. <https://doi.org/10.1111/j.1558-5646.1980.tb04790.x>
- Endler, J. A. (1990). On the measurement and classification of colour in studies of animal colour patterns. *Biological Journal of the Linnean Society*, 41, 315–352. <https://doi.org/10.1111/j.1095-8312.1990.tb00839.x>
- Endler, J. A. (2012). A framework for analysing colour pattern geometry: Adjacent colours. *Biological Journal of the Linnean Society*, 107, 233–253. <https://doi.org/10.1111/j.1095-8312.2012.01937.x>
- Endler, J. A., Cole, G. L., & Kranz, X. (2018). Boundary strength analysis: Combin-ing colour pattern geometry and coloured patch visual properties for use in predicting behaviour and fitness. *Methods in Ecology and Evolution*, 9(12), 2334–2348. <https://doi.org/10.1111/2041-210X.13073>
- Endler, J. A., Gaburro, J., & Kelley, L. A. (2014). Visual effects in great bowerbird sexual displays and their implications for signal design. *Proceedings of the Royal Society B: Biological Sciences*, 281, 20140235. <https://doi.org/10.1098/rspb.2014.0235>
- Endler, J. A., & Mappes, J. (2017). The current and future state of animal coloration research. *Philosophical Transactions of the Royal Society B: Biological Sciences*, 372, 20160352. <https://doi.org/10.1098/rstb.2016.0352>
- Endler, J. A., & Mielke, P. W. (2005). Comparing entire colour patterns as birds see them. *Biological Journal of the Linnean Society*, 86, 405–431. <https://doi.org/10.1111/j.1095-8312.2005.00540.x>
- Fleishman, L. J., Perez, C. W., Yeo, A. I., Cummings, K. J., Dick, S., & Almonte, E. (2016). Perceptual distance between colored stimuli in the lizard *Anolis sagrei*: Comparing visual system models to empirical results. *Behavioral Ecology and Sociobiology*, 70(4), 541–555. <https://doi.org/10.1007/s00265-016-2072-8>
- Gawryszewski, F. M. (2018). Color vision models: Some simulations, a general n-dimensional model, and the colourvision R package. *Ecology and Evolution*, 8, 8159–8170. <https://doi.org/10.1002/ece3.4288>
- de Ibarra, N. H., Giurfa, M., & Vorobyev, M. (2001). Detection of coloured patterns by honeybees through chromatic and achromatic cues. *Journal of Comparative Physiology A*, 187, 215–224. <https://doi.org/10.1007/s003590100192>
- Jiggins, C. D. (2016). *The ecology and evolution of Heliconius butterflies*. Oxford, England: Oxford University Press. <https://doi.org/10.1093/acprof:oso/9780199566570.001.0001>
- Kelber, A., Vorobyev, M., & Osorio, D. (2003). Animal colour vision – behavioural tests and physiological concepts. *Biological Reviews*, 78, 81–118. <https://doi.org/10.1017/S1464793102005985>
- Kemp, D. J., Herberstein, M. E., Fleishman, L. J., Endler, J. A., Bennett, A. T. D., Dyer, A. G., ... Whiting, M. J. (2015). An integrative framework for the appraisal of coloration in nature. *The American Naturalist*, 185, 705–724. <https://doi.org/10.1086/681021>
- Maia, R., Eliason, C. M., Bitton, P. P., Doucet, S. M., & Shawkey, M. D. (2013a). PAVO: An r package for the analysis, visualization and organization of spectral data. *Methods in Ecology and Evolution*, 4(10), 906–913.
- Maia, R., Rubenstein, D. R., & Shawkey, M. D. (2013b). Key ornamental innovations facilitate diversification in an avian radiation. *Proceedings of the National Academy of Sciences of the United States of America*, 110(26), 10687–10692. <https://doi.org/10.1073/pnas.1220784110>
- Maia, R., & White, T. E. (2018). Comparing colors using visual models. *Behavioral Ecology*, 29, 649–659. <https://doi.org/10.1093/beheco/ary017>
- Maier, E. J., & Bowmaker, J. K. (1993). Colour vision in the passeriform bird, *Leiothrix lutea*: Correlation of visual pigment absorbance and oil droplet transmission with spectral sensitivity. *Journal of Comparative Physiology A*, 172, 295–301. <https://doi.org/10.1007/BF00216611>
- Müller, F. (1879). *Ituna and Thyridia*: A remarkable case of mimicry in butterflies. *Transactions of the Entomological Society of London*, 1879, 20–29.
- Olsson, P., Lind, O., & Kelber, A. (2015). Bird colour vision: Behavioural thresholds reveal receptor noise. *Journal of Experimental Biology*, 218, 184–193. <https://doi.org/10.1242/jeb.111187>
- Olsson, P., Lind, O., & Kelber, A. (2017). Chromatic and achromatic vision: Parameter choice and limitations for reliable model predictions. *Behavioral Ecology*, 29, 273–282.
- Ooms, J. (2018). MAGICK: Advanced graphics and image-processing in R. CRAN. R package version 1.9.
- Pike, T. W. (2012). Preserving perceptual distances in chromaticity diagrams. *Behavioral Ecology*, 23, 723–728. <https://doi.org/10.1093/beheco/ars018>
- Pike, T. W. (2018). Quantifying camouflage and conspicuousness using visual salience. *Methods in Ecology and Evolution*, 9(8), 1883–1895. <https://doi.org/10.1111/2041-210X.13019>
- Renoult, J. P., Kelber, A., & Schaefer, H. M. (2017). Colour spaces in ecology and evolutionary biology. *Biological Reviews*, 92(1), 292–315. <https://doi.org/10.1111/brv.12230>

- Rojas, B., Devillechabrolle, J., & Endler, J. A. (2014). Paradox lost: Variable colour-pattern geometry is associated with differences in movement in aposematic frogs. *Biology Letters*, 10, 20140193. <https://doi.org/10.1098/rsbl.2014.0193>
- Rojas, B., & Endler, J. A. (2013). Sexual dimorphism and intra-populational colour pattern variation in the aposematic frog *Dendrobates tinctorius*. *Evolutionary Ecology*, 27, 739–753. <https://doi.org/10.1007/s10682-013-9640-4>
- Schnaitmann, C., Haikala, V., Abraham, E., Oberhauser, V., Thesstrup, T., Griesbeck, O., & Reiff, D. F. (2018). Color processing in the early visual system of *Drosophila*. *Cell*, 172, 318–330. <https://doi.org/10.1016/j.cell.2017.12.018>
- Smith, T., & Guild, J. (1931). The CIE colorimetric standards and their use. *Transactions of the Optical Society*, 33, 73. <https://doi.org/10.1088/1475-4878/33/3/301>
- Thoen, H. H., How, M. J., Chiou, T. H., & Marshall, J. (2014). A different form of color vision in mantis shrimp. *Science*, 343, 411–413. <https://doi.org/10.1126/science.1245824>
- Troje, N. (1993). Spectral categories in the learning behaviour of blowflies. *Zeitschrift für Naturforschung C*, 48, 96. <https://doi.org/10.1515/znc-1993-1-218>
- Troscianko, J., Skelhorn, J., & Stevens, M. (2017). Quantifying camouflage: How to predict detectability from appearance. *BMC Evolutionary Biology*, 17, 7. <https://doi.org/10.1186/s12862-016-0854-2>
- Troscianko, J., & Stevens, M. (2015). Image calibration and analysis toolbox—a free software suite for objectively measuring reflectance, colour and pattern. *Methods in Ecology and Evolution*, 6, 1320–1331. <https://doi.org/10.1111/2041-210X.12439>
- Vorobyev, M., Brandt, R., Peitsch, D., Laughlin, S. B., & Menzel, R. (2001). Colour thresholds and receptor noise: Behaviour and physiology compared. *Vision Research*, 41, 639–653. [https://doi.org/10.1016/S0042-6989\(00\)00288-1](https://doi.org/10.1016/S0042-6989(00)00288-1)
- Vorobyev, M., & Osorio, D. (1998). Receptor noise as a determinant of colour thresholds. *Proceedings of the Royal Society of London Series B: Biological Sciences*, 265, 351–358. <https://doi.org/10.1098/rspb.1998.0302>
- Westland, S., Ripamonti, C., & Cheung, V. (2012). *Computational colour science using MATLAB*. Chichester, UK: John Wiley & Sons. <https://doi.org/10.1002/9780470710890>
- White, T. E. (2017). Jewelled spiders manipulate colour-lure geometry to deceive prey. *Biology Letters*, 13, 20170027. <https://doi.org/10.1098/rsbl.2017.0027>
- White, T. E., Dalrymple, R. L., Noble, D. W. A., O'Hanlon, J. C., Zurek, D. B., & Umbers, K. D. L. (2015). Reproducible research in the study of biological coloration. *Animal Behaviour*, 106, 51–57. <https://doi.org/10.1016/j.anbehav.2015.05.007>
- White, T. E., & Kemp, D. J. (2016). Color polymorphic lures target different visual channels in prey. *Evolution*, 70, 1398–1408. <https://doi.org/10.1111/evo.12948>
- White, T. E., & Kemp, D. J. (2017). Colour polymorphic lures exploit innate preferences for spectral versus luminance cues in dipteran prey. *BMC Evolutionary Biology*, 17, 191. <https://doi.org/10.1186/s12862-017-1043-7>
- Wilts, B. D., Vey, A. J., Briscoe, A. D., & Stavenga, D. G. (2017). Longwing (*Heliconius*) butterflies combine a restricted set of pigmentary and structural coloration mechanisms. *BMC Evolutionary Biology*, 17, 226. <https://doi.org/10.1186/s12862-017-1073-1>

How to cite this article: Maia R, Gruson H, Endler JA, White TE. *pavo 2: New tools for the spectral and spatial analysis of colour in r*. *Methods Ecol Evol*. 2019;00:1–11. <https://doi.org/10.1111/2041-210X.13174>

Résumé grand public en français

Les couleurs iridescentes (définies comme des couleurs qui changent selon l'angle d'incidence ou d'observation) sont omni-présentes dans notre quotidien, aussi bien dans des objets artificiels comme les CD ou la peinture des voitures, que dans les objets naturels. En effet, on retrouve ces couleurs dans presque toutes les branches de l'arbre du vivant : chez les poissons, chez de nombreux insectes (des scarabées notamment) ou araignées, chez les oiseaux (les canards, les faisans, les étourneaux, les colibris). Elles sont générées par l'interaction physique de la lumière avec des structures régulières de taille nanométrique (réseau de diffraction ou structure multicouche). Et si la beauté de ces couleurs a frappé l'esprit des tous premiers naturalistes, force est de constater qu'aujourd'hui encore, elles restent sources de beaucoup de mystères pour les scientifiques.

Dans cette thèse, je me suis plus particulièrement intéressé aux couleurs iridescentes des colibris. En effet, si les couleurs iridescentes sont présentes chez de nombreux organismes, elles sont rarement aussi extraordinaires que chez les colibris. Un individu qui semble avoir la tête d'un rose criant à un moment donné, passe à un noir complet en un instant, lorsqu'il tourne même très légèrement la tête. Lors de l'élaboration de ce projet de thèse, j'ai donc cherché à identifier les mécanismes physiques impliqués dans la production de couleurs iridescentes d'une telle intensité. Et dans un deuxième temps, j'ai cherché à identifier les mécanismes évolutifs qui ont conduit chaque espèce à posséder plutôt telle ou telle couleur.

Mais ce projet a très vite été amené à évoluer puisque, si la mesure de couleurs non-iridescentes est bien connue et utilisée depuis longtemps, jusqu'ici, personne n'avait décrit comment on pouvait mesurer de manière fiable et objective des couleurs qui dépendent de l'angle. L'idée de mesurer chaque position de l'espace des angles a rapidement été abandonnée lorsque j'ai réalisé le temps nécessaire pour mesurer ne serait-ce qu'à une seule position. Il fallait donc que je comprenne comment les couleurs iridescentes variaient dans l'espace des angles, dans l'espoir de peut-être pouvoir réduire le nombre de mesures nécessaires. En m'appuyant sur la théorie qui décrit l'origine physique des couleurs iridescentes, je suis effectivement parvenu à démontrer qu'elles variaient de façon prévisible dans l'espace selon des fonctions mathématiques relativement simples que l'on pouvait entièrement décrire avec seulement 6 paramètres. Il n'était donc plus nécessaire de mesurer tout l'espace des angles mais seulement quelques positions bien choisies pour estimer les valeurs de

ces paramètres : un gain de temps considérable ! J'ai ensuite vérifié que cette méthode fonctionnait bien en la testant chez les colibris, mais aussi chez des espèces très différentes : les papillons *Morpho*, suggérant par là que cette méthode devrait effectivement être applicable chez n'importe quel organisme. Ce qui me plaisait avec cette méthode, c'est qu'elle proposait un protocole et des indices standards qui, en théorie, devraient marcher tout le temps. À l'inverse des méthodes développées spécifiquement à chaque fois pour mesurer une espèce donnée jusqu'ici, ma méthode permettait donc de comparer l'iridescence d'un organisme à l'autre, d'une étude à l'autre. Mais il aurait été dommage de ne pas pouvoir utiliser tous les travaux sur l'iridescence qui ont été conduits par le passé dans ces comparaisons : je me suis donc efforcé de faire un inventaire exhaustif des différentes méthodes utilisées jusqu'ici, pour pouvoir expliquer pourquoi elles me semblaient moins appropriées que la méthode que je proposais et comment il était possible de convertir leurs indices pour les comparer aux miens.

J'étais donc désormais équipé pour poursuivre mon travail sur les colibris. Ma première étude a porté sur les communautés de colibris en Équateur. En effet, il existe 365 espèces de colibris qui vivent partout en Amérique, jusqu'en Alaska mais il y a un gradient latitudinal de diversité très marqué : alors qu'il y a seulement 7 espèces de colibris dans toute l'Amérique de Nord, il y en a 132 rien qu'en Équateur. Mais une telle concentration de diversité a des conséquences : il est fréquent que des colibris d'espèces différentes s'hybrident, engendrant dans de nombreux cas une descendance non-fertile. D'un point de vue évolutif, puisque les hybrides ne peuvent pas transmettre leurs gènes (et ceux de leur parents) à leur descendance, on s'attend à ce qu'au fil des générations, leur fréquence (et la fréquence des accouplements interspécifiques) diminue. Autrement dit, on s'attend à la sélection progressive de mécanismes qui conduisent à la réduction du nombre d'hybrides. Un exemple d'un tel mécanisme serait une divergence dans l'apparence des espèces : peu à peu, les espèces se ressemblent de moins en moins et il n'y a plus d'accouplements interspécifiques. Mais, malgré tout, les individus ne peuvent pas devenir de n'importe quelle couleur : un oiseau entièrement rose dans le vert de la forêt tropicale serait rapidement la proie de nombreux prédateurs. C'est le perpétuel paradoxe lorsqu'on s'intéresse à l'évolution des couleurs : d'un côté, la sélection va favoriser les individus très voyants, qui parviennent à attirer de nombreux·ses partenaires sexuel·le·s, mais de l'autre, elle va aussi favoriser les individus très peu voyants, qui parviennent à échapper aux prédateurs. Un mécanisme courant par lequel ce paradoxe est résolu repose sur une répartition spatiale complexe des couleurs sur le corps des animaux. Les parties du corps souvent exposées aux prédateurs ressemblent généralement au feuillage, alors que les parties exposées aux partenaires potentiels sont resplendissantes. C'est particulièrement visible chez de nombreux papillons, que l'on ne détecte pas tant qu'ils ont les ailes fermées, et qui révèlent leurs riches couleurs lorsqu'ils déplient leurs ailes. On s'attend à quelque chose d'assez similaire chez les colibris d'équateur : la tête et la poitrine de l'oiseau sont

probablement liés à la communication et la séduction, alors que le dos est probablement lié au camouflage. À l'échelle de la communauté et au vu de ce que j'expliquais précédemment, on devrait observer de grandes différences de couleurs sur la tête et la poitrine des colibris qui vivent au même endroit. Et à l'inverse, puisqu'il existe un nombre limité de façons de se camoufler dans la forêt, on s'attend à ce qu'ils aient tous des couleurs similaires (et similaires au feuillage) sur le dos. J'ai testé ces prédictions sur 189 communautés de colibris en Équateur, qui abritent 112 espèces de colibris différentes. J'ai effectivement trouvé que les espèces qui vivent au même endroit ont tendance à avoir les mêmes couleurs sur le dos, et des couleurs très différentes sur le ventre mais, contrairement à ce que j'avais prévu, elles n'ont pas forcément des couleurs très différentes sur la tête. Cette différence par rapport à mon attendu théorique est peut-être simplement due au fait que de petites différences (juste sur le ventre, ou des différences sur autre chose que la couleur, comme le chant par exemple) sont suffisantes pour limiter les accouplements interspécifiques.

Ce travail laborieux de mesure de la couleur chez 112 espèces de colibris, sur différentes parties du corps, ainsi que le temps que j'ai passé dans les collections des muséums, m'ont fait prendre conscience de l'incroyable diversité de couleurs au sein de cette famille qui est apparue pourtant récemment. Ma seconde étude s'est donc penchée sur la source physique de cette diversité : quels sont les mécanismes exacts qui produisent l'iridescence chez les colibris ? Et à quel point diffèrent-ils d'une espèce à l'autre ? Des études précédentes donnaient déjà quelques pistes mais j'avais de bonnes raisons de penser que ce n'était qu'une vision très partielle : les structures de seulement 13 espèces parmi les 365 espèces de colibris ont été observées en détails jusqu'ici. Je me suis donc efforcé d'échantillonner un plus grand nombre d'espèces, avec des couleurs, des habitats et une histoire évolutive très différents. Et au vu des résultats de ma première étude, qui montrait que le dos et le ventre sont soumis à des processus évolutifs différents, j'ai échantillonné deux parties du corps (la gorge et le dos) chez chaque espèce. Pour chaque échantillon, j'ai mesuré la couleur avec la nouvelle méthode que j'avais développé précédemment, et j'ai fait des observations des structures sous-jacentes au microscope électronique à transmission. Mes observations confirment mes suspicions d'une grande diversité dans les structures à l'origine de l'iridescence chez les colibris, diversité bien plus grande que ce que les études précédentes laissaient présager. Un travail de corrélation entre les couleurs iridescentes mesurées et les structures sous-jacentes, couplé à de la modélisation optique, m'a permis de mettre en évidence le rôle des différentes caractéristiques des structures (nombre de couches, épaisseur des couches, etc.) dans la couleur qui en résulte. Néanmoins, pour certaines espèces, les structures observées sont tellement inhabituelles qu'il faudra probablement des études précises dans chaque cas (à l'inverse de mon étude qui voulait étudier la diversité à l'échelle de la famille) pour bien comprendre leur fonctionnement.

Au cours de ces études, j'ai également remarqué un biais dans une méthode classique pour l'étude de la couleur. Lorsqu'on veut quantifier la diversité en couleur d'une espèce ou d'un taxon, on calcule généralement le volume de l'enveloppe convexe obtenue à partir des points expérimentaux. L'idée sous-jacente est que si des couleurs extrêmes peuvent être produites, alors toutes les couleurs intermédiaires peuvent l'être aussi. Mais il s'agit d'une hypothèse très forte, et bien souvent pas valide dans le domaine de l'étude de la couleur. Cela conduit à des surestimations du volume de couleur d'une espèce ou d'un groupe d'espèces. J'ai donc proposé une approche alternative, plus générale, qui supprime cette hypothèse de convexité, et ainsi supprime le biais responsable de la surestimation du volume. J'ai principalement discuté l'avantage de cette méthode dans l'étude de la couleur mais il ne fait aucun doute qu'elle pourrait également être utilisée dans d'autres disciplines, qui utilisent également l'enveloppe convexe, sans qu'elle donne des résultats satisfaisants (par exemple, en écologie fonctionnelle, ou en paléontologie).

Ces trois ans de thèse, qui ont représenté ma plus longue immersion jusqu'ici dans le monde de la recherche, m'ont également fait prendre conscience de nombreux dysfonctionnements dans le système de publication scientifique et d'évaluation des chercheur·se·s. J'ai entrepris de nombreuses actions pour sensibiliser mon entourage à ces problèmes et pour partager ma connaissance de systèmes alternatifs qui proposent des solutions. Plus concrètement, j'ai contribué à l'initiative rOpenSci, qui propose une évaluation par les pairs de packages R. Ce projet est crucial dans un monde où la dépendance des résultats scientifiques aux logiciels est croissante et où le développement des logiciels est fait par des scientifiques qui ne sont pas nécessairement formés au développement. Mes contributions passées à des logiciels libres (non scientifiques) et mon intérêt pour le développement logiciel m'ont permis de rejoindre dans un premier temps un projet déjà existant : pavo, qui propose une large palette d'outils pour l'analyse des couleurs dans R. J'ai contribué à l'ajout de quelques nouvelles fonctionnalités (lecture de nouveaux formats de fichiers, algorithme plus précis et performant pour le calcul de certaines variables), et à la simplification et l'accélération du code déjà existant. Ce package a été publié (après relecture par les pairs) par Methods in Ecology and Evolution et cette expérience m'a encouragé à m'investir davantage dans cette voie : j'ai donc par la suite développé le package lightr qui offre pour la première fois un outil libre et gratuit pour lire les formats propriétaires produits par les spectrophotomètres lors de la mesure de la couleur (package contrôlé par rOpenSci et article publié dans le Journal of Open Source Software). J'ai également participé à l'élaboration du package R rrromeo (également relu par rOpenSci), qui permet d'accéder depuis R aux politiques des journaux en matière d'Open Access. Cet outil se révèle déjà précieux pour des documentalistes ou des chercheur·se·s en bibliométrie, comme en attestent les premiers retours de la communauté scientifique. Par ailleurs, j'ai contribué à sensibiliser des chercheurs à l'intérêt de publier les sources de leurs logiciels, sous licence libre, et je les ai accompagnés dans cette transition.

Pour conclure, au cours de ces trois ans, j'ai effectivement travaillé sur l'iridescence des colibris. J'ai dans un premier temps développé une nouvelle méthode qui propose un protocole clair, et répétable pour l'étude des couleurs iridescentes, protocole qui fonctionne aussi bien à l'échelle intra- qu'inter-spécifique, et sur une large variété d'espèces. J'ai ensuite montré qu'à l'échelle de la communauté, on observait des patrons qui suggèrent l'implication de différentes parties du corps dans différents processus écologiques : le ventre semble plutôt impliqué dans la communication et la reconnaissance spécifique alors que le dos semble davantage lié au camouflage. Néanmoins, ces résultats pourraient être complétés par une étude de micro-évolution : est-ce que des colibris d'une même espèce ont des couleurs différentes à différentes localités selon les espèces avec lesquelles ils vivent ? Sont-ils différents d'une localité à l'autre selon le feuillage dans lequel ils doivent se camoufler ? Cette diversité de scénarios évolutifs trouve aussi écho dans une diversité structurale sous-jacente : contrairement à ce qu'on croyait jusqu'ici, en se basant sur un très petit nombre d'études, les structures responsables de l'iridescence chez les colibris sont extrêmement différentes d'une étude à l'autre. Mais, je n'ai pas travaillé que sur l'iridescence des colibris : je me suis également intéressé à des questions méthodologiques plus larges, qui concernent de nombreuses disciplines en écologie et évolution, comme les problèmes liés à l'utilisation des enveloppes convexes et comment y remédier. Et j'ai aussi largement milité pour l'utilisation de pratiques plus ouvertes dans le monde scientifique, par des discussions ou un soutien personnel, ou par l'organisation d'atelier, l'écriture de billets de blog, etc. J'ai également largement contribué au développement d'outils et de logiciels scientifiques : soit en améliorant des outils existants, par ajout de fonctionnalité, ou par amélioration des performances ou de la documentation, ou soit en développant mes propres outils de zéro lorsqu'aucune base n'existe déjà. J'aimerais dans le futur m'impliquer davantage dans le développement d'outils techniques dédiés à l'ouverture de la science, comme des logiciels libres de publication qui viennent en appui au processus de revue par les pairs.

Origine et fonctions des couleurs iridescentes chez les colibris

La couleur constitue un trait particulièrement intéressant pour étudier les mécanismes de l'évolution car il s'agit d'un trait complexe, qui peut évoluer dans plusieurs dimensions, et qui est soumis à de nombreuses pressions évolutives, qui agissent généralement dans des directions opposées. Parmi les couleurs, il existe une classe qui a reçu relativement peu d'attention de la part des biologistes évolutifs jusqu'ici du fait de sa complexité et de la difficulté à la mesurer de manière fiable et comparable entre espèces : les couleurs iridescentes. Les couleurs iridescentes sont habituellement définies comme des couleurs qui changent selon l'angle d'observation ou d'illumination. Au cours de cette thèse, j'ai collaboré avec des biologistes et des physiciens et j'ai utilisé la théorie optique pour construire une nouvelle méthode de mesure pour ces couleurs, que j'ai ensuite testée sur les colibris et les papillons *Morpho*. J'ai également développé d'autres outils méthodologiques et des librairies logicielles pour l'étude des couleurs. Je me suis ensuite intéressé plus précisément aux couleurs iridescentes des colibris et à leur origine (i) proximale : par quels mécanismes les colibris produisent-ils leurs couleurs extraordinaires ? (ii) ultime : quels sont les processus qui contrôlent l'évolution de ces couleurs à l'échelle de la communauté toute entière ? J'ai découvert que les structures responsables de l'iridescence chez les colibris présentent bien plus de diversité que ce qu'on pensait jusqu'ici et ils ont également un type de structure qui n'a pour l'instant été observé dans aucun autre groupe. J'ai aussi montré qu'à l'échelle interspécifique, les couleurs iridescentes présentes sur le dos sont similaires parmi les espèces qui habitent la même communauté, ce qui suggère une sélection par l'environnement, pour le camouflage par exemple, alors que celles sur le ventre sont plus différentes qu'attendu au hasard, ce qui suggère une sélection pour la communication.

Origin and functions of iridescent colours in hummingbirds

The study of colour can offer valuable insights into the fine details of evolutionary mechanisms. It is indeed a complex trait, which can evolve along several dimensions, and which is controlled by multiple selective pressures with often opposed effects. Yet, there is one class of colours that has received few attention from evolutionary biologists: iridescent colours. This is due to the inherent complexity of these colours and the fact that their sole quantitative measurement is a challenge in itself. During my PhD, I worked with physicists and biologists and I used optical theory to propose a new measurement method for iridescent colours. I then validated this method empirically by showing that it produced reliable and repeatable estimates for both hummingbirds and *Morpho* butterflies. My work during these three years has also focused on the development of other methodological tools and software for the study of colours. I also focused more precisely on iridescent colours in hummingbirds. I mainly investigated two sides of this topic and tried to find out (i) the proximate causes of iridescence in hummingbirds: how do they produce the striking colours they are renowned for? (ii) the ultimate causes of iridescence: what are the evolutionary mechanisms which control the evolution of iridescence at the community level? I found out that the structures producing iridescence in hummingbirds are way more diverse than what we previously thought. They even display an usual type of structure which has not been described in any other group yet. I also showed that at the interspecific level, iridescent colours on the back of hummingbirds tend to be similar among species occupying the same communities, which suggests a possible role of the environment in the evolution of these colours, possibly for camouflage against predators. On the other hand, colours on the belly tend to be more similar than expected by chance among co-occurring species, which suggests a role of selection for communication.